CHAPTER 1

INTRODUCTION

1.1 Background of studies

Mould and die are one of the typical necessary tools for modern mass-production industries. Customer industries for moulds and dies range broadly over transportation, machinery, electrical, household goods, optical devices, toys and others. As these products and equipment consist mostly of parts, units (sub-assemblies) and components which are used in volume, mould and dies are supplied virtually to every manufacturing company. In terms of industrial applications, moulds and dies are classified into press dies, plastic mould die, casting dies, forging dies, powder metallurgy dies, rubber dies and ceramic dies.

As dies and moulds help in the fabrication of parts and components, their accuracy determines the final products quality such as, mirroring or matching the final intended shape. For example, when the required accuracy of a consumer good is stringent, it must be finished with the matching high accuracy such the moulds used to fabricate these parts are required to have much higher accuracy. Aluminium cans that contain beverages may injure consumers' lips with their notched tap. These cans are finished within the accuracy of 1 micron whereas the corresponding mould accuracy is in the magnitude of 0.1 micron (Horst et al., 2008).

In general, most moulds and dies are made through the machining of a hardened tool steel material (>60 HRC) or solid block. Milling process is preferable due to its flexibility and capability in creating a complex shape geometry of mould and die components (shown in Figure 1.1). However, there are several challenges in machining

with the materials such as rough machined surface, high cutting force and low material removal rate. The literature shows that even though optimal cutting conditions are employed for machining tool steel material, the produced surface roughness is still beyond the permissible tolerances (Azlan et al., 2017). The machining tolerances are generally achieved by subsequent manual finishing processes in essence to polishing and grinding in order to realize both the required geometry and surface finish. Notably, the aforementioned manufacturing techniques for mould and die fabrications tend to decrease productivity and create uncertainty in the component accuracy.

Hence, this thesis proposed a significant advancement on improving the mould fabrication process using a hybrid machining technique such as combining two established manufacturing processes into a new combined set-up known as rotary ultrasonic assisted end milling (RUAEM) whereby the advantages of each discrete process can be exploited synergistically.

The rotary ultrasonic assisted end milling (RUAEM) process of mould and die part was analyzed in this thesis. The project was initiated in collaboration with an automotive tool and die component manufacturer, Miyazu (Malaysia) Sdn. Bhd. The work piece material was hardened D2 tool steel material for all the components. During milling process of this component, large volumes of materials were removed with the risk of instability and tolerance violation. Traditionally, milling process followed by manual polishing process are employed to obtain the desired tolerances which tends to reduce productivity and increase the manufacturing costs.



Figure 1.1: Complex free-form shape die in the automotive industry

(www.mizayu.com.my)

1.2 Problem statement

1.2.1 Low manufacturing productivity

In general, the production of mould and die involves several stages starting from the design and cutter path generation such as CADCAM. The process continues with the rough machining process where the material is removed as fast as possible while leaving a semi-finishing allowance. In this stage, there is little or no emphasis on work piece dimensional accuracy or surface roughness. An end milling process is generally employed for this process due to the high efficiency of material removal and longer tool life.

Next, semi-finishing process is executed after the rough machining process where the remaining steps and shoulders from the roughing stage are removed and a finishing allowance of uniform thickness is left. This operation is essential in maintaining a relatively constant metal removal rate for subsequent finishing. This is particularly important at corners and other difficult areas to access. The aim is to minimize cutter deflection and tool wear during finishing.

Next, the finish machining process is conducted in which the final shape of the part is achieved using a ball nose end mill. Dimensional accuracy, gouge prevention and work

piece surface roughness are the most important criteria. As a result, finishing generally requires the largest amount of machining time due to the low depths of cut and slow feed rate.

Finally, in order to realize both the required geometry and surface finish, polishing and grinding process are performed manually by a skilled operator. Figure 1.2 shows steps involved in die making. Distinctly, the steps involved in mould and die fabrication tend to decrease productivity and create uncertainty in component accuracy.



Figure 1.2: Steps in die manufacturing (Donghao, 2018)

1.2.2 Rough machined surface

Manufacturing process of mould and die comprise of rough machining, finish machining, polishing and grinding process. However, the polishing and grinding process is

done by manually and require skill worker. Whereas the quality of machined surface produced by manual polishing and grinding difficult to get mirror surface quality. Also, mould and die material difficult to machine because of its high strength material and high rates of work hardening (Nguyen and Hsu, 2016). Then, the quality of produced part depends on the quality of the mould and dies. Besides that, the mould and die material is hard to machine by conventional end milling causing some distortions on machined surface and the cavity is machined to an oversize dimension of 0.3 mm (Altan et al., 2001). Also, after manual polishing and grinding process, it difficult to get mirror surface quality and surface roughness requirement for finishing the working surface of die should be achieved strictly. This is due to finishing the surface by hand with stones and sandpaper costs a lot of time and the surface roughness (Ra) value is not always satisfying the requirement perfectly (Donghao, 2018).

1.2.3 High machining force

One of the major challenges in milling of hardened mould and die materials is high machining force at cutting zone during interaction between cutting tool and work piece machined surface because mould and die material have excellent properties. The higher interaction between cutting tool and machined surface occurred because hardened mould and die material have excellent properties of high wear resistance, high compressive strength, good through hardening properties, high stability in hardening and good response to heat treatment and deep hardening and categorized as difficult to cut materials. During milling process, machining force is one of main factor that directly affected to dynamics effects, work piece roughness and tool deflection during milling machining of mould and die materials (Neto et al., 2016). Also, hardened steel material are difficult to machine because to their physical and mechanical properties such as high strength and low thermal

conductivity which causing the higher cutting force, higher cutting temperature and shorten tool life of cutting tool (Sun et al., 2010).

1.2.4 Low material removal rate

Die manufacturing process consists rough and finish machining. The purposes of finish machining to produce surface finish machined surface and rough machining process by conventional milling is to remove a large amount of material at a low rate. It was found that rough machining process by conventional end milling produce lower material removal rate which causing subsurface damage of machined surface because a difficult chip out of the cutting area between the cutting tool and work piece surface (Kalpakjian et al., 2014). Rough machining process by conventional machining difficult to control the chip flow during cutting zone and generated continuous chips, long chips and curled chips. Besides that, the mould and die material difficult to be machined during manufacturing process because of high strength material which causing low removes unwanted material from a work piece which aim to produce the desired shape. In conventional machining, material removal rate depends on the feed velocity of milling cutter, width of cut and depth of cut. The decrease low feed rate during conventional machining, causes the material removal rate slightly decreases because blunt cutting tool (Latif et al., 2017). The blunt cutting tool during conventional machining generate more heat between cutting tool and work piece machined surface that contribute the form of burr which resulting low material removal rate compared rotary ultrasonic assisted end milling. The suitable applied of vibration frequency on rotary ultrasonic assisted end milling obtained the most stable cutting process in relative stable region with achieving higher material removal rate and higher surface accuracy (Cao et al., 2015).

1.2.5 Challenges in machining hardened mould and die material

The demand of low tolerances and high quality products has forced manufacturing industry to continuously progress in quality control and machining technologies. One of the fundamental mould and die manufacturing processes is end milling. Typically, mould and die components are made from hardened material such as a tool steel with superior strength. Due to its high strength properties (>60 HRC), machining with these materials poses several problems. Few reported works on machining hardened material result in high cutting force (Okada et al., 2011), rapid tool wear (Begic et al., 2014), rough machined surface (Toh, 2006) and high machining temperature (Karaguzel et al., 2016). As a result, the milling process in dealing with these materials requires some special techniques such as light machining cut, low depth of cuts and slow feed in order to obtain a good result. However, those techniques result in longer machining time which hampers the productivity and increases the machining costs.

For manufacturers, the quality of mould and die components is directly evaluated with its surface roughness attribute because functional attributes of a product such as contact, wearing, heat transmission and coating are affected by the surface. For some of the applications, such as in the plastic production, the requirement for a mirror surface quality profile is crucial for aesthetic appearance. Therefore, the requirement for a smooth surface finish is vital for mould and die components which are nearly impossible to be achieved through the end milling process. Figure 1.3 and Figure 1.4 show an example of metal stamping die used in the automotive industry and mould for injection moulding in plastic industries respectively.

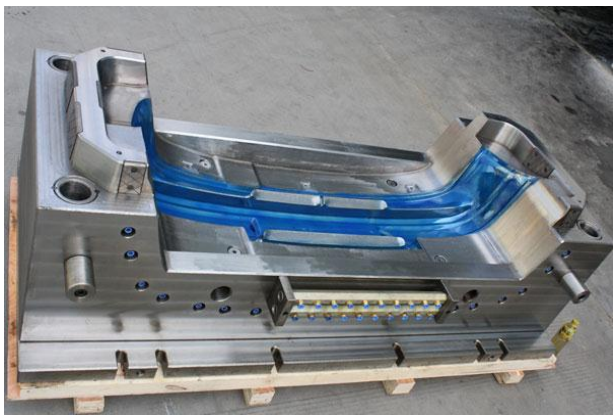


Figure 1.3: Example of metal stamping component in automotive industry

(www.xuhuimould.com)

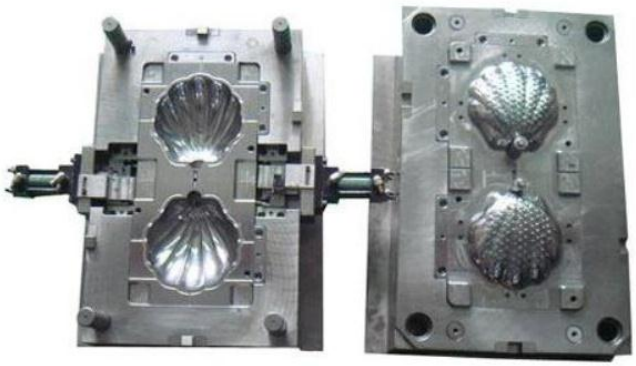


Figure 1.4: Mould for injection moulding in plastic industries (www.indiamart.com)

Figure 1.5 shows manual hand sanding polishing proceess by skill worker that applied in die industry. Otherwise, the surface roughness value after manual polishing by skilled worker cannot meet the requirements perfectly (0.6 μm – 0.8 μm) and highly depend on worker's experience (Donghao, 2018).



Figure 1.5: Manual hand sanding polishing process by skill worker that applied in die industry (Donghao, 2018)

Currently, to solve manual hand sanding polishing process by skill workers, the real application of ultrasonic assisted end milling (UAEM) in die industry is using hammering tool technique application with indirect high frequency micro-forging (about 220 strokes/second) as shown in Figure 1.6.



Figure 1.6: Peening tool application in industry with indirect high frequency micro-forging (Donghao, 2018)

It was found that, the new machining techniques using ultrasonic vibration known as rotary ultrasonic assisted end milling (RUAEM) is suitable technique compared to the

shot peening tool application due to high amplitude hammering impact may cause damage to the part surface (Donghao, 2018).

1.3 Preliminary proposed technical solution-rotary ultrasonic assisted end milling (RUAEM)

The existing techniques on achieving fine surface finish for mould and die components have a tendency to reduce the productivity and create uncertainty in the component accuracy. To overcome the disadvantages with the current practice, a practical yet effective solution is deemed necessary. The ultrasonic machining has been recently applied in mould and die industry for finishing of various precision parts such as mirror surface finishing of mould and die materials and precision micro machining of dies and molds (Jung et al., 2012). One of the possible and promising techniques is by combining or assisting the current end milling process with the ultrasonic vibration known as rotary ultrasonic assisted end milling (RUAEM), which has been proven to improve the performances of conventional machining process for some hard and brittle materials.

In this section, a preliminary proposed technical solution using the RUAEM is presented. The aim of this section is to provide an insight on the feasibility of RUAEM technique to improve the machined surface roughness value compared to normal end milling process (EM). To demonstrate this, a set of experimental runs between the RUAEM and normal end milling process (EM) process is performed. Details of the experimental runs including machining parameter, experimental design, cutting tool, surface roughness results and statistical ANOVA analysis are presented in Appendix A.

The preliminary experimental runs yield that the machined surface roughness values for RUAEM process are lower and better compared to normal end milling process (EM) process within the same cutting parameters conditions. The surface roughness values

for RUAEM range between 0.27 μm to 1.11 μm whereas the surface roughness values for EM range between 0.32 μm to 3.48 μm. Figure 1.7 shows the surface roughness values between RUAEM and EM process.

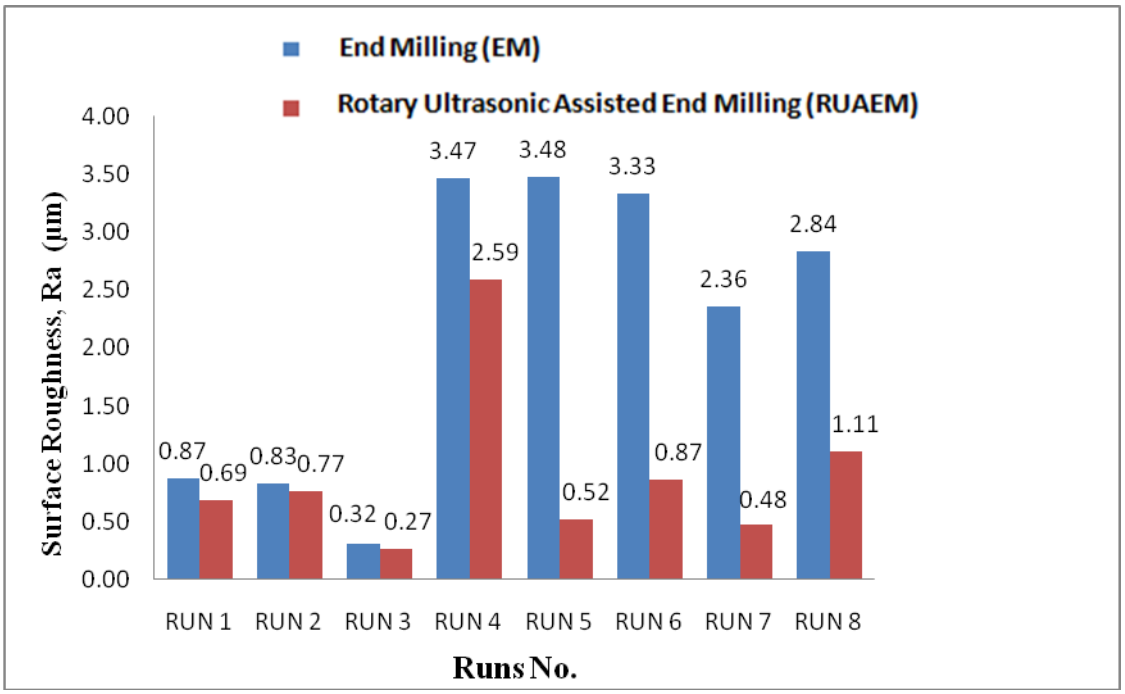
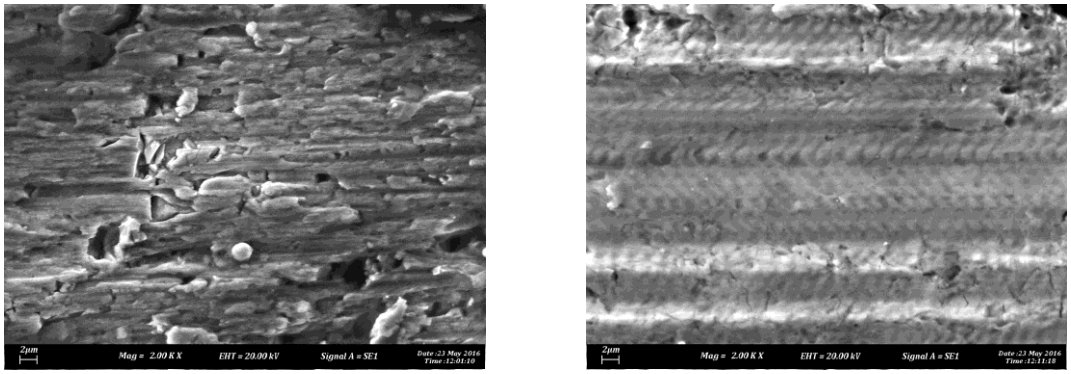


Figure 1.7: Surface roughness value between RUAEM and EM process

As an early hypothesis, the ultrasonic vibration presence in the rotating cutting tool can improve the surface roughness value up to 85%. The incorporation of the ultrasonic vibration creates an imposed static pressure on the workpiece surface grains, in which the workpiece surface is hammered into, and finally a peening surface is produced that improves the surface finish by reducing the peak height produced from the milling cutter as observed microscopically in Figure 1.8. In addition, ANOVA analysis yields that the cutting parameters in essence to cutting speed, feed rate and depth of cut have a significant effect on the surface roughness value.



(a) End milling (b) RUAEM

Figure 1.8: Macroscopic surface topographies for cutting speed, Vc = 3 m/min, feed = 100 mm/min, depth of cut, A_p = 12 μm

1.4 Summary

Based on the unproductive manufacturing activities that are associated with the fabrication of mould and die components and problems in machining hardened tool steel materials as well as with the feasibility of RUAEM in improving the surface roughness value, RUAEM is deemed suitable to be studied. Further investigation relates to the effects of machining parameters, such as, cutting speed, feed rate, depth of cut and ultrasonic parameters such as ultrasonic frequency and amplitude towards surface roughness value is essential to be conducted. In addition, to be more sound industry relevant, other machining performances such as cutting force and material removal rate need to be included in the analysis and optimised as a whole which will be the matters that will be discovered in this thesis.

1.5 Research objectives

Based on the problems faced in conventional machining of hardened materials and the tight tolerances requirements for mould and die components, this thesis proposed a

rotary ultrasonic assisted end milling (RUAEM) process. The specific objectives of this thesis are:

1. To investigate the effects of RUAEM parameters namely speed, feed rate, depth of cut, frequency, vibration amplitude, slurry concentration on the machining performances (surface roughness, cutting force, material removal rate) for hardened AISI D2 tool steel materials.
2. To develop a regression mathematical model on the relationship between each machining performance associated with RUAEM parameters.
3. To optimize the RUAEM parameters based on the multi objective performances criteria namely low surface roughness, low cutting force and high MRR. The optimization is achieved through response surface methodology (RSM) statistical technique. Multiple response routine with desirability function technique is employed for the optimization process. The outcome from this objective is a set of optimized RUAEM parameters associated with the machining performance.
4. To validate the effectiveness of the recommended RUAEM parameters based on the performance criteria.

1.6 Scope of work

In order to realize the objectives of the thesis, the following scope of works are proposed:

i) This thesis is focusing on a hybrid rotary ultrasonic assisted end milling machining (RUAEM) process to eliminate the manual polishing and grinding process to achieve a mirror surface finish profile. Critical aspects of the experimental research include machining parameters, cutting tool, machine capability, slurry concentration percentage and machining performance.

ii) All experiments are performed on a computer numerical control (CNC) vertical milling (HAAS CNC Milling VF-1) with 3 axis machining.

iii) Ultrasonic tool holder is employed in order to give the ultrasonic vibration to the cutting tools. The material used in this study is hardened steel material, AISI D2 with 60 HRC.

iv) The RUAEM ultrasonic frequency ranges between 20 kHz to 27 kHz.

v) A straight integral shank tool holder type EPH Hybrid TAC mills and a multilayer TiAlN coated carbide tool produced by Tungaloy Corporation are utilized for the machining process.

vi) The experiment is carried out under dry cutting condition with the addition of different volumetric percentage concentration (5 %, 10 %, 15 %, 20%) of alumina oxide and deionised water.

vii) The working principle is based on the following processes:

a) Series of experimental work according to design of experiment of response surface methodology with a set of cutting parameters (spindle speed, feed rate, depth of cut, frequency vibration and amplitude vibration).

b) Surface roughness, machining force and material removal rate are measured as machining performance evaluation and database generation.

c) Optimization of the cutting parameter based on the performances criteria is performed using the statistical tools.

1.7 Scope and limitation

i) The experiment used a straight shank of EPH Hybrid TAC mills type EPH11R010M06.0-2.

ii) The experiment used the XHGR110208ER-MJ AH730 coated carbide inserts with multilayer coating TiAlN.

iii) The experiment used ultrasonic tool holder assisted machining with type BT40.

iv) The capacity of RUAEM ultrasonic frequency and rotary ultrasonic tool holder ranges between 20 kHz to 27 kHz.

1.8 Significance of studies

This thesis focuses on employing an ultrasonic vibration to the end milling process aiming to increase the machining performances for hardened mould and die materials. This thesis is to contribute to a new scientific body of knowledge and a benchmark data of optimized RUAEM parameters that are effective on machining hardened mould and die materials. The new data on the effects of RUAEM parameters on the performances have the potential benefit in improving the productivity and component quality.

1.9 Thesis organization

The chapters of the thesis are organized as follows:

In Chapter 2, the relevant literature that relate to this current thesis is reviewed. In addition, this chapter provides more highlights in grinder less machining strategies with machining parameters (cutting speed, feed rate, depth of cut, frequency) using rotary ultrasonic assisted end milling machining (RUAEM) to improve a machined surfaced of mould and die materials. The machining performances such as surface roughness, cutting force, material removal rate (MRR) and surface topography are investigated as well. The purpose of reviewing these topics is to provide a theoretical base for the remainder of this thesis.

This chapter also reviews and provides general information on previous works related to the study. It discusses mould and die manufacturing, mould and die manufacturing process, mould and die material, related work in machining AISI D2 hardened steel, rotary ultrasonic assisted end milling machining (RUAEM) with working principles, cutting parameters for RUAEM such as cutting speed, feed rate, depth of cut, frequency, amplitude vibration and machining performances (surface roughness, cutting force, material removal rate). This chapter also covers the statistical analysis using design of an experiment (DOE).

Chapter 3 describes the experimental method including the experimental setup, procedures, machining used, machining strategies and equipment that are involved in measuring machining performances.

Chapter 4 demonstrates the experimental result and discussion. This chapter also comprises the comparison between ultrasonic assisted machining and conventional machining when machining hardened steel materials. Next, this chapter shows a comparison of rotary ultrasonic assisted end milling machining (RUAEM) with different percentage of slurry concentration. Furthermore, this chapter includes the effectiveness of machining using rotary ultrasonic assisted machining. The thesis concludes with a summary of contributions and suggestions for future work in Chapter 5.

CHAPTER 2

LITERATURE REVIEW

2.1 Introduction

This chapter reviews and provides general information on previous works related to the present thesis. It discusses mould and die manufacturing, mould and die manufacturing process, mould and die material, related work in machining AISI D2 hardened steel, rotary ultrasonic assisted machining (RUAM) with working principles, cutting parameters for RUAM such as cutting speed, feed rate, depth of cut, frequency, amplitude vibration and machining performances that relate to surface roughness, cutting force, material removal rate. This chapter also discusses the statistical analysis using design of an experiment (DOE).

2.2 Mould and die manufacturing

In the 21st century, mould and die industries are one of the important sectors in consumer products manufacturing. All production of consumer products, aerospace and automotive component by mass production are performed using mould and die production process. The manufacturing sector of aerospace and automotive require and demand a mirror surface quality profile and sophisticated free-form shape with high tolerance and high accuracy of mould and die surface.

Mould and die sector in Malaysia has grown rapidly over the three decades with the economic growth in demand for moulds and dies for manufactured parts and automotive components (MIDA, 2016). Malaysian Investment Development Authority (MIDA) approved 54 total of mould and die projects of RM 656.6 million in investments between

2013 and 2015. In addition, Malaysian Investment Development Authority (MIDA) has approved RM 37.9 million in investments for six (6) mould and die projects for the first six months of this year. Therefore, it is crucial that advanced manufacturing technologies meet demands for precision mould and die in the automotive industry with precision machined surface with lower surface roughness value and lower tolerances.

Therefore, the production process of mould and die is an important aspect of the entire production chain and represents a small investment from the overall value of its entire production cost (Altan et al., 2001). The quality of mould and die directly influencing the quality of the produced part components and mirror the needs for surface quality of machined surface to fulfill the product requirement. Based on the recent survey by Taegutec Global Supply Network Company, 41% of mould type tooling are produced by injection moulds. Figure 2.1 shows the ratio of the mould type tooling produced.

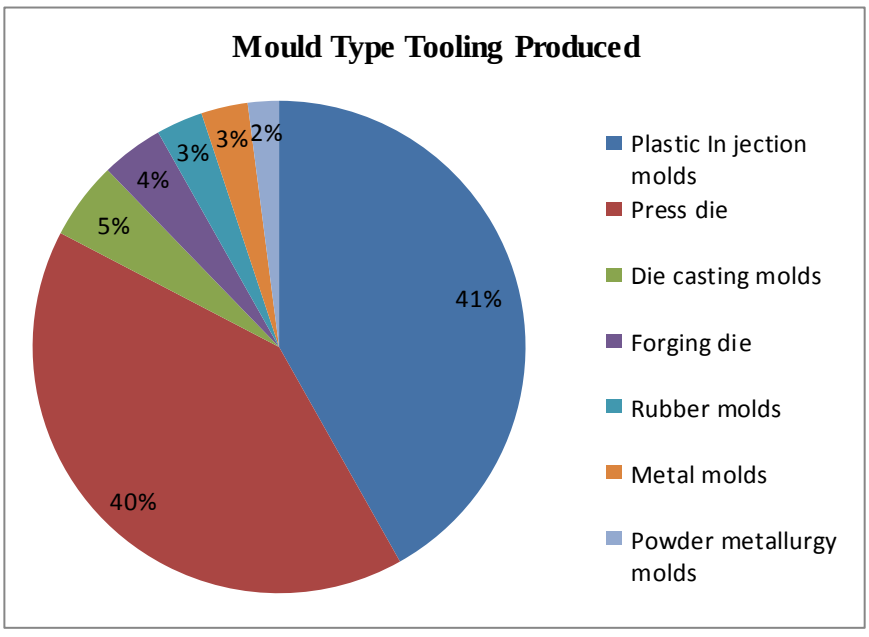


Figure 2.1: The ratio of the mould type tooling produced

The process of mould and die production comprises two successive stage namely mould machining and surface polishing (Grandguillaume et al., 2015). The finishing and critical process such as abrasion, grinding and polishing are utilized to polish the machined surface of mould and die material in producing mirror surface finish for mould and die making. The finishing process is an important process in making mould and die components because it involves a cleaning process by removing burrs left by machining, or providing protective and decorative surface of work piece.

In industries of automotive, aerospace and electronics which involve other post processes such as die casting, forging, plastic injection moulding, extrusion and so on, the hardened steel is commonly used in manufacturing mould and die.

2.3 Mould and die manufacturing process

Various, current machining techniques can be used in mould and die manufacturing process. It consists of a solid block by milling machining, casting process and powder metallurgy.

2.3.1 Solid block by milling machining

The machining mould and die material is from the solid block and machining process is done using CNC milling machine with ball nose end mills cutting tools (Güvenç and Srinivasan, 1997). In general, the production of mould and dies in industrial sector involves conventional machining (end milling) in the annealed (soft) state, followed by heat treatment, electrode manufacture, electro discharge machining (EDM) and finish grinding or hand grinding (Axinte and Dewes, 2002). The milling of mould and die components generate large benefits in reducing the manufacturing cost and production time compared to traditional method consisting of machining in the annealed condition, heat

treatment, electrical discharge machining, grinding and manual polishing (Gaitonde et al., 2016). Through the milling process, the metal is removed by a rotating multiple-tooth cutter with each tooth removes small amount of metal in each revolution of the spindle (Daud et al., 2009).

Besides, the machining of mould and die materials involves the conventional machining and non-conventional machining. In the conventional milling process, the work piece is set up manually by the machinist on the machine and conventional machining process features a direct contact of the tool and work piece or material. The cutting tool is physically in contact with the material being cut or processed. Conventional machining processes consist of three categories; single point cutting, multi-point cutting and abrasive machining. Single point cutting involves using a cutting tool with a single sharp edge to remove material from the work piece. Multi-point cutting process uses a cutting tool with many sharp teeth that moves against the work piece to remove material in milling process. In the milling process, the work piece is fed into the rotating tool along different paths and depths to create a variety of features.

Therefore, the main problem in conventional machining is to maintain dimensional tolerances and surface finish quality of the work piece. The problem is overcome through the non-conventional machining where computer numerical control (CNC) machines can be used to get more accurate and precise machining because there is no physical contact between the work piece and tool. For example, CNC machining and ultrasonic machining.

Then, computer numerical control (CNC) can be used in mould and die manufacturing process because it is the automation of machine tool that is operated by a computer assisted process to control general purpose machines from instruction generated by a processor. The programs consist of specific number and letters to move the spindle to various locations and depths stored in a memory system or storage media. CNC can be

adapted to any kind of machine or process like CNC milling centers, turning centers, boring machine, grinding machines and applied to metalworking machinery including mills, drills, boring machines and punch presses in mould and die manufacturing process. The objective of the application of CNC to metalworking operation is to reduce the machining cost, fixturing costs, tooling storage, required skills and to increase cutter life, automatically producing precision machined components.

Fixed 3 axis milling machine is the most popular method to gain high accuracy and smooth finish for the mould and die fabrication because of its sharp tools, rigid machines and fixtures and ample power. When the machining operation produces the final machined surface with an average surface roughness value (Ra) of less or equal to 0.5 μm, it is equal to that of manual polishing (Baptista and Antune Simões, 2000).

Moreover, the surface finish of machined surface is improved by a polishing process using EDM (Electrical discharge machine). Electrical discharge machining (EDM) is one of the techniques used for polishing the machined surfaces of mould and die. According to Thomas et al. (2016), electrical discharge machining (EDM) is a widely used method for processing the surface of mould and die material. The machining of mould and die surface takes a long time because of low material removal rate (Thomas et al., 2016). Machining of mould and die surface undergoes electrical discharge machining (EDM) process which involves many variables and challenges in maintaining an optimal of input machining parameters. Besides, the machining cost to produce mould and die surface is high. An alternative to improve the EDM process efficiency is by adding metal powder or alloy powder to the dielectric fluid. According to Thomas et al. (2016), when aluminium powder (300 μm-400μm) is mixed with the dielectric fluid for EDM machining of mould and die material, the material removal rate (MRR) increases, tool wear rate and surface

roughness value (Ra) of machined surface (TWR) decrease leading toward the improvement of the productivity and quality of the machining process.

2.3.2 Casting process

Casting process is one of the technique which can be used for mass mould and die components manufacturing process. Mould design is essential in the mould and die process because the shape and properties of the mould directly affect the finished product. Die casting process includes the melting of metal in the furnace and then later forcing it to enter into moulds with exact specifications using high pressure to produce a good finishing product. Die casting used in producing mould and die has an excellent dimensional accuracy and a smoothness of cast surfaces with the surface roughness value (Ra) of 1–2.5 micrometres. It requires secondary machining operations when the surface roughness (Ra) value of mould and die surface > 0.3 μm. Besides, one of the advantages using die casting in producing mould and die is rapid production rates and high tensile strength of casting as greater than 415 megapascals (60 kpsi).

Besides, the casting equipment and the dies components for die casting in mould and die manufacturing process are very costly. Therefore, die casting in mould and die manufacturing process is limited only to high-fluidity metals. During die casting process, the heat can cause the gas in the pores to expand and the mould and die surface to exfoliate with micro-cracks inside the part.

Abrasive machining such as milling process refers to the use of tools that are made of tiny, hard particles to remove material from a work piece. Abrasive machining such as milling process is used because each particle cuts into the work piece and removes a small chip of material. The purpose of abrasive machining of the milling process is to improve the surface finish of a part and shape a work piece and form features. It shows that the

milling process is the last process used to improve the quality surface finish of machined surface.

2.3.3 Powder metallurgy

Powder metallurgy is where metal powders are used as an agent to compress in mould and die for the manufacturing of metal parts. Powder metallurgy is suitable for processes such as mould and die, casting, forging and machining for making complex part of high strength and hard alloy with high quality surface. The parts are made using powder metallurgy which have a good dimensional accuracy and high quality surface profile.

Powder metallurgy for mould and die production offers a good dimensional accuracy control and reduced machining and finishing process with reduced scrap, waste and energy. Besides, the use of powder metallurgy in the manufacturing of mould and die, can increase the production rate of the complex parts with the use of automated equipment and few workers.

The use of powder metallurgy for mould and die production incurs a high cost because of size of parts, complexity shape of parts and press capacity. In addition, tooling and equipment are also costly for small production runs.

2.3.4 Remarks

Based on the three (3) methods in the mould and die manufacturing process, it is found that the milling process from the solid block is the best method to reduce time for mould and die polishing surface finish of work piece machined surface. However, the mould and die machined surface must still be polished to obtain desirable excellent surface finishes on mould and die components through achieving a ‘mirror’ aspect. A suitable

technique is required to eliminate the manual polishing and grinding process to achieve a mirror surface finish profile of mould and die material.

2.4 Mould and die material

Alloy steels with hardness greater than 30 HRC are commonly used in making mould and dies for production of automotive, electronics components and plastic moulding parts (Fallböhmer et al., 2000). Alloy steels used in making mould and die is hardened steel with Rockwell hardness between 30-51 HRC. An important criterion of making mould and die is the quality of the die or mould in terms of dimensional, geometrical and surface accuracy. If the surface quality of mould and die after machining is poor and does not meet the requirements, manual polishing and finishing work need to be performed. While manual polishing and finishing work of surface mould and die components give a satisfying surface accuracy, it often has a negative impact on the dimensional and geometrical accuracy. The main targets for the surface quality of mould and die is to reduce or eliminate manual polishing by improving the mirror surface quality, decreasing the production costs and lead times.

The requirement for the production of mould and die is a mirror surface finish profile with surface roughness (Ra) value of below 0.3 μm. The best surface finish of machined surface is generated with surface roughness value (Ra) of less than 0.5 μm which is equal to manual polishing (Kasim et al., 2013).

2.4.1 Hardened AISI D2 tool steel (AISI D2)

AISI D2 tool steel or JIS SKD 11 tool steel (Japanese equivalent of AISI D2) is a special category of steel for its high carbon, and high chromium alloyed with molybdenum and vanadium. AISI D2 is included in group D because of its intensive use in

manufacturing mould and die and has good properties of wear resistance and deep hardening (Koshy et al., 2002). AISI D2 tool steel is used in mould and die industry because of its high wear resistance, high compressive strength, good through hardening properties, high stability in hardening and good response to heat treatment. Many foreign standards exist for grading a tool steel specification. Mould and die are often made of hardened steel and difficult to machine under conventional cutting conditions (Kita et al., 2001), for example, Great Britain (BS4659), USA (AISI/SAE), Germany (W-Nr Din), Italy (UNI), Japan (JIS), France (AFNOR) and Spain (UNE). The D2 tool steel can be classified through its applications such as cold work steel, shock resisting steels, die casting die steel and die steel. D2 tool steel is used in mould and die industry, cutting tool manufacturing, aerospace and power generation industries (Abd Halim et al., 2014). Table 2.1 shows the properties of D2 tool steel. Besides, AISI D2 tool steel is a material which is difficult to be cut and machined because of its high abrasion resistance and high strength of material (Koshy et al., 2002).

Hardened steel, D2, is a special alloyed steel because it has the characteristics of high strength, impact toughness and very high wear resistance and cracking. The basic general alloy elements in hardened steel are tungsten, molybdenum, chromium and vanadium (Kalpakjian et al., 2014). Hardened steel is the most important metals in machining operations of mould and die industry. The basic types of tool and die steels are indicated in Table 2.2. Tool and die materials for cold working are 55-65 HRC hardness and hot working are hardened 30-55 HRC.

Table 2.1: D2 tool steel properties (% weight)

Chemical composition	**C**	**Si**	**Mn**	**Cr**	**Mo**	**V**
	1.55	0.3	0.4	11.8	0.8	0.5
Standard specification	AISI D2, JIS SKD 11					

Table 2.2: Types of tools and die steels (Kalpakjian et al., 2014)

Basic types of tool and dies steels		
Type	**AISI**	
High speed	M	(molybdenum base)
	T	(tungsten base)
Hot work	H1 to H19	(chromium base)
	H20 to H39	(tungsten base)
	H40 to H59	(molybdenum base)
Cold work	D	(high carbon, high chromium)
	A	(medium alloy, air hardening)
	O	(oil hardening)
Shock resisting	S	
Mold steels	P1 to P19	(low carbon)
	P20 to P39	(others)
Special purpose	L	(low carbon)
	F	(carbon-tungsten)
Water hardening	W	

Hardened steel, D2 is very important and popular for mould and die industries and generally machined using ball end milling, grinding or electrical discharge machine (Budak et al., 2004). Sculptured surfaces of hardened die steel are generally machined by the ball end milling and when the mirror surfaces is required, the rough surfaces will be polished (Shamoto et al., 2005). One problem arising from the machining of hardened steel process is the increase of thrust force (Wojciechowski and Konrad, 2012).

High speed steel is used in manufacturing mould for plastic injection moulding, stamping dies, extrusion dies, blow moulds, forming tools, structural components (Abou-El-Hossein et al., 2007), but it lacks popularity compared with AISI D2 tool steel for mould and die industries. Also, hardened steel (AISI D2) is stability during heat treatment, high hardness with abrasion resistance and suitable used in forming dies, stamping die and die manufacturing. It was observed by Amin et al. (2008), the ability of AISI D2 for the machining process in making moulds and die is very poor with high of surface roughness value and cutting temperature is significantly higher when machining hardened steel (AISI D2) with contribute the poor tool life of cutting tool. According by Bourithis et al. (2006), hardened steel developed to resist wear resistance at temperature of forming and cutting process. Hardened steel are used for many applications because low cost material, easily available with great resistance to tempering, has better hardness and machinability. The advantages choosing hardened steel (AISI D2) because of successful wear resistance, deep characteristic, high abrasion resistance and high strength properties (Halim et al., 2014). Marcel et al. (2014) uses a work piece material plate with the dimensions of 100 x 70 x 10 mm for machining Al alloy (AlMg4.5Mn) using rotary ultrasonic machining compared by Suzuki (2012). Suzuki (2012) used hardened steel work piece sizes (64 x 48 mm) for applying elliptical vibration cutting with a diamond tool, with nose radius of 1 mm.

2.4.2 Remarks

In terms of material, hardened tool steel AISI D2 is selected for mould and die manufacturing. According to Gundogar and Findik (1997), 28 steels are used in mould and die as listed in Table 2.3, but nine (9) steels are widely applied which consist of W1, O1, A2, D2, D4, M2, S1 and S5. Therefore, hardened AISI D2 tool steel is used because its characteristics are best-suited from the non-deforming properties, safety in hardening, impact toughness, high wear resistance to softening effect of heat, high compressive strength, good through hardening properties. It is very good also in wear resistance, high stability of hardening, response to heat treatment and accessibility with lower cost. Table 2.3 below shows the details of comparison between basic characteristics tool and die steel. The hardened tool steel (AISI D2) is stability during heat treatment, best safety in hardening, very good in wear resistance, high hardness with abrasion resistance and suitable used in forming dies, stamping die and die manufacturing. Besides that, AISI D2 is a cool work die steel and commonly used in the mould and die industry with classified as difficult to cut because their extreme toughness and resistance to flow (Becze et al., 2001). Hardened tool steel, AISI group of D2 with range 58-62 HRC are widely used in industry of blanking and cold forming dies and in-service hardened such as steel (Coldwell et al., 2003).

Table 2.3: Comparison of basic characteristics tool and die steel (Gundogar and Findik, 1997)

AISI	Non deforming	Safety in	Toughness	Resistance	Wear	Machinability
W1	Low	Fair	Good	Low	Fair	Best
W2	Low	Fair	Good	Low	Fair	Best
O1	Good	Good	Good	Low	Fair	Good
O2	Good	Good	Good	Low	Fair	Good
O6	Good	Good	Good	Low	Fair	Best
A2	Best	Best	Fair	Fair	Good	Fair
A4	Best	Best	Fair	Fair	Good	Fair
A6	Best	Best	Fair	Fair	Good	Fair
A7	Best	Best	Low	Fair	Best	V. Low
A8	Good	Best	Best	Good	Good	Fair
A10	Best	Best	Fair	Fair	Good	Good
D2	Best	Best	Low	Fair	V.Good	Low
D3	Good	Best	Low	Fair	V.Good	Low
D4	Best	Best	Low	Fair	V.Good	Low
D6	Best	Best	Low	Fair	V.Good	Low
D7	Best	Best	Low	Fair	Best	V. Low
S1	Fair	Good	Best	Fair	Fair	Fair
S2	Fair	Good	Best	Fair	Low	Fair
S4	Fair	Good	Best	Fair	Low	Fair
S5	Fair	Good	Best	Fair	Low	Fair
S7	Fair	Good	Best	Fair	Good	Fair
T1	Good	Good	Good	Best	V. Good	Fair
T15	Good	Good	Low	Best	Best	V. Low
M1	Good	Good	Good	Best	V. Good	Fair
M2	Good	Good	Good	Best	V. Good	Fair
M4	Good	Good	Good	Best	V. Good	Fair
L3	Fair	Good	Good	Low	Fair	Good
F2	Fair	Fair	Low	Low	Good	Fair

2.5 Review of related work in machining AISI D2 tool steel material

Studies and research work have been conducted in the machining of AISI D2 tool steel material for making mould and die components. Related work in machining AISI D2 tool steel material involves studying on machining parameters, cutting tools and machining performances.

2.5.1 Machining parameter

In machining AISI D2 tool steel material, critical aspects of machining parameters should be considered because it will directly affect the surface roughness (Ra) value of machined surface. Before starting a machining operation, various cutting conditions must be set such as cutting depth, milling width, tooth feed, cutting speed and rotation speed. Cutting condition is obtained through references by the manufacturers of cutting tool (Sandvik, Pramet, Seco) and technologists from the regulations of cutting conditions, or the operator using trial and error method (Pimenov, 2014).

Amin et al. (2008) analyzed the surface roughness of machined parts when end milling machining of hardened steel AISI D2 (60-62 HRC), under room temperature using machining parameters of cutting speed (50, 75, 100, 125, 150 m/min), feed rate (0.05, 0.1 mm/tooth) and depth of cut (1 mm) and produced the surface roughness (Ra) value of machined surface below 0.4 μm. As shown in Table 2.4 below, the influence of machining parameters on machining performance such as surface roughness (Ra) value, cutting force and material removal rate on machine surface has been studied. In addition, the effects of cutting parameters and tools material on different machinability aspects such as surface roughness, cutting force, material removal rate, tool wear during machining hardened AISI D2 tool steel are also investigated (Chinchanikar and Choudhury, 2015). According to literature, the parameters included cutting speed, feed rate and depth of cut as shown in Table 2.4.

Table 2.4: Literature on the study of the influence machining parameter when machining AISI D2 tool steel on machining performance

Author	Machining	Machining parameters	Machining performance evaluated	Comment
Amin et al. (2008)	Milling	Cutting speed, feed, depth of cut	Surface roughness, material removal rate, tool flank wear	Average surface roughness to increase with cutting speed
Thepsonthi et al. (2009)	High speed milling	Cutting speed, feed rate, lubricant mode	Surface roughness, cutting force, tool wear, tool life	Best surface roughness with pulsed jet mode at lower cutting velocity and lower feed rate
Heo et al. (2011)	HSM-Milling	Cutting speed, feed rate, axial depth of cut, radial depth of cut	Surface roughness	Surface roughness increased when critical load reduced
Wojciechowski and Konrad (2012)	Milling	Cutting speed, feed, inclination angle	Cutting force, tool wear	Lower cutting speed significantly higher tool life, lower cutting force and lower tool wear
Wojciechowski and Twardowski (2012)	Milling	Cutting speed, feed, inclination angle	Cutting force, tool wear	Lower cutting speed significantly

				lower cutting force and lower tool wear
Wang et al. (2014)	High speed milling	Cutting speed, feed, depth of cut	Chip formation and chip morphology	The increasing cutting speed, chip morphology was transform from continuous to deformation band
Pu and Singh (2013a)	High speed machining	Cutting speed, feed rate, axial depth of cut, width depth of cut	Surface integrity and tool wear	Higher cutting speed produced lower surface roughness value
Kiswanto et al. (2015)	Milling	Cutting speed, feed rate, machining time	Surface roughness, burr formation	Lower feed rate generated better surface roughness

The milling process is widely used in machining AISI D2 steel material with machining parameters like cutting speed, feed rate, depth of cut and investigation on machining performances of surface roughness, cutting force and material removal rate.

2.5.2 Cutting tools

The cutting tool is a critical part in mould and dies industry. In the context of machining, a cutting tool (or cutter) is any tool that is used to remove material from the work piece. There are many types of cutting tools widely used in machining AISI D2 tool steel material. To manufacture a mould and die, many different cutting tools are involved,

from deep hole drills to smallest flat end mills (Cakir et al., 2005). Cutting tool may be accomplished by single-point or multipoint tools. Single-point tools are used in turning, shaping, planing and similar operations, and removing material by means of one cutting edge whereas multipoint tools are used in milling and drilling process.

High speed tool steels (HSS) are often used only when the hardness of work piece does not exceed 280 Hv (28 RC). Many aerospace and alloyed products are fully heat-treated condition and normally the hardness is more than 280 Hv (28 RC). Therefore, carbide tipped tools are employed because they permit higher cutting speeds, feeds and are often more economical (Naresh et al., 2013).

Additionally, tool life of cutting tool is a very important factor in mould and die manufacturing. Tool life of cutting tool can affect cutting distribution of rough and finish cutting (Kita et al., 2001). The damage of the cutting edge can also affect the machining accuracy of mould and die components. Cutting tool performance is often measured through surface finish of the work piece and flank wear of the cutting tool (Camuşcu and Aslan, 2005).

2.5.2.1 Tungsten carbide flat end mills

Tungsten carbide flat end mills cutting tools are commonly used in machining AISI D2 tool steel. Tungsten carbide end milling cutter is used for the machining process using a CNC milling machine. An end mill cutting tool is generally employed for this process due to the high efficiency of material removal and longer tool life. However, in the case of hardened steels, a corner radius end mill or ball nose end mill is generally used. The advantage of tungsten carbide end milling cutter is its lasting life, high toughness and wearing features. Another advantage of using a tungsten carbide and mills is their high speed cutting of dry type process machining using a CNC machine. Tungsten carbide end

milling cutters are commonly used because they are good for high milling production (Dawes and Aspinwall, 1997).

2.5.2.2 Solid carbide ball nose

The solid carbide ball nose of cutting tools are often used in machining AISI D2 tool steel with different diameters, flutes, degrees of helix angle, diameters, length and micro grains respectively. The solid carbide ball nose cutting tools are used in machining AISI D2 tool steel. They provide better wear resistance and produce a low surface roughness (Ra) value of machined surface. An experiment (Koshy et al., 2002) used solid carbide ball nose with coated carbide as a cutting tool on face milling experiments of AISI D2 tool steel. In production mould and die by conventional machining (end milling), the ball nose cutting tools are used for machine components and gave the lowest work piece surface roughness with less compressive residual stress distribution below the machined surface without directly in their hardened state condition (Axinte and Dewes, 2002). Also, solid carbide ball nose is special cutting tool for mould manufacture and used in machining hardened AISI D2 cold work tool steel (58 HRC) to identify the tool wear mechanisms based on the analysis of flank wear patterns with suitable cutting parameters (Tomas et al., 2014). Solid carbide provide better strength compared than high speed steel because it is extremely heat resistant which used in high speed machining application on hardened tool steel material. Besides, solid carbide suitable for heavy feed rate and can be operated 2 to 3 times faster compared others cutting tools. Solid carbide ball nose consisting of different flutes such single flute, two flute, third flute and fourth flute. The solid carbide ball with 2 flute is suitable and excellent for slot milling machining because easily to allow for more chip carrying capacity moving out from the cutting zone. The standard coatings for solid carbide ball nose is titanium nitride (TiN), titanium carbonitride (TiCN), titanium

aluminum nitride (TiAlN), aluminum titanium nitride (AlTiN), zirconium nitride (ZrN) and uncoated tools. Hence, solid carbide ball nose with coating of titanium aluminum nitride (TiAlN) always used in machining hardened tool steel (AISI D2) because has higher strength hardness and higher oxidation temperature compared titanium nitride (TiN) and titanium carbonitride (TiCN).

2.5.2.3 Polycrystalline diamond (PCD) tool

Polycrystalline diamond cutting tool is a diamond tool with diamond grains fixed onto the tool through special bonding materials. Polycrystalline is a super hard tool material which is sintered under high temperature and high pressure by diamond microcrystal (Liu et al., 2002). PCD cutting tools have excellent mechanical properties and good thermal properties (Zhou et al., 2003). The special capabilities of polycrystalline diamond cutting tool (PCD) is in machining of hard metal and has a strong wear resistance. PCD tools are one of the special tools materials for high precision machining cutting, grinding materials and cost effective tools materials (Paulo Davim and Monteiro Baptista, 2000; Zhang et al., 2011). Zhou et al. (2003) studied the effect of polycrystalline diamond cutting tool when ultrasonic vibration assisted cutting on the machining of AISI D2 tool steel material. Figure 2.2 shows the ratio of the Polycrystalline diamond cutting tool.



Figure 2.2: The polycrystalline diamond cutting tool (https://www.amanatool.com)

2.5.2.4 Coating carbide insert with multilayer coating TiAlN

Coated carbide inserts with multilayer coating TiAlN with the straight shank produced by Tungaloy company is selected as the cutting tools on slot milling machining of AISI D2 tool steel material work piece using conventional machining and rotary ultrasonic assisted end milling machining (RUAEM). The specific description of straight shank type EPH Hybrid TAC Mills used is EPH11R010M06.0-2. EPH type of shank from Hybrid TAC mills Tungaloy company is a high precision milling process which generates low cutting force, high productivity levels and high accuracy machining compared to solid carbide end mills. The insert from EPH Hybrid TAC mills of XHGR110208ER-MJ AH730 is a precision insert for multipurpose ground machining. This type of cutting tool can be used for hole enlarging, plunging, pocket milling, ramping, shoulder milling, shoulder milling with radius, side milling and slot milling. Then, the cutting tool of XHGR110208ER-MJ AH730 is used for slot milling machining.

The coating cutting tool with TiAlN has extended tool life during machining of hardened steel material, AISI D2 (Kang et al., 2008). The coating with TiAlN has been applied to improve the mechanical and oxidation properties. It shows that TiAlN coating is better compared by TiAlSiN coatings. The coating with TiAlN can increased the cutting tool life and anti-wear properties (Wojciechowski and Twardowski, 2012). Pu and Singh (2013b) reported that cutting tool coated with TiAlN is the best carbide tools and its tool life be three times higher than TiCN coated carbide. Besides that, end milling of hardened steel material by coated carbide tool was improved surface finish and can delay welding of chips on the tool which prolong the tool life (Gaitonde et al., 2016). The new coating for cutting tool can make improvement in mechanical and chemical properties of tungsten carbide tool which increased lifetime of cutting tool, increased production rate and decreased in consumption of cutting fluid during milling process. The coated cutting tool

will be able to protect the main layer of the cutting tool from the high temperature occurred between machined surface and tool during milling process (Ucun et al., 2013). Also, it observed that coated cutting tool with TiAlN possess high corrosion endurance and resistance to chip adherence. The performance of the TiAlN coating cutting tool was better in term corrosion and produced a better quality of the machined surface compared uncoated cutting tool.

2.5.2.5 Remarks

A suitable cutting tool used in this experiment is coated carbide inserts with multilayer coating TiAlN and straight shank because coated carbide insert can produce excellent work piece machined surface with low surface roughness, low cutting force, low tool wear rate and high material removal rate.

2.5.3 Machinability of milling AISI D2 hardened tool steel

Problems encountered in machining AISI D2 hardened tool steel material include rough machined surface, rapid tool wear, high machining force and machining temperature. Few studies have investigated machining of hardened D2 tool steel, focusing on improvement of machining performance, such as surface roughness, cutting force and tool wear. The effectiveness of machining performances such as surface roughness and cutting force depends on milling machining parameters (Izamshah et al., 2010). Besides, the optimum surface roughness can be obtained through investigating mains factor of milling machining including speed, feed rate and depth of cut (Rawangwong et al., 2014). Research and studies on machining performance (surface roughness, machining force, tool wear and cutting temperature) effects when machining AISI D2 hardened steel are very important to evaluate the quality of machined surface of a work piece.

2.5.3.1 Surface roughness

Hardened AISI D2 tool steel is widely used in the manufacturing industry such as injection moulding process, manufacturing of cold forming tools, engineering parts, mould and die and need a new advanced machining of a process to improve surface finish of machined surfaces. Excellent surface finish of tool steel parts is an important factor for measuring the quality of a product in mould and die industry. The improvement of a surface roughness of final machined surface will reduce the cost of labour and time needed to complete the final machined surface mould and die parts (Tsai et al., 2016). The greatest challenge in the machining of hardened AISI D2 tool steel in mould and die industry is the requirement of a fine surface finish of machined surface. The lower the cutting force during machining of tool steel can generate fine surface finish of machined surface whereas the high machining force during machining causes a rough machined surface that has been machined with high magnitude of surface roughness. Therefore, manufacturing sectors need to produce a high accuracy finished products and good surface quality (Azlan et al., 2016). Kumar et al. (2014) claimed that ultrasonic vibration assisted machining successfully improved a machined surface with lower surface roughness (Ra) value because the uniform alternating cycle between tool and work piece produces lower friction with lower temperature and reduced subsurface cracking. Table 2.5 summarizes the machining performance of surface roughness (Ra) value obtained from the study of other researchers on machining AISI D2 hardened steel in the milling process.

Table 2.5: List of studies on machining performance of surface roughness (Ra) value obtained on machining AISI D2 hardened steel in milling process

Author/Year	**Method**	**Ra (μm)**
Axinte and Dewes (2002)	High speed milling	0.36-2.18 μm
Moriwaki et al. (2004)	Ultrasonic elliptical vibration milling	0.11 μm
Kovac (2012)	Face milling	1.05 μm
Jasni et al. (2012)	High speed milling	0.2-0.45 μm
Pu and Singh (2013b)	High speed milling	0.2 μm
Halim and Kasim (2014)	High speed milling	0.213 μm
Izamshah et al. (2014)	Milling	1.5 μm
Rasidi et al. (2014)	Ultrasonic vibration assisted micro-milling	0.2 μm
Gaitonde et al. (2016)	Milling	0.34 μm
Kundor et al. (2016)	Hard milling	0.10-0.37 μm

2.5.3.2 Machining force

Machining force is a force that is generated by the cutting tool during machining processes and very important a milling operation. The main factors that influencing the milling operation, the part accuracy and the tool life is the machining force. The machining force is associated with machining temperature, dynamic phenomena, roughness increase, tool wear and so on. The research about machining force and its modelling is one of the classic research areas of machining processes. The modelling and calculation of machining force can be estimated according on the machining parameters, material and cutting tool

material (Lamikiz et al., 2004). Also, machining force has been used to clarify the cutting process which directly affected tool wear, cutting temperature, residual stress and surface integrity (Zhang et al., 2013).

The total cutting force is divided into two (2) components in the horizontal and vertical direction. The component in horizontal component is called cutting force (Fc) and vertical direction components are called thrust force (F_D). Figure 2.3 shows a schematic diagram of cutting force component during milling machining.

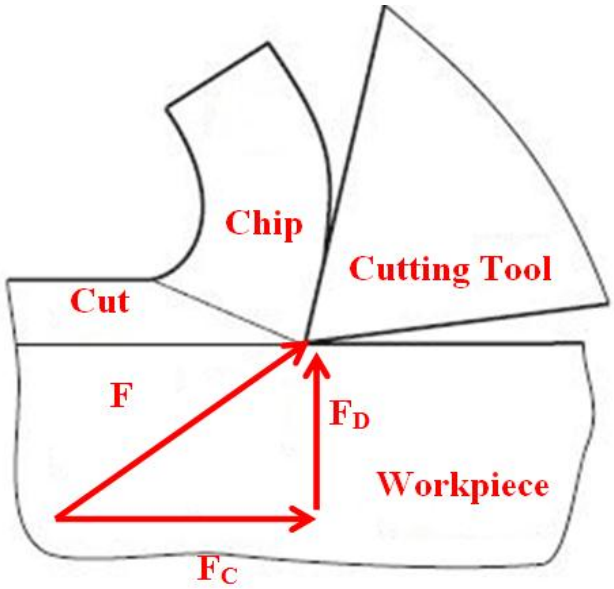


Figure 2.3: Schematic diagram of cutting force component during milling machining

Resultant cutting force (F_R) is utilized as the measurement of the cutting force in this study and its analysis. The machining performances such as cutting force will be measured for evaluation in order to improve a surface quality of work piece machined surface.

Hardened tool steel, AISI D2, generally machined by the ball end milling and rough surface was polished manually when mirror surface is required (Shamoto et al., 2005) where the high cutting force occurs, thus, causing a rapid tool wear. To solve this problem,

the non-conventional machining through rotary ultrasonic assisted end machining is required to replace a conventional machining in order to improve machining performance such as cutting force. Table 2.6 summarizes the machining performance of cutting force value obtained from the study of other researchers on machining AISI D2 hardened steel in milling process. Kumar et al. (2014) reported that the ultrasonic vibration assisted milling of machining hardened steel generated tool velocity exceeds the chip velocity which produces a reversed tool-chip friction force and consequently reduces the cutting force (thrust force). In the end milling process, the cutting tool rotates on an axis vertical to the work piece. The tangential force is in the direction of cutting speed, the radial force is in the radial direction of cutter feed and axial cutting force is in the cutter axial direction (Wu et al., 2013). Gaitonde et al. (2016) reported that the cutting force increases at higher values of feed rate because the work piece machined surface material presents more resistance to cutter in the cutting direction, hence, increasing friction when AISI D2 hardened steel material is milling using coated tungsten carbide inserts in dry cutting condition. An experiment conducted by Jung et al. (2012) revealed that the thrust force increases as the cutting distance increases when applying the elliptical vibration cutting of hardened die steel in the milling process using single crystalline diamond tools.

Table 2.6: List of research on machining performance of cutting force obtained on machining AISI D2 hardened steel in the milling process

Author/ Year	**Method**	**Cutting Force**
Saedon et al. (2012)	Micro end milling	~3.2 N-11.3N (Feed Force,Fx) ~2.7N-18.8N

		(Thrust Force, Fz)
Srinivasa and Shunmugam (2013)	Micro end milling	~3.25N-9.56N (Feed Force,Fx) ~2.21N-8.38N (Transverse Force, Fy)
Gaitonde et al. (2016)	Milling	~57.97 N-536.3 N

2.5.3.3 Tool wear

Tool wear is the gradual failure process of cutting tool during machining process (Kalpakjian et al., 2014). The effects of tool wear during machining is poor machined surface with high surface roughness value, increased cutting force, increased cutting temperature and cause tool damage. Regular tool wear mechanism occurred in the milling process when the cutting tool resists the mechanical and thermal shock of the milling process. In addition, the tool life of cutting tool depends on more frequency caused by chipping, cracks and breakage of the edge of tool during cutting zone between interaction tool and machined surface. Also, the factors that influence of the quality machined surface and economic of machining is the tool wear (Zhou et al., 2006). Figure 2.4 shows the photographic view of the wear pattern in milling process.

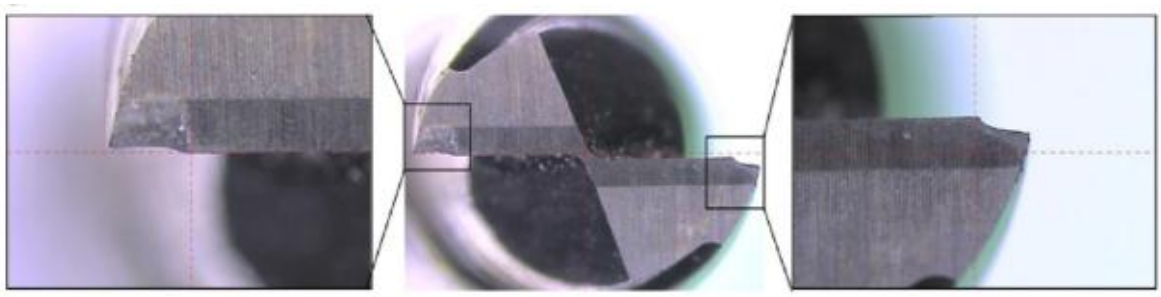


Figure 2.4: Photographic view of the wear pattern in milling (Ding et al., 2010)

In general, the hardness of hardened steel material, AISI D2, for mould and die is 40 ~ 60 HRC. The hardness of hardened steel material is very high which causes the strength of the material to be very high and difficult to be machined. Subsequently it leads to poor machined surface and rapid tool wear because high hardness of this material and high machining force during the machining of hardened steel materials. Kumar et al. (2014) reported that the ultrasonic vibration assisted milling on difficult to machine material can reduce the force during the machining, stresses and periodic separation by helping the cutting tool to release stresses which will reduce a tool wear. In addition, tool wear is an important criteria in evaluating the effectiveness of the milling process and it will affect quality assurance and quality of the work piece of machined surface. Kundor et al. (2016) reported that wear rate is much higher and flank wear of the cutting tool grows faster at the higher feed rate of 0.04 mm/tooth during the milling experiment test using CNC vertical milling machine with end milling coated tungsten carbide as a cutting tool of machining AISI D2 hardened steel.

2.5.3.4 Cutting temperature

Cutting temperature during milling machining process of mould and die material affects tool wear, machined surface quality and chip shape (Sekulic et al., 2010). Gaitonde et al. (2016) reported that minimum cutting temperature can be achieved when applying lower depth of cut (Doc), lower cutting speed and medium value of feed rate during milling AISI D2 hardened steel coated tungsten carbide inserts. Jasni et al. (2012) found that the flank wear propagates with the rise in cutting temperature during milling process and built up edge (BUE) starts to occur at length of cut of 100 mm through high speed milling of AISI D2 hardened steel using TiAlN/AlCrN multilayer coated carbide inserts in dry cutting condition. The tool wear deterioration often starts from the early stage until it

reaches flank wear of 0.3 mm. The presence of built up edge (BUE) during milling process can increase the tool wear rate (Hossein and Yahya, 2005). The increase of temperature between cutting tool and the work piece machined surface will cause the reduction of the hardness of the work piece machined surface. When using ultrasonic assisted machining in machining AISI D2 hardened steel, the ultrasonic oscillation is superimposed onto the conventional spindle rotation, causing the cutting edges of the tool periodically lift from the material and the cutting temperature of the tool significantly decreases because lower speed required for fiber break-up is delivered by energy ultrasonic oscillation (Feucht et al., 2014).

The tool life of cutting tool depends on the cutting temperature, tool wear and may affect the surface quality of machined surface. Higher cutting force and higher temperature during milling process caused by the rubbing between the stuck chips and the work piece surface, which generated the reddish colour that appear on the tool tips and lead notch wear on the cutting tool (Kasim et al., 2013). Then, high cutting temperature during machining occurred when strong adhesion interaction between tool and work piece machined surface which increase tool wear (Khan and Rahman, 2014). When the tool wear increased, it caused the chemical reaction and adhesion between cutting tool and machined surface. Research by Arsecularatne et al. (2006) reported that cutting force (Fx, Fy, Fz) increased with increasing of tool wear during machining hardened steel, AISI D2. The increasing of tool wears during machining because broken chips generated due to the influence of the rake face groove and obstacle created by tool wear. Kumar et al. (2014) reported that vibration assisted machining facilitate consecutive overlapping of tool paths during milling process result in chips that are thinner compared by conventional milling and contribute to reduction in tool forces and heat generated during milling process.

2.5.3.5 Remarks

In machining AISI D2 tool steel hardened material, the lowest surface roughness value of the work piece of machined surface can be obtained through ultrasonic elliptical vibration machining with its value of 0.11 μm, followed by hard milling of 0.10 μm and ultrasonic vibration assisted micro-milling of 0.2 μm respectively. Hence, the ultrasonic vibration machining can be used in machining of machined surface hardened steel material with lower surface roughness value. The ultrasonic vibration assisted milling of machining hardened steel produces a reversed tool-chip friction force and it can reduce the machining force (cutting force) compared to the conventional milling process (Rasidi et al., 2015). Besides, the ultrasonic vibration assisted milling of machining hardened steel can extend the life of cutting tool when a periodic separation occurs by helping the cutting tool to release stresses which reduces a tool wear. In addition, using ultrasonic assisted machining in machining AISI D2 hardened steel can reduce the cutting tool temperature because lower speed is required for fiber break-up during milling machining. Studies on surface roughness, machining force and material removal rate in milling AISI D2 hardened steel are scarce. Many studies focus on turning process in conventional and non-conventional methods. Hence, rotary ultrasonic assisted end milling (RUAEM) is required for machining AISI D2 steel to obtain an excellent quality of machined surface of mould and die components.

2.6 Rotary ultrasonic assisted machining (RUAM)

2.6.1 Ultrasonic machining (USM)

Ultrasonic machining (USM) is categorized as non-conventional mechanical material removal process and also known as ultrasonic abrasive machining, ultrasonic cutting, ultrasonic drilling and slurry drilling (Kumar et al., 2008b). According to Singh et

al. (2014), the ultrasonic machining (USM) uses a high frequency electrical energy and generates high frequency electrical energy which is converted into mechanical vibration through a transducer which is then transmitted to an energy focusing through devices such as horn or tool assembly.

Ultrasonic machining can be classified as vibration machines. Ultrasonic machining (USM) is a machining operation using vibration tool oscillating at ultrasonic frequencies (18-20 kHz) and aided by abrasive slurry that flows freely between the tool and the work piece to remove material from the work piece. According to Routara et al. (2011), ultrasonic machining is non-conventional machining with low material removal rates and operates at ultrasonic frequency ranging between 20-40 kHz. According to Kalpakjian et al. (2014), the concept of ultrasonic machining (USM) refers to material being removed from a surface by micro chipping hammering, aided by fine abrasive grains in a water slurry with vibration of 20 kHz frequency and 0.0125-0.075 mm of amplitude. The principle of ultrasonic machine is utilized during the interaction between tool with the work piece or medium to be treated. The tool is vibrated with a specific direction, frequency and intensity. According to Astashev et al. (2014), the vibration is generated by a transducer and transmitted to the tool using a vibration system, often with a change in direction and amplitude. The vibration tool oscillating with amplitude 10 to 40 μm imposes a static pressure on the abrasive grains, hammered into the work piece surface, causing chipping of fine particles and forming the required tool shape. Lee and Chan (1997) revealed that material removal rate (MRR) and surface roughness (Ra) will increase when the amplitude of vibration increases, static load increases and size of abrasive increases when using K-type magnetic ferrite as work piece through ultrasonic machining. Besides, the material removal rate depends on the amount of energy exerted to the materials.

Zhixin et al. (1997) showed that the efficiency of combined machining is three times more than that of ultrasonic machining and the surface integrity is not significantly different when using the combined machining technology of ultrasonic machining and electrical discharge machining for machining of all conductive hard and brittle material. Figure 2.5 shows a schematic diagram of ultrasonic machining (USM).

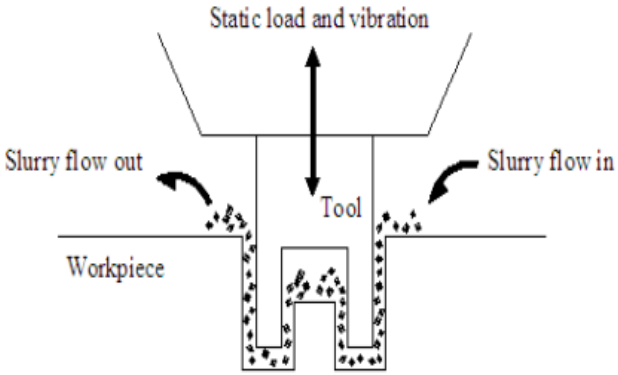


Figure 2.5: Schematic diagram of ultrasonic machining (USM) (Khoo et al., 2008)

The surface roughness value (Ra) of machined surface for any work piece material decreases with the decrease in the grain size of abrasive slurry during ultrasonic machining (Komaraiah et al., 1988). In addition, an ultrasonic machining (USM) with abrasive slurry causes the low removal material rate. To solve this problem, rotary ultrasonic machining (RUM) is used to produce low surface roughness value, low cutting force and increase a material removal rate during the slot milling of hardened mould and die materials.

2.6.2 Rotary ultrasonic machining (RUM)

Kuo and Tsao (2012) reported that rotary ultrasonic machining (RUM) using energy of micro-oscillations to remove material in hammering actions. Rotary ultrasonic

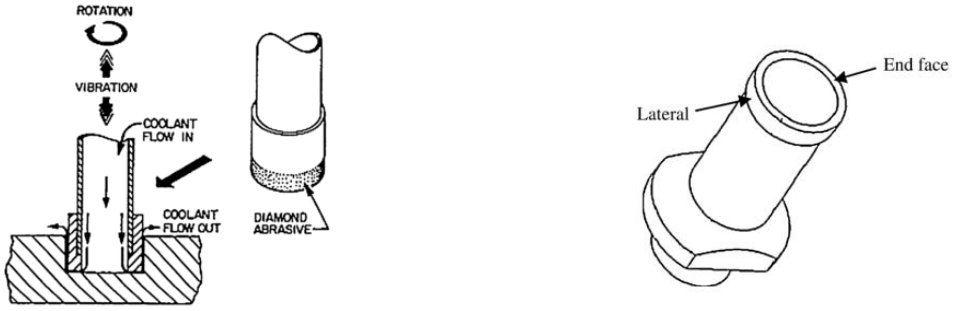
machining (RUM) is categorized as hybrid machining process because of a combination between material removal mechanisms of diamond grinding and ultrasonic machining (Cong et al., 2011). When using a rotary ultrasonic machining (RUM) for milling hard and brittle materials, the repeated hammering action generated by the ultrasonic energy is transferred to the material, causing plastic deformation fractures. Effective and efficient machining can be obtained using rotary ultrasonic vibration machining. The principle of machining process using rotary ultrasonic machining (RUM) is rotating tool vibrates axially at an ultrasonic frequency (Cong et al., 2011) and tools fed towards the work surface at a constant feed (Singh and Singhal, 2015). According to Lauwers et al. (2008), the system of mechanical ultrasonic vibration is generated by a piezo-actuator integrated with the actor system of the tool holder. The surface roughness value (Ra) of machined surface for any work piece material generated by rotary ultrasonic machining (RUM) is lower compared to a conventional ultrasonic machining (USM) (Komaraiah et al., 1988). The advantage of using rotary ultrasonic machining (RUM) is it can provide a much higher material removal rate, deep holes, fine precision machining and perform the contour machining of brittle and hard material (Ya et al., 2002). The rotary ultrasonic machining (RUM) generates better surface roughness value, Ra (lower surface roughness) because the possibility of removal of the ridges of the work piece machined surface subjects to the rotation al movement. Kuruc and Peterka (2014) used rotary ultrasonic machining (RUM) based on abrasive removing mechanism and ultrasonic vibrating diamond particles which are bonded on the active part of a rotating tool for machining poly-crystalline cubic boron nitride (PCBN). The result of this experiment showed that rotary ultrasonic machining (RUM) can machine PBCN with a low surface roughness value with Ra of 0.24 µm, Rz of 2.834 µm. In general, rotary ultrasonic machining (RUM) is deemed suitable for finishing of hard and brittle material's surface.

2.6.2.1 Working principle of RUM

Rotary ultrasonic machining (RUM) is a non-traditional machining process and used for machining brittle and ductile material such as hardened steel, ceramics and composite materials (Cong et al., 2011). It also combines the material removal mechanisms between diamond grinding and ultrasonic machining (Shiou and Ciou, 2008). A tool is mounted on a rotary spindle and attached to a piezo-electric transducer to produce the rotary and ultrasonic motion (Churi, 2010). Therefore, Pei et al. (1995) stated that rotary ultrasonic machining (RUM) is a hybrid machining process that combines the material removal mechanisms of diamond grinding and USM, resulting in higher material removal rate (MRR) than that obtained by either diamond grinding or USM.

Besides, the rotary ultrasonic machining is rotating core drill with metal-bonded diamond abrasives which is ultrasonically vibrated. The slurry has to be fed between work piece and cutting tools are replaced with abrasives bonded to the tool and rotating core drill fed toward the work piece at a constant pressure or a constant feed rate.

Therefore, in the process of rotary ultrasonic machining (RUM), the abrasive slurry is replaced by a tool with metal bonded diamonds abrasives and the tool is vibrated ultrasonically and rotated with constant pressure pressed against to the work piece surface (Kalpakjian et al., 2014). Figure 2.6 shows a schematic diagram of rotary ultrasonic machining. According to Churi (2010), no study has been reported on RUM of titanium alloy, silicon carbide and dental ceramics.



(a) (b)

Figure 2.6: Schematic diagram of rotary ultrasonic machining (RUM) (Zeng et al., 2005)

The cutting tool employed for rotary ultrasonic machining (RUM) is a core drill with metal bonded diamond abrasives with rotating tool vibrates moves along the axial direction toward the work piece and the vibration of rotating tool at ultrasonic frequency above 20 kHz. Figure 2.7 shows a diagram of rotary ultrasonic machining (RUM).

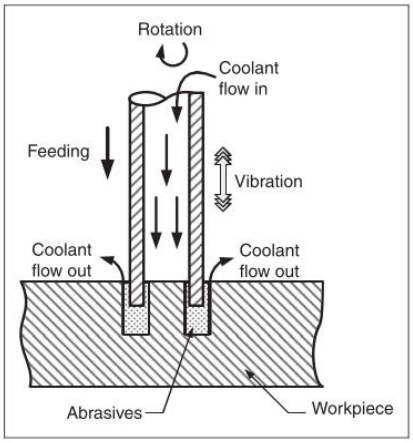


Figure 2.7: Rotary ultrasonic machining (RUM) (Khoo et al., 2008)

2.6.3 Rotary ultrasonic assisted machining (RUAM)

Rotary ultrasonic assisted machining (RUAM) is based on ultrasonic machining (USM). All the concepts and techniques of ultrasonic machining (USM) apply to rotary

ultrasonic assisted machining (RUAM). The new milling machining method using ultrasonic vibration technique is successfully applied to the difficult to cut materials machining (Jung et al., 2012). According to Lauwers et al. (2010), ultrasonic assisted machining is used for grinding process with a tool or work piece is vibrated at 15-15 kHz and amplitudes vibration range is 15-20 μm for machining ZrO2 with grinding tools diameters of 2, 3 and 5 mm are used to make holes and slots. The tool holder system has a significant influence on the obtained amplitude of the vibration and the vibration of the tool and work piece indicate more surface craters (near surface cracks) due to material break out.

RUAM consists of 1 dimensional vibration assisted machining (1D VAM), 2 dimensional vibrations assisted machining (2D VAM) and elliptical vibration machining (3D VAM). The machining method for 1D VAM is the tool tips driven in a small reciprocating and 2D VAM uses elliptical motion whose center moves in the cutting velocity direction (Brehl and Dow, 2008a). Ultrasonic assisted machining is also applied in ceramics components manufacturing industry (Lauwers et al., 2008). The application of ultrasonic vibration assisted cutting in machining of hardened materials is an effective method for improving precision machine parts, reducing cutting force, improving finished surface quality of material and reducing tool wear (Ma et al., 2004; Xing et al., 2013; Feucht et al., 2014). However Chern and Chang (2006) reported that slot surface roughness micro milling of aluminium alloys can be improved using assisted vibration cutting with end mills of diameter 1 mm cutting tools.

Tsai et al. (2016) indicated that the ultrasonic assisted milling produces an excellent surface roughness (Ra) value of 0.136 μm at an ultrasonic amplitude of 2.20 μm compared to conventional milling with the surface roughness (Ra) value of 0.236 μm within the same machining parameters. Hence, the surface roughness (Ra) by ultrasonic assisted milling

generates a better finish compared to conventional machining. Ultrasonic assisted milling generates “hammer effect” during the milling process and because of high frequency vibration, the cutter teeth will hammer the work piece surface constantly.

2.6.3.1 Working principle of RUAM (1D VAM)

Studies on rotary ultrasonic assisted machining of hardened steels are limited. Brehl and Dow (2008) stated that vibration assisted machining (VAM) used a small amplitude, high frequency tool displacement for the cutting motion of the tool tip during machining process. Vibration assisted machining includes 1 dimensional vibration assisted machining (1D VAM), 2 dimensional vibration assisted machining (2D VAM) and elliptical vibration machining (3D VAM). The concept of 1 dimensional vibration assisted machining (1D VAM) is shown in Figure 2.8 in which the cutting tool is driven harmonically in linear path and relative to a work piece moving at upfeed velocity.

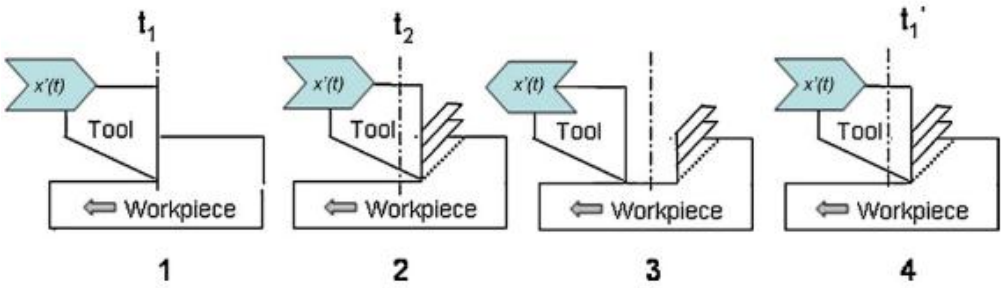


Figure 2.8: 1 dimensional vibration assisted machining (1D VAM) (Brehl and Dow, 2008a)

The t_1 is the time of initial contact with uncut material and the t_2 is designated as the time the tool breaks contact with the work piece material at the end of its cutting motion. In step 1 of Figure 2.5, the tool velocity *x’(t)* relative to the work is greater than zero. Initially, the cutting tool rake face has just come into contact with the uncut material

and started to cut. Then, in step 2, the tool is at the limit of the linear vibration of initial contact with the uncut work piece material designated as t_2 in Figure 2.5. Next, in step 3, *x'(t)* has reversed tool breaks contact with the work piece material at the end of its cutting motion which is designated t_2. Lastly, in step 4, *x'(t)* is again positive and the tool is shown advancing into contact with the work piece as it commences to another cutting cycle.

1 dimensional vibration assisted machining (1D VAM) is a simple setup, easy to install and can be used in the existing CNC (computer numerical control) machine. Then, 1D VAM can be employed at the normal cutting tools with lower machining cost. It is found that the surface roughness value of machined surface generated by 1D VAM is not very smooth and needs a better improvement.

2.6.3.2 Working principle of RUAM (2D VAM)

2D VAM (2 dimensional vibration assisted machining) consists of a combination between vertical harmonic motion to the horizontal motion of 1D VAM which causes the cutting tool to move in circle or ellipsis and superimpose on the upfeed motion of the work piece (Brehl and Dow, 2008b). 2 dimensional vibration assisted machining is material cutting process through a series of overlapping ellipses in which the distance the work piece moves each cycle is small compared to the horizontal vibration amplitude.

The major axis of the ellipse for 2D VAM is the cutting force and the minor axis is the thrust force. When the tool progresses moving in its elliptical path, the uncut chip area for each point increases and the tool motion relative to the work piece causes the chance in rake angle and clearance angle. 2D VAM (2 dimensional vibration assisted machining) uses a diamond tool and is mounted on the end of the beam and generated 2 dimensional elliptical cutting by combining two bending vibrations at the right angle (Brehl and Dow, 2008b).

Two dimensional vibration assisted machining (2D VAM) uses diamond as a cutting tool and is mounted onto the end of the beam. 2D VAM provides longer tool life compared to 1D VAM when using diamond as a cutting tool for the same depth of cut, tool geometry and tool work piece material combination (Brehl and Dow, 2008b). The surface roughness (Ra) value decreases approximately 40 % using 1D VAM and 95 % decreased using 2D VAM. However, the diamond cutting tool used for 2D VAM is difficult to obtain and very expensive which contributes higher machining cost than 1D VAM cutting tools.

2.6.3.3 Working principle of RUAM (3D VAM)

3D VAM (3 dimensional vibration assisted machining) is a machining method using rotary ultrasonic assisted machining by ultrasonic elliptical vibration cutting method. Shamoto et al. (2005) used ultrasonic elliptical vibration cutting method to apply mirror surface machining of hardened die steel and this method is used to eliminate the polishing process. Based on the ultrasonic elliptical vibration cutting, the cutting tool is vibrated elliptically and fed along the sculptured surface according to the required methods. Suzuki (2012) reported that ultrasonic elliptical vibration system can decrease the tool wear effectively and produce mirror surface machining of the steel material when applying ultrasonic elliptical vibration with the 4 axis control into ultra precision cutting of the steel materials using single crystal diamond as tool materials. Figure 2.9 and 2.10 respectively show the ultrasonic elliptical vibration cutting for the three dimensional free surface of steel materials and development of sculpturing using elliptical vibration cutting.

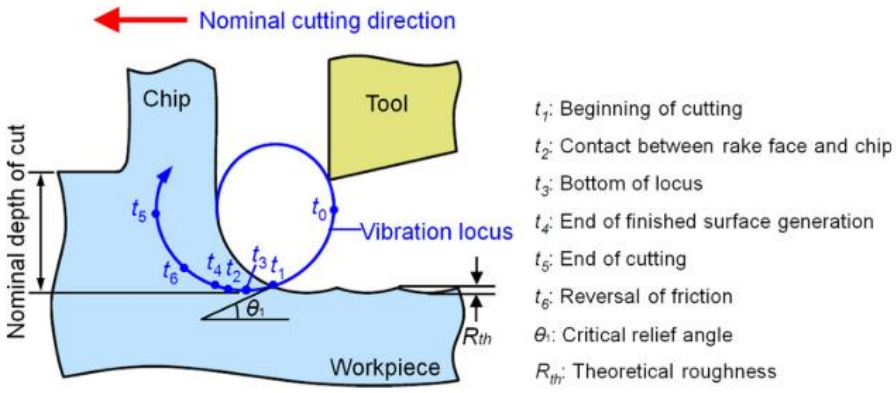


Figure 2.9: Ultrasonic elliptical vibration cutting (Zhang et al., 2016)

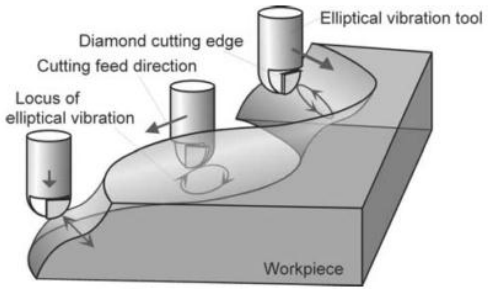


Figure 2.10: Ultrasonic elliptical vibration cutting for the three dimensional free surface of steel materials (Suzuki, 2012)

According to Feucht et al. (2014), ultrasonic vibration machining (1D VAM, 2D VAM, 3D VAM) improves surface roughness value, particle flow of chips in the working zone of the tool, constant machining quality, flow of chips, lowers temperature at the tool, reduces tool wear and a cutting force during machining. However, it is found that the 3D VAM (3 dimensional vibration assisted machining) is difficult in the machining of hardened steel material AISI D2 because of its complication in the processes and availability in lab scale only. 3D VAM (3 dimensional vibration assisted machining) is carried out on a simple block surface and not replicated in the actual mould and die surface.

2.6.4 Remarks

Based on literature, rotary ultrasonic assisted end milling (RUAEM) is possible to be used in industry because of its performance in producing a better surface finish, reducing cost and extending tool life. Extended tool life ensures that the vibration assisted machining (VAM) generates the better surface finish of machined surface at an economical cutting distance compared to the conventional machining (Brehl and Dow, 2008a). According to Jianguo et al. (2016), the 3D VAM (ultrasonic elliptical vibration) system is using a single crystal diamond as a tool material for milling process of machined surface hardened steel material (AISI D2). On the other hand, single crystal diamond tools are not suitable to steel machining because of the strong chemical affinity in mechanical elements (Zhang et al., 2013) and the appropriate method of suitable cutting tools should be proposed for machining of hardened steel material surface.

Therefore, this thesis will implement rotary ultrasonic assisted end milling (RUAEM) and abrasive slurry using coated carbide inserts with multilayer coating of TiAlN as cutting tools to decrease a surface roughness value (Ra), reduce cutting force and increase the material removal rate during milling process of hardened steel material, AISI D2.

2.6.5 Mechanic of RUAM and abrasive slurry

In machining AISI D2 hardened steel using rotary ultrasonic assisted end milling machining (RUAEM) on the machining slot, the theoretical modelling can be shown by sinusodial graph and cutting tolerances displacement. Figure 2.11 shows the vibration amplitude and frequency of the vibration. The vibration amplitude (value of ΔW) is displacement of the cutting tolerance displacement (Rasidi et al., 2014) whereas the frequency vibration is a wave length.

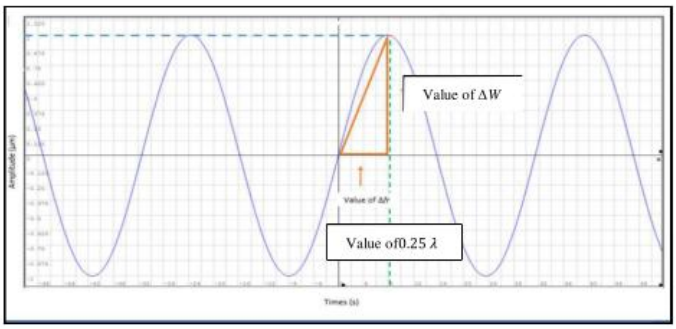


Figure 2.11: Value of vibration amplitude (ΔW) and frequency vibration (λ) (Rasidi et al., 2014)

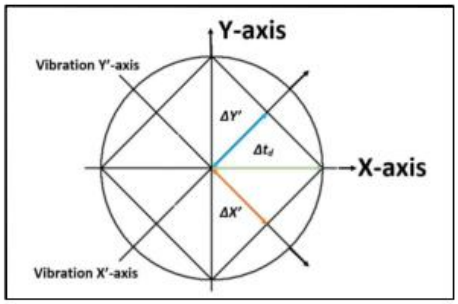


Figure 2.12: Value of vibration amplitude (ΔW) and frequency vibration (λ) In x-axis and y-axis (Rasidi et al., 2014)

According to Figure 2.12, the cutting tolerance displacement is an amplitude vibration motion in x-axis, ΔX' and y-axis, ΔY'. The formula of cutting tolerance displacement is shown in Equation 2.1.

$$\Delta t_d = \sqrt{\Delta X'^2 + \Delta Y'^2} \quad (2.1)$$

The feed rate of ultrasonic vibration assisted machining motion of the machining slot is shown in Equation 2.1. The feed rate of ultrasonic vibration assisted machining (Fv) motion depends on cutting tolerance displacement and machining feed rate (*fr*) as shown in Equation 2.2. The Figure 2.13 shows the effect of amplitude vibration on slot machining.

$$Fv = fr + \left(\left(\frac{d\Delta}{dt} t_d \right) / 60 \right) \tag{2.2}$$

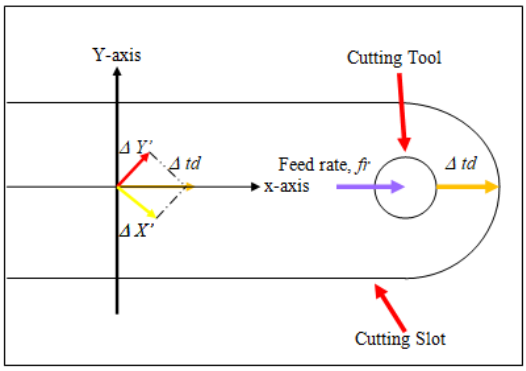


Figure 2.13: Effect of amplitude vibration on slot machining

The mechanic of material removal process for ultrasonic machining is similar to grinding process or single tool cutting process or particle displacing or fracturing the work surface (Agarwal, 2015a). The process of ultrasonic machining involves the shocking movement and abrasive cutting under the tip of the vibrating tool. The mechanism of material removal processes for ultrasonic machining is shown in Figure 2.14.

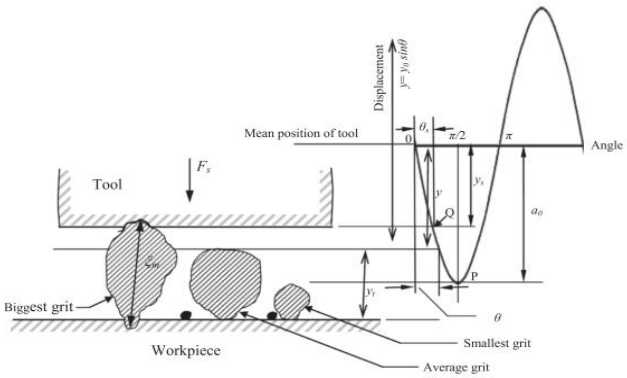


Figure 2.14: Mechanism of material removal process on ultrasonic machining (Agarwal, 2015a)

The mechanism of material removal processes of ultrasonic machining is caused by the effect of the impact indentation and fracture phenomena. The impact indentation process is a grit pushed by the end face of cutting tool head and it penetrates the work piece surface which causes crack impact initiation and development in the brittle work piece material. The fracture phenomena are cracks develop in an intermittent fashion with a cyclic impact, causing a layer of the local work piece beneath the grits to spall into tiny pieces in one of the layer strikes. Then, the hardness of the material depends on fracture stress. If the lower fracture stresses, the material is harder. Table 2.7 shows the list of the material brittleness and ultrasonic machinability of different materials.

Table 2.7: Material brittleness and ultrasonic machinability (Kuo and Tsao, 2012)

Type of material	**Brittleness**	**Machinability**
Glass, quartz, ceramics, diamond	>2	Easy
Hard alloy, hardened steel, Titanium alloy	1-2	Average
Lead, mild steel, copper	<1	Difficult

In addition, rotary ultrasonic machining combines the two (2) methods of material removal mechanism of the ultrasonic machining process and grinding process (Pei et al., 1995). There are three (3) material removal mechanisms including hammering (indentation and crushing under the impact of the ultrasonic vibrations), abrasion (the rotation motion of the cutting tool) and extraction (generate from the simultaneous action of ultrasonic vibration and the rotation motion of the cutting tool). Then, the combination of three material removal mechanisms causes the higher material removal rates in rotary ultrasonic machining compared to conventional machining. Figure 2.15 shows the three

(3) material removal mechanisms. The circular holes, cavity, flat surface and milling slot can be machined by rotary ultrasonic machining because of the rotating motion of the tool on the work piece machined surface.

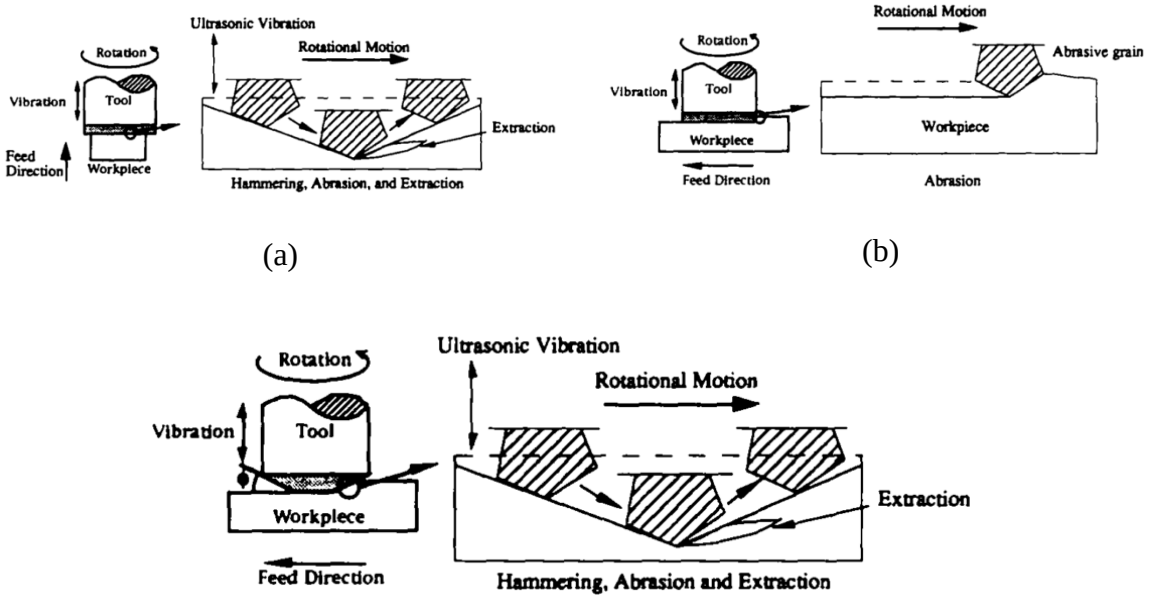
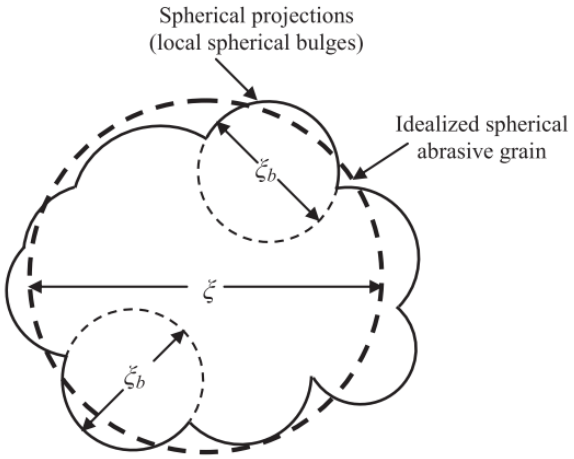
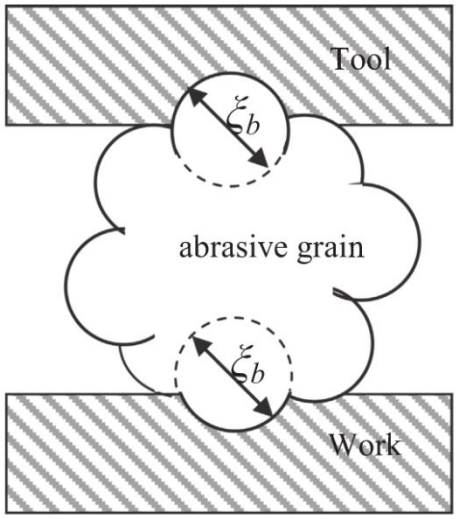


Figure 2.15: Three of the material removal mechanisms in rotary ultrasonic machining including : (a) hammering, (b) abrasion (c) and extraction (Pei et al., 1995)

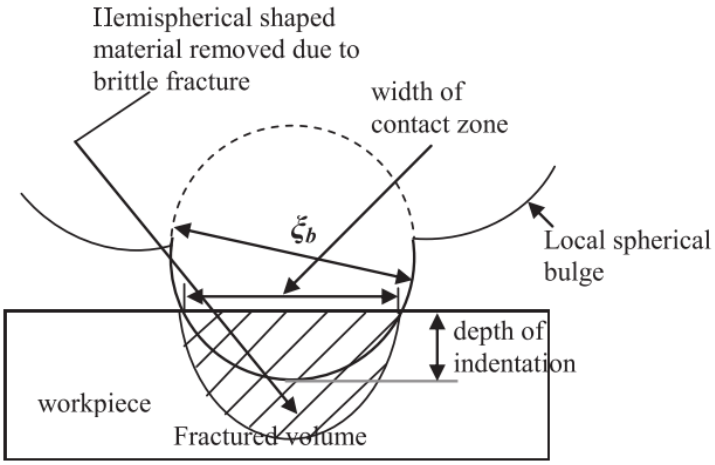
Besides, when using an abrasive slurry of alumina oxide in assisting the machining process of rotary ultrasonic assisted machining of AISI D2 tool steel material, the indentation between the abrasive grit onto the work piece and the cutting tool occurs. The indentation process between the abrasive grit onto the work piece and the cutting tool generates the local spherical bulges contact to the surfaces and are characterized by ξb and by ξ. Where's, the ξb is the deflection of local spherical bulges and ξ is the diameter of spherical. Figure 2.16 (a), (b), (c) show the indentation process between the abrasive grit onto the work piece and the cutting tool where the contact zone is established with the same grows and the contact zone is circular in nature.



(a) Schematic representation of abrasive grain (spherical projections on the abrasive grain)



(b) Interaction between grain and work piece and tool



(c) Indentation geometry after the impact of grain on the work piece

Figure 2.16: The indentation process between the abrasive grit onto the work piece, the cutting tool which the contact zone is established with the same grows and the contact zone is circular in nature (Agarwal, 2015b)

The formula for impulse (Ms) due to the variable contact static force, F_s during acting over contact portion of the cycle for rotary ultrasonic machining is given by:

$$\mathrm{Ms} = f.Fs \tag{2.3}$$

Where, f is frequency and F_s is static force. Then, the contact force for rotary ultrasonic machining at a time, t is given by:

$$Fct = \int_{yxt}^{\xi m} \pi\, dHw\;\; \delta' wt\varphi(\xi)\, \mathrm{d}\xi \tag{2.4}$$

Where, π is 3.142, *dHw* is changes ratio of work piece hardness (Hw), *δ'wt* is the indentation in the work piece at the time (t), $\varphi(\xi)$ is the size distribution of grains and dξ is changes for particle of grains size. The Equation 2.4 can be used when the maximum gap between the tool and the work piece allowable in ultrasonic machining has the same magnitude as the amplitude of vibration and causes the size of the grits which can participate in the machining.

In addition, the contact force for rotary ultrasonic machining is given as:

$$Fct = \int_{yxt}^{\xi m} \pi\, Hw\;\; (\delta wt - \delta t)\varphi(\xi)\, \xi \tag{2.5}$$

Then, the impulse force due to the contact force during the contact period from θs to π/2 is given as follows:

$$Mct = \frac{1.095\, f.\; N.\; Hw}{2.\, \xi} \int_{\theta s}^{\pi/2} \int_{yt}^{\xi m} (\delta wt - \delta t) \left(1 - \left(\frac{\xi - \xi'}{\xi'}\right)^2\right)^3 \mathrm{d}\xi\, .\, \mathrm{d}\,\theta \tag{2.6}$$

By inserting the static force impulse (Ms) to the contact force impulse *(Mct)*, the static force is given by:

$$Fs = \frac{0.545.\ N.\ Hw}{\xi} \int_{\theta s}^{\pi/2} \int_{yt}^{\xi m} (\delta wt - \delta t) \left(1 - \left(\frac{\xi - \xi'}{\xi'}\right)^2\right)^3 d\xi \,.\, d\,\theta \qquad (2.7)$$

The formula of material removal rate for rotary ultrasonic assisted milling involve volume of fractured per grid size (Vg), radius of the contact indentation zone (rc^3), the number of particles of size (ξ) and the frequency (f). The formula of volume of fractured per grid size, Vg is given by the hemispherical portion (Agarwal, 2015c) as shown in Equation 2.8.

$$Vg = (2/3)\ X\ \pi\ X\ r_c^3 \qquad (2.8)$$

Where, rc^3 is radius of the contact indentation zone. Then, $r_c = l_c/2$, where l_c is width of contact indentation zone. The calculation for material removal rate, M_R to all abrasive grains of diameter, ξ is shown in Equation 2.9.

$$M_R = Vg\ \ X\ \ \varphi(\xi)\ \ X\ f \qquad (2.9)$$

Where, Vg is the volume fractured per grit, $\varphi(\xi)$ is the number of particles of size ξ and f is the frequency. It indicates that the material removal rate depends on the volume fractured per grit, number of particles of size and ultrasonic frequency on slot milling using rotary ultrasonic assisted machining.

2.6.6 Hammering effect from RUAEM

Hammering effect is the one of primary mechanism in rotary ultrasonic machining where the cutting cool were ultrasonically vibrated and hammering during milling machining (Pei et al., 1995). Rotary ultrasonic assisted end milling as advanced machining

technique including hammering action (indentation and crushing under impact of the ultrasonic vibration), abrasion (rotation motion of cutting tool) and extraction (generated by the simultaneous of ultrasonic vibration and rotational of cutting tool) action during milling process (Lee et al., 2008) as illustrated in Figure 2.14. Also, primary mechanism in rotary ultrasonic assisted end milling is the hammering action of abrasive slurry particles into work piece material. Direct hammering of abrasive slurry particles on the work piece by the tool during rotary ultrasonic machining, generating material removal rate and particle crushing on work piece machined surface (Vo, 1986). The increasing material removal rate achieved by increasing the grit size of abrasive slurry particles which decreasing the surface density of abrasive slurry particles and causing a greater augmentation of the effective stress due to each size of abrasive slurry particle acting on the work piece machined surface (Agarwal, 2015a). During the hammering process of abrasive slurry particles into work piece machined surface, the material removal rate (MRR) increases as the abrasive slurry grit size increases to an optimal value of abrasive slurry grit size because the coarser abrasive slurry particle cause more damage of material (Khoo et al., 2008a) and micro chipping by impact of the free moving abrasive slurry particles that fly across the machining gap (Rupinder and Khamba, 2006) which strike the work piece machined surface at random location (EI-Hofy, 2005). Hammering effect to cutting tool during rotary ultrasonic machining causing the cutting tool losses contact with the chips on the specified amplitude vibration with resulting in decreasing of cutting force, improving the tool life of cutting tool and improving surface finish of machined surface with low surface roughness (Ra) values (Chavoshi and Luo, 2015). While, the hammering effect to work piece during rotary ultrasonic machining causing hammering action is transferred to the material which causes fracture before plastic deformation and resulting in increasing the material removal rate (Kei and Chung, 2012).

2.6.7 Cutting parameter for RUAEM

2.6.7.1 Cutting speed

A detailed knowledge of cutting parameter for milling process is very important and useful to improve productivity and surface quality. The main purpose of this study is to investigate and propose an optimal cutting conditions to achieve a mirror surface finish profile of machined surface for mould and die material of AISI D2 hardened steel. Optimization routines are considered for the finish milling and better surface of sculptured profile of hardened AISI D2 tool steel.

The series of cutting tests were performed with a set of cutting parameter (spindle speed, feed rate, depth of cut, frequency, amplitude vibration) based on the Taguchi design of experiment orthogonal arrays. The machining performance parameters chosen for this study are surface roughness, machining force and material removal rate. These machining parameters were measured for machining performance evaluation and database generation. The optimization of cutting parameters such as spindle speed, feed rate and depth of cut, can get a better surface integrity of end milling cutting (Masmiati, 2015). The process to get the optimization of machining parameters is made based on few factors; decrease cutting speeds, better surface quality, better dimensional and accuracy of the work piece shape at lower tool wear (Soković et al., 2004).

The machining parameters used for machining AISI D2 hardened steel, using rotary ultrasonic vibration machining (RUAM) are cutting speed or spindle speed, feed rate, depth of cut, vibration amplitude,vibration frequency, abrasive grit size, grit concentration and coolant. Churi et al. (2007) reported that the controlled variables involved in ultrasonic machining (USM) are rotational speed, vibration amplitude and frequency, diamond type, size and concentration, bond type, coolant type and pressure and many more.

The cutting speed is defined as the tool moves through the material at a rotational frequency of the spindle of the machine, measured in revolution per minute for cutting material using CNC machines. The higher cutting speed during ultrasonic machining causes the ductile percentage of machined work piece to be higher where the higher ductile percentage generates the fined of machined surface (Pei and Ferreira, 1999). The low feed rate during the slot milling with rotary ultrasonic assisted machining causes the contact pressure on the machined surface to be less along with the lower value surface roughness.

The cutting speed is an important parameter for grinder less process machining strategies of hardened mould and die materials. The cutting speed is a significant factor which can affect the surface quality of a part that has been milled. The cutting speed also has a strong influence on tool life when the machining process is conducted (Filho, 2002).

a) Rotational speed for ultrasonic assisted machining

Besides, rotational speed is used in milling process through rotary ultrasonic assisted machining (RUAM) of AISI D2 hardened steel. The rotational speed is defined as an object rotating around an axis and the number of turns of the object is divided by time, specified as revolutions per minute (rpm) for cutting materials using a machine. The rotational speed is an important parameter for machining strategies of ultrasonic vibration machining hardened mould and die materials. The rotational speed is a significant factor which can affect the surface quality of a part that has been milled. The rotational speed also has a strong influence on tool life when the machining process is conducted (Filho, 2002). Table 2.8 summarizes the rotational speed used by researchers on ultrasonic machining in milling process with different materials.

Table 2.8: List of studies on the rotational speed used on ultrasonic machining in milling process with different materials

Author/Year	Material	Method	Speed	Comments
Shamoto et al. (2005)	Hardened die Steel, HRC 40 and HRC 54 ~Cutting tool-single crystal diamond tools	3 Degree of freedom (DOF) ultrasonic vibration ~Ultrasonic elliptical vibration cutting	HRC 54 (Flat) 0.2 m/min (32 rpm) HRC 40 (Spherical) less 1.34 m/min (213rpm)	Cutting speed is significant factor that affected to surface roughness of work piece machined surface
Lauwers et al. (2010)	ZrO2-based ceramics materials (TM2 and TM2.5)	~Ultrasonic assisted machining ~Vibration mechanical ultrasonic piezo-actuator integrated within the actor system of the tool holder	6000 rpm	Cutting speed constant
Kuo and Tsao (2012)	Brittle material	Rotary ultrasonic machining	5000 rpm	Higher rotation speed produced higher removal rates
Suzuki (2012)	Hardened steel materials: ~HRC40 (JIS:NAK80) ~HRC53 (JIS: SUS420J2) ~HRC54 (JIS: SUS420J2)	Ultrasonic elliptical vibration system with the 4 axis control	Spherical 0-1.27 m/min (0-202 rpm) Machined Molds 0.64 m/min (102 rpm) Textures Grooves 0.2 m/min (32 rpm)	Cutting speed during machining is low with less 5 m/min

			Sculptured letters 1 m/min (159 rpm)	
Lian et al. (2013)	Al 6061	Ultrasonic vibration assisted micro-milling (UVAM) with longitudinal vibration	150,000 rpm	High cutting speed during machining
Kuruc and Peterka (2014)	Poly-crystalline cubic boron nitride (PCBN) material.	Rotary ultrasonic vibration machining (RUM)	8000 rpm	Constant cutting speed
Marcel et al. (2014)	Al alloy is AW 5083(AlMg4.5Mn)	~Rotary ultrasonic machining ~Ultrasonic oscillation is provided by an ultrasonic generator with a piezo-ceramic convertor	5000-7000 rpm	Surface roughness value (Ra) decrease at 0.59 µm on 6000 rpm of cutting speed

2.6.7.2 Feed rate

The second parameter used in rotary ultrasonic assisted end milling machining (RUAEM) is feed rate. The feed rate is a relative velocity of the cutter which should move through the material being cut. Feed rate is directly proportional to the motion of the tool and the work piece. During machining operation, when the other parameters are constant, the feed rate is the most important and influential parameter that will affect a surface roughness (Ra) value on machined surfaces. The feed rate is the major factor that affects the surface roughness (Ra) value of machined surface in milling process (Alabdullah et al., 2016). The feed rate also depends on the motion of the cutter and work piece. When, a cutter removes more unwanted material from a work piece, it can generate more heat between work piece and cutting tools and reduce a tool life. Consequently, the feed rate

increase can reduce a cutter life. When the feed rate reduces during the machining process, the cutter life improves because it does not stress the hardness of the cutter material.

According to Feucht et al. (2014) the increased feed rate can reduce tool wear during flexible integration of ultrasonic assisted machining of hard and brittle materials, composites materials, metal alloys and advanced materials such as ceramics and glasses. Table 2.9 summarizes the feed rate used on ultrasonic machining in milling process with different materials.

Table 2.9: List of research on the feed rate used on ultrasonic machining in milling process with different materials

Author/Year	Material	Method	Feed rate	Comments
Shamoto et al. (2005)	~Hardened die Steel, HRC 54 or HRC 40 ~Cutting tool-single crystal diamond tools	~3 Degree of freedom (DOF) ultrasonic vibration ~Ultrasonic elliptical vibration cutting	Flat (HRC 54) 20 μm (20 X 10^{-3}mm) Spherical (HRC 40) 15 μm (15 X 10^{-3}mm)	Lower feed rate during machining
Lauwers et al. (2010)	ZrO2-based ceramics materials (TM2 and TM2.5)	~Ultrasonic assisted machining ~Mechanical ultrasonic piezo-actuator integrated within the actor system of the tool holder	~125 mm/min, ~250 mm/min, ~500 mm/min	The increasing the feed rate can reduced the axial tool wear
Kuo and	Brittle material	Rotary ultrasonic	0.1 mm/s (6	The increasing

Tsao (2012)		machining	mm/min), 0.2 mm/s (12 mm/min), 0.3 mm/s (18 mm/min)	of feed rate caused the increasing of surface roughness
Suzuki (2012)	Hardened steel materials ~HRC40 (JIS:NAK80) ~HRC53 (JIS: SUS420J2) ~HRC54 (JIS:SUS420J2)	Ultrasonic elliptical vibration system with the 4 axis control	Spherical Surfaced 15 µm/rev (15 X 10^{-3} mm) Machined Molds 20 µm/rev 920 X 10^{-3} mm) Sculptured letters 20 µm/rev (20 X 10^{-3} mm)	Lower feed rate during machining
Lian et al. (2013)	Al 6061	Ultrasonic vibration assisted micro-milling (UVAM) with longitudinal vibration	0.5 mm/s (30 mm/min)	The feed rate of cutting tool is magnified 100 X
Kuruc and Peterka (2014)	Poly-crystalline cubic boron nitride (PCBN) material.	Rotary ultrasonic vibration machining (RUM)	300 mm/min	Constant feed rate
Marcel et al. (2014)	Al alloy is AW 5083(AlMg4.5Mn)	~Rotary ultrasonic machining ~Ultrasonic oscillation is provided by an ultrasonic	100-500 mm/min	Lower feed rate of 100 mm/min reduced of surface roughness value (0.59 µm)

generator

with a piezo-

ceramic convertor.

2.6.7.3 Depth of cut

The third machining parameter used in rotary ultrasonic assisted machining is depth of cut (Doc). It refers to the layer removed from the work piece in a single pass. It is measured perpendicular to the machined surface. Therefore, the depth of cut is defined as the measurement of the width and depth of the cutter or tool cut into the work piece. The unit measurement for Doc is inches or millimetre. Machining performances (tool life, surface finish, dimensional accuracy of part) are likely to be influenced by the depth of cut (DOC). Tool life can increase when the depth of cut increases.

Ideal cutting condition using an end mill cutter is shown in Figure 2.17 where the precise geometry of cutting tool is interrelated to the depth of cut of the pocket versus how many flutes involved on milling cutting. Table 2.10 summarizes the depth of cut used by researchers on rotary ultrasonic assisted machining in milling with different materials.

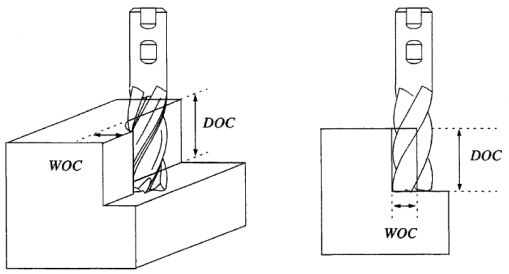


Figure 2.17: The idea of cutting condition using an end milling cutter, where the woc (width of cut), doc (depth of cut) (Trent, 1999)

Table 2.10: List of research on depth of cut used by rotary ultrasonic assisted end milling with different material

Author/Year	Material Used	Method	Doc	Comments
Shamoto et al. (2005)	~Hardened die Steel, HRC 54 or HRC 40 ~Cutting tool- single crystal diamond tools	~3 Degree of freedom (DOF) Ultrasonic vibration ~Ultrasonic elliptical vibration Cutting	~HRC 54 (Flat) 3 μm ~HRC 40 (Sphere) 3 μm	Lower depth of cut during machining
J. Kumar et al. (2008b)	~High carbon steel ~Titanium and its alloys	Ultrasonic machining	1 mm	Constant depth of cut
Kuo and Tsao (2012)	Brittle material	Rotary ultrasonic machining	1 mm, 2 mm, 3mm	Depth of cut increase causes the increase of surface roughness
Suzuki (2012)	Hardened steel materials ~HRC40 (JIS:NAK80) ~HRC53 (JIS: SUS420J2) ~HRC54 (JIS: SUS420J2)	Ultrasonic elliptical vibration system with the 4 axis control	Spherical 3 μm Machined Molds 5 μm Textures Grooves 2.5 μm Sculptured letters 20 μm	Lower depth of cut during mcahining
Lian et al. (2013)	Al 6061	Ultrasonic vibration assisted micro-milling (UVAM) with	1μm	Constant depth of cut

		longitudinal vibration		
Kuruc and Peterka (2014)	Poly-crystalline cubic boron nitride (PCBN) material	Rotary ultrasonic vibration machining (RUM)	0.003 mm	Constant depth of cut
Marcel et al. (2014)	Al alloy is AW 5083(AlMg4.5Mn)	~Rotary ultrasonic machining ~Ultrasonic oscillation is provided by an ultrasonic generator with a piezo-ceramic convertor	0.1 mm (constant)	Constant depth of cut

2.6.7.4 Frequency

The fourth machining parameter used in rotary ultrasonic assisted end milling (RUAEM) machining is frequency. Definition of frequency is the number of periods or regularly occurring events of any given kind in units of time (second). Also, frequency is the number of cycles or completed alternations per unit time of a wave or oscillation. Ultrasonic vibration cutting mechanism was incluenced by frequency vibration of cutting tool which improve machining quality, stability of processing device, long life cutting tool and easily removing chip breaking (Zou et al., 2015). Ultrasonic machining convert a low frequency electrical energy to a high frequency electrical energy signal and transmit to a transducer (Singh and Khamba, 2006). Then, the transducer switch high frequency electrical energy signal into mechanical vibration and transmitted via the energy accumulation device namely horn. The cutting tool vibrate along its longitudinal axis at high frequency which is over than or equal frequency of 20 kHz. The cutting tool vibration due to high frequency will cause the abrasive particle present in slurry between cutting tool and work piece surface which impact to work piece machined surface causing material

removal process by micro chipping. The suitable abbrasive slurry used is silicon carbide, boron carbide, alumina oxide and pumped in cutting zone area. Table 2.11 summarizes the frequency of vibration used on ultrasonic machining in milling process with different materials.

Table 2.11: List of research on the frequency of vibration used in ultrasonic machining

Author/Year	Material Used	Method	Frequency	Comments
Shamoto et al. (2005)	~Hardened die Steel, HRC 54 or HRC 40 ~Cutting tool-single crystal diamond tools	~3 Degree of freedom (DOF) ultrasonic vibration ~Ultrasonic elliptical vibration cutting	HRC 54 (Flat) 34.4 kHz HRC 40 (Sphere) 34.4 kHz	Constant with high frequency
Kumar et al. (2008b)	~High carbon steel ~Titanium and its alloys	Ultrasonic machining	21 kHz	Constant frequency
Lauwers et al. (2010)	ZrO2-based ceramics materials (TM2 and TM2.5)	Ultrasonic assisted machining ~Mechanical ultrasonic piezo-actuator integrated within the actor system of the tool holder	16.505kHz	The frequency is set to resonant
Kuo and Tsao (2012)	Brittle material	Rotary ultrasonic machining	22 kHz	Constant frequency
Suzuki (2012)	Hardened steel materials ~HRC40 (JIS:NAK80) ~HRC53 (JIS:	Ultrasonic elliptical vibration system with the 4 axis control	Spherical 34.4 kHz Machined Molds 38 kHz	Frequency above 30 kHz

	SUS420J2) ~HRC54 (JIS: SUS420J2)		Textures Grooves 38 kHz Sculptured letters 36 kHz	
Lian et al. (2013)	Al 6061	Ultrasonic vibration assisted micro-milling (UVAM) with longitudinal vibration	38 KHz	Inherent high a frequency of 38 KHz and tool teeth hammer work piece constantly
Kuruc and Peterka (2014)	Poly-crystalline cubic boron nitride (PCBN) material	Rotary ultrasonic vibration machining (RUM)	21.6 kHz	Constant frequency
Marcel et al. (2014)	Al alloy is AW 5083(AlMg4.5Mn)	~Rotary ultrasonic machining ~Ultrasonic oscillation is provided by an ultrasonic generator with a piezo-ceramic convertor	21.467 kHz	Constant frequency

2.6.7.5 Amplitude

The fifth machining parameter used in rotary ultrasonic assisted end milling (RUAEM) machining is amplitude vibration. Amplitude vibration is defined as the maximum displacement of vibrating particle or body from its position of rest. According to Agarwal (2015a), amplitude vibration is caused by velocity of abrasive particle at the interface between work piece and cutting tool. Figure 2.18 shows the amplitude vibration

effect to RUAEM. The increasing of amplitude vibration during rotary ultrasonic machining generates higher material removal rate and leads to effective flushing away of debris and chips between cutting tool and work piece machined surface at cutting zone area (Khoo et al., 2008b). Using the larger vibration amplitude during rotary ultrasonic assisted machining causing the greater the material removal rate per active grain which causes higher kinetic energy grits strike the work piece machined surface (Tawakoli et al., 2008). Due to ultrasonic impact occurs, causes a reduction in friction during machining because ultrasonic vibration applying additional stress to assist in breaking the work piece surface microstructure and the material more easily begin to rollover as well as more micro cracking propagation in the cutting zone area which cause by an effective interaction between abrasive grits slurry and work piece machined surface. Ultrasonic vibration generated ultrasonic impulse energy to ultrasonic cleaning function which helps to eliminate waste around the cutting zone area between cutting tool, help wash away the chips and machined surface and thus reduction of the machining force (Liu et al., 2012). Also, rotary ultrasonic machining with suitable amplitude vibration during machining can improved chip removal rate, reduced tool wear with prolong the tool life, improve surface quality of machined surface, reduced cutting force with minimum torque, remove excess heat more efficiently at cutting zone area and higher material removal rate. The application of low vibration amplitude and small abrasive particle slurry used in rotary ultrasonic machining reduce the machining rates with superior surface finish of work piece machined surface (Viswanath et al., 2014). Table 2.12 summarizes the amplitude of vibration used on ultrasonic machining in milling process with different materials.

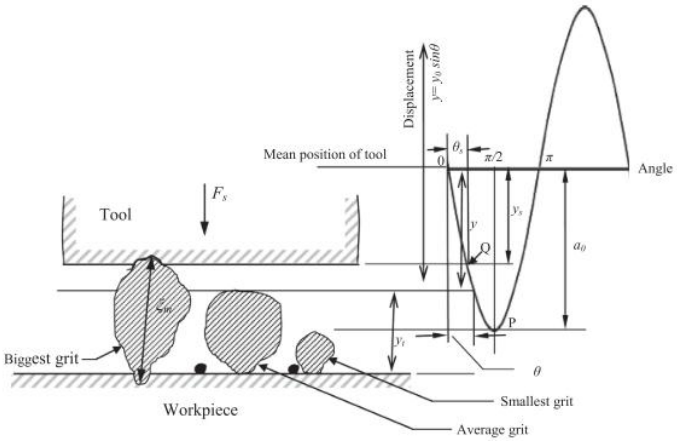


Figure 2.18: Amplitude of vibration for RUAEM (Agarwal, 2015a)

Table 2.12: List of research on the amplitude of vibration used in ultrasonic machining

Author/Year	Material Used	Method	Amplitude	Comments
Shamoto et al. (2005)	~Hardened die Steel, HRC 54 or HRC 40 ~Cutting tool-single crystal diamond tools	~3 Degree of freedom (DOF) Ultrasonic vibration ~Ultrasonic elliptical vibration cutting	HRC 54 (Flat) 8-8-4 μm (U-V-Z) HRC 40 (Sphere) 6-6-3 μm (U-V-Z)	The amplitudes of the three directional vibrations was developed
Kumar et al. (2008b)	~High carbon steel ~Titanium and its alloys	Ultrasonic machining	25.3–25.6 μm	Amplitude vibration promotes efficiency work piece machined surface
Lauwers et al. (2010)	ZrO2-based ceramics materials (TM2 and TM2.5)	~Ultrasonic assisted machining ~Mechanical ultrasonic piezo-actuator integrated within the actor system of the tool holder	~(vf:100mm/min, ap: 10μm) ~(vf:500mm/min, ap: 30μm) ~ap: 20μm, tool rotation 6000rpm, feedrate	The amplitude vibration reduced force and tool wear

			500mm/min.	
Kuo and Tsao (2012)	Brittle material	Rotary ultrasonic machining	25.0 µm	Amplitude vibration does not affect the machined surface
Suzuki (2012)	Hardened steel materials ~HRC40 (JIS:NAK80) ~HRC53 (JIS: SUS420J2) ~HRC54 (JIS: SUS420J2)	~Ultrasonic elliptical vibration system with the 4 axis controls	Spherical 6-6-3 μm_{p-p} Machined Molds 4 μm_{p-p} Textures Grooves 4 μm_{p-p} Sculptured letters 2-4 μm_{p-p}	Amplitude vibration in the depth of cut direction and lower amplitude of below 6 µm
Lian et al. (2013)	Al 6061	Ultrasonic vibration assisted micro-milling (UVAM) with longitudinal vibration	11µm, 15µm and 19µm	The bigger of ultrasonic vibration amplitude is not the better
Kuruc and Peterka (2014)	Poly-crystalline cubic boron nitride (PCBN) material.	Rotary ultrasonic vibration machining (RUM)	6 µm	Constant amplitude
Marcel et al. (2014)	Al alloy is AW 5083(AlMg4.5Mn)	Rotary ultrasonic machining	6 µm	Constant amplitude

2.6.7.6 Abrasive slurry

The abrasive slurry and grain size particles used in ultrasonic machining (USM), rotary ultrasonic machining (RUM) and rotary ultrasonic assisted machining (RUAM) is significantly affecting the material removal rate (MRR) of work piece and proven to improve the quality of machined surface with low surface roughness value (Singh, 2012).

The surface roughness (Ra) value of machined surface is directly proportional to slurry concentration during ultrasonic machining (Kumar and Khamba, 2007).

Slurry contains a mixture of solids and liquid, which generally based on water. When the more abrasive particle slurry during rotary ultrasonic assisted machining, more materials are removed. In the different volumetric percentage of slurry concentration, there are many small abrasive particles in the slurry which assist the material removal rate during slot milling. In theory, the small abrasive particle in volumetric slurry concentration produce a small crater which generates a small surface roughness (Ra) value of machined surface (Gupta et al., 2013). An experiment by Pei et al. (2013) proved that the abrasive particle moves toward the center of machining area during vibration and abrasive particle is randomly distributed hence, improving the surface roughness of machined surface. Singh and Khamba (2008) used three (3) different slurries namely silicon carbide (SiC), boron carbide (B_4C) and alumina (Al_2O_3) with different slurry concentration in ultrasonic machining. The concentration of particles in the slurry can be determined by volume percentage (C_v) and weight percentage (C_m). The three (3) different slurry concentration of 15%, 20% and 25% with three (3) slurry types (silicon carbide (SiC), boron carbide (B_4C) and alumina (Al_2O_3) were used in ultrasonic machining which significantly improve the material removal rate with 28% contribution in comparison to other factors (Singh and Khamba, 2007). Singh and Khamba (2007) found that the abrasive slurry concentration increases the material removal rate (MRR) on ultrasonic machining. The calculation of slurry concentration is shown in the Equation 3.1.

$$\% \text{ Slurry concentration} = (\text{Weight of dry solids})/(\text{Weight of dry solids} + \text{weight of liquid phase}) \quad (2.10)$$

The use of appropriate slurry which is accurately conveyed to cutting zone between cutting tool and surface being machined during slot milling using rotary ultrasonic assisted machining, causes repetitive impacts of the tool on the grains of the abrasive material, falling the grains slurry onto the treated surface, leading to the work piece material fracture and cavity formation with the shape mirror formed of the tool (Astashev and Babitsky, 2014). Besides, a slurry acts as a coolant and as fresh abrasive is pumped to the cutting zone between rotary ultrasonic tool holder (ultrasonic horn), cutting tool, work piece machined surface, allowing efficient energy transfer which can remove debris from the cutting zone (Singh and Khamba, 2006). Goswami and Chakraborty (2015) indicated that value of maximum material removal rate (MRR) can be achieved at higher volumetric and higher concentration of abrasive particle in slurry using ultrasonic machining.

Alumina oxide as abrasive slurry is made from high purity alumina oxide powder and suitable for polishing purposes. Alumina oxide as abrasive slurry suitable for polishing process of hardened steel material by using rotary ultrasonic assisted end milling technique (RUAEM). The vibration of cutting tool using rotary ultrasonic assisted end milling causes the abrasive particles held in slurry between the cutting tool and the work piece machined surface, which impact to the work piece surface causing material removal by micro chipping and improve surface roughness value with lower cutting force (Singh, 2014).

2.7 Machining performances for RUAEM

The main goal of this thesis is to study, investigate and analyze the effect or influence of machining parameters (cutting speed, feed rate, depth cut, frequency, amplitude) for AISI D2 hardened die and mould material on the machining performances (surface roughness, cutting force, material removal rate) during slot milling process.

Machining refers to any of various processes in which a piece of raw material is cut into a desired final shape and size by a controlled material removal process. Machining processes can be expressed as the removal of a certain selected areas from a part in order to obtain a desired shape or finish. Machining can create a variety of features and shape including holes, slots, pockets, flat surfaces, and even complex surface contours. Machining is often considered the most common and versatile of all manufacturing processes. Machining is needed for the production of specialized component in automotive industries, aerospace, marine, mass production industry and industries. The best mode of machining is required to produce the best productivity and quality of components and products (Ozoegwu et al., 2012). The machining for AISI D2 hardened steel is done by non-traditional machining using a computer application. Non-traditional machining is using computer application including CNC (computer numerical control) for machining process. Rotary ultrasonic machining can be used for machining hard material and providing excellent work piece machine surface, fine precision, low cutting force and higher material removal rate (Ya et al., 2002). New machining strategy was applied by applying rotary ultrasonic assisted end milling (RUAEM) using abrasive slurry. The abrasive slurry used for slot milling using rotary ultrasonic assisted end milling machining (RUAEM) is alumina oxide slurry of 5%, 10%, 15%, 20% volumetric concentration with distrilled water mixture. Percentage alumina oxide slurry of 5% to 20% volumetric concentration with distrilled water mixture was selected based on the literature review. The machining performances for rotary ultrasonic assisted end milling machining are surface roughness, resultant cutting force and material removal rate. Another analysis used to support machining performance is macroscopic evaluation of machined surface quality and heat effected in RUAEM machining.

2.7.1 Surface roughness

The surface finish is the smoothness of the final work piece machined surface or finished final product. A mirror surface finish profile is in high demand for mould and die industry, hence, surface finish is paramount to be addressed and investigated. Surface finish is generated by the interaction of the cutting edges and the microstructure of the material being cut in machining process. Another description of surface finish includes the texture, the flaw, the material and any coating applied. The peaks and valleys of the surface were measured using parameter Ra (arithmetical mean deviation of the assessed slot) at a location of work piece machined surface as shown in Figure 2.19. Maximum value of Ra (surface roughness) is taken for each slot and average value is calculated as the input to surface roughness response. In addition, stereo microscope is used for the macroscopic observation of machined surface.

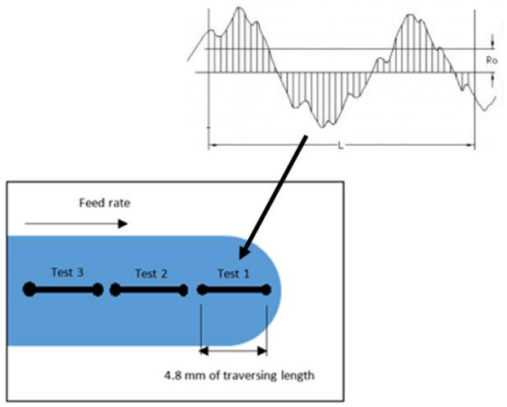


Figure 2.19: The surface roughness measuring location

Besides, the work piece surface roughness is the most important criteria for grinding and polishing process to get a mirror surface sculptured profile of hardened mould and die material. Therefore, surface roughness is an important measurement of product quality (Rawangwong et al., 2014). Surface finish ranges from 1.5 to 3.8 μm (Ra-value) for

milling free-machining steels and nonferrous material. According to Zhang et al. (2011), the improvement of surface roughness value is observed through ultrasonic vibration machining of slot milling hardened steel. Then, Feucht et al. (2014) reported that ultrasonic vibration assisted machining has been shown as the latest technology in machining hardened mould and die material resulting in the improvement of the surface roughness of machined surface, decrease of process force and reduction of a tool wear for cutting tool. The microstructure on machined surface changes is caused by thermal, mechanical and chemical energy reaction between chemical composition of steel and surface microstructure changes during machining (Yan et al., 2011). Jung et al. (2012) reported that mirror quality surfaces with surface roughness (Ra) value of 0.013μm are obtained when applying ultrasonic elliptical vibration milling cutting method of hardened die steel and using a single crystal diamond tool with a nose radius of 1.0 mm as a cutting tool. Rasidi et al. (2014) reported that ultrasonic vibration assisted micro milling improves surface roughness (Ra) value of machined surface about 0.20 μm using 2 flute flat end mill 0.5 mm diameter as a cutting tool. Tsai et al. (2016) investigated a machining performance of surface roughness of AISI 420 mould steel work piece using cemented carbide flat-end milling cutters of 6 mm in diameter with 2 teeth as a cutting tool on milling machining using ultrasonic assisted end milling. The results indicated that the improvement of surface roughness (Ra) value with the decrease from 0.236 μm to 0.136 μm when applying ultrasonic assisted end milling at ultrasonic amplitude of 2.20 μm and 20 kHz frequency respectively. The surface roughness of work piece machined surface with ultrasonic assisted end milling shows better surface finish, uniformity and smoothness compared to unassisted machining under the same conditions. The summary of machining performance of surface roughness obtained by rotary ultrasonic assisted machining of AISI D2 hardened steel in milling process is shown in Table 2.13.

Table 2.13: The summary of machining performance of surface roughness obtained by rotary ultrasonic assisted machining of AISI D2 hardened steel in milling process

Author/Year	Method	Surface roughness (Ra)
Jung et al. (2012)	Ultrasonic elliptical vibration milling cutting	0.013 μm
Rasidi et al. (2014)	Ultrasonic vibration assisted micro milling	0.20 μm
Tsai et al. (2016)	Ultrasonic assisted milling	0.174 μm

2.7.2 Cutting force

Cutting force is defined as a force that is generated by the cutting tool during machining processes. The cutting force during a milling operation is very important because it is very useful in determining the requirements of the machine tool to cut a work piece material efficiently, determine the size of the cutting tool and analyze the machining process based on different works and combined tool materials. Nath and Rahman (2008) reported that ultrasonic vibration cutting increases the life of cutting tool by lowering the cutting force during machining through reduction of friction between the tool and work piece. The machining process using ultrasonic vibration reduces the friction between chips and machined surface, causing the chip produced to be thinner and thrust force to be reduced on milling process because the additional pressure is applied to assist in breaking the microstructure of machined surface and it can also reduce plastic deformation of the machined surface (Tawakoli et al., 2008). This condition occurs during the slot machining using rotary ultrasonic assisted machining, the frequency vibration and amplitude vibrations help the slot cutting processes in ductile and brittle conditions and causing the resultant force needed for the milled work piece surfaces decreases (Ibrahim et al., 2011).

Wu et al. (2011) carried out a research on machining performances of cutting force during rotary ultrasonic machining of aluminium as work piece material. This research revealed that the axial cutting force is lower when the spindle speed of rotary ultrasonic machining increases because the indentation depth of abrasive particles into the work piece machined surface becomes smaller. Pei and Ferreira (1999) reported that the cutting force increases when the speed, feed rate, depth of cut and vibration amplitude increase on rotary ultrasonic face milling of ceramic work piece plat using water as coolant. The milling cutting forces components for *Fx*, *Fy* and *Fz* during slot milling of hardened steel material by RUAEM is shown in Figure 2.20.

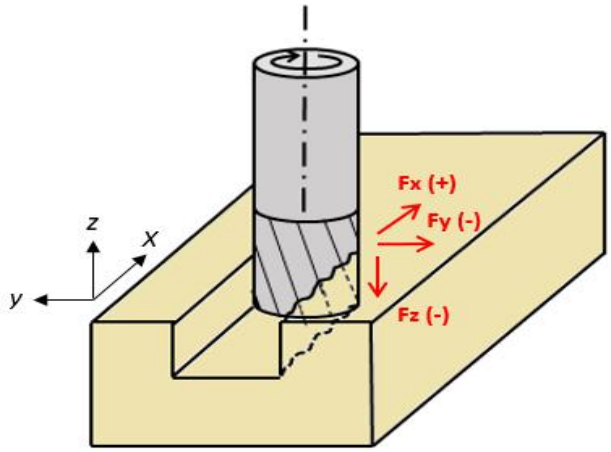


Figure 2.20: Milling cutting forces component for F_x, F_y, and F_z for RUAEM

2.7.3 Material removal rate

Material removal rate (MRR) is the volume of material removed by machining process divided with the total machining time (Bertsche et al., 2013). According to Kuo and Tsao (2012), the material removal rate refers to material removed per unit time and the calculation of material removal rate depends on tool shape, length of material slot milled, width of the slot milled and the depth of cut of the machining slot. The *l* is the length of slot, *w* is the width of the slot and *h* is the depth of cut of the machining slot.

In addition, the material removal rate varies according to the depth of cut of the machining slot. The feed rate will determine the overall milling time taken and a higher feed rate produces higher material removal resulting in a more efficient process (Kuo and Tsao, 2012). In RUAEM, the materials are removed by the interaction between the shearing from milling cutter and vibration amplitude either with or without the presence of abrasive slurry. The interaction creates a high momentum of shearing impact on the machined surface that produces a localized fatigue stress, causing a continuous impact and micro chipping phenomenon (Jain et al., 2011). Then, the microstructure which appears on the surface machined surface is significantly changed by the material removal process which may improve and damage the machined surface (Jawahir et al., 2011). Narasimha (1993) proved that the material removal rate (MRR) in rotary ultrasonic machining is 3 to 4 times greater compared to conventional ultrasonic machining.

The mechanics of material removal process for RUAEM are complicated and the mechanistic model to quantify the rate of material removal precisely is non-existence, hence, the most suitable and practical method to measure MRR is through measuring the weight of material loses per specific time. The material removal rate formula (Bertsche et al., 2013) is shown in Equation 2.11.

$$MRR\ (\frac{mg}{\text{min}}) = \frac{\text{Weight before machining} - \text{Weight after machining}}{\text{Machining Time}} \quad (2.11)$$

Rotary ultrasonic machining is the best technique and method for machining hardened steel material and cutting tool vibration frequency where rotation increases the material removal rate and simultaneously increases quality of surface finishing and the stability or reliability of cutting process (Singh, 2012).

2.7.4 Remarks

Based on literature, studies on machining performances of surface roughness (Ra), resultant cutting force (F_R) and material removal rate (MRR) on rotary ultrasonic assisted end milling in machining of AISI D2 hardened tool steel are scarce. New research techniques need to be carried out to investigate the effect of RUAEM machining on machining parameters namely surface roughness, cutting force and material removal rate for machining AISI D2 tool steel.

2.8 Statistical analysis

Design of experiment (DOE) is a statistical analytical method to determine the relationship between machining parameters that affect the machining performance or the machining output (response) of the process. The design of experiment (DOE) is a tool to find cause and effect of a machining process. DOE can control the effects of parameters in the machining process and its helps to minimize the number of experiments and time usage with low usage of material resources. Besides, DOE is a process planning of an experiment using statistical analysis to make conclusion from the data obtained and it can reduce the variability and error during experiments compared to a conventional approach of one factor at a time. According to Halim and Kasim (2014), design of experiments (DOE) is a statistical structured approach used to determine the relationship between cause and effect and important method to reduce problems encountered in the experiment. DOE tool is commonly utilized in most studies to investigate the effects of rotary ultrasonic assisted machining parameters for hardened mould and die material on machining performances like Full Factorial, Taguchi and Response surface methodology (RSM).

Kiswanto et al. (2015) used full factorial experimental design to determine the relationship between machining parameters and machining response and ascertain which

machining parameters are significantly affected to surface roughness value. This experiment involves the design of 33 full factorial design through 27 run of experiments for slot milling operation of aluminium alloy AA100 using micro milling machining. Wu et al. (2011) applied full factorial design for dynamic process modeling for rotary ultrasonic machining of alumina. Four input variables are utilized such as; spindle speed, feed rate, ultrasonic vibration power and diamond grid size. A total of 16 experiments were carried out to investigate the significant factors that affect the value surface roughness (Ra). Through the full factorial design, the number of runs for experiments can be reduced depending on the number of machining parameters involved. The reduction in the number of experiments it can save machining time, manpower, materials, cutting tools, machinery and other equipment.

Another design of experiment (DOE) tool which can be used is the Taguchi method where it can improve the quality and performance. Shiou and Ciou (2008) reported that Taguchi method is used to determine the effect of several parameters by conducting matrix experiments. The Taguchi method is selected to obtain the optimal vibration assisted spherical polishing parameters and investigate the effects of polishing parameters on the surface roughness of machined surface. Naresh et al. (2013) used Taguchi method to indicate the impact of process parameters on machining performances such as surface roughness, machining force and delamination factors. This experiment is run according to four (4) parameters, 3 levels and produces 27 experimental runs. The results yield that the Taguchi method is saving experiment runs and time, reducing the cost and determining the significant factors quickly.

The last tool of design of experiment (DOE) used is response surface methodology (RSM). Response surface methodology (RSM) is an important tool of DOE in analyzing results obtained in machining experiments. Response surface methodology (RSM) is

defined as a mathematical and statistical technique for the modeling and analysis of experiments which show the significant effect of independent factors with the response. Response surface methodology is very convenient and the most efficient use in the field of machining engineering in studying cutting tools, surface roughness and machining force (Noordin et al., 2004; Hossein et al., 2007; Campatelli and Scippa, 2012). The main purpose of using RSM in experimental design is to optimize the machining response and develop a mathematical model and empirical relationship between response and machining parameters (Mishra et al., 2014). Another objective of using response surface methodology is to optimize the response and determine the response variables (Y) which is generated due to several independent quantitative factors (X_1, X_2,….,X_K). RSM generates a precise map based on mathematical models such as response surface plot and contour plot which put all responses together through optimization approach (Anderson and Whitcomb, 2005). A review of design of experiments (DOE) method shows that the DOE method has its own function and own advantages based on machining process, objective, method, sample size, material, cutting tools, machining time and available cost of machining process.

2.8.1 Taguchi method

Taguchi method is tool for designing of an experiment in various areas including metal cutting. The Taguchi method was introduced by Genichi Taguchi, a Japanese quality management consultant (Shahrom et al., 2013). The method is improving the response quality with a minimum run of an experiment, cost and time. Taguchi also creates a standard orthogonal array to include as many factors as possible. The choice is left to user to select either the standard or column-merging method oridle-column, subject to the number of factors, interactions and levels needed. Taguchi method is an experimental

optimization technique to choose design parameter settings. It is indeed, a simple and significant approach to optimize design for performance, quality and cost.

In quality engineering, a manufacturing process that causes a product output performance deviates from its original design is called noise factors. Noise factors which occur in a machining process are called inner noise factors. Taguchi parameter design is a significant tool for robust engineering (Said et al., 2013). Robust design engineering is an important tool to obtain product and process conditions which are very sensitive to the various causes that effect the production and produce high quality of products with minimum cost. Based on Taguchi method, robust design is the best way to reduce the effect of noise factors on machining performance during slot cutting. S/N ratio is used in experiments to improve the measurement quality of variation ranging by points. The standard parameters of S/N ratio are indicated in Table 2.14.

Table 2.14: Standard parameter of S/N ratio (source: manual of design experiment)

Type of S/N ratio	**Objective**
Smaller the better: $\frac{S}{N} = 10\ \mathrm{Log}\left[\frac{1}{\bar{y}^2 + s^2}\right]$	Minimize the response
Target – the –best: $\frac{S}{N} = 10\ \log\left[\frac{y^{-2}}{s^2_{n-1}}\right]$	Target the response at the desired value
Larger the best: $\frac{S}{N} = -10\ \mathrm{Log}\left[\frac{1}{n}\sum_{i=1}^{n}\frac{1}{y_i^2}\right]$	Maximize the response

Moreover, the second tool for Taguchi method is orthogonal arrays. Orthogonal arrays are used to reduce the number of experimental runs and contain the amount of controllable factors to be tested in experiments. The notation of an orthogonal array in Taguchi method can be illustrated with an example of L_4 (2^3) array. Alphabet "L" is derived from Latin-Graeco orthogonal array. 4 indicates the number of experimental runs involved in Taguchi method design. 2 shows the number of level and 3 shows the number of experimental factors. The notation of orthogonal arrays is shown in Figure 2.21. For example, the orthogonal array for L_4 refers to four experimental runs conducted when applying the Taguchi design method.

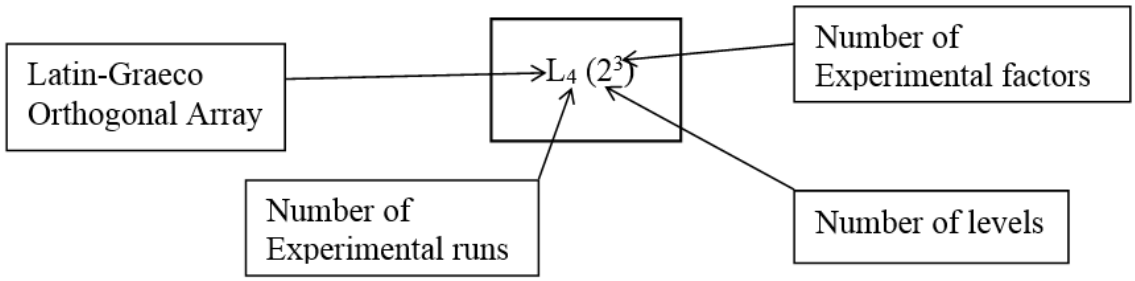


Figure 2.21: The notation of orthogonal array using Taguchi design method

2.8.2 Response surface methodology (RSM) analysis and optimization method

Response surface methodology (RSM) is a mathematical and statistical method that is to create, enhance and optimize a process. Response surface methodology can find a relationship between several factors that affect one or more response variables. Response surface methodology consists of statistical experimental design, regression of modelling technique and optimization process. The main purpose of using RSM is to get an optimal response of experimental designs. The design optimization in response surface methodology is intended to reduce the cost of analysis method. In the response surface

methodology, the equation and ANOVA analysis generated are essential to analyze the results obtained. The degree of significance of each factor is easily obtained using response surface methodology. The response surface methodology is a mathematical and statistical technique which can generate an empirical model based on the relationship between an experimental design and experimental data. In RSM, the relationship between a multiple parameters variables and single response can be modelled as a polynomial equation generated from regression analysis (Tsai et al., 2010). Besides, fit linear or square model can be used to indicate the experimental condition and optimization process. The equation generated is known as a response surface and graphically generated by a contour plot for optimal solution analysis. There are a few stages required to be considered before optimization process the experimental result by utilizing RSM application. The first step is the selection of an independent parameter or variable which gives a critical effect on the experimental process through screening processes which are related to the objective of the experimental research and experience gained by the researchers based on an experimental study conducted. The second step is a selection of an experimental design (polynomial modelling) to conduct the experiment based on experimental matrix. The third step is to determine a polynomial function fitted to the data obtained from the experiments that have been carried out. The fourth step is to evaluate based on the experimental results obtained for the polynomial functions according to sum of squares and lack of fit evaluated by analysis of variances (ANOVA). The fifth step is setting an initial estimation of optimum working condition of the systems and then moving closely to the actual optimum area. The sixth step is to ascertain the optimum value for each independent variable.

2.8.2.1 Screening of the independent variables

Screening is the most important strategy when there are many factors or variables involved in this research and it is very difficult to determine the effects of small contribution for each factor. Screening experiments is essential to select the independent variables or factors that contribute to the major effects and abolish the unnecessary variables. Apart from that, screening experiment is to determine control factors, response variables and quality characteristic such as larger the better (LTB), nominal the best (NTB), smaller the better of response variables (Tsai et al., 2010). According to Seifert et al. (1998), a screening experiment is conducted to determine the experimental factors and interaction between factors and response that have significant affect on the result. Full factorial or fractional factorial designs with linear or second order interaction models are commonly used in screening studies (Seifert et al., 1998).

2.8.2.2 Selection of polynomial modelling

The polynomial modelling is used to see reaction values when its control factors setting are given. When the actual function of the response becomes linear, the first order model is approaching. When, the optimization system of the response forms curvatures, the higher polynomial degree, for example, second order model (quadratic) or third order model (cubic) can be fitted.

2.8.2.3 Fit polynomial functions to experimental data

The next step after measuring experimental data is to fit polynomial function or mathematical equation to the data collected from the experiments in order to determine the behaviour of the measured value of the result from the experiments in accordance to a selected polynomial model. The polynomial function or mathematical equation is

generated through the method of least squares (MLS) and it can produce a minimum range of residual error between the sum of square actual data with an estimation of the data.

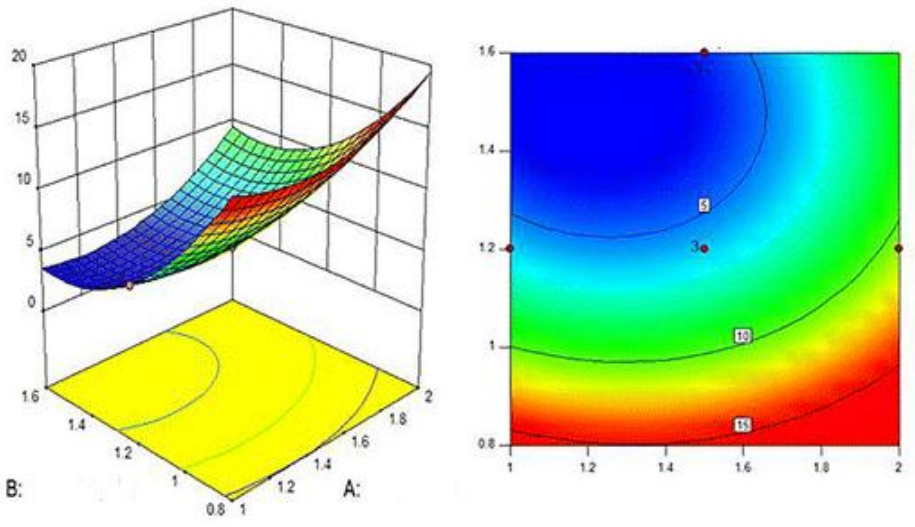
2.8.2.4 Evaluation of fitted polynomial function

Analysis of variance (ANOVA) is a one technique in statistical methods which is used to evaluate the adequacy of a fitted model by estimating the sum of squares and lack of fit test of the model. The total sum of squares in analysis of variance (ANOVA) represents the sum of variation that can be associate with various factors. The regression sum of squares of variation associate with the relationship between x and y factors. The sequential sum of square in analysis of variance (ANOVA) is an analysis which compares between models by adding the model terms to those that exist in the model and subject to the order of the factors entering into the model. The statistical test which is known as the p-value is used to distinguish whether the experimental results fall below the significance level and if it happens, the results are statistically significant. When the p-value becomes smaller, where the p-value is less than 0.05, the model terms are deemed significant. The small p-value indicates the highest polynomial model. The confidence level represents the degree of the confidence that the statistical finding result does not happen coincidentally or by sampling error. In addition, the standard of confidence level in numerous statistical test is 95%, with 5% confidence level or p-value.

2.8.2.5 Optimum operating conditions

The optimum operating conditions have been acquired through response surface analysis and is represented by the graphical behaviour graphs such as response surface plot and contour plot. Contour plot is an important graphical graph in the study of the response surface. The response surface plot and contour plot through design expert software help to

characterize, the form of surface by locating the optimal precision. All the graphical behaviour graphs show the significant effect of independent factors with the response. Figure 2.22 shows a response surface plot and contour plot which describes a surface with a maximum design and analysis of experiments.



(a) Response surface plot (b) Contour plot

Figure 2.22: Response surface plot and contour plot which describes a surface with a maximum design and analysis of experiments (Douglas, 2009)

2.8.3 Analysis of variances (ANOVA)

Analysis of variances (ANOVA) is applied to identify the most significant factors that affect the machining response (Yang et al., 2009). From the ANOVA analysis, the "Model F-value" is calculated using a formula of a model mean square divided by a residual mean square. Then, the F-ratio is the interaction between the variance of the response, rejection, and acceptance in which a significant machining parameters can be determined. Besides, the F-ratio contains information on the effect of a factor or interaction either significant or not. In ANOVA analysis, when the "p-value" is less than 0.05 ($p <$

0.05), hence, the terms in the model have a significant effect on the machining responses such as; surface roughness, cutting force, material removal rate and others. p-value is correlated with the F-ratio. When the F-value ratio is higher, then the p-value is smaller.

The analysis of variances (ANOVA), consists of three values of confidence level, namely 90%, 95% and 99% with the critical value of 10%, 5% and 1% respectively. When, the critical value is smaller, the confidence level is greater and more suitable for a high-risk machining response. Joshua et al. (2015) applied confidence level of 95% in end milling of aluminium 6061 through minimum quantity lubricants (MQL) method. In order to compare between the residual error and pure error, the lack of fit test is used. The result of lack of fit test shows that the residual error is larger than pure error, indicating this model is not deemed suitable to represent the experimental research. In short, the experimental results with the smallest p-value for the lack of fitting test should not be chosen.

In addition, the analysis of variances (ANOVA) calculates the regression model to complete all polynomial models and produces the sequential model sum of squares which consists of linear, quadratic, 2 factor interaction (2FI) and cubic. The results generated by the sequential model sum of squares can be utilized, as a guide to select the higher order polynomial where the additional terms are significant. Besides, the analysis of variances (ANOVA) can generate the summary of a statistical model and can calculate the statistical values such as the sum of square, mean square, F-value, standard deviation, R-squared, adjusted R-squared and predicted R-squared. This statistical model and statistical values are essential to identify the most significant factor that affect machining response.

Analysis of variance (ANOVA) is also used to evaluate the significant effects of individual independent factors and it is an important method to evaluate the polynomial model. In ANOVA analysis, statistical data, such as F-test and p-values can be used to assess the impact of individual, independent variables. F-test is used to test the variance

data, interaction and significance of each factor (Singh et al., 2014). Apart from that, F-test also examines the null hypothesis. When the null hypothesis states, $H_0 : \mu_1 = \mu_1$, this shows that the variance of two populations (factor and response) is equal. When, the F-value is approaching the value of 1, it indicates equality of variance for both the population hence, it can be accepted.

In addition, the F-value is directly proportional to the p-value. When, the F-value is larger and far from the value of 1, it is found that p-value is small and approaching the value of 1. The possibility to reject the null hypothesis is through the p-value. The null hypothesis, H_0 can be rejected when it is found that the p value is smaller than 0.05 ($p < 0.05$), indicating that the factor gives a significant effect to the response. When the statistical results show that p-value is larger than 0.05 ($p > 0.05$), the factors give insignificant effect to the response and do not affect the response.

2.8.4 Optimization

The final stage in the design of experiments is an optimization process by considering all the various factors. In the optimization process, verification is done by comparing experimental results obtained with a set of parameters that have the best response combination. Optimization process consists of single response and multiple response. In Design Expert software, optimization choice consists of numerical optimization, graphical optimization and point prediction. The best method of optimization process is using a multiple response optimization. Multiple response optimization techniques tend to improve the machining performance, production time and reduce cost for mould and die manufacturing.

In this study, desirability function and overlay plot are two techniques that can be applied to optimize multiple responses. The aim of this optimization process is to produce

the best machining parameters on slot milling of hardened mould and die materials using rotary ultrasonic assisted machining with the highest material removal rate and the lowest surface roughness and cutting force.

Values from the machining parameters related to the performances were converted into each individual desirability (d_i) scale. On each of the individual parameter function, the conditions are included to search for the closest value that meet the desired response. The scale of the individual desirability, d is ranged between 0 to 1 in which to represent less desire and fully desire respectively. This conversion helps to make it possible for summing and pooling the response values on different orders of magnitude. By summing up each of the individual desirability's, the total desirability (D) can be achieved. The total desirability function (D) is defined as the weighted geometric of the individual desirability (d_{indi}) and can be written as:

$$D = \sqrt[m]{d_1 d_2 \ \ldots d_m} \tag{2.12}$$

Number of responses analyzed in the optimization processes were denoted as m. Thus, the simultaneous optimization process was reduced to find the level of factors that demonstrate the maximum overall desirability. There are several types of transformations possible for obtaining individual desirability (Marcos et al., 2008). Thus, if the target value (T) for the response y is a maximum, the individual desirability (d_{ind}) is described by the following equation:

$$d_{ind} = \begin{cases} 0 \ if y < 1 \\ \left(\frac{y-l}{T-l}\right)^2 \ if l \leq y \leq T \\ 1 \ if y > t \end{cases} \tag{2.13}$$

Where l is the lower acceptable value to the response and y is the weight. Thus, when y = 1, the desirability function is linear. When y > 1 is chosen, a major importance is given to the points near to target value. When y < 1 is chosen, this last demand is of least importance. However, if the target value for the response y is minimum, the individual desirability (d_{ind}) is given by:

$$d_{ind} = \begin{cases} 1 \; if T < y \\ \left(\frac{U-y}{U-y}\right)^t \; if T \leq y \leq U \\ 0 \; if y > U \end{cases} \tag{2.14}$$

Where U is the upper acceptable value to the response and t is a weight. The same idea for y is applied for t to attribute levels of importance to the target value. If the target value (T) is located between the lower limit and the upper limit, then, a bilateral desirability function must be used. This function is expressed by the following equation. As demonstrated, t and y control the variation rate of the desirability functions. When these parameters are varied, it is feasible to attribute different desirability to the responses and, consequently, to increase or decrease the range of acceptable values in the optimization process.

$$d_{ind} = \begin{cases} 0 \; if y < l \\ \left(\frac{y-l}{T-l}\right) if l \leq y \leq T \\ \left(\frac{U-y}{U-T}\right)^t \; if T \leq y \leq U \\ 0 \; if y > U \end{cases} \tag{2.15}$$

Based on Equation (4.5) to (4.8), the desirability function was developed to search for the closest desired response namely the lowest surface roughness, lowest force and highest MRR value.

2.9 Summary

This chapter has reviewed literature on mould and die manufacturing and related components. Hardened tool steel AISI D2 is the best and suitable material for mould and die manufacturing because it has the characteristics of high wear resistance, high compressive strength, good through hardening properties, impact toughness, high stability in hardening and good response to heat treatment compared to other materials. The detailed knowledge about machining parameters of cutting speed, feed rate, depth of cut, frequency and amplitude vibration when milling process is very important and useful to improve productivity and machining performance in terms of surface quality, cutting force and material removal rate.

Hence, this thesis proposed a significant advancement on improving the mould fabrication process using a hybrid machining technique such as combining two established machining processes into a new combined set-up known as rotary ultrasonic assisted end milling (RUAEM). Cutting conditions for slot milling machining of rotary ultrasonic assisted end milling (RUAEM) are dry cutting (without any lubricant, oil, fluid, liquid cooling) and using 5%, 10%, 15%, 20% volumetric concentration of alumina oxide slurries with distrilled water as a transport medium for slurry, during slot milling experiments. Then, rotary ultrasonic assisted machining is required in machining AISI D2 hardened tool steel material to obtain an excellent quality of machined surfaces, higher material removal rate and lower machining force in comparison to conventional machining with the same cutting conditions parameters using different machining parameters, advanced cutting tools and advanced machining techniques in order to get a mirror machined surface.

CHAPTER 3

RESEARCH METHODOLOGY

3.1 Introduction

This chapter presents the methodology of the thesis which includes equipment, tools, procedure, technique, method used for collecting data and analysis of the data. The design of experiments (Doe) was used in this experiment for the purposes of planning and providing detailed analyses of the experiments.

Firstly, all the necessary fundamental knowledge of the concept, theories, and practice on machining of hardened mould and die material were identified. Factors such as machining parameters, material properties and performance measurement were identified and analyzed. Based on the literature, the preliminary technical solutions on the design criteria were proposed. Then, project planning was carried out so as to minimize the risks and failure of the project. The experimental setup for the equipment and instrument was designed and fabricated to suit the particular CNC machining centre. Statistical technique analysis was used to obtain the mathematical relationships between one or more independent variables obtained through full factorial analysis, Taguchi method and response surface methodology (RSM).

The method used for this thesis was a milling process with ultrasonic assisted vibration machining strategies of hardened mould and die material. In addition, the effect of machining parameters on surface roughness of hardened steel material by milling operation (slot milling) was also conducted using an ultrasonic tool holder assisted milling. The surface roughness of work piece is the major factor for satisfactory condition of the work piece under slot milling operation. Moreover, scanning electron microscopy (SEM)

was used to investigate the surface topography of machined surface by ultrasonic assisted vibration machining. In short, this chapter covers the material preparation until the final analysis of the experiments.

3.2 Research flowchart

This chapter describes briefly the process flow for this thesis. It presents the research method and procedures which are divided into three stages, as displayed in Figure 3.1.

Stage 1: Screening the most significant variables for further analysis.

Stage 2: Optimizing the variables values based on the performance criteria.

Stage 3: Validating the suggested optimal value between the predicted and experiment.

In the screening stage, Taguchi experimental design technique was used to eliminate the non-significant factors that had the least influence on the machining responses such as surface roughness, cutting force and material removal rate. Various factors may influence the response of the system studied, and it is essentially difficult to distinguish and control the little contributions from each one. Subsequently, it is important to choose those factors with significant impacts. Screening designs should be implemented to identify which of the few trial factors present more significant effects. Analysis of variance (ANOVA) and signal to noise (S/N) ratio and were utilized to identify and analyze the significance of the variables that affected the machining performance. Factors distinguished as insignificant will be wiped out for further analysis. The removal of distinguished factors helps to enhance the optimization of result obtained as the analysis will only focus on the most important and significant variables that affected the machining performance. The beginning of the screening stage was to create a process planning which

included preparation of materials according to the specified dimensions, machining parameters, part design, jig and tooling design. Then, Taguchi design technique was selected in the screening stage because its ability to reduce the variation around the design space. The selected variables were analyzed for cutting speed, feed rate, depth of cut, frequency, amplitude vibration and slurry abrasive concentration. A total of twenty-seven (27) runs were designed according to the L_{27} orthogonal arrays matrix. The machining performance such as surface roughness, cutting force and material removal rate was measured. Then, a screening process was carried out for all the machining parameters that affected machining performance during rotary ultrasonic assisted end milling (RUAEM) experiments. Variables identified as insignificant factors were eliminated for further analysis. The elimination helped to enhance the optimization of result obtained as the analysis would only concentrate on the most significant variables that affected machining performance.

Subsequently, response surface methodology (RSM) with historical data analysis (HDD) was used for design of experiment, analysis and optimization process for rotary ultrasonic assisted end milling (RUAEM) experiments with slurry abrasive. After RUAEM experiments with slurry abrasive was carried out, surface roughness, cutting force and material removal rate were measured and analysed using Design Expert 7.0. Then, ANOVA analysis was used to generate the mathematical equation for each performance of surface roughness, cutting force and material removal rate with based interaction on machining parameters in rotary ultrasonic assisted and milling. After the experiments, results were analysed and the optimization process was carried out.

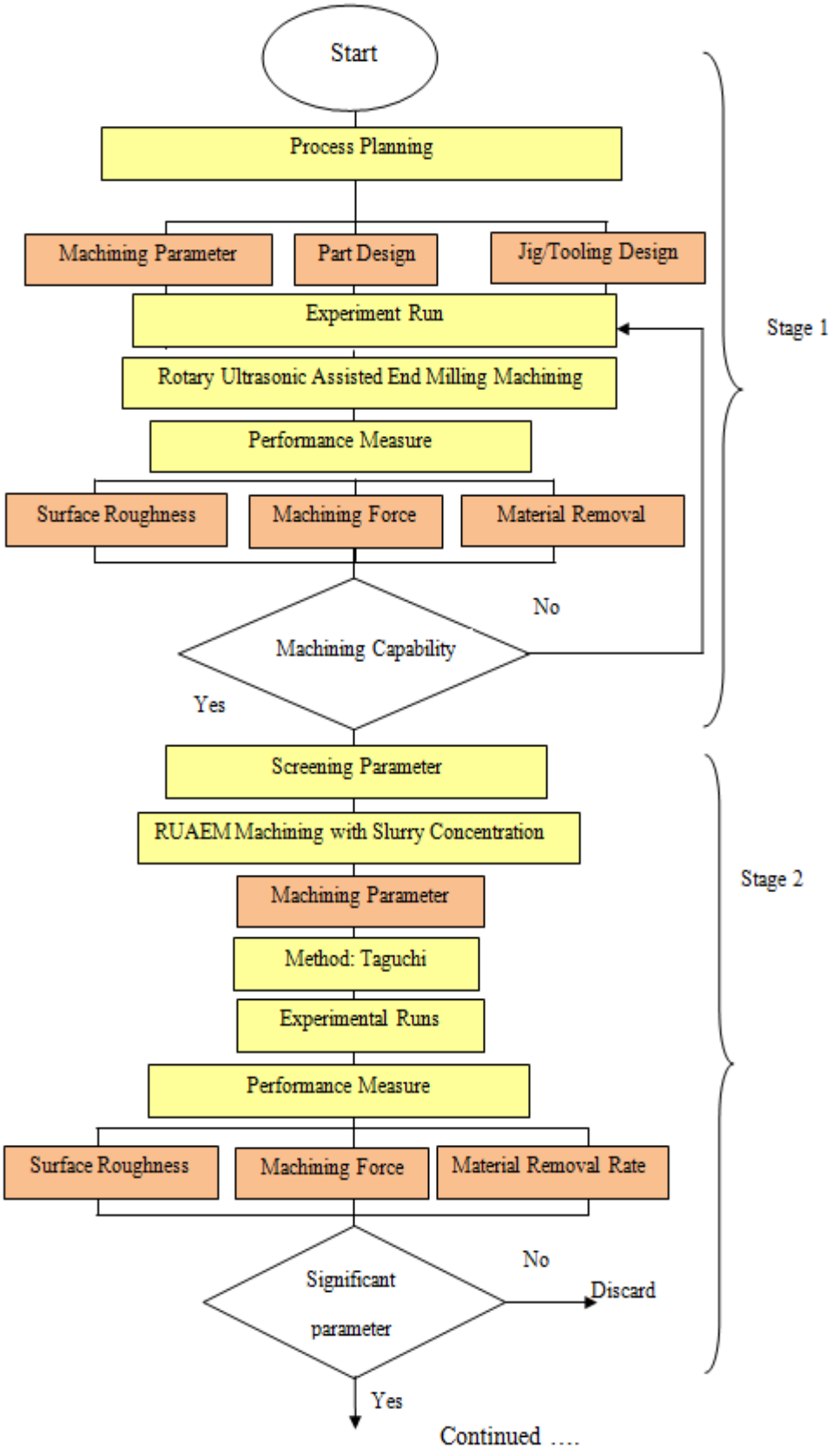
The next step to be conducted was the optimization procedure in order to select the most significant variables and eliminate the non-significant variables. The optimization process was carried out based on all machining parameters involved in RUAEM

experiments. A design matrix based on HDD was generated for further analysis of the selected variables obtained from the screening process by taking into account the machining performance in terms of surface roughness, cutting force and material removal rate. For optimization routine, the developed function of each performance used and the procedure were analyzed by adopting the desirability function approach. Then, individual desirability index, goals index and regions index would be the input for the optimization process. After optimization process was carried out, the overall desirability within the design spaces and the predicted optimal variables was generated. Then, the overlay plot of each performance associated with the machining parameters was developed for visual characterization of the feasible optimized region. Optimization stages based on the optimum conditions to generate a minimum surface roughness, minimum cutting force and high material removal rate. In the optimization stage process, verification is implemented by comparing the results with a set of parameters that have the best response combination. In Design Expert software analysis, an optimization stages consists of numerical optimization, graphical optimization and point prediction. The best method of optimization stages process is using a multiple response optimization. Furthermore, the multiple response optimizations is the method for the optimum desire response condition to be achieved. The advantage using of multiple response optimization techniques is improving the machining performance, aiming to improve the production time and reduce cost in mould and die manufacturing.

The desirability function and overlay plot are two techniques that can be applied to optimize multiple responses. The goal of this optimization stage is to generate the best machining parameters on slot milling of hardened mould and die material using rotary ultrasonic assisted end milling machining with the lowest surface roughness, lowest resultant cutting force (F_R) and high material removal rate. In the optimization stage

process, verification is done by comparing the results with a set of parameters that have the best solution response combination. Besides that, numerical optimization was used with set goals for each response for the optimization process conducted. The goals of machining parameters such as cutting speed, feed rate, depth of cut, frequency vibration, amplitude vibration and slurry concentration have been set as in range. Then, the goals of machining performance such as surface roughness, resultant force (F_R) have been set as minimum and material removal rate (MRR) has been set as maximum.

Lastly, a validation process was performed using the most effective parameters that could highly respond and assess amount of the relative errors between the predicted and experimental results. The Figure 3.1 below shows a flowchart of research activities involved in the slot machining of hardened steel material using RUAEM.


Start
Process Planning
Machining Parameter
Part Design
Jig/Tooling Design
Experiment Run
Rotary Ultrasonic Assisted End Milling Machining
Performance Measure
Surface Roughness
Machining Force
Material Removal
No
Machining Capability
Yes
Stage 1
Screening Parameter
RUAEM Machining with Slurry Concentration
Machining Parameter
Method: Taguchi
Experimental Runs
Performance Measure
Surface Roughness
Machining Force
Material Removal Rate
No
Significant parameter
Discard
Yes
Stage 2
Continued ….

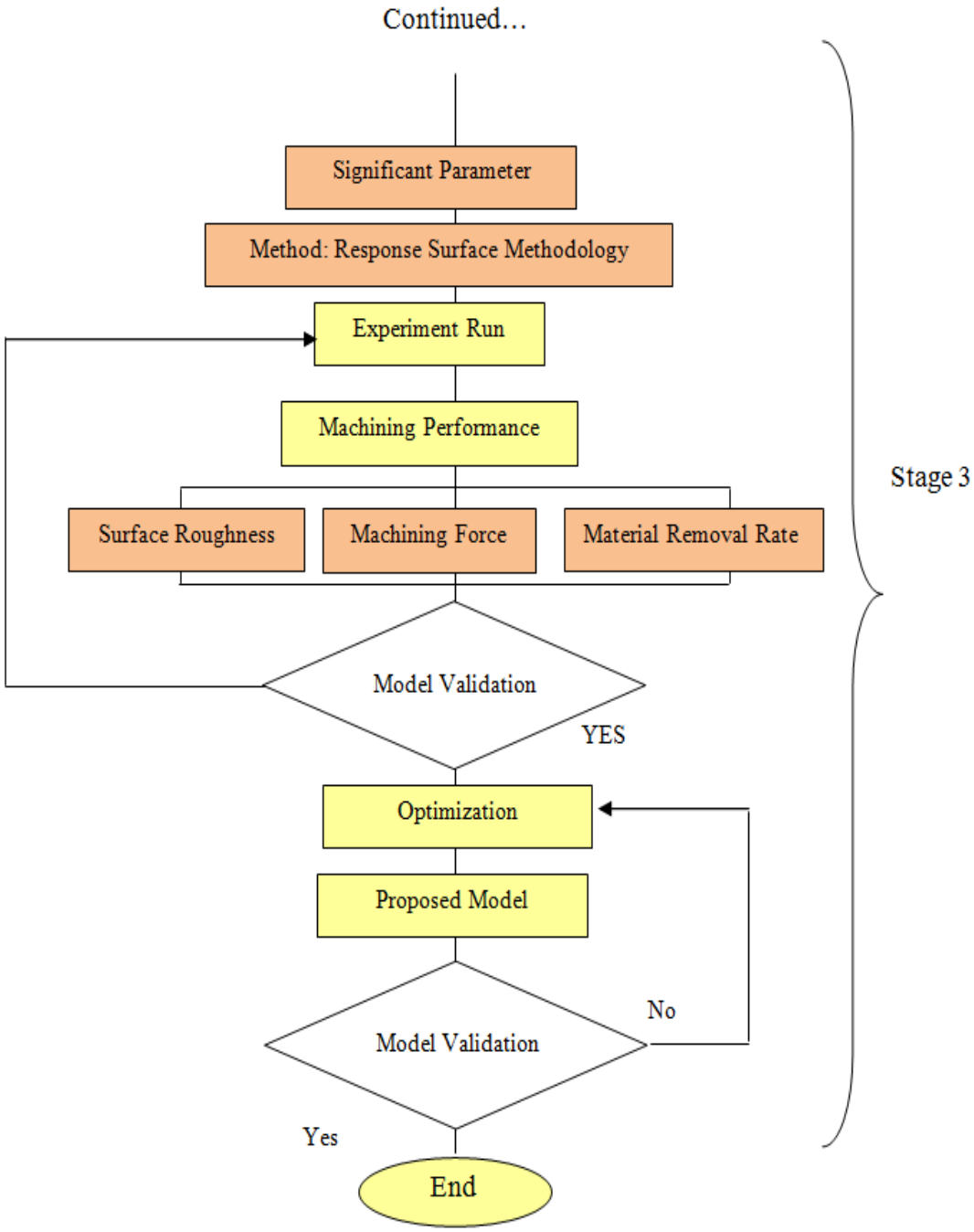


Figure 3.1: Flow chart of research activities

3.3 Work piece material and cutting tools

3.3.1 Work piece material

The work piece material employed in this study was a rectangular block of hardened AISI D2 cold work tool steel with the dimensions of 100mm × 100mm × 20mm (W×L×H) and Rockwell hardness of 61 HRC.

According to the ISO 8688-2 International Standard for tool life testing in milling (part 2: end milling), the recommended work piece shall be a bar or billet of rectangular cross-section with a minimum width of 2 times the cutter diameter and minimum length of 10 times the cutter diameter but preferably with a recommended length of times the cutter diameter. A formula of the recommended work piece for end milling is as follows:

Minimum Width = Minimum Width = 2 X cutter diameter

Minimum Length = Minimum Length = 10 X cutter diameter

Recommended Length = Recommended Length = 20 X the cutter diameter ISO 8688-2: 1998 (E)

The chemical material composition of AISI D2 tool steel is shown in Table 3.1.

Table 3.1: Chemical composition of AISI D2 tool steel

Composition	**C**	**Si**	**Mn**	**Cr**	**Mo**	**V**
% weight	1.55	0.3	0.4	11.8	0.8	0.8

A horizontal band saw from Wasbek Manufacturer was used to cut the work piece material into the smaller blocks of 100mm × 100mm × 20mm (W×L×H) in a rectangular shape before underwent slot milling machining test. While, the Bridgeport vertical milling

machine was used for facing and squaring the work piece (raw material) into a rectangular shape. The raw material of AISI D2 tool steel was skimmed down to 0.5 mm by vertical milling machine to remove any surface problem, cracks or any defects from the manufacturing process (Kasim et al., 2013). The last process for work piece preparation was done using surface grinding machine. The machine was used for last surface finishing processes for a work piece in preparation, aiming to get a perfectly flat work piece surface. The surface roughness (Ra) value of work piece surface before slot milling by RUAEM is about 0.905 μm (micrometer). The cutting process and work piece facing surface process are shown in Appendix B. This experiment was implemented with 162 runs of slot milling with different cutting speeds, feed rates, depths of cut, frequencies of vibration and amplitude vibrations by conventional machining, conventional rotary ultrasonic assisted end milling machining (RUAEM) with 5%, 10%, 15%, 20% volumetric concentration of alumina oxide slurry-distrilled water mixture to investigate relationships between cutting parameters and machining performances (surface roughness, cutting force, material removal rate) and work piece after slot milling experiments. The cutting length of slot milling was performed for conventional machining, conventional rotary ultrasonic assisted end milling machining (RUAEM) with 5%, 10%, 15%, 20% volumetric concentration of alumina oxide slurry-distrilled water mixture is 100 mm and parallel to cutting axis. Figure 3.2 shows AISI D2 hardened tool steel material used in this experiment.

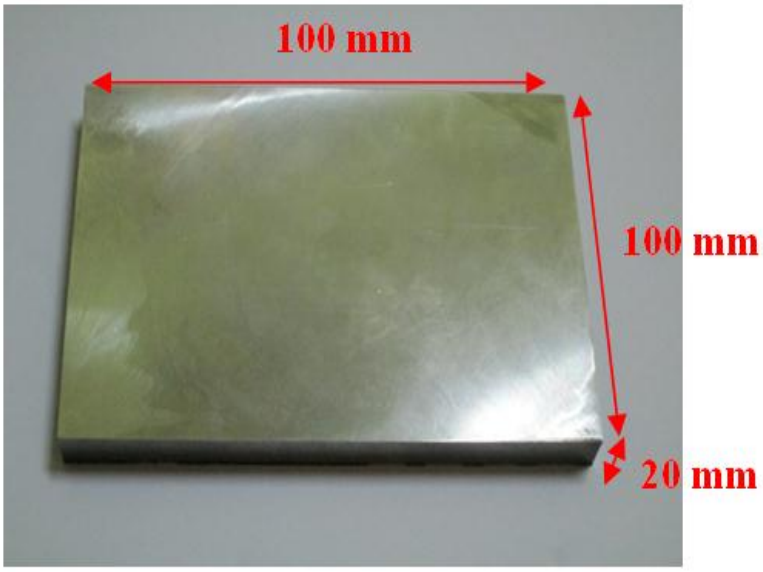


Figure 3.2: AISI D2 hardened steel work piece

3.3.2 Cutting tools

A cutting tool is any tool used for any machining operation that involves removal process of metal from work piece by shear deformation and cutting action. The material used to make a cutting tool or cutter must be harder than the material to be machined. The cutting edge geometry of a cutting tool such as rake angle, corner radius, clearance angle and the condition of cutting edge is an important factor for choosing a suitable cutting tool in machining operations that involve high precision machining.

The new cutting tools were used for each new run experiments to produce a better result from each run with high surface finish of machined surface.

3.3.2.1 Cutting tool materials

Many materials are generally used for making cutting tools such as high speed steels, stellite, hard metals, cermets, sialons, ceramics, silicon carbide, cubic boron nitride and diamonds.

3.3.2.2 Cutting tool requirement

The ideal cutting tools must have the best performance when machining processes and the criteria of ideal cutting tool are as follows:

a. Hot hardness. When machining processes occur, the tools can maintain sharpness and consistent cutting edge with the increasing of temperature during machining.

b. Endurance to thermal shock. The tools have resistance to the continuous cycle of heating and cooling, which always occur during the machining process.

c. Lack of affinity. Lack of affinity occurs when there is an interaction between cutting tool and work piece. Any degree of lack affinity between cutting tool and work piece will lead to a formation of built up edge (BUE) with poor chip breaking ability, high force generated during machining and poor surface finish of machined surface.

d. Resistance to oxidation processes. The cutting edge of cutting tools should have an excellent condition during the machining process to obtain a high resistance to oxidation process.

3.3.2.3 Cutting tool for machining AISI D2 hardened steel

For this experiment, an integral shank tool was used for each set of experimental condition. The type of integral shank tool used was a straight shank mounted on BT40 tool holder of HAAS CNC machine for highly strong, rigid and precise foundation with less vibration and effective distribution of cutting forces. The straight shank used for this experiment was purchased from the Tungaloy Company (Member IMC Group) of EPH Hybrid TAC mills series because it fits with ultrasonic tool holder assisted milling. Figure 3.3 shows the cutting tool from Tungaloy company used in this experiment. The specific description of straight shank of EPH Hybrid TAC mills used was EPH11R010M06.0-2.

Figure 3.4 shows EPH body specifications of the cutting tool used in these experiments. EPH type of shank from Hybrid TAC Mills Tungaloy company is a high precision milling process with low cutting force, high productivity levels and high accuracy machining compared to solid carbide end mills. Figure 3.5 shows a straight shank of cutting tools with coated carbide insert. Coated carbide inserts with multilayer coating TiAlN produced by the Tungaloy company was selected as the cutting tools for machining the work piece. The XHGR110208ER-MJ AH730 from the EPH Hybrid TAC Mills of the Tungaloy company was a precision insert for the multipurpose ground machining. The type insert used in slot milling for conventional machining, conventional rotary ultrasonic assisted end milling machining (RUAEM) with 5%, 10%, 15%, 20% volumetric concentration of alumina oxide slurry-distrilled is type of XHGR110208ER-MJ AH730 coated with TiAlN with coating thickness of 2-5 microns, 2 point cutter teeth, 0.8 mm of corner radius and 11 mm of overall insert length. The specification of the XHGR110208ER-MJ AH730 insert is shown in Table 3.2. The picture of the XHGR110208ER-MJ AH730 insert is shown in Figure 3.6. This type of cutting tool can be used for hole enlarging, plunging, pocket milling, ramping, shoulder milling, shoulder milling with radius, side milling and slot milling.



Figure 3.3: Cutting tool (shank)

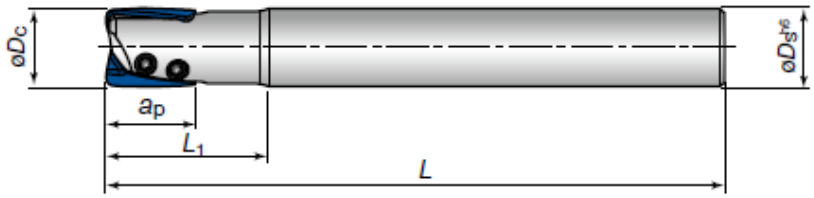


Figure 3.4: EPH body specification

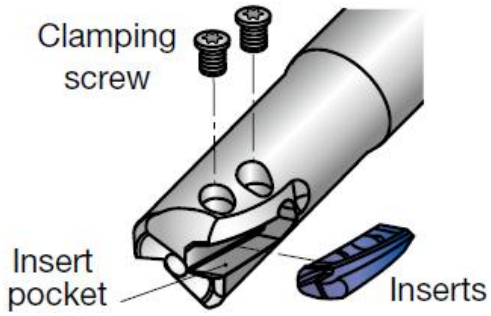


Figure 3.5: Straight shank specification with coated carbide insert

Table 3.2: The specification of the XHGR110208ER-MJ AH730 insert

Type	**XHGR110208ER-MJ AH730**
Shape	Rectangle
Grade	AH730
Coating	TiAlN
Applicable material	Steel
Insert edge length	0.433″
Cutting length	0.394″
Corner radius	0.031″
Cutting edge material	C

(http://www.cmtindustrial.com/catalogue/product/247874)

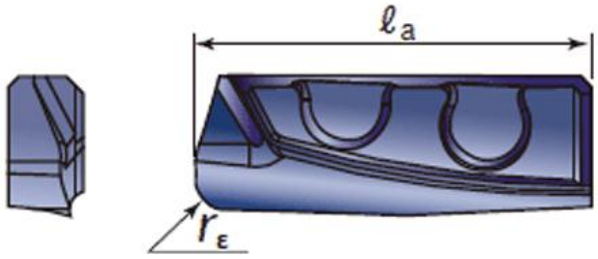


Figure 3.6: Type XHGR110208ER-MJ AH730 insert was used for this experiment

The procedure of EPH insert mounting is illustrated in Appendix C.

3.4 RUAEM machine and equipment

The equipment used in RUAEM experiment was the ultrasonic tool holder assisted machining (BT40), amplitude meter (digital) and computer numerical control (CNC) milling machine.

3.4.1 Ultrasonic tool holder assisted machining (BT40)

Ultrasonic tool holder assisted machining is categorized as ultrasonic vibration cutting because it is influenced by the important parameters of vibration frequency. It is also suitable for machining hard to cut materials. The advantages of using the ultrasonic vibration cutting (ultrasonic tool holder assisted machining) are low vibration cutting with low power consumption, high accuracy of machined surface, low surface roughness of machined surface, tool life of cutting tools and various materials cutting. Ultrasonic tool holder assisted machining is designed to collet stucture and is deemed suitable for BT40 CNC (computer numerical control) machine tool holder which is compatible with all kinds of cutting tools. The features of the ultrasonic tool holder assisted machining is simple design structure, easy to plug-in, simple modification and easy to install.

The type of ultrasonic tool holder assisted machining is the NUTH-BT40-ER-11. It is equipped with 3 pin connectors for AC (alternating current) power input and comes with an input control box AC (alternating current) 110~220 Vac (volts electrical pressure of alternating current) power input which can be select by switch. Ultrasonic output terminals contain 2 pin connectors for connecting to the spindle or ultrasonic tool holder. The controller I/O inputs fit with interconnect controller (12 pin connector) and control box. The control box connects to the ultrasonic tool holder through 12 pin connectors to control the functions. The ultrasonic control box specification and pin connectors are shown in Tables 3.3 (a) and 3.3 (b) respectively. Table 3.4 shows the NUTH-BT40-ER-11 specifications.

Table 3.3 (a): Ultrasonic control box specification

Ultrasonic control box specification	
Dimension	Length 325 mm X Width 262 mm X high 90 mm
Weight	5 kg
Input power	110 ~ 220 VAC selected by switch
Power frequency	47 Hz ~ 63 Hz
Frequency	20 ~ 27 kHz
Maximum output power	300 W
Frequency scanning modes	Manual or PLC I/O control
Display panel	Power On Indicator
	Ultrasonic output indicator
	Malfunction light
The controller signal input I/O	Ultrasonic control box power up

	Ultrasonic output
	Frequency scan
	Abnormal signal warning
Manual control	Ultrasonic scan
	Ultrasonic output

Table 3.3 (b): Pin connector

Pin connector no.	**Explanation**
1	No
2 (red)	Frequency scanning control, use DC24+12 V driving
3 (orange)	Output control
4	No
5	No
6	No
7 (black)	GND
8	No
9	No
10	NO
11 (yellow)	Alarm contacts
12 (green)	Alarm contacts

Table 3.4: Ultrasonic tool holder NUTH-BT40-ER-11 specification

Ultrasonic tool holder NUTH-BT40-ER-11 specification	
Holder Type	BT 40
Weight	3.5 kg
Input Power	110 V, 220 AC 50/60 Hz
Maximum output	300 W
Tool Speed	Max. 6000 rpm
Tool Interface	ER-11
Ultrasonic Power	100~220 V
Operating Frequency	20 ~ 27 kHz
Frequency Adjustment	Auto Search
Power Adjustment	Manual
Vibration Average	< 20 μm

Figure 3.7 and 3.8 show the dimensional drawing and ultrasonic tool holder of NUTH-BT40-ER-11 used in the experiments. The power supply converter electrical supplied high frequency electrical energy whereas the high frequency electrical energy is distributed to a piezoelectric converter, converting the electrical energy into mechanical vibration.

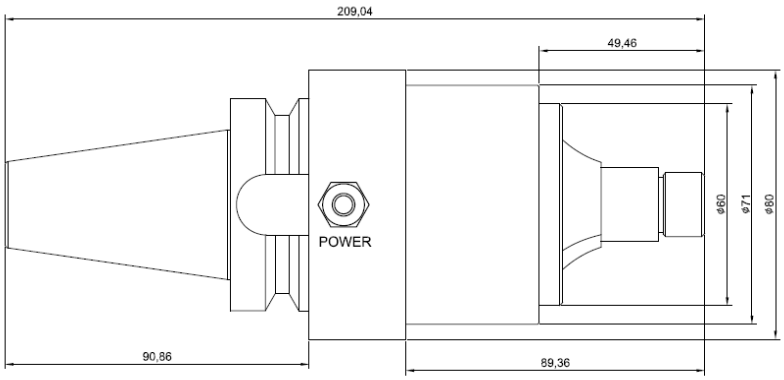


Figure 3.7: The dimensional drawing of ultrasonic tool holder NUTH-BT40-ER-11

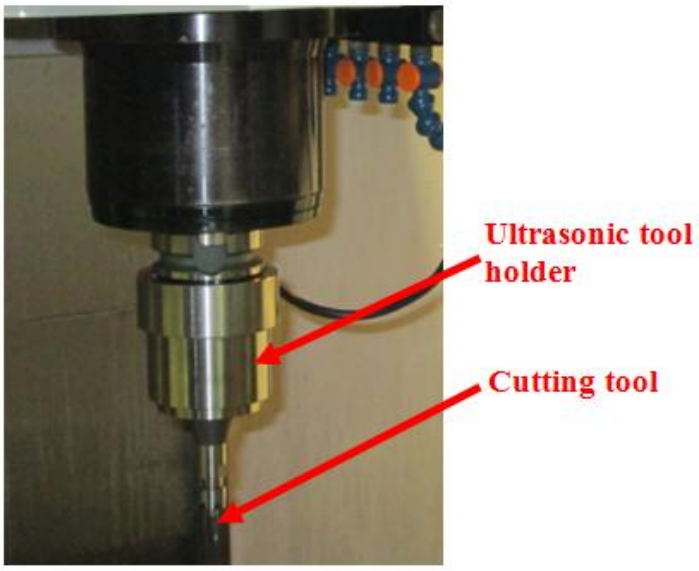


Figure 3.8: Ultrasonic tool holder NUTH-BT40-ER-11

The amplifier would strengthen the ultrasonic vibration and the ultrasonic vibration was delivered to the rotating cutting tools. The rotating cutting tool with ultrasonic vibration vibrated in the perpendicular direction of the work piece surface. The function of the ultrasonic spindle control system was to scan, control and generate suitable vibration frequency output during the milling machining. The ultrasonic processor control system equipped with ultrasonic tool holder is schematically illustrated in Figure 3.9.



Figure 3.9: The ultrasonic processor control system equipped with ultrasonic tool holder

3.4.2 Amplitude meter (digital)

A dial indicator method is the measurement of vibration amplitude in rotary ultrasonic machining (RUM) used in industry (Cong et al., 2011). In this experiment, the equipment used for measurement of vibration amplitude in hybrid rotary ultrasonic assisted machining was an amplitude meter with digital reading. This amplitude meter (digital) measured variations of ultrasonic amplitude output with digital reading. The accuracy of the measurement reading was 1 μm (micrometer). Figure 3.10 shows the amplitude meter (digital) equipment used for measurement of vibration amplitude during ultrasonic assisted machining.



Figure 3.10: Amplitude meter (digitally reading) used in the measurement of amplitude vibration

3.4.3 Computer numerical control (CNC) milling machine

This experimental work was conducted using a computer numerical control (CNC) milling machine with 3 axes to ensure the cutting speed, feed rate, depth of cut and cutting force were applied successfully. The machining process was conducted in dry cutting and abrasive slurry (namely alumina oxide) condition using a Kistler dynamometer to measure a cutting force. A dynamometer was very sensitive to coolant or fluid during the machining process. The ultrasonic vibration assisted machining for milling process carried out on CNC milling machine namely HAAS VF-1. The CNC vertical milling (HAAS CNC milling VF-1) specification is shown in Appendix D and Table 3.6 shows the machines, equipments and software used for the experiment.

3.5 RUAEM experiment setup

The experiment set up for rotary ultrasonic assisted end milling machining on slot milling AISI D2 hardened tool steel material involved ultrasonic tool holder assisted machining, ultrasonic processor with frequency controller, amplitude controller using DC power supply and calibration of vibration amplitude and frequency.

3.5.1 Rotary ultrasonic assisted machining equipped with an ultrasonic tool holder

The equipment consists of ultrasonic tool holder assisted machining, ultrasonic controller, cutting tools and Kristler dynamometer for measuring cutting force in 3 directions (Fx, Fy, Fz). The experiment setup is shown in Figure 3.11 and Figure 3.12.

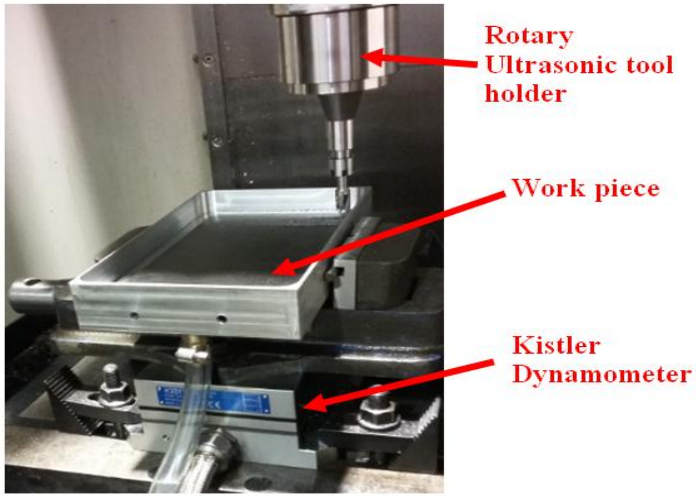


Figure 3.11: An experimental setup of ultrasonic tool holder with Kistler dynamometer



Figure 3.12: Experimental setup of rotary ultrasonic assisted end milling machining with Kistler dynamometer, frequency controller and voltage controller

3.5.2 Ultrasonic processor with frequency controller

The ultrasonic tool holder was controlled manually by ultrasonic processor using a frequency controller. The ultrasonic processor scanned the ultrasonic tool holder with the cutting tool to produce a rotary vibration machining during slot milling operation. The frequency input was manually entered to the frequency controller. The minimum frequency operating of ultrasonic tool holder was 20,000 Hz (20 kHz) whereas the maximum frequency operation was 27,000 Hz (27 kHz). Frequency between 20,000 Hz (20 kHz) to

27,000 Hz (27 kHz) was chosen because the capacity of RUAEM ultrasonic frequency and rotary ultrasonic tool holder ranges between 20 kHz to 27 kHz. The frequency output from frequency controller was measured by 3 in 1 EMF multimeter. Figure 3.13 shows the ultrasonic processor with frequency controller and 3 in 1 EMF multimeter.



Figure 3.13: An experimental setup of ultrasonic processor and frequency controller

3.5.3 Amplitude controller using DC power supply

The DC power supply was used to produce voltage and generate amplitude vibration for ultrasonic tool holder during slot milling cutting. Figure 3.14 shows a DC power supply used to generate voltage.

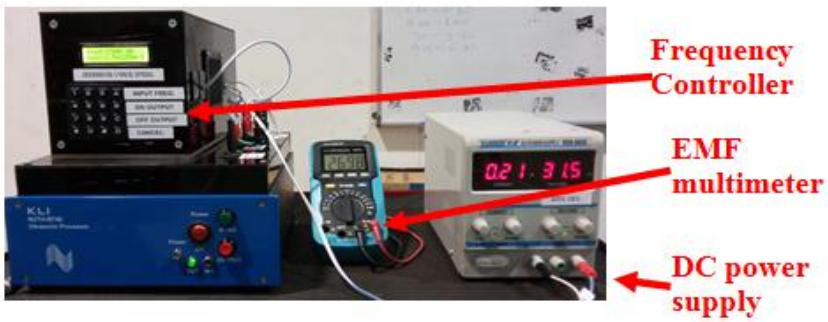


Figure 3.14: An experimental setup of DC power supply with ultrasonic processor and frequency controller

3.5.4 Calibration of vibration amplitude and frequency

The calibration process was carried out before starting the experiments. The calibration process involved the frequency, voltage and vibration amplitude. Figure 3.15 shows the setup for the calibration process. Table 3.5 shows the value of calibration of vibration amplitude with frequency and voltage input settings. According to Table 3.5, calibration of amplitude vibration and frequency with voltage and current input shows that the calibration error for frequency and amplitude vibration which were ranging between 0.5 % to 1.8 % and 0.7 % to 3 % respectively. The low calibration error for frequency and amplitude vibration which less 10% clearly indicated that the calibration amplitude and frequency very well and therefore the result obtained from this experiment is high accuracy with minimum errors.

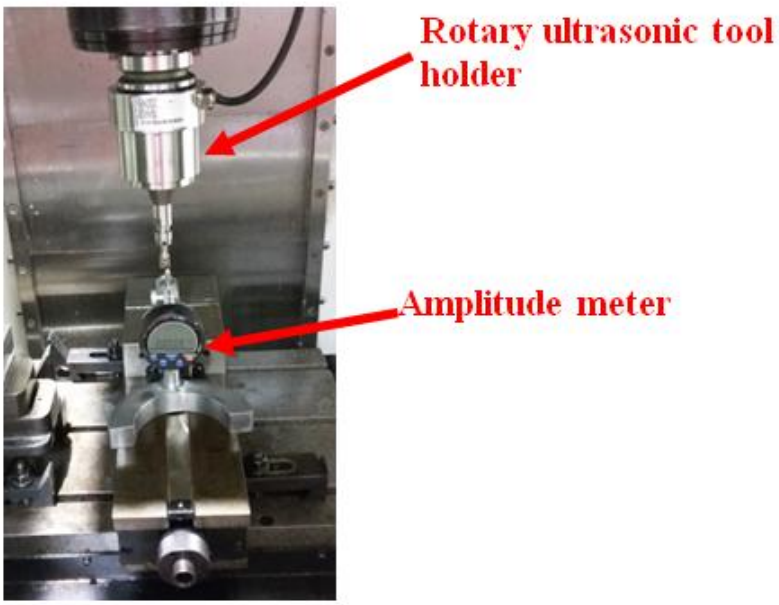


Figure 3.15: The setup of calibration process for vibration amplitude with the control by frequency input

Table 3.5: The value of calibration of vibration amplitude with frequency and voltage input settings

Input Frequency from Control Box (kHz)-Estimated Value	Input Frequency from Control Box (kHz)-Actual Value	Calibration Error-Frequency (%)	Voltage input from DC power supply (Volt)	Current, Output from DC power supply (Ampere)	Vibration amplitude generated by amplitude meter (μ meter)-Estimated Value	Vibration amplitude generated by amplitude meter (μ meter)-Actual Value	Calibration Error-Amplitude (%)
20.0 kHz	19.7 Hz	1.5 %	15 V	0.13 A	1 μm	0.97 μm	3 %
20.0 kHz	19.8 Hz	1.0 %	31.5 V	0.22 A	2 μm	1.98 μm	1 %
20.0 kHz	19.9 Hz	0.5 %	48 V	0.31 A	3 μm	2.98 μm	0.7 %
23.0 kHz	22.6 Hz	1.8 %	15 V	0.17 A	1 μm	0.97 μm	3 %
23.0 kHz	22.7 Hz	1.3 %	31.5 V	0.31 A	2 μm	1.97 μm	1.5 %
23.0 kHz	22.8 Hz	0.8 %	48 V	0.47 A	3 μm	2.98 μm	0.7 %
27.0 kHz	26.6 Hz	1.5 %	15 V	0.17 A	1 μm	0.97 μm	3 %
27.0 kHz	26.7 Hz	1.1 %	31.5 V	0.31 A	2 μm	1.98 μm	1 %
27.0 kHz	26.8 Hz	0.7 %	48 V	0.48 A	3 μm	2.98 μm	0.7 %

3.6 Machining performance measurement

The machining performance measurement involved measurements in terms of surface roughness, cutting force, material removal rate and qualitative.

3.6.1 Surface roughness measurement

Surface measurement could be classified as surface metrology because it determines the topography of the surface. The surface measurements include surface finish, surface texture, structural characterization and surface profile roughness. Surface roughness is called surface profile, Ra. Surface roughness is associated with the surface finish which is a topography scale of texture on the surface. Besides, the surface roughness is the vertical variation over a measured distance and the arithmetic average of all departures of the roughness profile from the center line within the appraisal length.

The surface roughness measurement for machining hard to cut materials (hardened steel, AISI D2) using rotary ultrasonic assisted machining is arithmetic mean surface roughness average, Ra. The standard for the roughness average is ISO 4287, BS 1134, ANSI B46.1 and DIN 4768. The R profile is the default assessment length of the roughness parameters. Prior to the measurement of surface roughness, the surface roughness equipment of Mitutoyo Surftest SJ-301 was calibrated before the measurement process using a standard plate from Mitutoyo instrument manufacture.

The machined surface is measured parallel to the slot cutting direction (Chen et al., 2005). The cut off wavelength (λc) used in surface roughness measurement was $\lambda c = 0.8$ mm. The evaluation length (EVA-L) used in surface roughness measurement was 4 mm. Surface roughness measurement was performed 10 times at random locations along the slot milling. The equipment used in surface roughness measurement was surface roughness tester (surface quality or roughness measurement).

3.6.1.1 Surface roughness tester (surface quality or roughness measurement)

Surface finish is also known as surface texture or surface topography which is the nature of a surface defined by 3 characteristics namely lay, surface roughness, and

waviness. The surface finishing is a broad range of industrial processes that alter the surface of a manufactured item to achieve a certain property and very important characteristic of a product after machining processes. The surface roughness of the material in most research is measured by Mitutoyo Surftest SJ-301.

The machined surface part for measuring is surface roughness and Ra is measured. Ra is the first roughness parameters that is developed and refers to the average deviation of the profile from the mean line. Besides, Ra is known as mean average roughness. Table 3.6 illustrates the Mitutoyo SJ301.

3.6.2 Cutting force measurement

Cutting force is the high compressive and frictional contact stresses between the tool face and work piece materials. The importance of cutting force measurement in slot milling machining is its ability to optimize cutting parameters and improve a cutting process. The cutting force can be measured and analysed using a sophisticated sensor. The sophisticated sensor can record a magnitude of cutting force during milling, grinding, turning, drilling and tapping process. Chen (2000) indicated that the feed force is the minimal of three force components whereas the thrust force is the highest component among the three force components when using ultrasonic vibration assisted machining Zhou et al. (2003) and resultant cutting force is the most important cutting force component compared to other force components. In this experiment, resultant cutting force (F_R) was measured during the slot milling using rotary ultrasonic assisted end milling (RUAEM) of hardened steel material. The measurement of cutting force can be achieved by a stationary or rotating dynamometer and the acquired signal is assessed with the aid of electronic hardware and supported software. Kistler dynamometers was used to measure all of the cutting force components (Fx, Fy,Fz) during slot milling machining in this study.

Before conducting the cutting force measurement process, the dynamometer, charge amplifier and control units were switched on for 30 minutes for warming up purposes.

Calibration for cutting force measurement was carried out by placing a weight of 0.5 to 1 kg and compared with results obtained from the DynoWare display screen and 1 kg standard block. The equipment used in cutting force measurement was Kistler dynamometer, control unit type 5233A and DynoWare Software.

3.6.2.1 Kistler dynamometer

The cutting forces were measured using dynamometer in three (3) linear directions of forces namely Fx (feed force), Fy (feed normal force) and Fz (thrust force) using Kistler piezoelectric dynamometer Type 9257B with built-in charge amplifier and 4 measuring ranges switchable. In addition, the Kistler dynamometer comprises four 3-components sensors, fitted under high preload between base plate and cover plate. A 3-channel charge amplifier is ready to be installed in the dynamometer. The output signal produced from the dynamometer is low impedance and the integrated cable is connected from the dynamometer to the control unit type 5233A1. The control unit can measure all the component of cutting forces in x-axis (Fx), y-axis (Fy) and Z-axis (Fz). Figure 3.16 shows the dynamometer and control unit of 5233A1 used for measuring the cutting forces during slot milling machining. Table 3.6 shows the Kistler dynamometer.



Figure 3.16: The dynamometer and control unit used for cutting force measurement during slot milling machining

3.6.2.2 Control unit type 5233A

The control unit type 5233 A is an external control unit for the range of selection, reset and operate as shown in Table 3.6. The range of cutting force in Fx direction and Fy direction is between 500N to 5KN whereas the cutting force in Fz direction is 1KN to 10 KN. The signals from the dynamometer were acquired at a sampling rate of 1 ms intervals using Kistler DAQ card and analyzed using the Kistler DynoWare software. the control unit type 5233A is shown in Table 3.6.

3.6.2.3 DynoWare software

The software used for measuring the cutting force is DynoWare. DynoWare is a general purpose data acquisition and display software package deemed suitable for cutting force and general dynamometer application. It is designed to combine the performance of the proven line of Kistler quartz dynamometer with modern computer technology. DynoWare is quickly to setup, record and display reaction forces and moments. DynoWare is a simple operation, configuration and control of Kistler measuring instruments through RS-232C or IEEE 488 interface; powerful graphics functionality; useful signal evaluation

and calculation functions; simultaneous recording of up to 8 measuring channels; this software is also ideal for recording and evaluating any physical quantity measurement. Table 3.6 shows a DynoWare software to measure a magnitude of cutting forces.

The measuring range of hardware (M.U.) and the hardware sensitivity (mV/M.U.) of cutting force measurement was updated before carrying out the measurement. The measuring range of hardware for cutting forces on all axis is 5000 N (Fx), 5000 N (Fy) and 10,000 (Fz) respectively whereas the sensitivity of hardware for cutting forces on all axis is 1.00 (Fx), 1.00 (Fy) and 0.50 (Fz) respectively. All settings for the measuring range (M.U.) and hardware sensitivity (mV/M.U.) are based on recommendations from the Kistler dynamometer manufacturer. Figure 3.17 shows the setting for the measuring range (M.U.) and hardware sensitivity (MV/M.U.).

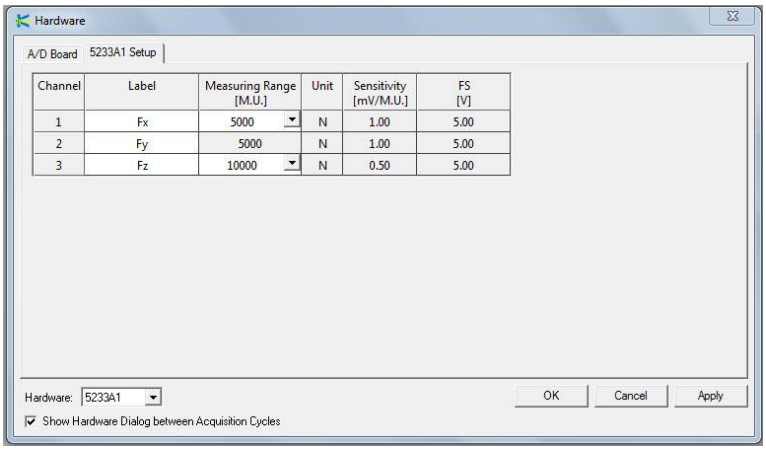


Figure 3.17: The setting for measuring range (M.U.) and hardware sensitivity (MV/M.U.) as recommended by Kistler manufacture

3.6.3 Material removal rate measurement

The material removal rate for this experiment was measured through the total weight of material removed by the total machining time. Total weight material removed is the amount of weight material removed in order to produce a machined slot and total

machining time is the total machining time taken to produce a machined slot during machining (Bertsche et al., 2013). The equipment used in the material removal rate measurement are EDM (electro discharge machining) Wire cut, ultrasonic cleaning and weighing scale. The detail explanation of EDM (electro discharge machining) wire cut and ultrasonic cleaner is shown in Appendix E. The total weight of removed material was measured by a digital weighing scale machine. Table 3.6 shows the weighing scale used in the experiments for measuring weight of removed material in order to produce a machined slot.

3.6.4 Qualitative measurement

Qualitative measurement is a measurement used to measure the quality of work piece machined surface after slot milling machining by rotary ultrasonic assisted end milling machining. The equipment used are Rockwell hardness machine, optical microscope and scanning electron microscopy (SEM).

3.6.4.1 Rockwell hardness machine

The definition of hardness according to the Metal Handbook is the measure resistance of metal to plastic deformation by surface indentation. The meaning of resistance of metal refers to stiffness, temper and resistance to scratching, abrasion, or cutting. When, the hardness of metal increases, the metal resistant to deformation increases. The hardness test often used in research areas and industry sectors are Brinell hardness test, Rockwell hardness test and Vickers hardness test. According to the American Society for Testing and Materials (ASTM), the Rockwell hardness test is a commonly used technique for hardness test.

The type of Rockwell hardness testing was used for measurement of AISI D2 hardened steel work piece before undergoing the process of slots machining. The principle of Rockwell hardness test is measuring hardness of materials according to the net increment depth of load applied. Diamond indenter is used in Rockwell hardness testing for measurement of hardness of AISI D2 hardened steel work piece. The hardness scale of C is used for Rockwell hardness testing because the AISI D2 hardened steel is categorized as hard material. In testing AISI D2 hardened steel, a 120°(degrees) diamond indenter is used and 150 kg load is directly applied to the hardened steel work piece to measure AISI D2 hardened steel hardness. The Rockwell hardness machine and process of measuring work piece hardness are shown in Table 3.6.

3.6.4.2 Optical microscope

Optical microscope is to capture a digital image of machined surface and observe burr and chip formation by slot milling operation using ultrasonic vibration cutting. The model of optical microscope used for experiments is originated from EMZ-Meiji. The stereo microscope was used in this experiment to observe and measure the surface roughness of machined surface of material after the completion of slot milling process in wet and dry cutting condition with different cutting parameters (cutting speed, feed rate, depth of cut) under low magnification images (1.0X, 1.2X, 1.5X, 2.0X, 2.5X, 3.0X, 3.5X, 4.0X, 5.0X, 6.0X, 7.0X magnification). Table 3.6 shows the optical microscope used in this experiment. The specifications of stereo microscope is shown in Appendix E.

3.6.4.3 Scanning electron microscopy (SEM)

Scanning electron microscopy is a kind of electron microscope instrument that generates image and picture of a specimen or a sample by analysing it with an engaged

lights of electrons. The electrons react with the atoms in the specimen, creating different signals that contain data on the surface morphology, chemical composition and crystalline structure of the specimen. The high energy of electron scans the specimen in the raster scan pattern to produce signals of the surface specimens and an image of the specimen. Table 3.6 shows the scanning electron microscopy (SEM) machine used in the measurement of machining performance. The specification of scanning electron microscopy (SEM) used in the measurement of surface topography is shown in Appendix F.

3.7 Summary of machine, equipment and software

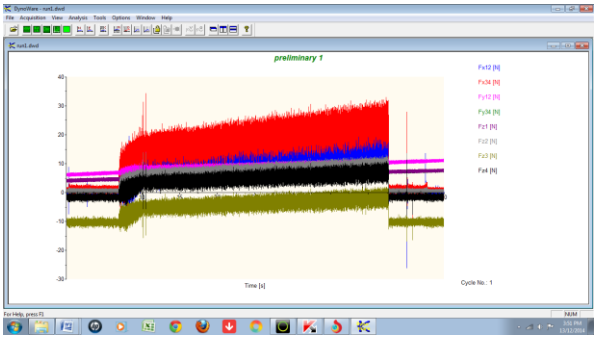
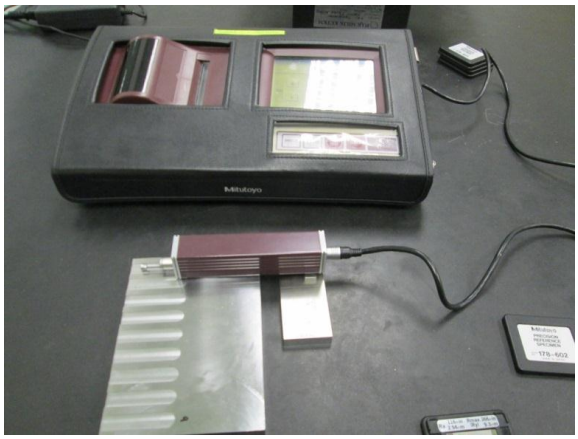
Equipment and machine were divided into four (4) main category; equipment for machining experiments, measurement of experimental results, sample preparation and performance measurement using scanning electron microscopic (SEM) for data analysis purposes.

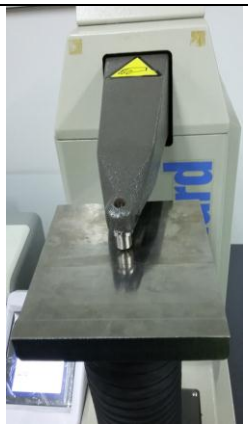
3.7.1 Machine, equipment and software

All the experiments performed 3 axis CNC vertical milling (HAAS CNC milling VF-1) with BT40 tool holder. End milling operation was operated under dry cutting conditions and slurries (namely alumina oxide) with 10 micrometer to 30 micrometer depth of cut. Down milling method was used to get better outcomes such as improved surface finish, less heat generation, larger tool life, better geometrical accuracy and compressive stresses favourable for carbide edges. Table 3.6 shows the machines, equipment and software used for the experiment.

Table 3.6: Machines, equipments and software used for the experiment

No.	Machines /Equipment / Software	Purpose
(a)	CNC Milling Machine-HAAS (VF-1) 3-Axis vertical milling 	Slot milling process
(b)	Kistler dynamometer Type 9257B 	Force measurement
(c)	Control unit Type 5233A 	Force measurement

(d)	Dynoware 	Data acquisition and force analysis
(e)	Surface roughness tester 	Surface roughness measurement
(f)	Weighing scale 	Material removal rate measurement by total weight of material removed

(g)	Rockwell Hardness Machine		Measurement of work piece material hardness
			
(h)	EDM (Electro Discharge Machining) Wirecut		Cutting the finished slot machined work piece material into smaller size
			
(i)	Ultrasonic Cleaner		Cleaning the specimen
			

(j)	Optical Microscope 	Captured digital image of machined surface,
(k)	Scanning Electron Microscopy (SEM) 	Captured, generate image and picture of a specimen or a sample by checking it with an engaged lights of electron

3.8 Experimental design of experiment (DOE) and statistical analysis

This section explains the experimental design of experiment (DOE) and statistical analysis method which were applied in this thesis. For the screening purposes, the Taguchi statistical technique was used. Taguchi approach is totally based on statistical design of experiments and this can economically satisfy the needs of problem solving and product/process design optimization (Ghani et al., 2004). Taguchi method can reduce the time required for experimental investigation. Taguchi method is also effective in

investigating the effects of multiple factors on performance as well as analysing the influence of individual factors to determine the most influential factor.

For the optimization purposes, response surface methodology (RSM) is the most suitable method used for optimizing the control factors that affect the machining performances during slot milling machining. The optimization process for machining parameters during slot milling machining involves surface roughness, cutting force and material removal rate. The RSM was chosen for optimization purpose because of its ability to get the functional relationship between the response (surface roughness, cutting force, material removal rate) of the slot milling machining with the cutting speed, feed rate, depth of cut, frequency and amplitude vibration. Details on the Taguchi and response surface methodology (RSM) techniques were utilized in this thesis as described in Section 3.7.1 and 3.7.2 respectively.

This thesis used three (3) experimental design layouts; full factorial design for screening purposes, Taguchi OA for design of experiments and response surface methodology (historical data design) for analysis and optimization purposes. The software used for the run sequence of experiments was DOE such as Design Expert 7.0.0. The analysis of variance (ANOVA) was used as a statistical method analysis of both experiments.

3.8.1 Design of experiment (DOE)

The main purpose using DOE in experiments is to produce optimization results. Figure 3.18 shows the schematic diagram of the process factors and responses that affect the machining process.

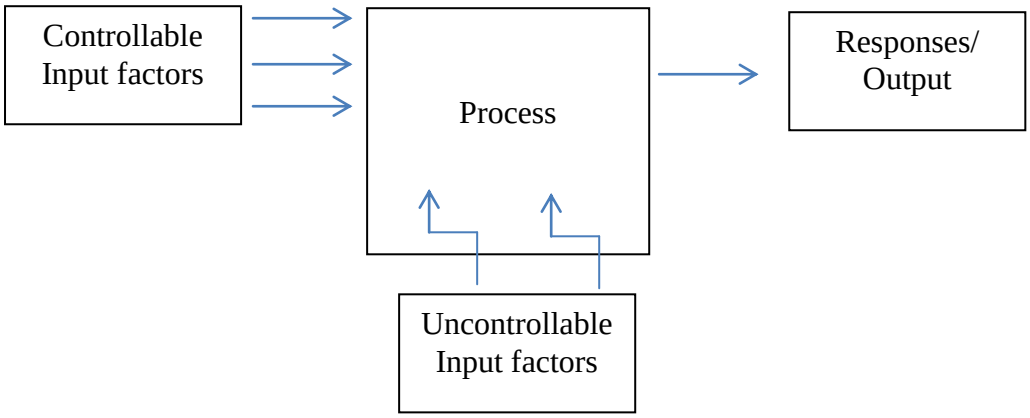


Figure 3.18: The process factors and responses that affected the process

The design of experiments (DOE) is also used to make decisions on the results obtained by engaging a lot of unknown parameters. It is an essential instrument to diminish the time required for experimentation and investigate the effects of multiple factors on performance by determining the most influential factor (Said et al., 2013).

3.8.2 Taguchi statistical technique

Taguchi statistical technique was used in this study to identify the control factors that mainly affected machining performances such as surface roughness, cutting force and material removal rate. Taguchi method is used for design of experiment (DOE) to determine other significant effects such as the interaction among slot milling machining parameters. It is a suitable method to solve the problems with minimum number of trials as compared with a full factorial design.

The Taguchi statistical technique consists of two major tools, namely single over signal noise ratio (S/N ratio) and orthogonal arrays. Signal noise ratio (S/N ratio) measures quality by focusing on variation. Table 3.7 shows the orthogonal array for five (5) factors and three levels used in this experiment which requires 27 experiments needs to be run. The type of S/N ratio of "smaller the better' was used for analysing the results due to the

minimum surface roughness, minimum cutting force and maximum material removal rate which improved work piece machined surface. The details of Taguchi statistical technique and formula for calculating "smaller the better" characteristics are discussed in Section 2.7.1.

Table 3.7: L^{27} orthogonal arrays for five factors and three levels

Runs No.	**Factor 1:** (A) Cutting speed (rpm)	**Factor 2:** (B) Feed rate (mm/min)	**Factor 3:** (C) Depth of cut (μm)	**Factor 4:** (D) Frequency (kHz)	**Factor 5:** (E) Amplitude (μm)
1	0	1	-1	0	0
2	0	0	1	-1	-1
3	0	0	1	-1	0
4	1	1	0	-1	-1
5	1	1	0	-1	0
6	0	-1	0	1	-1
7	0	-1	0	1	0
8	1	0	-1	1	1
9	1	0	-1	1	0
10	0	1	-1	0	1
11	-1	-1	-1	-1	-1
12	-1	1	1	1	-1
13	1	-1	1	0	0
14	1	-1	1	0	-1

15	-1	-1	-1	-1	1
16	0	1	-1	0	-1
17	-1	-1	-1	-1	0
18	-1	0	0	0	-1
19	-1	1	1	1	1
20	-1	0	0	0	1
21	-1	1	1	1	0
22	1	-1	1	0	1
23	1	1	0	-1	1
24	0	0	1	-1	1
25	1	0	-1	1	-1
26	0	-1	0	1	1
27	-1	0	0	0	0

3.8.3 Response surface methodology (RSM)

Response surface methodology (RSM) is essential to analyze results obtained in machining experiments. Response surface methodology (RSM) is a mathematical and statistical technique for the modeling and analysis of experiment which shows the significant effect of independent factors with the response. Response surface methodology is very convenient and the most efficient in the field of machining engineering that involves the study of cutting tools, surface roughness and machining force, (Noordin et al., 2004; Hossein et al., 2007; Campatelli and Scippa, 2012). The main objective of using response surface methodology is to optimize the response and determine the response variables (Y) generated due to several quantitative and independent factors (X_1, X_2,….,X_K). RSM generates the precise map based on mathematical model such as response surface

plot and contour plot which put all responses together through optimization approach (Anderson and Whitcomb, 2005).

3.8.3.1 RSM historical data analysis

Historical data analysis is one of the statistical approaches and included in the response surface methodology (RSM) tools intended for the optimization process. Historical data methods in the response surface methodology (RSM) tend to analyze the interaction between independent variables and responses (Aremu et al., 2014). By applying the historical data method, a predictive model and graph response can be developed. In historical data design, the minimum and maximum value for each numeric factor is specified. The numeric factor can be determined according to the number of cutting parameters (factors) used in machining experiments.

3.8.3.2 Analysis of variance (ANOVA)

Analysis of variances (ANOVA) was used to determine the significant factors that influence responses such as surface roughness, cutting force and material removal rate during experiments (Zhang et al., 2007). According to Joshua et al. (2015), the analysis of variance is used to investigate the significant machining parameters that affect the surface roughness value. The results of ANOVA showed that a positive correlation was found between analysis of variance (ANOVA) and probability F value. Besides, the value of probability was small, Prob > F, less than 0.0001 %. The predictive model was confirmed when using analysis of variance (ANOVA) at 5% significant level. In addition, the analysis of variance (ANOVA) is to investigate the effect of each process parameter on the machining performance characteristic of the interest to be studied (Kumar et al., 2008a). Izamshah et al. (2013) stated that the model terms are significant when the values factor

processing of "Prob > F" are less than 0.0500 and significant level at 95 % confidence interval (Elhadie et al., 2011). According to Noordin et al. (2004), the values of "Prob > F" can be compared with the desired probability. These finding shows a positive correlation between analysis of variance (ANOVA) and F value where the analysis of variance (ANOVA) is correlated with the probability of F value.

The software used to analyze the data from the experiment was Design Expert with 7.0 versions. The steps used to analyze the data are as follows (Anon, 2002):

a) Firstly, the transformation was chosen. Choosing a transformation is an important step to analyze the response. An initial step is to set transformation as "None". When the transformation is set to "None", the value of lambda = 1.0 and was designated as y' = y. This software can also diagnose the most suitable type of transformation. When, a ratio of maximum to minimum response is greater than 10, then, a transformation is required.

b) Second, the fit summary stage, the software calculated the regression to complete all polynomial models and produced sequential model sum of squares which consisted of linear, quadratic, 2 factor interaction (2FI) and cubic. From the sequential model sum of squares, the higher order polynomial could be selected where the additional terms are significant. This software would also generate the model summary statistics and calculated the statistical values such as the sum of square, mean square, F-value, standard deviation, R-squared, adjusted R-squared and predicted R-squared. Based on these results, a suitable model that focused on maximizing the "adjusted R-squared" and the "predicted R-squared".

c) Third, performed the modelling process. For modelling process, the process order and selection depended on the model summary statistics. In the model stage, all the main factors (A, B, C, D, E) and interaction factors (AB, AC, AD, BD, CD, DE)

were listed and selected for ANOVA analysis. Interaction factors could be removed or repealed to improve the value of R-squared, adjusted R-squared and subsequently improved the model.

d) Fourth, analysis of variances (ANOVA) was conducted to determine the controllable factor influencing the response factors such as surface roughness and optimal cutting combination (Zhang et al., 2007; Yang et al., 2009). Analysis of variances (ANOVA) also displayed all the factors of the model chosen and generated model F-value, indicating whether the model is significant or not. ANOVA analysis showed the results of the sum of square, mean square, F-value, Prob>F, standard deviation, mean, standard deviation, mean, R-squared, Adj R-squared, pred R-squared and adeq precision. Apart from that, the p-value was also displayed on each factor selected. The P-value or "Prob > F" less than 0.0050 indicated that model term is significant. If the significant value was lower, appropriate transformation process should be chosen to remove interaction factors with high p value in order to increase the significant values. When, the p-value is high, the probability of machining parameters affect the machining performances (surface roughness, cutting force, material removal rate) is low (Toh, 2006). The ANOVA results showed that the model was significant when the F test model showed a low probability value, with (p model > F) <0.05 (Aremu et al., 2014). Interaction for the model was highly significant when the F-value for interaction was high and p value was low. The criteria that determine the model is good and reasonable when the value of R-squared is close to 1 (Elhadie et al., 2011).

e) Fifth, the purpose of diagnostic process was for a model validation. The diagnostic process is essential to verify the factor that may have affected the response during the experiment (Kasim et al., 2014). Several types of plot can be generated from the

diagnostic process such as normal probability, residual vs predicted, residual vs run, residual vs factor, outlier T, Cook's distance, leverage, predicted vs actual and Box Cox graph. Several types of plot that can be generated from the diagnostic process is as follows (Stat-Ease, 2002):

i. Normal probability plot. It indicates that a set of data has a normal distribution or not. A good distribution of data is when the data follow a normal distribution in a straight line (Izamshah et al., 2013). When the data are plotted in S shape, then, it indicates the form of data is scattered with abnormal distribution, indicating a bad response. In addition, when the data are plotted in a nearly linear pattern, it showed the normal distribution, indicating the best model for this data set.

ii. Residual vs predicted plot. This plot indicates the comparison of residual and predicted with the display in the range observed. This plot is also used to confirm the constant variance assumption.

iii. Residual vs run. The plot is very similar to the residual vs predicted plot, but the difference is on the x-axis. Based on the residual vs run plot, the experimental data that shy away from the prediction target which affect the response are able to be identified.

iv. Residual vs factor. This plot shows the residual for the selected factor. This plots indicate whether a variant that is not calculated for the model is different at the level of factor. All data are within control when all data occur in the range of upper limits and lower limits.

v. Outlier T. This plot shows the response data included or not included in the range of upper limits and lower limits. It can also show whether the model is suitable in a variety of parameters that have been set.

vi. Cook's distance. The Cook's distance is to study the effect of data point when performing regression analysis. This plot is clearly indicating every value of response on each experimental run. In addition, it can identify a data point that has a negative impact on the regression model.

vii. Leverage vs run. This plot can measure how each point affects the model. The score for leverage ranges from 0 to 1. The leverage value of 1 refers to any error such as experimental and measurement with related response value to be formed into a model and can be predicted accurately.

viii. Predicted vs actual. The predicted vs actual plot is to compare the predicted value with actual values and show the model that predict the data.

ix. Box Cox graph. Box Cox plot for power transformation is used to identify an appropriate exponent (Lambda = l) to transform data into a normal shape. The Lambda value indicates the power to which all data should be raised.

f) The model graph. The model graph plot shows the relationships between factor and response. The model graph is displayed in the form of perturbation, one factor, interaction, contour, 3D surface and cube. The contour graph shows the pattern of response with factors whereas the cube graph shows the effect of response with machining factors.

3.9 Optimization and validation process

3.9.1 Optimization process

The final stage in the design of experiments (DOE) is an optimization process which considers all the various machining parameters such as; cutting speed, feed rate, depth of cut, frequency vibration, amplitude vibration and slurry concentration (5%, 10%,

15%, 20%) on machining performances (surface roughness, cutting force, material removal rate). Optimization choices are based on the optimum conditions to generate a minimum surface roughness, minimum cutting force and high material removal rate. In the optimization process, verification is done by comparing the results with a set of parameters that have the best response combination. In Design Expert software, an optimization choice consists of numerical optimization, graphical optimization and point prediction. The best method of optimization process is using a multiple response optimization. The benefit of multiple response optimization techniques is improving the machining performance, aiming to improve the production time and reduce cost in mould and die manufacturing. Furthermore, the multiple response optimizations is the method for the optimum desire response condition to be achieved.

In this study, desirability function and overlay plot are two techniques that can be applied to optimize multiple responses. The aim of this optimization process is to produce the best machining parameters on slot milling of hardened mould and die material using rotary ultrasonic assisted end milling machining with the lowest surface roughness, lowest resultant cutting force (F_R) and high material removal rate. In the optimization process, verification is done by comparing the results with a set of parameters that have the best response combination. When the optimization process was conducted, numerical optimization was used with set goals for each response. The goals of machining parameters such as cutting speed, feed rate, depth of cut, frequency vibration, amplitude vibration and slurry concentration have been set as in range. While the goals of machining performance such as surface roughness and resultant force (F_R) have been set as minimum, material removal rate (MRR) has been set as maximum.

Then, the response optimizations such as surface roughness (Ra), resultant cutting force (F_R) and material removal rate (MRR) have been set to high priority with high

important scale in analysis using the Design Expert software. The optimization solution is selected based on the best solution with consideration between factors, response and constraints such as cost, efficiency and practically. According to the Design Expert software, the best proposed solution for optimizing the effects of rotary ultrasonic assisted machining parameters (speed, feed rate, depth of cut, frequency and vibration amplitude, % slurry concentration) on slot milling for hardened mould and die material on machining performances (surface roughness, cutting force, material removal) is on solution number 2 which is based on a combination of the lowest surface roughness (Ra) value, lowest resultant force (F_R) and higher material removal rate (MRR).

The other criteria taken into consideration for the selected optimization solution were volumetric slurry concentration of alumina oxide–water mixture. The selected RUAEM parameter with different volumetric slurry concentrations of alumina oxide–water mixture was used for optimization process.

3.9.2 Validation process

The validation process is conducted by comparing the results with calculations using the generated formula based on the machining model predicted values (Yang et al., 2009). Besides, the validation process is performed using the most effective parameters that have the high influence to response. Then, the validation process was conducted to measure the differences of the bias error between the predicted and experimental results. Validation processes were done to assess the amount of the relative error between the predicted and experimental results. The relative error is calculated using the formula as shown:

$$Relative\ Error\ (\%) = \frac{(Predicted\ Value - Actual\ Value)}{Predicted\ Value} \times 100 \quad (3.1)$$

The experiment for this validation is done by comparing the result of surface roughness (Ra) value of machined surface, resultant force (F_R), material removal rate (MRR) between predicted values and actual experiments after slot machining using Rotary ultrasonic assisted end milling (RUAEM).

3.10 Procedure of experiment process

3.10.1 Machining parameters and experiment design matrix

Machining parameters for ultrasonic assisted end milling machining for the slot machining test depend on literature review and recommendations from cutting tool manufacturer. Machining parameters used in the slot machining test were cutting speed, feed rate, depth of cut, frequency vibration, amplitude vibration and % concentration of abrasive slurry concentration. Cutting speed is the rate or the speed difference between the cutting tool and the work piece surface is cut and independent of the machining utilized. The measurement unit of cutting speed on meter per minute (m/min). The three (3) level of cutting speed (-1, 0, +1) are used in the slot machining test for hard to cut material such as hardened steel, AISI D2. While, the feed rate is the relative speed at which the cutter is progressing along the work piece and feed rate units rely upon the movement of the device and work piece.

Table 3.8 shows the machining parameters and experiment design matrix respectively used in the slot machining test of AISI D2 hardened steel materials. The process to get the optimization of machining parameters is made based on factors like

lower cutting speeds, better surface quality, better dimensional and accuracy of the work piece shape at lower tool wear (Soković et al., 2004).

Table 3.8: Machining parameters used for slot machining test for RUAEM

Machining parameters	**Symbol**	**Unit**
Cutting speed	Vc	rpm
Feed rate	f	mm/min
Depth of cut	Doc	µm
Frequency vibration	f	kHz
Amplitude vibration	A	µm
Abrasive slurry	%	Percentage concentration

3.10.2 Independent variable and dependent variable

This experiment was carried out to obtain the interaction between machining parameters and machining performance. The independent variable is defined as inputs or causes for variation that occurs whereas the dependent variables is the effect, output, outcome or result whose variety is being concentrated on.

The machining parameters are categorized as independent variables such as cutting speed, feed rate and depth of cut. The dependent variable is categorized as machining performances namely as surface roughness, cutting forces and material removal rate. Table 3.9 shows a level of independent variables involved in the ultrasonic assisted machining process for hard to cut materials. The number of value for cutting speed (Vc), feed rate (f), depth of cut (d), frequency vibration (f), amplitude vibration (A) and abrasive slurry of alumina oxide (%) was set based on literature review in Section 2.6.7 (cutting parameter for RUAEM).

Table 3.9: Level of independent variables

Machining parameters variables	Level		
	-1	0	+1
Cutting speed, Vc (rpm)	30	90	150
Feed rate, f (mm/min)	5	25	45
Depth of cut, d (μm)	10	20	30
Frequency vibration, f (kHz)	20	23	27
Amplitude vibration, A (μm)	1	2	3
Abrasive slurry of Alumina Oxide (%)	0	10	20

3.10.3 Experiment design matrix

All experiment runs for rotary ultrasonic assisted end milling for slot milling of hardened steel material (AISI D2) are based on machining parameters, level of independent variables and experiment design matrix. Table 3.10 shows the experiment design matrix used for the slot machining test for RUAEM.

Table 3.10: Experiment design matrix used for slot machining test for RUAEM

Machining parameters						
Run	**Method (% concentration)**	**Vc (rpm)**	**F (mm/ min)**	**DoC (μm)**	**f (Hz)**	**A (μm)**
1	RUAM	90	45	10	23,000	2
	RUAM with 5 % slurry	90	45	10	23,000	2
	RUAM with 10 % slurry	90	45	10	23,000	2

	RUAM with 15 % slurry	90	45	10	23,000	2
	RUAM with 20 % slurry	90	45	10	23,000	2
	Conventional	90	45	10	-	-
2	RUAM	90	25	30	20,000	1
	RUAM with 5 % slurry	90	25	30	20,000	1
	RUAM with 10 % slurry	90	25	30	20,000	1
	RUAM with 15 % slurry	90	25	30	20,000	1
	RUAM with 20 % slurry	90	25	30	20,000	1
	Conventional	90	25	30	-	-
3	RUAM	90	25	30	20,000	2
	RUAM with 5 % slurry	90	25	30	20,000	2
	RUAM with 10 % slurry	90	25	30	20,000	2
	RUAM with 15 % slurry	90	25	30	20,000	2
	RUAM with 20 % slurry	90	25	30	20,000	2
	Conventional	90	25	30	-	-
4	RUAM	150	45	20	20,000	1
	RUAM with 5 % slurry	150	45	20	20,000	1
	RUAM with 10 % slurry	150	45	20	20,000	1
	RUAM with 15 % slurry	150	45	20	20,000	1
	RUAM with 20 % slurry	150	45	20	20,000	1
	Conventional	150	45	20	-	-
5	RUAM	150	45	20	20,000	2
	RUAM with 5 % slurry	150	45	20	20,000	2
	RUAM with 10 % slurry	150	45	20	20,000	2

	RUAM with 15 % slurry	150	45	20	20,000	2
	RUAM with 20 % slurry	150	45	20	20,000	2
	Conventional	150	45	20	-	-
6	RUAM	90	5	20	27,000	1
	RUAM with 5 % slurry	90	5	20	27,000	1
	RUAM with 10 % slurry	90	5	20	27,000	1
	RUAM with 15 % slurry	90	5	20	27,000	1
	RUAM with 20 % slurry	90	5	20	27,000	1
	Conventional	90	5	20	-	-
7	RUAM	90	5	20	27,000	2
	RUAM with 5 % slurry	90	5	20	27,000	2
	RUAM with 10 % slurry	90	5	20	27,000	2
	RUAM with 15 % slurry	90	5	20	27,000	2
	RUAM with 20 % slurry	90	5	20	27,000	2
	Conventional	90	5	20	-	-
8	RUAM	150	25	10	27,000	3
	RUAM with 5 % slurry	150	25	10	27,000	3
	RUAM with 10 % slurry	150	25	10	27,000	3
	RUAM with 15 % slurry	150	25	10	27,000	3
	RUAM with 20 % slurry	150	25	10	27,000	3
	Conventional	150	25	10	-	-
9	RUAM	150	25	10	27,000	2
	RUAM with 5 % slurry	150	25	10	27,000	2
	RUAM with 10 % slurry	150	25	10	27,000	2

	RUAM with 15 % slurry	150	25	10	27,000	2
	RUAM with 20 % slurry	150	25	10	27,000	2
	Conventional	150	25	10	-	-
10	RUAM	90	45	10	23,000	3
	RUAM with 5 % slurry	90	45	10	23,000	3
	RUAM with 10 % slurry	90	45	10	23,000	3
	RUAM with 15 % slurry	90	45	10	23,000	3
	RUAM with 20 % slurry	90	45	10	23,000	3
	Conventional	90	45	10	-	-
11	RUAM	30	5	10	20,000	1
	RUAM with 5 % slurry	30	5	10	20,000	1
	RUAM with 10 % slurry	30	5	10	20,000	1
	RUAM with 15 % slurry	30	5	10	20,000	1
	RUAM with 20 % slurry	30	5	10	20,000	1
	Conventional	30	5	10	-	-
12	RUAM	30	45	30	27,000	1
	RUAM with 5 % slurry	30	45	30	27,000	1
	RUAM with 10 % slurry	30	45	30	27,000	1
	RUAM with 15 % slurry	30	45	30	27,000	1
	RUAM with 20 % slurry	30	45	30	27,000	1
	Conventional	30	45	30	-	-
13	RUAM	150	5	30	23,000	2
	RUAM with 5 % slurry	150	5	30	23,000	2
	RUAM with 10 % slurry	150	5	30	23,000	2

	RUAM with 15 % slurry	150	5	30	23,000	2
	RUAM with 20 % slurry	150	5	30	23,000	2
	Conventional	150	5	30	-	-
14	RUAM	150	5	30	23,000	1
	RUAM with 5 % slurry	150	5	30	23,000	1
	RUAM with 10 % slurry	150	5	30	23,000	1
	RUAM with 15 % slurry	150	5	30	23,000	1
	RUAM with 20 % slurry	150	5	30	23,000	1
	Conventional	150	5	30	-	-
15	RUAM	30	5	10	20,000	3
	RUAM with 5 % slurry	30	5	10	20,000	3
	RUAM with 10 % slurry	30	5	10	20,000	3
	RUAM with 15 % slurry	30	5	10	20,000	3
	RUAM with 20 % slurry	30	5	10	20,000	3
	Conventional	30	5	10	-	-
16	RUAM	90	45	10	23,000	1
	RUAM with 5 % slurry	90	45	10	23,000	1
	RUAM with 10 % slurry	90	45	10	23,000	1
	RUAM with 15 % slurry	90	45	10	23,000	1
	RUAM with 20 % slurry	90	45	10	23,000	1
	Conventional	90	45	10	-	-
17	RUAM	30	5	10	20,000	2
	RUAM with 5 % slurry	30	5	10	20,000	2
	RUAM with 10 % slurry	30	5	10	20,000	2

	RUAM with 15 % slurry	30	5	10	20,000	2
	RUAM with 20 % slurry	30	5	10	20,000	2
	Conventional	30	5	10	-	-
18	RUAM	30	25	20	23,000	1
	RUAM with 5 % slurry	30	25	20	23,000	1
	RUAM with 10 % slurry	30	25	20	23,000	1
	RUAM with 15 % slurry	30	25	20	23,000	1
	RUAM with 20 % slurry	30	25	20	23,000	1
	Conventional	30	25	20	-	-
19	RUAM	30	45	30	27,000	3
	RUAM with 5 % slurry	30	45	30	27,000	3
	RUAM with 10 % slurry	30	45	30	27,000	3
	RUAM with 15 % slurry	30	45	30	27,000	3
	RUAM with 20 % slurry	30	45	30	27,000	3
	Conventional	30	45	30	-	-
20	RUAM	30	25	20	23,000	3
	RUAM with 5 % slurry	30	25	20	23,000	3
	RUAM with 10 % slurry	30	25	20	23,000	3
	RUAM with 15 % slurry	30	25	20	23,000	3
	RUAM with 20 % slurry	30	25	20	23,000	3
	Conventional	30	25	20	-	-
21	RUAM	30	45	30	27,000	2
	RUAM with 5 % slurry	30	45	30	27,000	2
	RUAM with 10 % slurry	30	45	30	27,000	2

	RUAM with 15 % slurry	30	45	30	27,000	2
	RUAM with 20 % slurry	30	45	30	27,000	2
	Conventional	30	45	30	-	-
22	RUAM	150	5	30	23,000	3
	RUAM with 5 % slurry	150	5	30	23,000	3
	RUAM with 10 % slurry	150	5	30	23,000	3
	RUAM with 15 % slurry	150	5	30	23,000	3
	RUAM with 20 % slurry	150	5	30	23,000	3
	Conventional	150	5	30	-	-
23	RUAM	150	45	20	20,000	3
	RUAM with 5 % slurry	150	45	20	20,000	3
	RUAM with 10 % slurry	150	45	20	20,000	3
	RUAM with 15 % slurry	150	45	20	20,000	3
	RUAM with 20 % slurry	150	45	20	20,000	3
	Conventional	150	45	20	-	-
24	RUAM	90	25	30	20,000	3
	RUAM with 5 % slurry	90	25	30	20,000	3
	RUAM with 10 % slurry	90	25	30	20,000	3
	RUAM with 15 % slurry	90	25	30	20,000	3
	RUAM with 20 % slurry	90	25	30	20,000	3
	Conventional	90	25	30	-	-
25	RUAM	150	25	10	27,000	1
	RUAM with 5 % slurry	150	25	10	27,000	1
	RUAM with 10 % slurry	150	25	10	27,000	1

	RUAM with 15 % slurry	150	25	10	27,000	1
	RUAM with 20 % slurry	150	25	10	27,000	1
	Conventional	150	25	10	-	-
26	RUAM	90	5	20	27,000	3
	RUAM with 5 % slurry	90	5	20	27,000	3
	RUAM with 10 % slurry	90	5	20	27,000	3
	RUAM with 15 % slurry	90	5	20	27,000	3
	RUAM with 20 % slurry	90	5	20	27,000	3
	Conventional	90	5	20	-	-
27	RUAM	30	25	20	23,000	2
	RUAM with 5 % slurry	30	25	20	23,000	2
	RUAM with 10 % slurry	30	25	20	23,000	2
	RUAM with 15 % slurry	30	25	20	23,000	2
	RUAM with 20 % slurry	30	25	20	23,000	2
	Conventional	30	25	20	-	-

3.10.4 Machining procedure

Before conducting the slot machining test, material hardness was measured using Rockwell hardness machine according to ISO 8688-1: 1989 (E)–International Standard (Page 2 and Page 3). Slot machining test for hard to cut materials (hardened AISI D2 steel) depended on machining parameters as shown in Table 3.7 and dimensional of work piece used. The work piece with accurate dimension and cutting tools is drawn in Solid Works software and AutoCAD software. After drawing work piece and cutting tool, the work piece and cutting tool drawing will be exported to EgdeCAM V9 software for the purpose of simulation.

Machining experiment was carried out based on Table 3.7 (machining parameters used for the slot machining test) and drawing the part of a work piece for machining is shown in Figure 3.19. The Figure shows a drawing of the part of a work piece for rotary ultrasonic assisted machining using AutoCAD software.

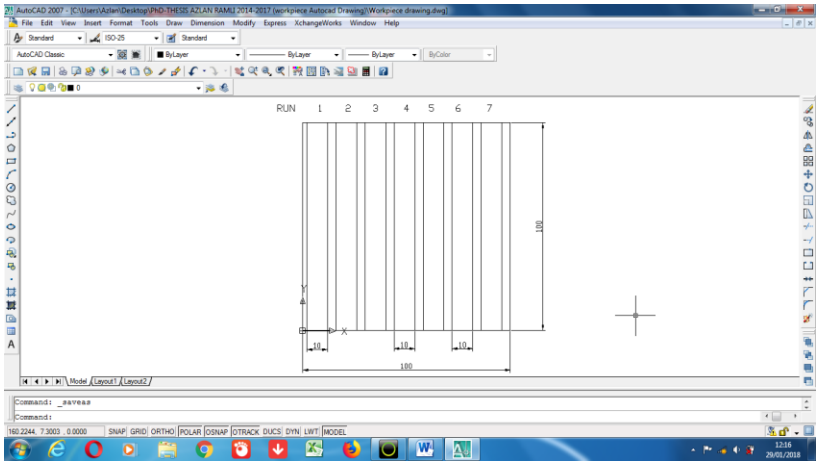


Figure 3.19: Drawing of the part of a work piece for rotary ultrasonic assisted machining using AutoCAD software

After the machining part of the work piece for rotary ultrasonic machining was successful in the simulation process, the machining program using G-code and M-code could be generated. The machining program using G-code and M-code CNC could be transferred or keyed in manually to control CNC machine panel. Figure 3.20 and 3.21 respectively shows the CNC control panel for keying in manually the machining program and G-code and M-code program. Before the slot machining process was carried out, the material of hardened steel, AISI D2 must be skimmed down to 0.5 mm by vertical milling and polishing process by surface grinding machine to dispel any deformity or any surface issue from the previous manufacturing process. According to Kasim et al. (2013), the block

of work piece material must be skimmed with maximum 0.5 mm on the surface of work piece to eliminate any deformity and surface issue from the past manufacturing process.



Figure 3.20: CNC control panel used for key in of machining program

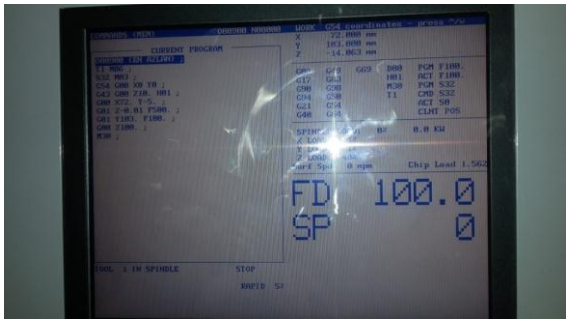


Figure 3.21: G-code and M-code of machining program which enter manually to control panel

After the completion of the slot machining program entering into the CNC control panel, slot machining run would start until the machining test was complete. In addition, the cutting tool condition was checked before performing the experiment to avoid an error of machining performance through a visual inspection. The setting of CNC machine datum is shown in Appendix F.

3.10.5 Cutting condition

Cutting conditions for slot milling machining of rotary ultrasonic assisted end milling (RUAEM) are dry cutting (without any lubricant, oil, fluid, liquid cooling) and using 5%, 10%, 15%, 20% volumetric concentration of alumina oxide slurries with distrilled water as a transport medium for slurry, during slot milling experiments. Using water as a transport medium for alumina oxide slurry is the best option to provide a better removal rate during the machining process (Singh and Gianender, 2012).

3.10.6 Preparation of alumina oxide slurry

The abrasive slurry used for slot milling using rotary ultrasonic assisted end milling machining (RUAEM) is alumina oxide slurry of 5%, 10%, 15%, 20% volumetric concentration with distrilled water mixture. Percentage alumina oxide slurry of 5% to 20% volumetric concentration with distrilled water mixture was selected based on the literature review conducted in Chapter 2 (2.6.7.6: abrasive slurry). The mixture was prepared using hot plate stirrer type SB 162-3 with brand of Stuart. The step preparation of alumina oxide slurry are as follows:

a) Firstly, weigh an empty beaker. The mass of empty beaker is 96.89 gram.

b) Secondly, weigh an empty beaker with 500 ml of distrilled water. The mass of empty beaker with 500 ml of distrilled water is 594.34 gram.

c) Thirdly, the mass of 500 ml of distrilled water was calculated. The mass of 500 ml of distrilled water is 497.45 gram.

d) Fourthly, the 5 % volumetric concentration of alumina oxide slurry was measure.

5 % concentration = 0.05

$$0.05 = \frac{X}{(X + 497.45)}$$

$$0.05\ (X + 497.45) = X$$

$$0.05\ X + 24.8725 = X$$

$$X - 0.05\ X = 24.825$$

$$0.95\ X = 24.8245$$

X = 26.1815 gram of alumina oxide/500 ml distrilled water

e) Fifthly, 26.1815 gram of alumina oxide mixed with 500 ml of distrilled water in beaker and stir the two ingredients together until well combined. After that, 5% volumetric concentration of alumina oxide slurries with distrilled water was conveyed between cutting tool and work piece surface during slot milling by RUAEM. The same calculation and process is repeated for 10%, 15%, 20% volumetric concentration of alumina oxide slurries with distrilled water.

3.10.7 Computer numerical control (CNC) machining procedure

Computer numerical control (CNC) is a computer-assisted process to control general purpose machines from instructions generated by a processor and stored in a memory in a memory system or storage media (tape, disk, chip) for the current and future use as well as future use.

Firstly, the part needed machining must be drawn using the computer aided design (CAD) using AutoCAD. Secondly, a machine part needed for machining, was converted into a computer aided manufacturing (CAM) and the program using G-code and M-code must be developed before starting the machining process. The computer aided

manufacturing (CAM) could generate G-code and M-code for machining of hardened mould and die AISI D2 using CNC HAAS Milling machine VF-1.

Before the experimental machining process was carried out, CNC machine would be allowed to operate without load for 30 minutes. After that, the work piece material was checked through visual inspection to ensure the position of the work piece was in a flat position and the work piece was clamped firmly and neatly on the CNC machine vise. Before the real experimental machining test, the test run or pilot test of hybrid rotary ultrasonic assisted machining was carried out using current machining parameters and tools that were not accounted for in the machining process. After that, the actual hybrid rotary ultrasonic assisted machining was carried out.

3.10.8 Computer aided manufacturing (CAM) modelling and simulation

Before conducting the rotary ultrasonic assisted machining process, the machined part drawing through AutoCAD software must be created earlier before converting it into CAM format. In this study, Edge CAM V9 was used for generating G-code and M-code for machining of hardened mould and die material using CNC HAAS milling machine VF-1. When using the edge CAM V9 software, the machining parameters, such as the choice of cutting tool, feed rate and spindle speed must be set as the tool path generators.

3.11 Summary

This methodology chapter describes the flow of this thesis which include research flow chart, work piece material, cutting tools, equipment used for machining experiment and performance measurement. This chapter also discusses the procedure of experiment process consisting of steps of research namely machining parameters, experimental design and experimental setup. Then, the validation process and optimization are presented.

CHAPTER 4

RESULT AND DISCUSSION

4.1 Introduction

This chapter presents and discusses the experimental results obtained according to the chosen methodology. The results are presented and discussed statistically and scientifically in two parts as described in Section 3.2. The first part of this chapter presents and discusses the results on the response surface methodology analysis which are divided to six sections according to the performance measured in Section 4.2 - surface roughness (Ra) results and analysis, Section 4.3 - resultant force (Fr) results and analysis, Section 4.4 – material removal rate (MRR) results and analysis, Section 4.5 – multi response optimizations results and Section 4.6 - macroscopic evaluation of machined surface quality. In addition, Sections 4.2 to 4.4 present, statistical analysis of variance (ANOVA) and mathematical model of the performance correlated with the machining parameters. Furthermore, statistical diagnostic test to evaluate the fitness of the developed mathematical is also discussed and 3D response surface plots are introduced as functions of performance and machining parameters.

Based on the developed mathematical function of each individual response correlated with the machining parameters, results on the multi-criteria optimization (Section 4.5) are presented for the second part of this chapter. Then, validation results are presented and the amount of bias error between the predicted optimal variables values such as machining parameters and experimental results are discussed. In Section 4.6, macroscopic evaluation of machined surface quality is presented and discussed.

4.2 Surface roughness (Ra) result and analysis

It is widely acknowledged in the machining industry that one of the main reasons for extensive application of machining hard materials (mostly steels with hardness more than 60 HRC) is to achieve high surface quality and eliminate the use of grinding as a costly and time-consuming finishing operation (Taylor and Kishawy, 2002; Grzesik, 2008). Hence, achieving good surface quality is one of the primary concerns when hard machining is employed.

Surface roughness was measured using surface roughness tester machine as shown in Table 3.6(e) (Mitutoyo SJ-400). Prior to the measurement of surface roughness, the surface roughness equipment of Mitutoyo Surftest SJ-400 was calibrated before the measurement process using a standard plate from Mitutoyo instrument manufacture. The machined surface is measured parallel to the slot cutting direction. The cut off wavelength (λc) used in surface roughness measurement was $\lambda c = 0.8$ mm. The evaluation length (EVA-L) used in surface roughness measurement was 4 mm. The peaks and valleys of the surface were measured using parameter Ra (arithmetical mean deviation of the assessed slot) at 10 differents locations along the machined slot length and were repeated 3 times as shown in Figure 4.1. Maximum value of Ra was taken for each slot and average value was calculated as input to surface roughness response. Table 4.1 and Figure 4.2 depict the experimental results for the surface roughness and comparison between the runs respectively.

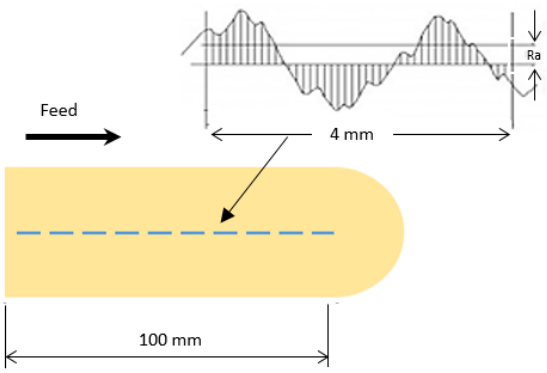
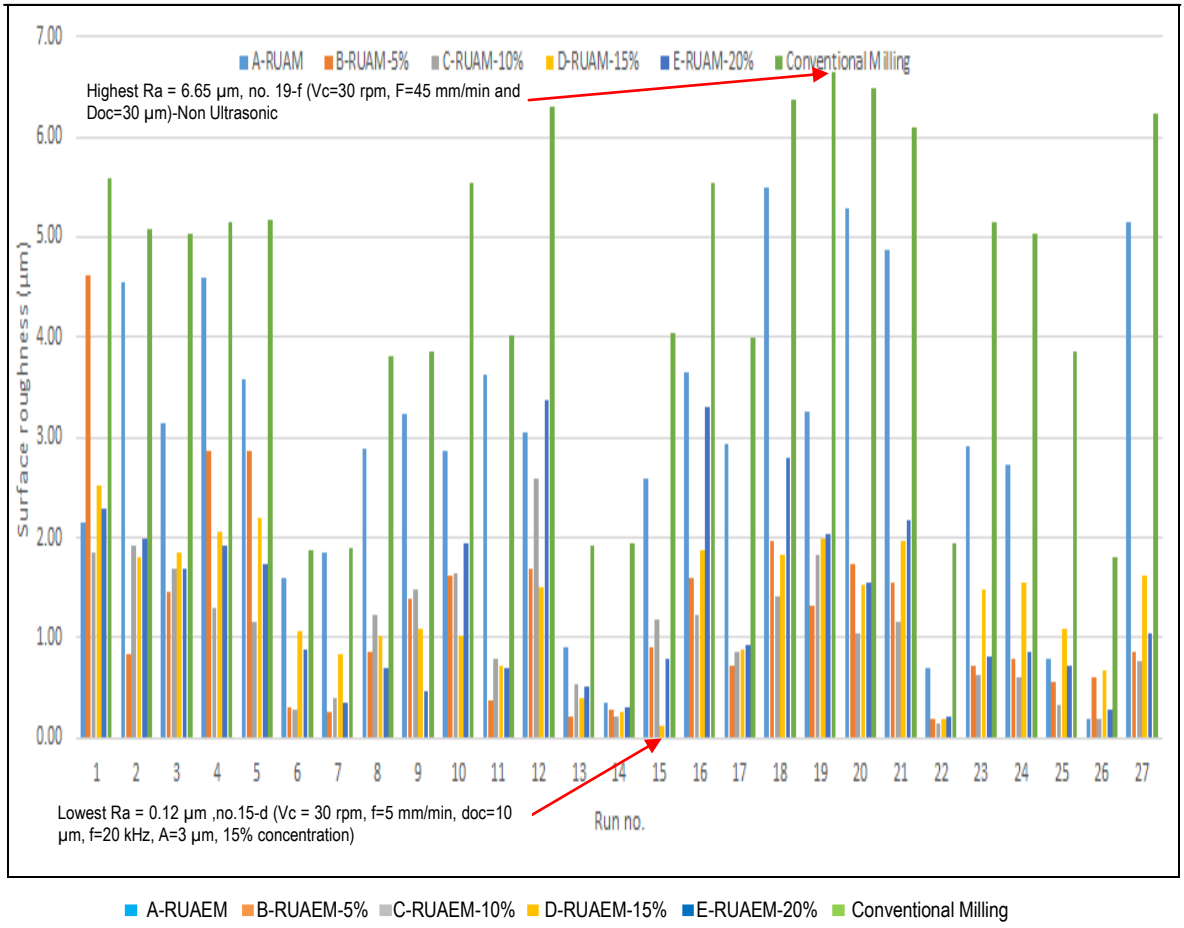


Figure 4.1: Surface roughness measuring location on each slot of milled surface

According to Table 4.1, the average surface roughness value of slot bottom surfaces varied between 0.12 to 6.65 µm with the overall mean of 2.06 µm. One major thing to be highlighted from the result is for all of the RUAEM experimental runs (denoted as a-e in the Table 4.1) the surface roughness values are dramatically decreased after ultrasonic vibration is applied compared to conventional milling process (denoted as f in the Table 4.1). The results are consistent with the preliminary experimental work performed (Appendix 1). In addition, variations seen in the values indicated that RUAEM cutting parameter has a significant effect on the response values (surface roughness). It can be observed that the combination of runs no. 15-d (Speed of 30 rpm, 5 mm/min feed rate, 10 µm depth of cut, frequency of 20 kHz, 3 µm amplitude and 15% concentration) produces the lowest surface roughness with an average value of 0.12 µm.



Remarks: A-RUAEM with 0% slurry, B-RUAEM with 5% slurry, C-RUAEM with 10% slurry, D-RUAEM with 15% slurry, E-RUAEM with 20% slurry, Conventional machining

Figure 4.2: Comparison of surface roughness between the runs

The results show that the optimal combination of RUAEM cutting parameter can produce smooth surface roughness and for this case it provides a deterioration of surface roughness due to the complexity of the relative motion between the tool and the work piece after ultrasonic vibration is applied. It is very clear that ultrasonic vibration greatly changes the movement pattern of tool tips, causing the tool tips to separate from the work piece repeatedly and regularly. In this RUAEM experimental work, the tool produces nearly 20-27 kHz vibrations in the axial direction within 1 s, creating small tool marks on slot bottom surface compared to that in conventional milling process. This is caused by contact force

(Fc) acts only over the portion of the cycle between 0 s to 1 s during RUAEM with causing deformation in the grit and the work piece. Contact force between the tool and the abrasive particle is effective only during a small portion of the cycle and motion of the cutting tool in condition of free sinusoidal motion under the loaded condition.

Meanwhile, the combination of run no. 19-f (Non-ultrasonic, speed of 30 rpm, 45 mm/min feed rate and 30 µm depth of cut) produced the highest surface roughness with an average value of 6.65 µm. Apart from the non-presence of ultrasonic vibration, one of the main reason for the high surface roughness value obtained from the combination of this run is due to the combination of slow cutting speed as well with high feed rate which decreases the shearing action (Yang et al, 2003). In consequence, the tendency for the material to break and release its bonds is greatly exaggerated and the chips will actually pull additional material from within the cut edge leaving a "cratered" or dimpled surface along the surface which produced a rough surface. Consequently, in both RUAEM and conventional milling process, the selection of cutting parameters and vibrating parameters affects the topography of machined surface and has a direct impact on the surface roughness value. Thus, ANOVA test is performed in order to understand the effects and contribution of the parameter on the response.

4.2.1 Statistical ANOVA and mathematical model development

Based on the experimental results in Table 4.1, a statistical ANOVA is generated to further investigate the effects of each parameter on the surface roughness. Table 4.2 tabulates the ANOVA results. Analysis of variance (ANOVA) is to investigate which main machining parameters that significantly affect machining performances (Kumar et al., 2013). Analysis of variances (ANOVA) with 5 % significance level (95 % confidence

level) is to identify which machining factors that significantly affect the surface roughness value of machined surface when slot milling of hardened steel materials.

Table 4.2: ANOVA result for the surface roughness

Source	Sum of	DF	Mean	F	p-value	
Model	42.87	26	1.65	26.08	< 0.0001	
A	2.10	1	2.10	33.16	< 0.0001	
B	2.90	1	2.90	45.89	< 0.0001	
C	0.04	1	0.04	0.58	0.4482	
D	0.00	1	0.00	0.02	0.8849	
E	0.03	1	0.03	0.43	0.5139	
F	0.62	1	0.62	9.76	0.0022	
A^2	0.03	1	0.03	0.53	0.4675	
B^2	0.79	1	0.79	12.47	0.0006	
C^2	0.05	1	0.05	0.86	0.3561	
D^2	0.00	1	0.00	0.05	0.8272	
E^2	0.14	1	0.14	2.18	0.1422	
F^2	3.75	1	3.75	59.39	< 0.0001	
AB	0.36	1	0.36	5.64	0.0189	
AC	0.10	1	0.10	1.55	0.2152	
AD	0.07	1	0.07	1.05	0.3077	
AE	0.02	1	0.02	0.34	0.5636	
AF	0.01	1	0.01	0.20	0.6580	
BD	0.00	1	0.00	0.05	0.8190	
BE	0.13	1	0.13	1.99	0.1604	
BF	0.01	1	0.01	0.08	0.7758	
CD	0.11	1	0.11	1.68	0.1971	
CE	0.37	1	0.37	5.85	0.0170	
CF	0.11	1	0.11	1.76	0.1868	
DE	0.08	1	0.08	1.25	0.2659	
DF	0.15	1	0.15	2.37	0.1256	
EF	0.01	1	0.01	0.20	0.6585	
Residual	8.53	135	0.06			
Lack of Fit	7.33	107	0.07	1.60	0.0780	not significant
Pure Error	1.20	28	0.04			
Cor. Total	51.41	161				

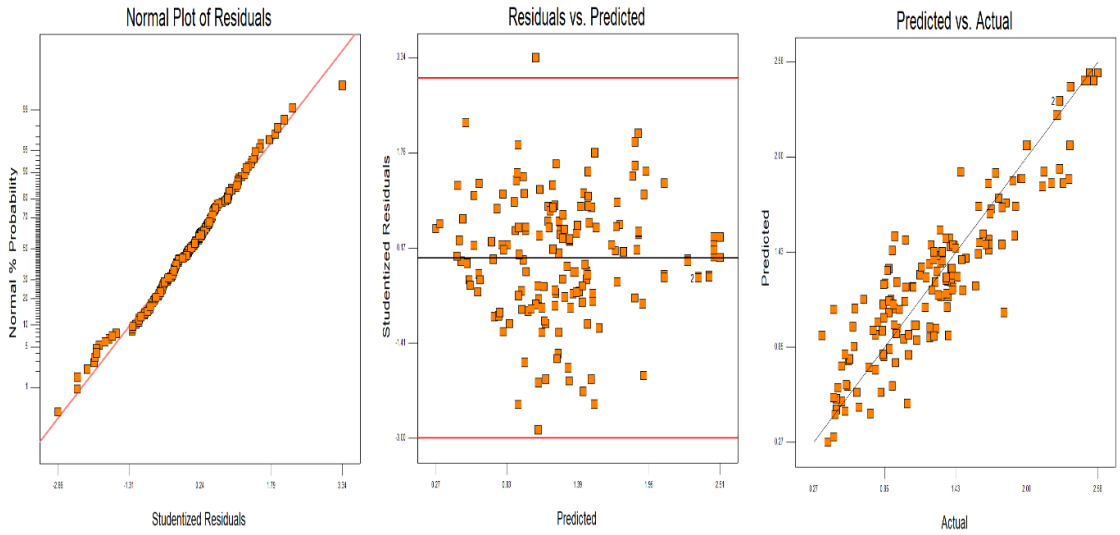
From the ANOVA, it shows that the generated model is significant, with p-value of <0.0001 and F-value of 26.08, indicating that there is only a 0.01% chance that the model could occur due to noise. Izamshah et al. (2013) states that the model terms are significant when the value factor processing of *Prob > F* is less than 0.0500. In addition, when value of *Prob>F* is less than 0.0500, then, the model terms are significant and in this case, the strongest machining parameter factors that affects the surface roughness value in the design space are denoted in codes; A, B, F, B^2, F^2, AB and CE. The R-Squared of 0.834 (83.4 %)

is in reasonable agreement with the Adj R-squared of 0.802 (80.2 %) which shows the adequacy of the model in predicting the response in the design space. The adequacy of the model in predicting the response help to validate the appropriate parameters affect the response. It shows that machining parameters such as speed, feed rate, slurry concentration and amplitude strongly affect the surface roughness value.

Based on the limit of independent variables that have been studied, a quadratic mathematical equation for the surface roughness as a function of machining parameter is as follows:

$$\begin{aligned}\text{Sqrt(Ra)} = {} & 1.07 - 0.2A + 0.38B + 0.037C + 0.032D - 0.11E - 0.35F + \\ & 0.034A^2 - 0.22B^2 + 0.048C^2 + 0.051D^2 - 0.16E^2 + 0.4F^2 + \\ & 0.15AB + 0.11AC + 0.058AD - 0.027AE + 0.017AF + 0.014BD \\ & - 0.073BE - 0.011BF + 0.08CD - 0.12CE + 0.052CF + 0.2DE + \\ & 0.23DF - 0.025EF \end{aligned} \quad (4.1)$$

It can be noted from the equation; the weak model terms are also included in order to maximize the fitness of the developed function. Furthermore, statistical diagnostic test to evaluate the fitness of the developed mathematical model is performed as shown in Figure 4.3 (a) to (c) which correspondingly show the normal, residuals vs predicted, and predicted vs actual plots of residuals. It can be observed that, the normal plot of residuals indicates that the residuals follow a normal distribution in a scatter plot straight line. In addition, the residuals versus predicted plot are also showing a randomly scattered (constant range of residuals across the graph) with just only one point outside the outlier limit. Lastly, from the predicted versus actual plots, the points are split evenly by 45 degree line, verifying the model fitness.



(a) (b) (c)

Figure 4.3: Statistical diagnostic test

To further analyze the interaction between machining parameters and surface roughness in the design space graphically, 3d surface response plot is developed. Figure 4.4 illustrates the interaction of surface roughness between cutting speed and feed rate. It can be seen that the interaction between cutting speed and feed rate significantly affects surface roughness value and can be modelled as a quadratic function. The 3D plot indicates that the lowest surface roughness lies in the region in which cutting speed is high and has low feed rate. One of the possible reasons is because high spindle speed within certain vibration frequency will affect the exact tool trajectory by shortening the cutting period, producing less cutter marks on the machined surface as shown in Figure 4.5. In addition, the surface roughness value increases as feed rate increases. This is due to the thrust forces presence which act on the work piece surface that affect the machining stability which, in turn, increase the roughness value.

For RUAEM, the ultrasonic vibration improves the machined surface formation. The reason of this improvement can be explained in terms of the alteration of chip formation mechanism by the ultrasonic vibration process. Furthermore, the mental material

of processing area is pried off the matrix little by little in RUAEM owing to the rapid separation of the cutter and work piece, therefore, more uniform surface can be obtained compared to that in conventional milling (Shen et al., 2011).

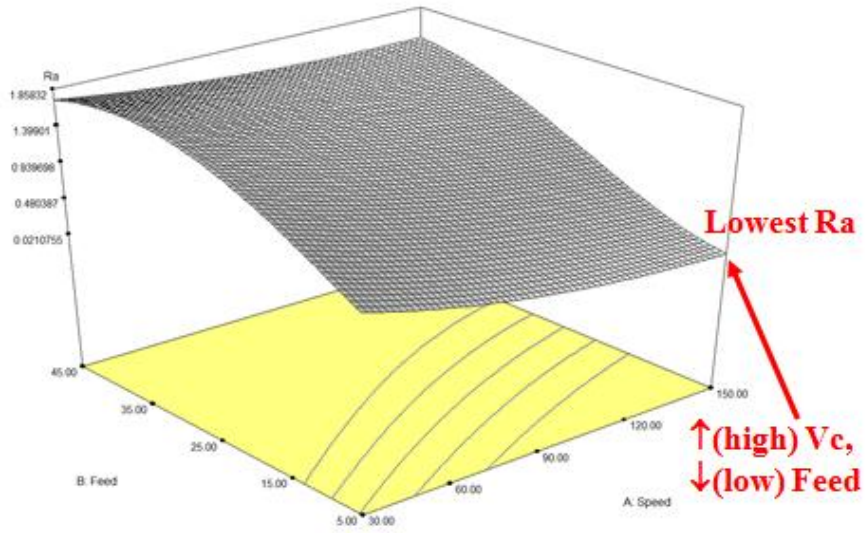
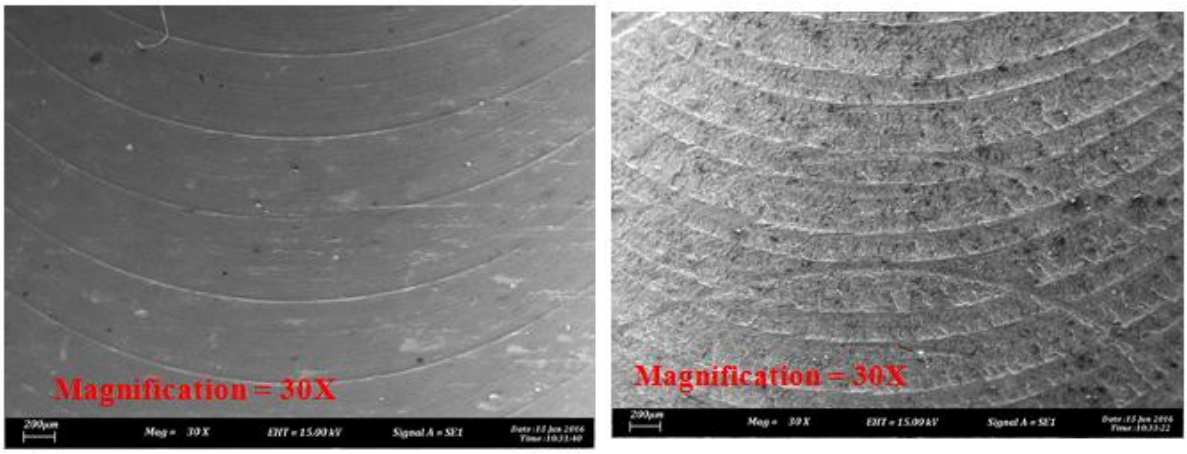


Figure 4.4: Interaction between cutting speed and feed rate on surface roughness



Conventional milling RUAEM

Figure 4.5: Cutter marks formation for conventional milling and RUAEM (Mag. = 30X)

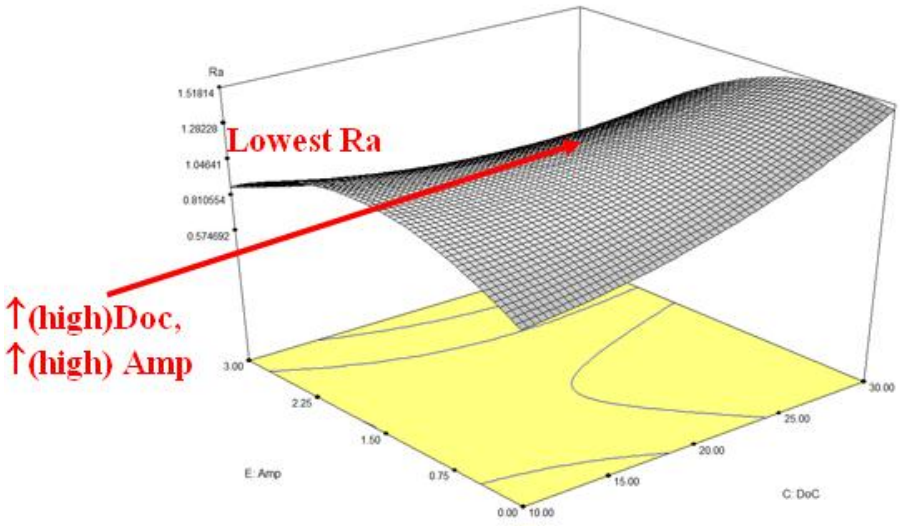
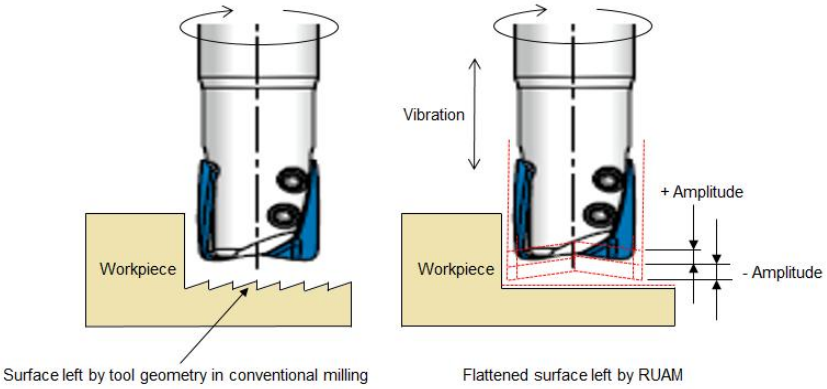
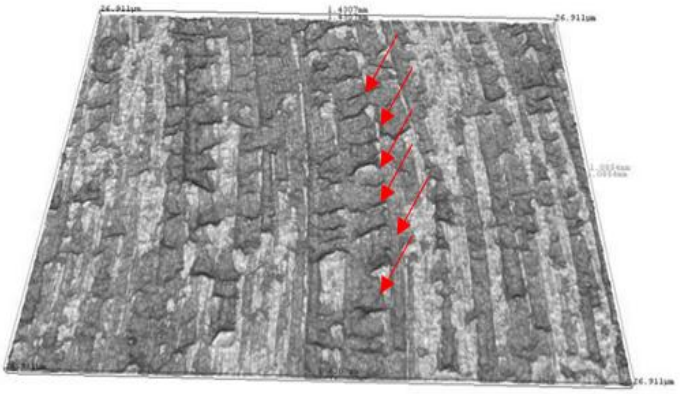


Figure 4.6: Interaction between vibration amplitude and depth of cut on surface roughness

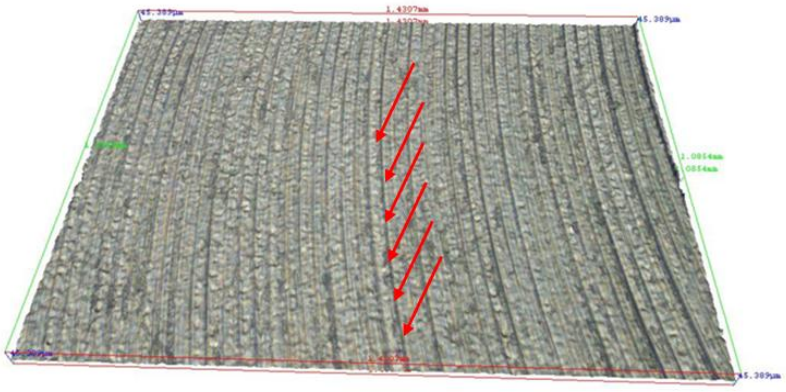
This could be explained in terms of the vibration amplitude is highly vibrating in an axial direction to the work piece surface, the energy at the cutter tip also increases due to the increase in the intensity of vibrations which, in turn, increases the impact on the work piece surface as illustrated in Figure 4.6. Consequently, creating hammering action that increases the localized stress force on the surface. This localized stress flattened the cutter marks left by the cutter teeth, thus, reducing the peak height and improving the surface roughness value as illustrated in Figure 4.7. Thus, in RUAEM, selection of cutting parameters and vibrating parameters affects the topography of machined surface and has a direct impact on the surface roughness value.



(a) Comparison of machined surface



(b) Conventional flattened machined surface

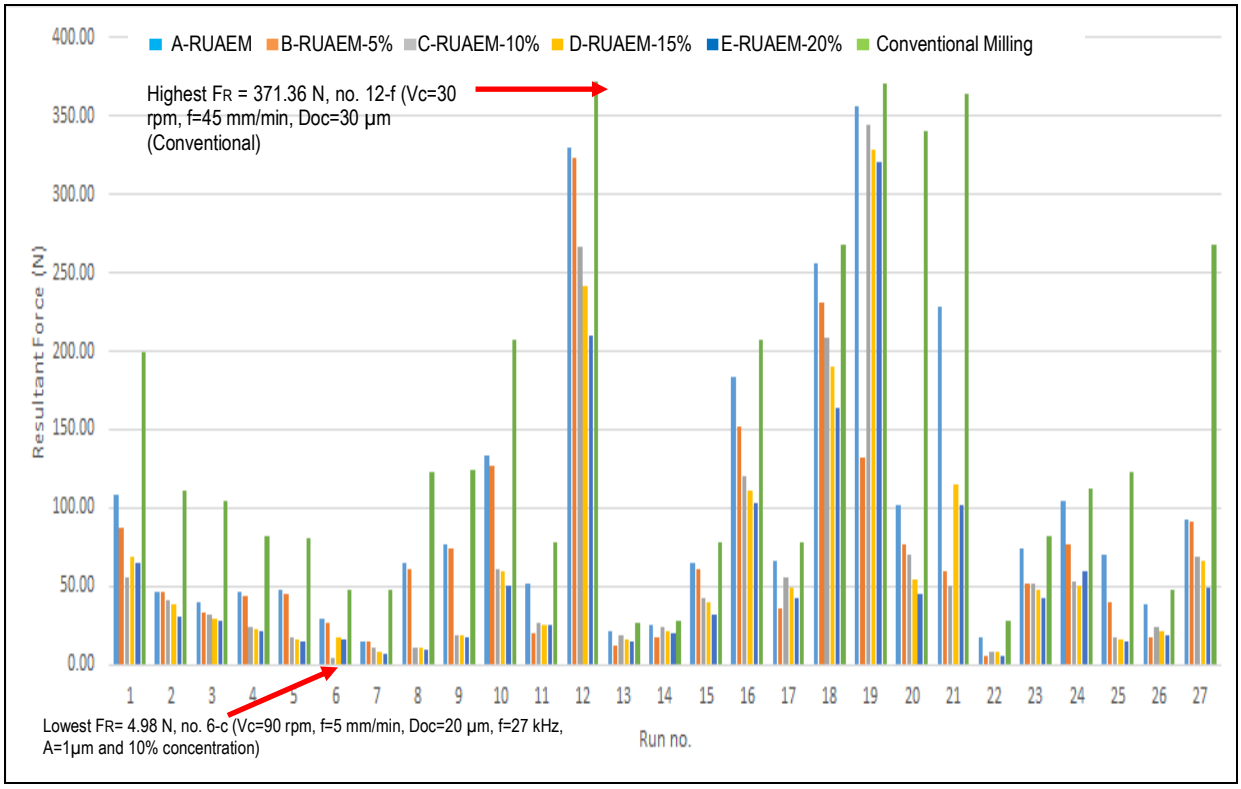


(c) RUAEM flattened machined surface

Figure 4.7: Machined surface topography for RUAEM showing the flattened surface from the hammering action in axial direction

4.3 Resultant force (F_R) result and analysis

Cutting force measurements were acquired using a set of apparatus which consists of Kistler 9257B dynamometer, Kistler 5070A charge amplifier and Kistler DynoWare Version 2.4 software as in Table 3.6 (b), (c) and (d). Firstly, the maximum absolute value of the cutting force amplitude in one cutting period is measured. Then, the average values of F_{max} amongst all cutting periods in one milling experiment are taken as the three force components F_x, F_y, and F_z. Then, the resultant cutting force ($F_{resultant}$) is determined by $F_{resultant} = \sqrt{Fx^2 + Fy^2 + Fz^2}$. In the end milling process, the cutting tool rotates on an axis vertical to the work piece. The tangential force (*Fx*) is in the direction of cutting speed, the radial force is in the radial direction of cutter feed (*Fy*) and axial cutting force is in the cutter axial direction (Wu et al., 2013). Gaitonde et al. (2016) reported that the cutting force increases at higher values of feed rate because the work piece machined surface material presents more resistance to cutter in the cutting direction, hence, increasing friction when machining hardened steel material.



Remarks: A-RUAEM with 0% slurry, B-RUAEM with 5% slurry, C-RUAEM with 10% slurry, D-RUAEM with 15% slurry, E-RUAEM with 20% slurry, Conventional machining

Figure 4.8: Comparison of resultant force between the runs

According to Table 4.3 and Figure 4.8, the Resultant Force values generated during the milling process varied between 4.98 N to371.36 N with the overall mean of 82.78 N. All the RUAEM experimental runs (denoted as a-e in the Table 4.3) and the cutting force values are dramatically decreased after ultrasonic vibration is applied compared to conventional milling process (denoted as f in the table). In addition, variations seen in the values indicated that RUAEM cutting parameter has a significant effect on the response values (resultant force). It can be observed that the combination of runs no. 6-c (Speed of 90 rpm, 5 mm/min feed rate, 20 µm depth of cut, frequency of 27 kHz, 1 µm amplitude and 10% concentration) produced the lowest resultant force with 4.98 N value. The results showed that an optimal combination of RUAEM cutting parameter can reduce the

magnitude of the cutting forces. One of the possible reasons of the decrease in the cutting force magnitude is, in RUAEM the ultrasonic vibration causes a high-frequency which interrupted the cutting process such as the cutter tooth is periodically in contact with the work piece. Owing to this action, the cutting chips were easily ejected from the cutting zone and removed the heat efficiently as well as helped the cutting fluid to reach the cutting area. In addition, the periodical separation between cutter tooth and work piece minimized the excessive accumulation heat, reduced the friction between the tool and work piece, and as a result helped to reduce the cutting force.

Meanwhile, the combination of run no. 12-f (Non-ultrasonic, speed of 30 rpm, 45 mm/min feed rate and 30 µm depth of cut) produced the highest resultant force with a value of 371.36 N. Apart from the non-presence of ultrasonic vibration, one of the main reasons for the high cutting force value obtained from the combination of this run was due to the combination of slow cutting speed as well with high feed rate which decreased the shearing action (Yang et al., 2003). In consequence, the tendency for the material to break and release its bonds was greatly exaggerated and the chips would pull additional material from within the cut edge, thus, producing high cutting force. Apart from the cutting force, the combination from this cutting parameter produced a rough machined surface as shown in Table 4.1. Consequently, in both RUAEM and conventional milling process, the selection of cutting parameters and vibrating parameters affected the magnitude of cutting forces produced. Therefore, in order to understand the effects and contribution of the parameters on the response clearly, ANOVA test was performed.

Table 4.4: ANOVA result for the resultant force

Source	Sum of squares	DF	Mean square	F-value	p-value Prob>F	
Model	136.09	21	6.48	32.17	< 0.0001	
A	16.33	1	16.33	81.05	< 0.0001	
B	7.88	1	7.88	39.12	< 0.0001	
C	1.50	1	1.50	7.46	0.0071	
D	3.37	1	3.37	16.71	< 0.0001	
E	1.07	1	1.07	5.31	0.0227	
F	0.41	1	0.41	2.06	0.1534	
AB	4.34	1	4.34	21.56	< 0.0001	
AC	0.36	1	0.36	1.79	0.1834	
AD	0.27	1	0.27	1.34	0.2485	
AE	0.22	1	0.22	1.07	0.3025	
AF	1.21	1	1.21	5.98	0.0157	
BC	1.08	1	1.08	5.36	0.0221	
BD	0.04	1	0.04	0.18	0.6747	
BE	0.00	1	0.00	0.00	0.9871	
BF	0.10	1	0.10	0.51	0.4770	
CD	0.50	1	0.50	2.49	0.1168	
CE	0.94	1	0.94	4.65	0.0327	
CF	1.56	1	1.56	7.75	0.0061	
DE	0.99	1	0.99	4.91	0.0283	
DF	0.06	1	0.06	0.32	0.5721	
EF	0.00	1	0.00	0.00	0.9532	
Residual	28.20	140	0.20			
Lack of fit	23.62	112	0.21	1.29	0.2233	not significant
Pure error	4.59	28	0.16			
Cor. total	164.29	161				

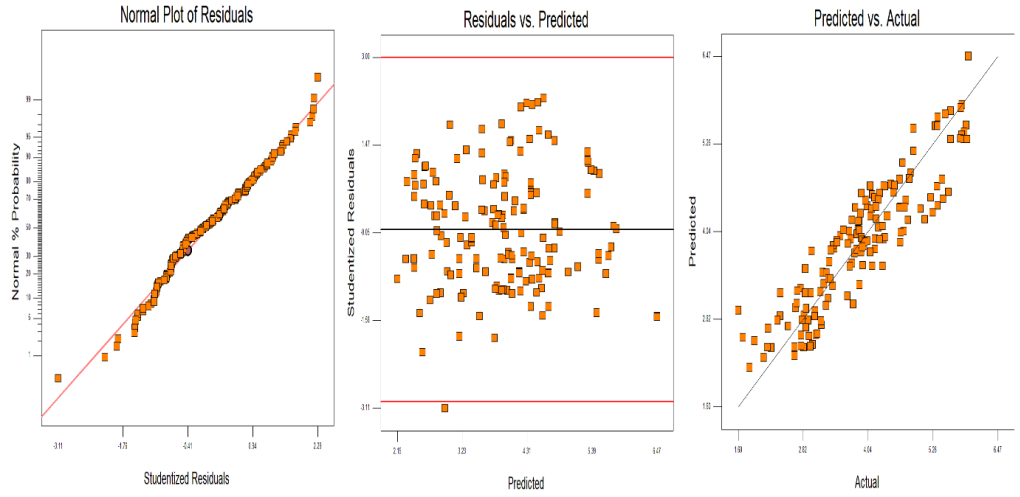
The ANOVA results (Table 4.4) showed that the generated model was significant, with p-value of <0.0001 and F-value of 32.17 indicating that there was only a 0.01% chance that the model could occur due to noise. In addition, values of Prob>F were less than 0.0500, indicating that the model terms are significant and in this case, the strongest machining parameters factors that affect the cutting force value in the design space are denoted in A, B, C, D, E, AB, AF, BC, CE, CF and DE which are significant model terms. The R-squared of 0.828 was in reasonable agreement with the Adj R-squared of 0.803, hence, the model was adequate in predicting the response in the design space. Machining parameters such as speed, feed rate, depth of cut, vibration frequency and amplitude strongly affected the cutting force value.

Based on the limits of independent variables that have been studied, a two factor interaction mathematical equation for the resultant force as a function of machining parameter is as follows:

$$\begin{aligned} Ln(Fr) = {} & 4.56-0.68A+0.59B-0.22C-1.02D+0.41E-0.26F-0.55AB- \\ & 0.16AC+0.12AD-0.085AE-0.16AF+0.25BC+0.046BD+1.467x10^{-003}BE- \\ & 0.050BF+0.17CD-0.19CE+0.19CF-0.52DE-0.13DF-5.801x10^{-003}EF \end{aligned} \quad (4.2)$$

It can be noted from the equation; the weak model terms were also included in order to maximize the fitness of the developed function. Furthermore, statistical diagnostic test to evaluate the fitness of the developed mathematical model was performed as shown in Figure 4.9 (a) to (c) which correspondingly show the normal, residuals vs predicted, and predicted vs actual plots of residuals. It can be observed that, the normal plot of residuals indicates that the residuals follow a normal distribution in straight line of a scatter plot. In

addition, the residuals vs predicted plot also showed a randomly scattered (constant range of residuals across the graph) with just only one point outside the outlier limit. Then, from the predicted vs actual plots, it can be seen that the points were split evenly by 45 degree line which confirmed the model fitness.



(a) (b) (c)

Figure 4.9: Statistical diagnostic test

To further analyze the interaction between machining parameters and cutting force in the design space graphically, 3d surface response plot was developed. Based on the ANOVA, all the RUAEM parameters have significant effects on the cutting force magnitude and therefore, the discussion on the cutting force effect on parameter is divided in three categories; effects on milling parameter, ultrasonic parameter and combination between milling and ultrasonic parameter. Firstly, for the effects on milling parameter, Figure 4.10 and 4.11 illustrate the interaction of cutting speed and feed rate on cutting force and interaction between depth of cut and feed rate on cutting force respectively. It can be seen that the interaction between cutting speed and feed rate significantly affects

cutting force value, indicating that the lowest cutting force lies in the region in which cutting speed are high and feed rate are low. On the other hand, for higher values of feed rate, an increase in cutting speed greatly reduces the cutting force magnitude. In addition, for the interaction between depth of cut and feed rate it shows that at the region when the feed rate is high, the work piece material became more resistance to cutter in the cutting direction and increases the friction, thus leading to the increase in cutting force magnitude. A further increase in depth of cut increases the chip load (material to be removed) per unit of time, thus, contributing to higher cutting force. It is also observed that the increase in cutting force is larger when the feed rate increases from medium to the highest value (Hosseini et al., 2016).

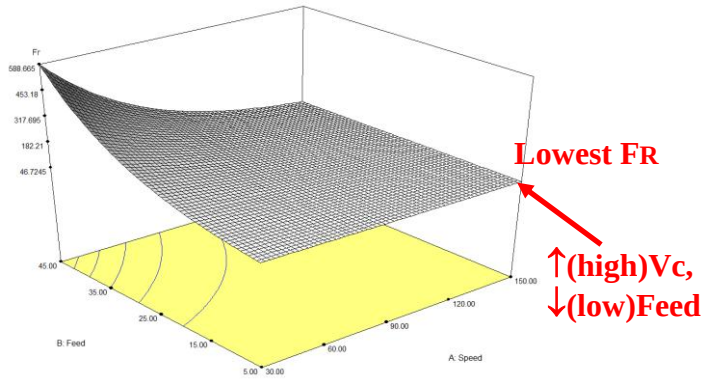


Figure 4.10: Interaction between cutting speed and feed rate on resultant force

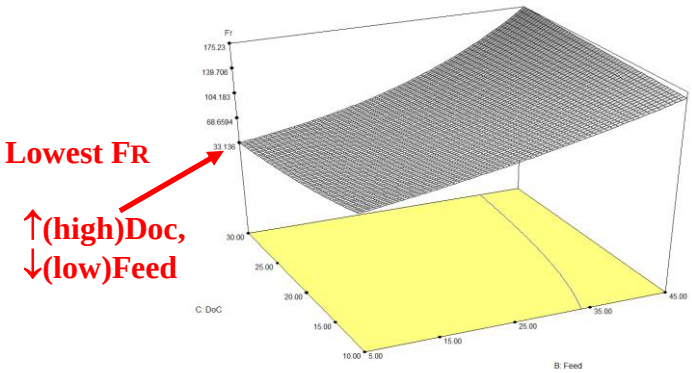


Figure 4.11: Interaction between depth of cut and feed rate on resultant force

Secondly is the effects on ultrasonic parameters. Figure 4.12 shows the 3d surface response plot on the interaction between vibration amplitude and frequency on the cutting force. The plot indicated that, cutting force magnitude increased at the region in which the vibration amplitude was at the highest with low frequency. To discuss the probability of this circumstances, two perspectives of hypothesis can be made. The first perspective is too high vibration amplitude and low frequency create an unstable machining condition known as chatter that generates force vibration thus, increasing the total cutting force magnitude. The second perspective is when the vibration amplitudes are too high, the energy at the cutter tip also increase due to increase in the intensity of vibrations which in turn increase the impact of abrasive particles on the work piece surface. Consequently, creating hammering action that increases the localized stress force on the surface, thus, increases the total cutting force magnitude.

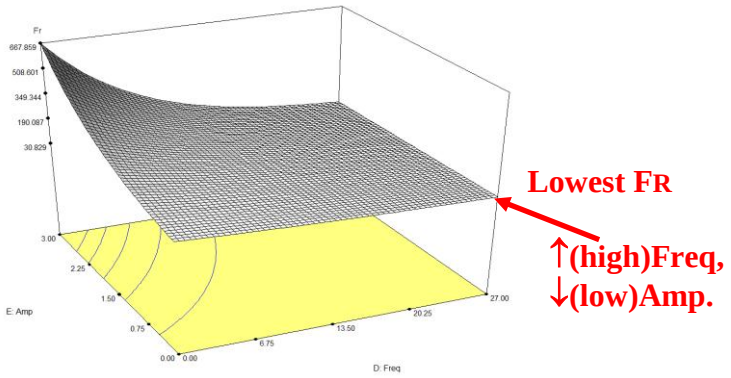


Figure 4.12: Interaction between vibration amplitude and frequency on resultant force

The decrease in cutting force was also observed when the vibration amplitudes were lower and frequency increased from medium to the highest value. The reason of this improvement can be explained in terms of the alteration of chip formation mechanism by the ultrasonic vibration process that creates an interrupted cutting action that changes the

cutting force profile as shown in Figure 4.13. In RUAEM, the ultrasonic vibration causes the cutting forces to oscillate over a wide range periodically. The cutting force value constantly returns to zero position and a similar pulse-like cutting force profile appears. As with conventional milling condition, the cutter teeth are always in contact with the work piece, creating a sine curve force pattern (Shen and Xu, 2017). According to Figure 4.13, the force pattern in sine curve and Δ t is the effective cutting time that the particle is in the contact the work piece machined surface (Zhang et al., 2013). When the cutting time start in zero position, the effective cutting time is zero and after finished one cycle cutting process, the effective cutting time is also increasing (Δ t). Then, the force (F) acts on abrasive slurry particles only on the effective cutting time (Δ t) during the cycle time. During the effective cutting time (Δ t), the abrasive slurry particles are directly contact with the vibration cutting tool and the work piece machined surface both. The effective cutting time (Δ t) for conventional milling is longer time period for one cycle cutting process compared by RUAEM machining which result in an increase the cutting force for conventional milling. The shorter effective cutting time (Δ t) and repeated cycle for RUAEM milling can reduce the time that the particle is in the contact the work piece machined surface which result in decrease the cutting force for RUAEM machining.

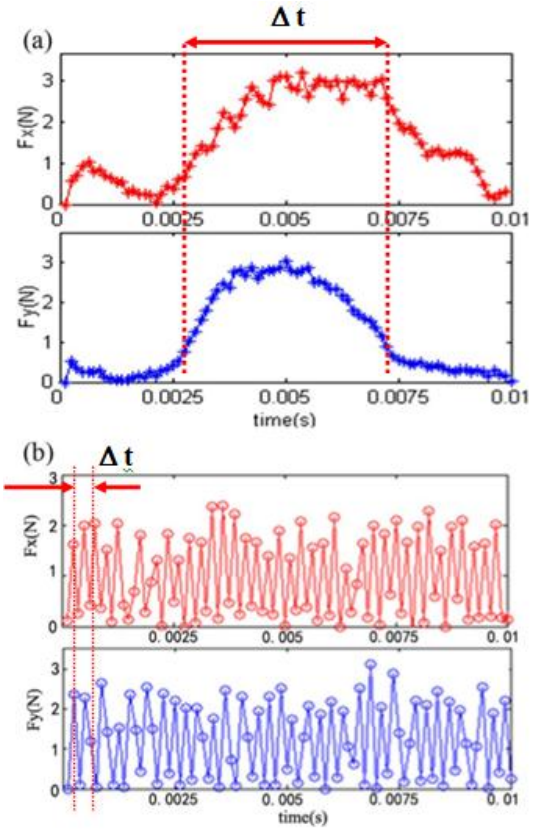


Figure 4.13: Cutting force profile between (a) Conventional milling and (b) RUAEM

Thirdly is the effects of combination between milling and ultrasonic parameter where Figure 4.14 and 4.15 show the interaction between vibration amplitude-depth of cut and interaction between cutting speed-slurry concentration; and slurry concentration and depth of cut on cutting force respectively. The plot indicated that, cutting force magnitude increased as the vibration amplitude increased and gradually decreased at lower depth of cut. The argument for this causes is similar to that previous discussion that relate to the increase in the intensity of vibrations which creates a hammering action and in turn, increases the localized stress force on the surface. In addition, the cutting force is gradually decreasing as the depth of cut decreases.

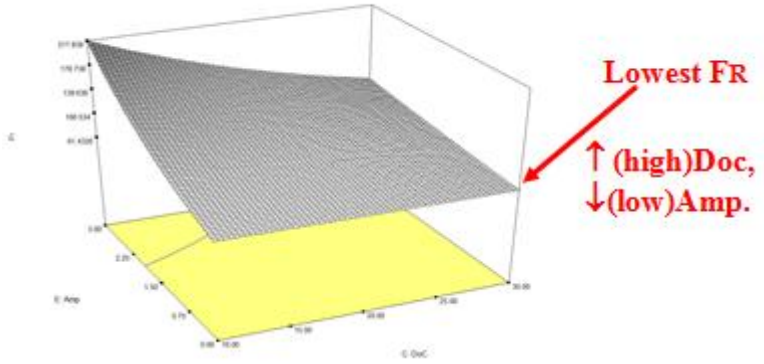


Figure 4.14: Interaction between vibration amplitude and depth of cut on resultant force

Figure 4.15 shows the 3D response surface graph of interaction between cutting speed and slurry concentration. It indicated that the maximum cutting force occurred on condition of higher slurry concentration and lower speed. One of the main reasons for the high cutting force value obtained from the combination of this parameter is due to the increase in the abrasive grain density that oscillates at high frequency and creates a high impact on the surface. Each of the abrasive grain has its own potential energy and as the density increases, the cumulative impact on the surface also increases, thus, elevating the total cutting force magnitude as demonstrated in Figure 4.16.

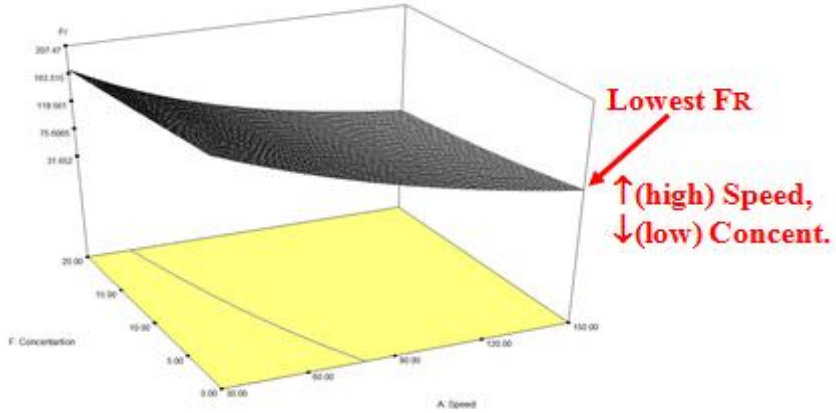


Figure 4.15: Interaction between cutting speed and slurry concentration on resultant force

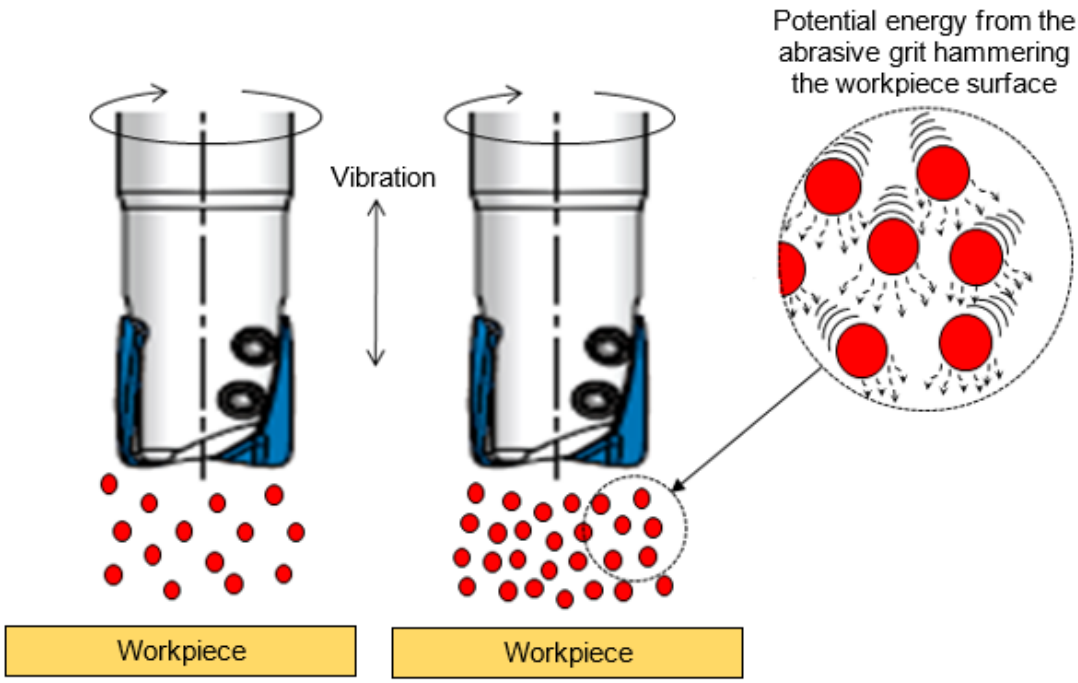


Figure 4.16: Effects of abrasive slurry concentration on resultant force

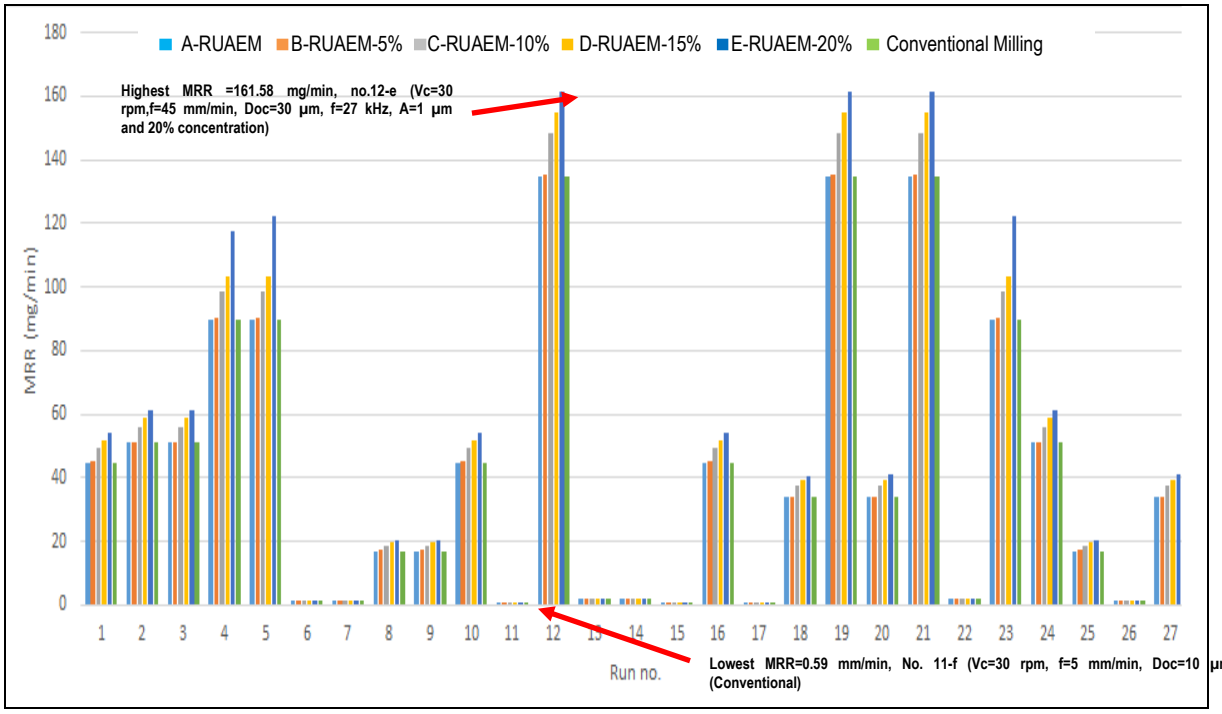
4.4 Material removal rate (MRR) result and analysis

The material removal rate (MRR) refers to the volume removed in the form of chips over a certain time during material-removing machining processes. In the production technology, MRR is one of the important factors as it is used as the basis for measuring and rating the productivity of tools and machines. In RUAEM, the materials are removed by the interaction between the shearing from milling cutter and vibration amplitude either with or without the presence of abrasive slurry. The interaction creates a high momentum of shearing impact on the machined surface that produces a localized fatigue stress, causing a continuous impact and micro chipping occurrence (Jain et al., 2011).

The mechanics of material removal process for RUAEM are complicated and the non-existence of the mechanistic model to quantify the rate of material removal precisely, hence, the most suitable and practical method to measure MRR are by measuring the weight of material loses per specific time which is depicted as:

$$MRR\ (\frac{mg}{\text{min}}) = \frac{\text{Weight before machining} - \text{Weight after machining}}{\text{Machining Time}} \quad (4.3)$$

The weight of the sample was measured using the precision weighing scale before performing the machining process. Once the machining process was completed, the samples were cleaned using the ultrasonic cleaner machine before weighing to measure the total loss of weight which was removed. Table 3.6 (f) and (k) show the equipment used for the MRR measurement. The machining slot was set to 100 mm in length and the times taken to complete the slot distance were recorded. The MRR results are tabulated in Table 4.5 and Figure 4.17.



Remarks: A-RUAEM with 0% slurry, B-RUAEM with 5% slurry, C-RUAEM with 10% slurry, D-RUAEM with 15% slurry, E-RUAEM with 20% slurry, Conventional machining

Figure 4.17: Comparison of material removal rate between the runs

According to Table 4.5, the average MRR value for all the runs varied between 0.562 to 161.58 mg/min with the overall mean of 45.04 mg/min. The variations seen in the MRR values indicate that the factors such as cutting parameters have the significant effect on the response values (MRR). The combination of runs no. 12-e (Speed of 30 rpm, 45 mm/min feed rate, 30 µm depth of cut, frequency of 27 kHz, 1 µm amplitude and 20% concentration) produced the highest MRR with an average value of 161.58 mg/min. As with conventional milling process, the MRR value was dependent on the combination between feed rate and depth of cut values such higher values increased the MRR. However, for the case of RUAEM, others than feed rate and depth of cut; frequency, amplitude and slurry concentration affected MRR values. In RUAEM, additional material removal mechanism was created by the impact of abrasive particle to the work piece surface which

increased the MRR. Apart from that, the obtained result shows that the optimal combination of RUAEM cutting parameter could increase the MRR values.

Besides, the combination of run no. 11-f (Non-ultrasonic, speed of 30 rpm, 5 mm/min feed rate and 10 μm depth of cut) produced the lowest MRR with an average value of 0.56 mg/min. Apart from the non-presence of ultrasonic vibration, one of the main reasons for the lower MRR value obtained from the combination of this run is due to the combination of low feed rate as well with low depth of cut which removes the work piece material in less time and slow speed. Consequently, in both RUAEM and conventional milling process, the selection of cutting parameters and vibrating parameters affects the MRR value. Therefore, in order to understand the effects and contribution of the parameters on the response clearly, ANOVA test is performed.

Table 4.6: ANOVA result for material removal rate

Source	**Sum of squares**	**DF**	**Mean square**	**F-value**	**p-value Prob>F**
Model	2012.96	21	95.86	44.39	< 0.0001
A	35.03	1	35.03	16.23	< 0.0001
B	313.99	1	313.99	145.42	< 0.0001
C	78.29	1	78.29	36.26	< 0.0001
D	5.01	1	5.01	2.32	0.1298
E	10.11	1	10.11	4.68	0.0322
F	0.23	1	0.23	0.11	0.7443
AB	7.36	1	7.36	3.41	0.0669
AC	9.61	1	9.61	4.45	0.0367
AD	16.58	1	16.58	7.68	0.0063
AE	27.89	1	27.89	12.92	0.0005
AF	0.04	1	0.04	0.02	0.8989
BC	3.43	1	3.43	1.59	0.2098

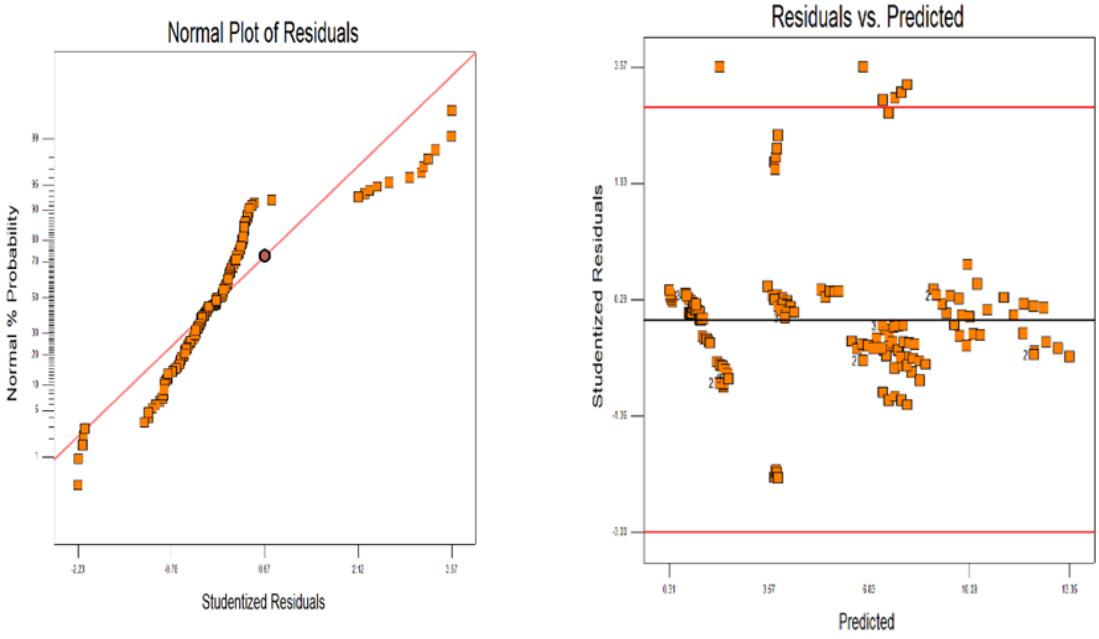
BD	2.63	1	2.63	1.22	0.2717	
BE	4.43	1	4.43	2.05	0.1543	
BF	2.44	1	2.44	1.13	0.2898	
CD	2.34	1	2.34	1.08	0.2996	
CE	3.15	1	3.15	1.46	0.2292	
CF	0.19	1	0.19	0.09	0.7682	
DE	2.94	1	2.94	1.36	0.2450	
DF	0.07	1	0.07	0.03	0.8565	
EF	0.14	1	0.14	0.06	0.8025	
Residual	302.28	140	2.16			
Lack of fit	64.21	112	0.57	0.07	1.0000	not significant
Pure error	238.07	28	8.50			
Cor. total	2315.24	161				

The results show that the generated model was significant, with p-value of <0.0001 and F-value of 44.39 indicating that there was only a 0.01% chance that the model could occur due to noise. In addition, Prob>F value was less than 0.0500, indicating that the model terms were significant and in this case, the strongest machining parameter factor that affected the MRR value in the design space were denoted as code A, B, C, E, AC, AD and AE in significant model terms. The R-squared of 0.870 was in a reasonable agreement with the Adj R-squared of 0.850 which shows the adequacy of the model in predicting the response in the design space. It shows that machining parameters such as speed, feed rate, depth of cut and amplitude strongly affected the MRR value.

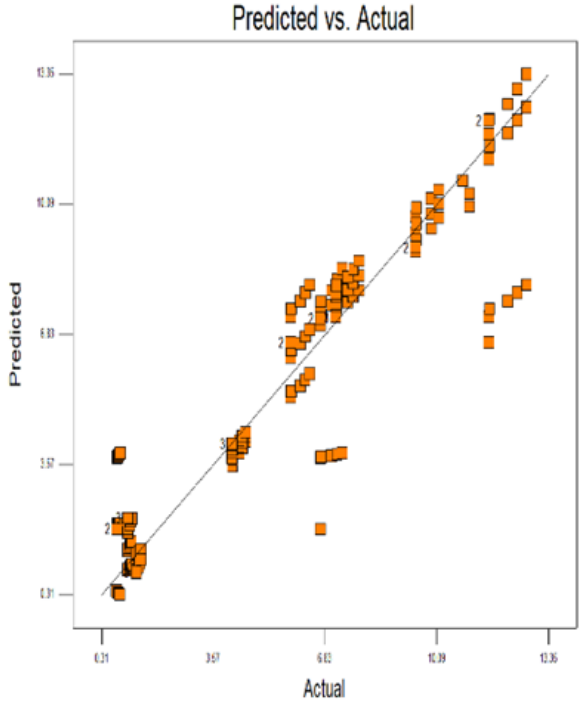
Based on the limits of independent variable that have been studied, a two factor interaction mathematical equation for the MRR as a function of machining parameter is as follows:

$$\text{Sqrt(MRR)} = 6.59 - 1.00A + 3.69B + 1.62C - 1.25D + 1.26E + 0.19F + 0.72AB - 0.82AC + 0.91AD - 0.96AE - 0.028AF + 0.44BC + 0.39BD - 0.43BE + 0.24BF + 0.37CD - 0.35CE + 0.067CF - 0.89DE + 0.14DF + 0.081EF \quad (4.4)$$

It can be noted from the equation; the weak model terms were also included in order to maximize the fitness of the developed function. Furthermore, statistical diagnostic test to evaluate the fitness of the developed mathematical model were performed as shown in Figure 4.18 (a) to (c) which correspondingly showed the normal, residuals vs predicted, and predicted vs actual plots of residuals. The normal plot of residuals indicated that the residuals followed a normal distribution in a straight line of scatter plot. Distribution of data is good condition because all data condition line up nicely. Then, the residual versus predicted plots were observed that material removal rate data a randomly scattered (constant range of residuals a cross the graph) with minor points outside the outlier limit. The predicted versus actual plots useful to present a detect outlier values are predicted by the model and all the points of material removal rate data were split evenly by 45 degree line which confirm the model fitness and show good agreement between the predicted value of material removal rate acquired from the model and actual experiment data.



(a) (b)



(c)

Figure 4.18: Statistical diagnostic test

To further analyze the interaction between machining parameters and MRR in the design space graphically, 3d surface response plots were developed. In terms of both techniques such as, conventional milling and RUAEM, the MRR values were greatly dependent on cutting speed, feed rate and depth of cut value. Figure 4.19 to 4.21 illustrate the two factors interaction of MRR between speed and feed rate; speed and depth of cut; feed rate and depth of cut respectively.

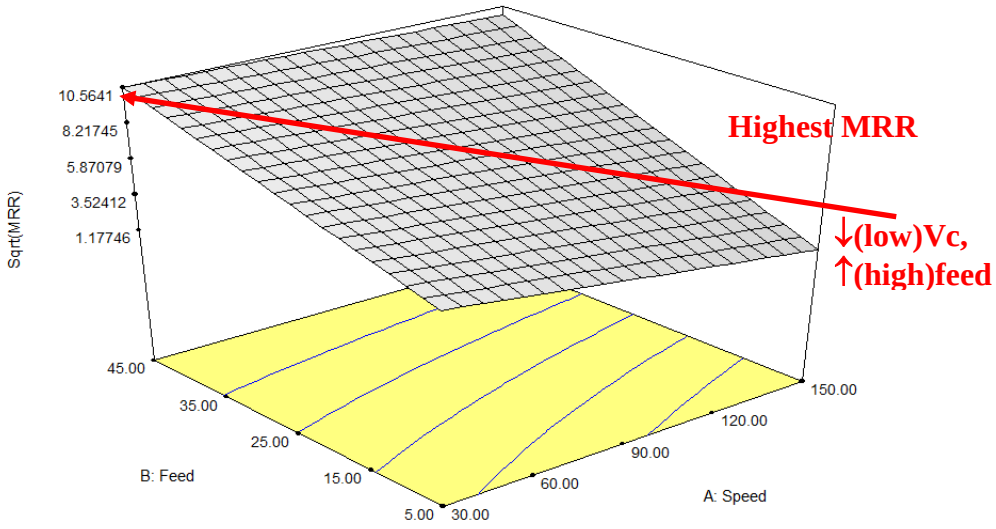


Figure 4.19: Interaction between cutting speed and feed rate on MRR

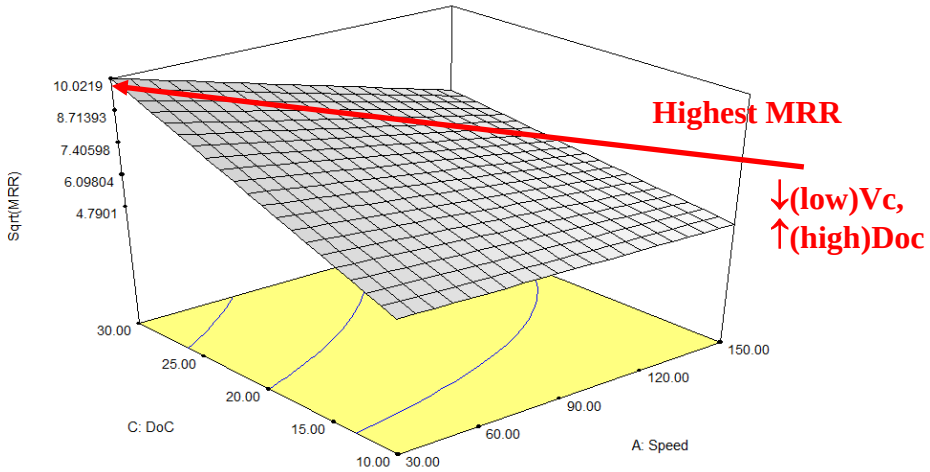


Figure 4.20: Interaction between cutting speed and depth of cut on MRR

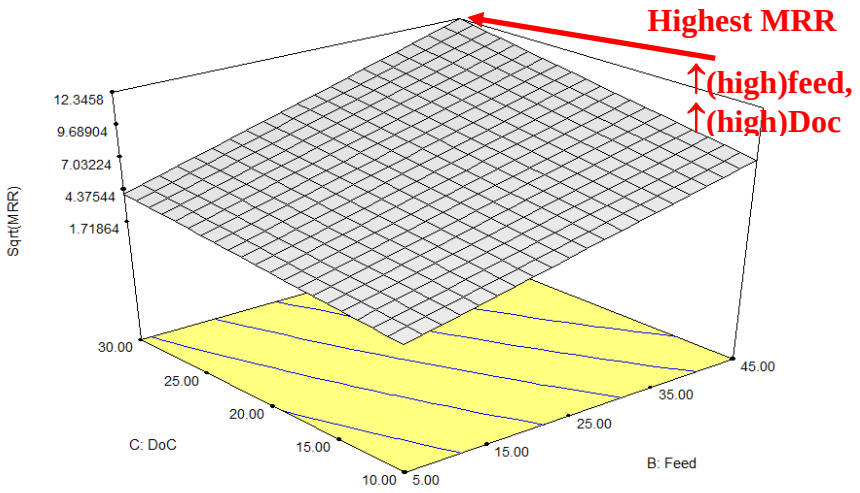


Figure 4.21: Interaction between feed rate and depth of cut on MRR

The 3D plots indicated that the highest MRR lay in the region in which feed rate and depth of cut were high whilst cutting speed was low. Obviously, the higher the feed rate and depth of cut values resulted in more material been removed in certain period of time, thus, increasing the MRR value. In addition, the MRR value increased as the cutting speed decreased. One of the possible reasons is when the cutting speed is low, the shearing process by the cutter teeth on the material can be done completely without any excessive material left, thus, increasing the MRR value.

In the context of RUAEM parameter, it is observed that vibration amplitude and abrasive slurry concentration had significant effect on the MRR value. Figure 4.22 shows the surface plot for the interaction between vibration amplitude and abrasive slurry concentration on MRR. It can be observed that the interaction between vibration amplitude and abrasive slurry concentration significantly affected the MRR value and could be modelled as two-factor interaction function. The 3D plot indicated that the highest MRR lay in the region in which both factors were maximum. In addition, as the number of abrasive particles increase, consequently the total micro chipping area increased, thus,

increasing the MRR value as depicted in Figure 4.23. The improvement on the MRR values can be related to the additional material removal mechanism by the high energy hammering action such high amplitude produced from the vibrated abrasive particles as depicted in Figure 4.24. The higher amplitude produces deeper chipping depth on the work piece surface such as increasing volume of material being removed. Also, the effect of the vibration of the cutting tool causes the abrasive slurry particles held in the slurry between work piece machined surface and the cutting tool which high energy hammering impact and generate high material removal rate by micro chipping (Thoe et al., 1998).

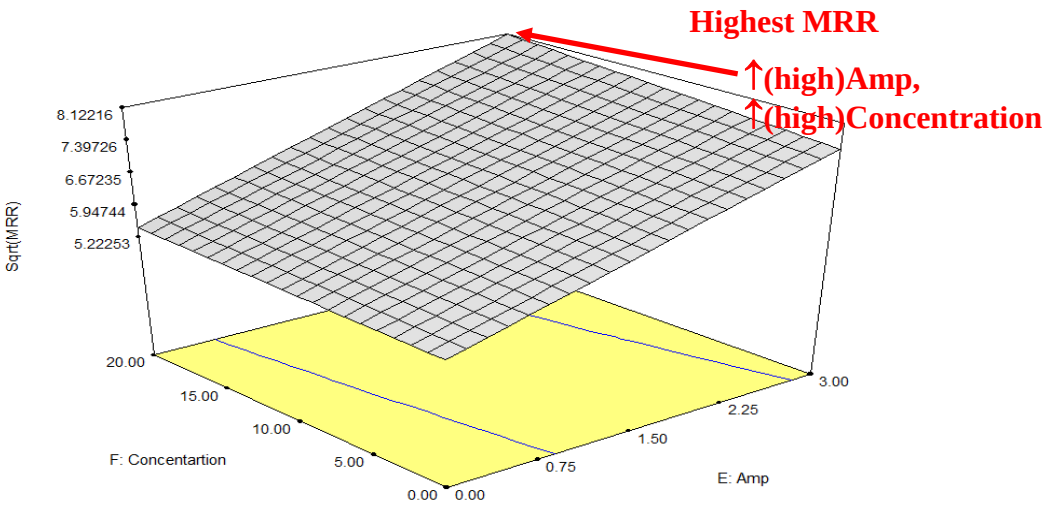


Figure 4.22: Interaction between vibration amplitude and abrasive concentration on MRR

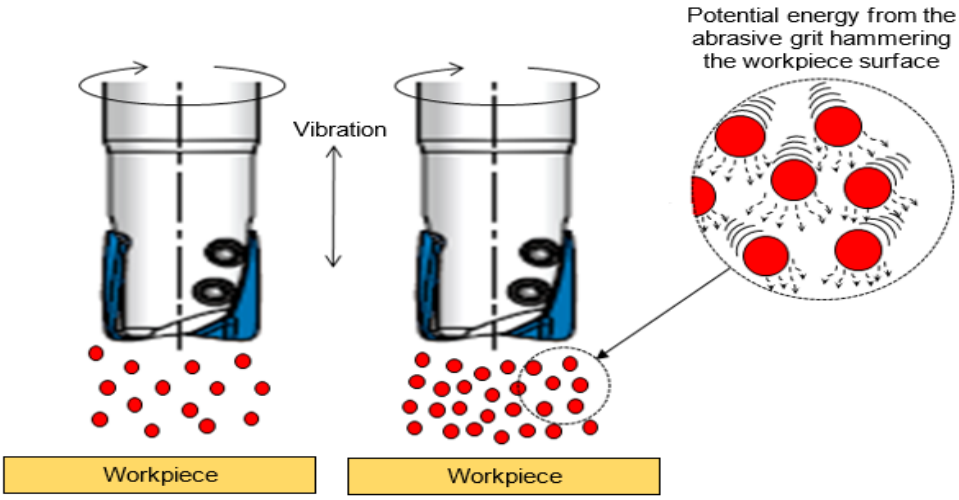


Figure 4.23: Effects of abrasive slurry concentration and vibration amplitude on MRR value

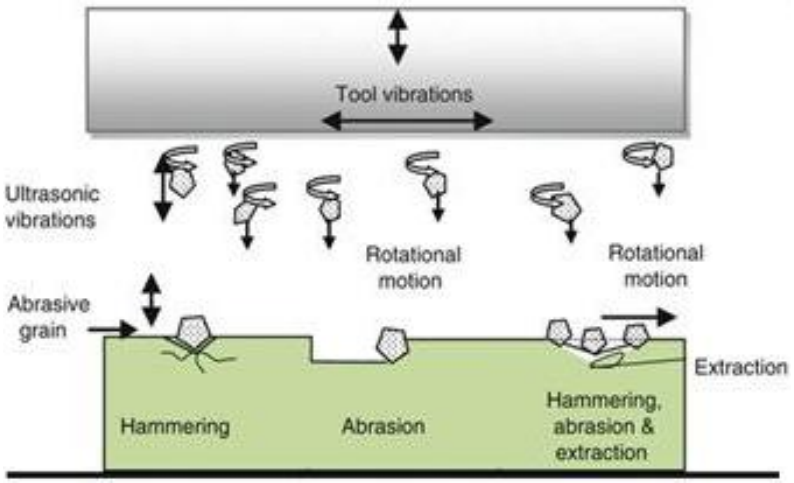


Figure 4.24: Material removal rate mechanism for RUAEM

4.5 Multiple response optimizations result

The developed mathematical function of each individual machining performances response such as, surface roughness, cutting force and material removal rate, was correlated with the machining parameter. Then, multi response optimization result are presented followed by the validation result.

Multiple response optimizations allowed for a set of optimum desire response condition to be achieved. All the desired responses can be simultaneously optimized or at least kept in the desired range. Multiple response technique was to increase the process efficiency, targeting to increase the quality, cost and time. In this study, there were two techniques applied for the multiple responses optimization namely; desirability function and overlay plot. The aim of this optimization process was to establish an optimum set of machining parameters that produced a combination of low surface roughness, low cutting force and high material removal rate.

The desirability function was developed to search for the closest desired response namely the lowest surface roughness, lowest force and highest MRR value. However, because the main goal of this thesis was to eliminate the manual grinding polishing process, the targeted surface roughness values were limited in the range between 0.1 to 0.2 μm and the weight was assigned to 5. The targeted surface roughness value ranges were equivalent to A-3 Level Grade#15 diamond high polish part specification as shown in Figure 4.25 (society of the plastic industry (SPI) finish guide for mold polishing. Table 4.7 tabulates the performances goals and the constraint for the factors which aims to achieve multiple desired goals simultaneously.

SPI FINISH GUIDE FOR MOLD POLISHING

Level	Description	Typical Applications
A-1	Grade #3 Diamond	Lens / Mirror – requires 420 SS material
A-2	Grade #6 Diamond	High Polish parts
A-3	Grade #15 Diamond	High polish parts
B-1	600 Grit paper	Medium polish parts
B-2	400 Grit paper	Medium polish
B-3	320 Grit paper	Med – Low polish
C-1	600 Stone	Low polish parts
C-2	400 Stone	Low polish parts
C-3	320 Stone	Low polish parts
D-1	Dry Blast Glass Bead	Satin finish
D-2	Dry Blast # 240 Oxide	Dull finish
D-3	Dry Blast # 24 Oxide	Dull finish

https://www.canadianmetalworking.com/article/metalfinishing/art-vs-science-the-world-of-metal-polishing

Figure 4.25: Society of the plastic industry (SPI) finish guide for mold polishing

Table 4.7: Goal and constraint for the factors and responses

Factor/response	**Goal**	**Lower limit**	**Upper limit**	**Weight**
Speed (RPM)	in range	30	150	3
Feed rate (mm/min)	in range	5	45	3
Depth of cut (µm)	in range	10	30	3
Vibration frequency (kHz)	in range	20	27	3
Vibration amplitude (µm)	in range	0	3	3
Slurry concentration (mg)	in range	0	20	3
Surface roughness (µm)	minimize	0.1	0.2	5
Cutting force (N)	minimize	4.98	371.4	1
Material removal rate (mg/min)	maximize	0.56	161.6	1

Constructed from the targeted goal and the constraint preset value, a total of 17 solutions with its desirability levels were proposed as tabulated in Table 4.8. Desirability level that is closer to 1, indicates that the goals can be reach. In other words, the higher the desirability index represents the closest the response towards target or optimum values. As shown in the table, the proposed solutions have the desirability index in the range of 0.19 to 0.87.

Table 4.8: Result for multiple response optimizations solutions

No.	Vc (rpm)	F (mm/min)	DoC (µm)	Freq (kHz)	Amp (µm)	Slurry (%)	Ra (µm)	Fr (N)	MRR (mg/min)	Desirability
1	111.45	5.75	27.05	21	3.00	13.26	0.100	19.43	9.78	0.87
2	115.00	5.01	29.66	22	3.00	11.84	0.100	15.40	8.34	0.87
3	133.50	8.82	24.66	20	2.96	11.72	0.100	24.17	7.50	0.77
4	115.27	5.00	17.34	20	1.85	15.00	0.100	29.75	2.31	0.73
5	119.53	5.00	21.13	20	1.15	10.85	0.100	27.66	1.99	0.69
6	115.00	5.00	21.27	20	0.75	15.10	0.098	23.61	1.65	0.68
7	140.03	5.00	25.95	22	2.33	12.10	0.100	16.80	1.98	0.67
8	107.94	5.27	17.09	20	1.19	13.39	0.100	30.03	1.51	0.66
9	115.00	5.64	20.70	20	0.75	10.88	0.100	27.84	1.88	0.66
10	144.67	7.75	25.99	22	3.00	12.88	0.100	15.24	3.45	0.64
11	130.89	5.00	25.20	20	0.61	13.67	0.100	20.69	1.94	0.64
12	127.76	5.00	19.06	24	2.09	12.88	0.100	21.08	1.23	0.63
13	117.46	5.00	13.85	20	1.60	17.20	0.100	29.65	0.93	0.59
14	117.19	5.15	23.72	24	0.42	9.81	0.100	21.20	1.69	0.56
15	138.49	7.70	12.23	20	3.00	7.85	0.100	64.06	3.12	0.54
16	103.43	7.97	14.72	20	0.43	15.00	0.099	28.20	0.84	0.54
17	113.32	11.74	10.52	20	0.03	18.86	0.128	23.08	0.63	0.19

Based on Table 4.8, solution number 1 and 2 had the highest desirability index such as 0.87. These two solutions were further analysed based on compromised decision between responses and the constraints such as cost, efficiency and practicality. In this experiment, the proposed solution number 1 was chosen as the best solution for the optimization of machining parameter (combination of 111.45 rpm, 5.75 mm/min feed rate,

27.05 µm depth of cut, 20.91 kHz vibration frequency, 3 µm amplitude and 13.26 % abrasive concentration) based on the combination of targeted surface roughness value of 0.1 µm, minimum resultant force and maximum material removal rate value which were predicted to be 19.43 Newton and 9.78 mg/min respectively. The trade of between solution 1 and 2 were made based on the highest predicted MRR value which affected the production time and could significantly reduce the machining cost. Although the resultant force from solution 2 were slightly lower than solution 1 to ~4 Newton, the force increment value was not too severe and would not impair the cutting tool and work piece surface due to the presence of the abrasive slurry. The abrasive slurry acted as a cutting fluid that cooled the cutting zone temperature.

Therefore, based on the arguments, solution 1 was selected as the best optimization run that fulfilled the desired responses. Figure 4.26 depicts the desirability ramp for the optimization process between parameters and responses. In addition, perturbation plot as shown in Figure 4.27 was created to illustrate how a function of a certain factor responded as the level of that factor changes to desirability (Oh et al., 1995). A steep slope or curvature in the plots indicates sensitivity of the response factor that can help to compare the effects of all factors at a particular point in the design space.

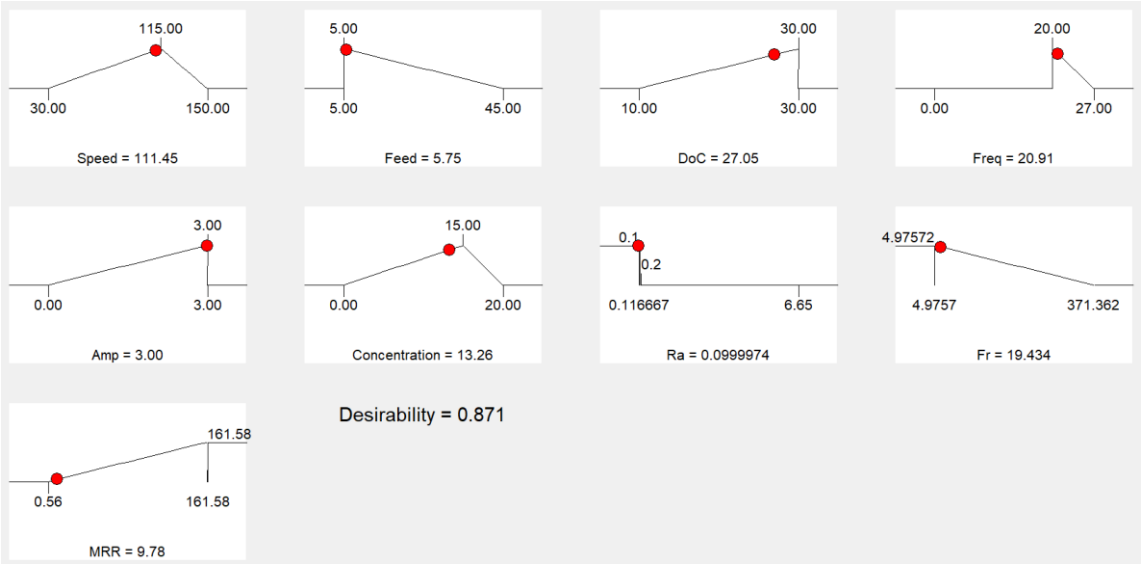


Figure 4.26: Desirability ramp for the optimization process between parameters and responses

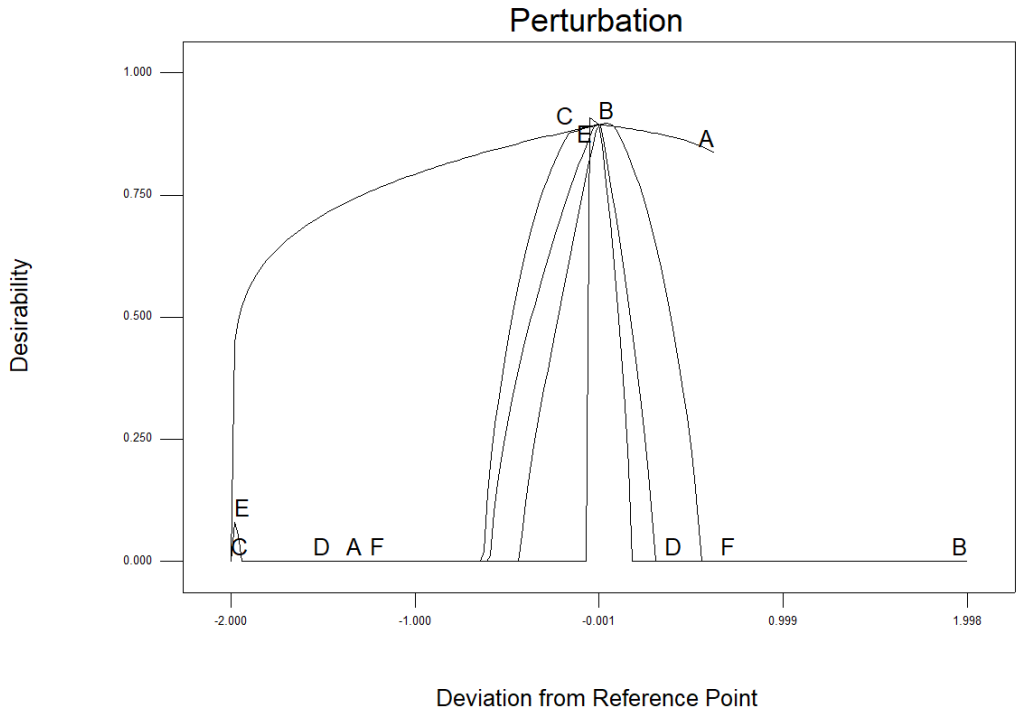


Figure 4.27: Perturbation plot for the optimization process based on desirability

4.5.1 Validation process

Based on the selected optimized cutting parameters (combination of 111.45 rpm, 5.75 mm/min feed rate, 27.05 µm depth of cut, 20.91 kHz vibration frequency, 3 µm amplitude and 13.26 % abrasive concentration), a triplicate experiment was set up to validate the effectiveness of the optimization model. Validation processes were done to assess amount of the relative error between the predicted and experimental results. The relative error is calculated using the formula as follows:

$$Relative\ Error\ (\%) = \frac{(Predicted\ Value - Actual\ Value)}{Predicted\ Value} \times 100 \quad (4.9)$$

4.5.1.1 Surface roughness

Table 4.9 and Figure 4.28 tabulated the validation score for surface roughness values between predicted and experimental results. According to Table 4.9, validation results for surface roughness values shows the correlation between experimental and selected solution which were ranging between 76.0% to 92.0% with an average correlation of 89.7%. The low average relative errors of approximately 10% from the predicted values clearly indicated that the model fitted the experimental data very well and therefore, optimized the targeted surface roughness value efficiently within the specified range of cutting parameters, hence, confirmed the proposed optimization parameter.

Table 4.9: Validation result for surface roughness

Validation Number	Predicted (µm)	Actual (µm)	Residual error (%)	Correlation (%)
1		0.092	8.0	92.0
2	0.10	0.124	24.0	76.0
3		0.115	15.0	85.0
Average	0.10	0.11	10.3	89.7

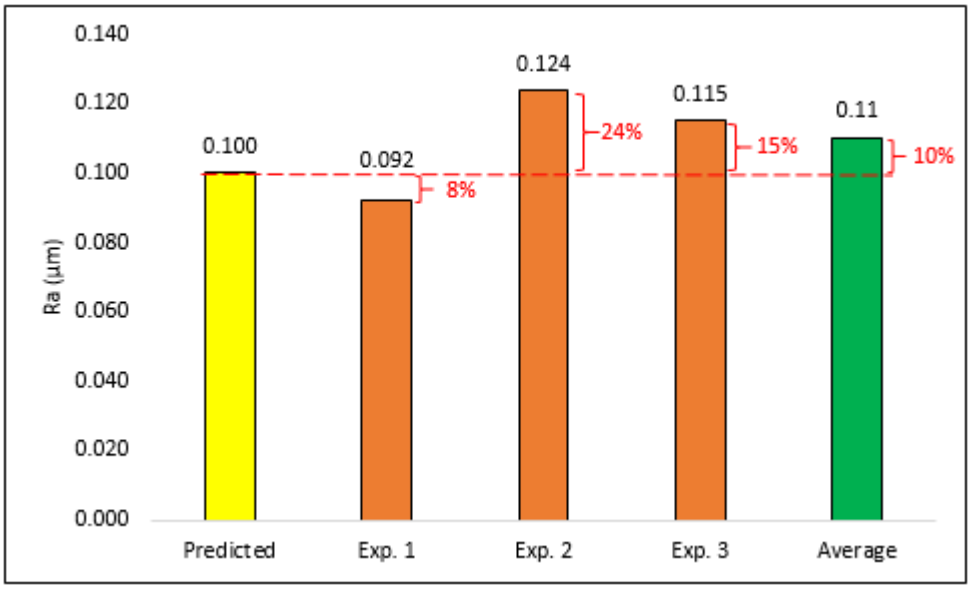


Figure 4.28: Comparison between predicted and actual values for surface roughness

4.5.1.2 Resultant force (F_R)

Table 4.10 and Figure 4.29 tabulated the validation score for resultant force values between predicted and experimental results. According to Table 4.10, validation results for resultant force values showed the correlation between experimental and selected solution were in the range between 81.0% to 85.9% with an average correlation of 84.1%. Although the average relative errors of approximately 15.9% from the predicted values are high,

from a practical stand point, the errors are still in the considerable accepted ranges due to the unstable and dynamic of the cutting force generated (Dikshit, et al., 2017). In addition, the sensitivity of the acquired signal force is also one of the factors that affected the value.

Table 4.10: Validation for resultant force

Validation Number	Predicted (N)	Actual (N)	Residual Error (%)	Correlation (%)
1		23.12	19.0	81.0
2	19.43	22.27	14.6	85.4
3		22.18	14.1	85.9
Average	19.43	22.52	15.9	84.1

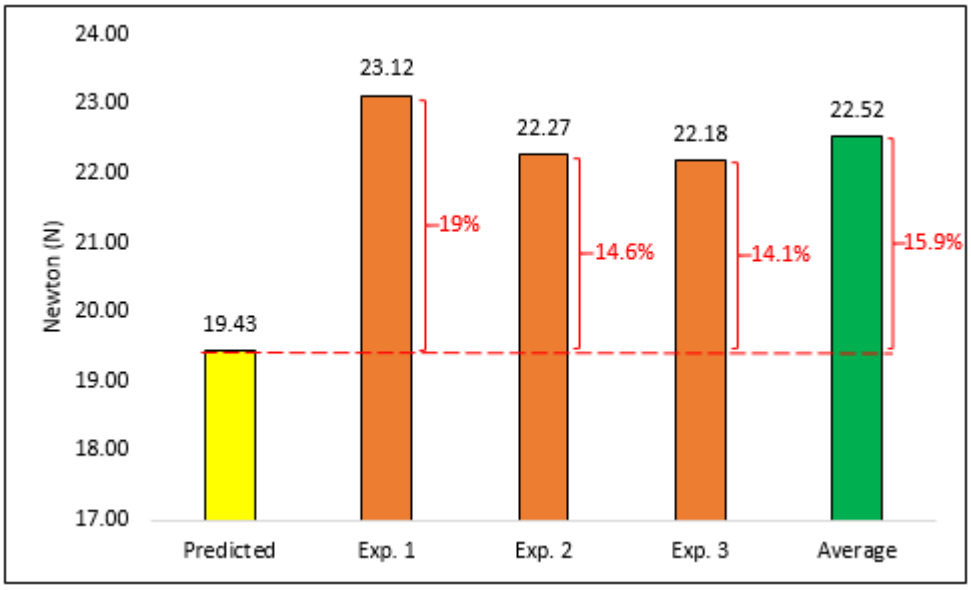


Figure 4.29: Comparison between predicted and actual values for resultant force

4.5.1.3 Material removal rate

Table 4.11 and Figure 4.30 tabulated the validation score for material removal rate values between predicted and experimental results. According to Table 4.11, validation results for resultant force values showed the correlation between experimental and selected solution which were in the ranges between 76.0 % to 92.0 % with an average correlation of 89.7%. The low average relative errors of approximately 10% from the predicted values clearly indicated that the model fitted the experimental data very well and therefore optimized the targeted material removal rate value efficiently within the specified range of cutting parameters, hence, confirming the proposed optimization parameters.

Table 4.11: Validation result for material removal rate

Validation Number	**Predicted (µm)**	**Actual (µm)**	**Residual Error (%)**	**Correlation (%)**
1		0.092	8.0	92.0
2	0.10	0.124	24.0	76.0
3		0.115	15.0	85.0
Average	0.10	0.11	10.3	89.7

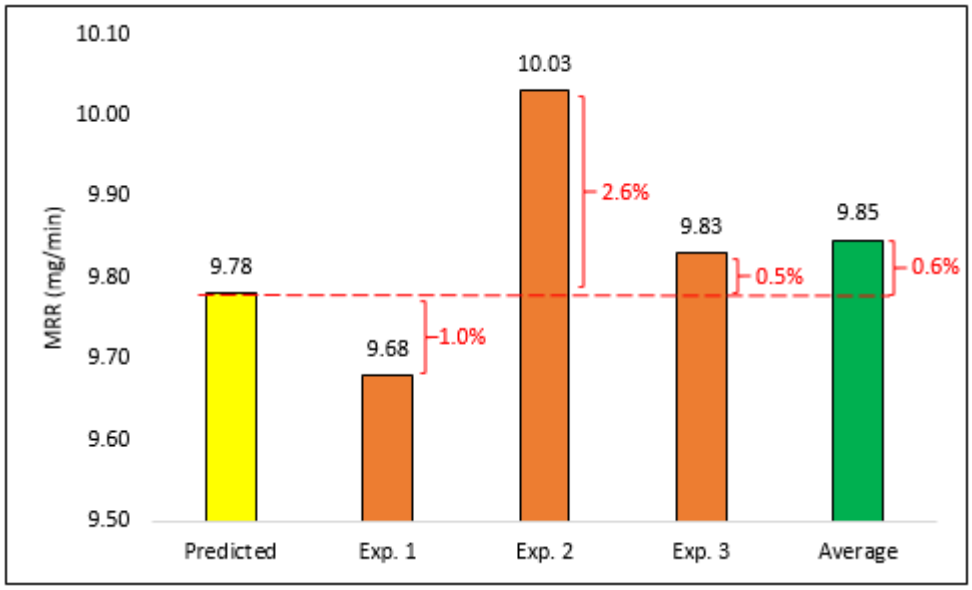


Figure 4.30: Comparison between predicted and actual values for material removal rate

Macroscopic observation was used to evaluate on the optimized machined surface finish. Figure 4.31 shows the observed machined surface. It shows that the suggested optimized parameters produced a smooth and shiny machined surface with fine and consistent cutter feed marks, thus, validating the optimization model.

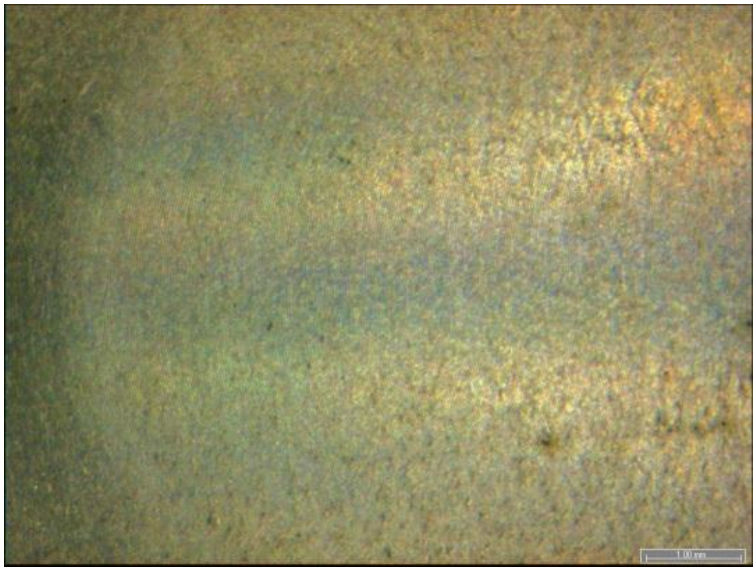


Figure 4.31: Optimized machined surface

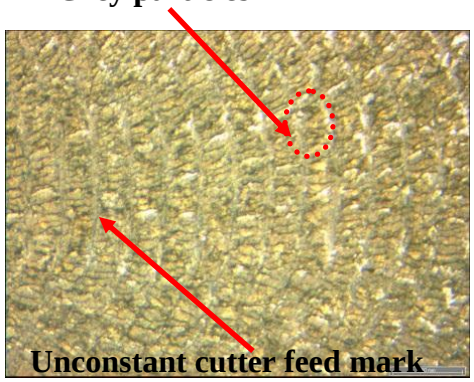
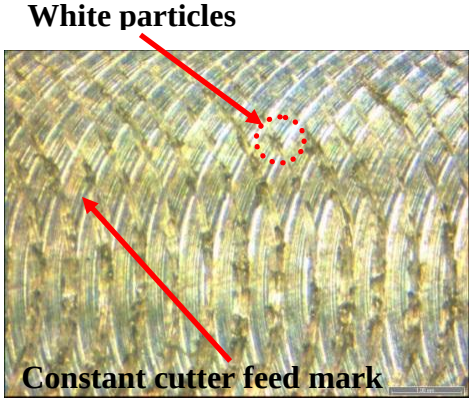
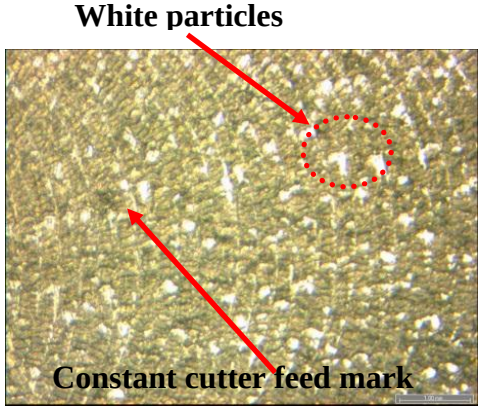
4.6 Macroscopic evaluation of machined surface quality

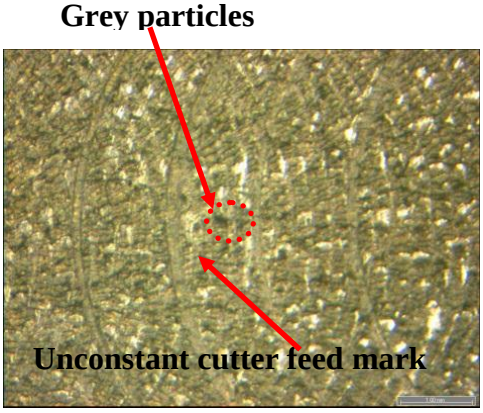
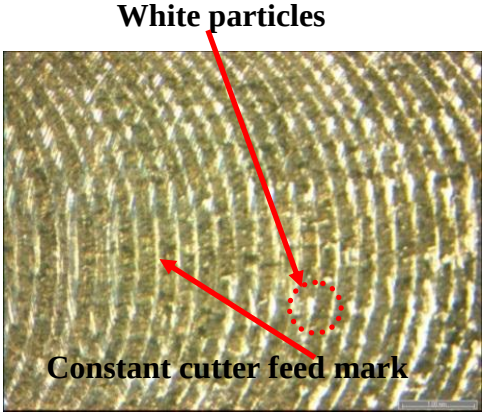
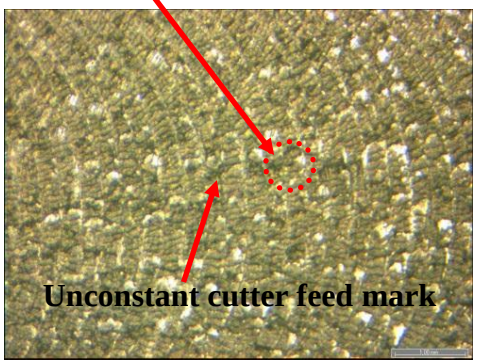
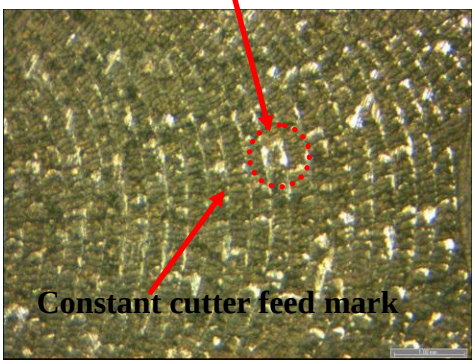
Macroscopic observations evaluation has been carried out to investigate and evaluate the machined surface quality for both machining techniques conventional and ultrasonic machining with different cutting conditions such as, speed, feed rate, depth of cut, ultrasonic frequency, ultrasonic amplitude and slurry concentration. Discussion on the machined surface quality is made based on two categories. In the first category, discussion is based on the comparison between conventional machining technique compared to rotary ultrasonic assisted machining (without the present of aluminum oxide slurry). As for the second category, discussion is based on the rotary ultrasonic assisted machining with different composition of aluminum oxide slurry (5%, 10%, 15% and 20% concentration).

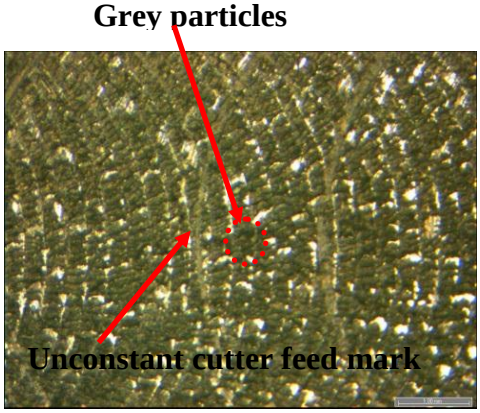
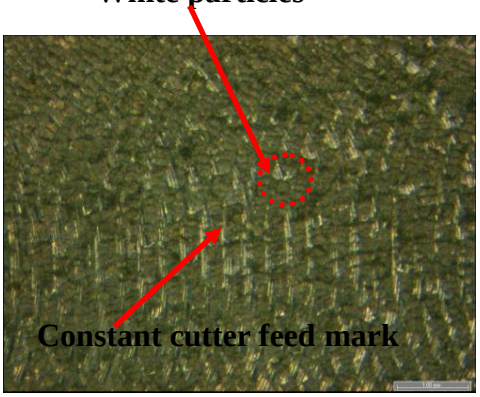
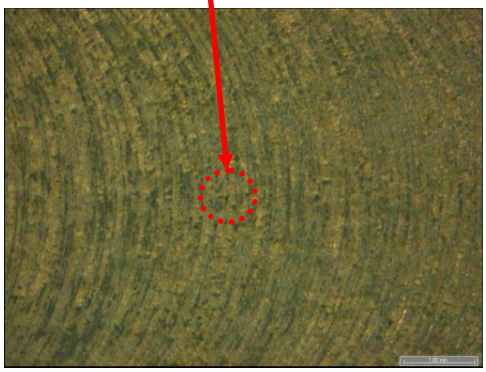
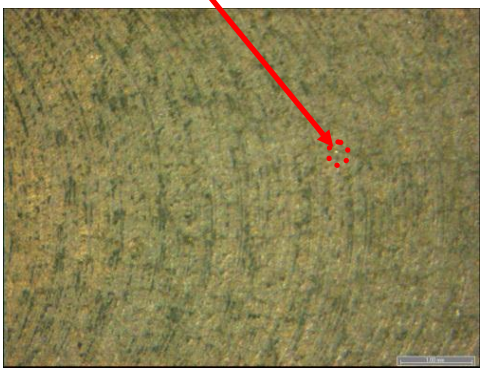
4.6.1 Machined surface quality between conventional machining and RUAEM (no slurry)

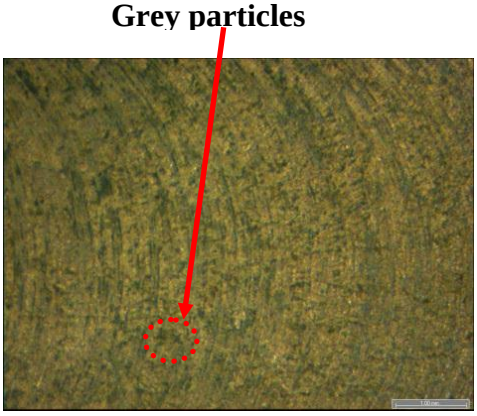
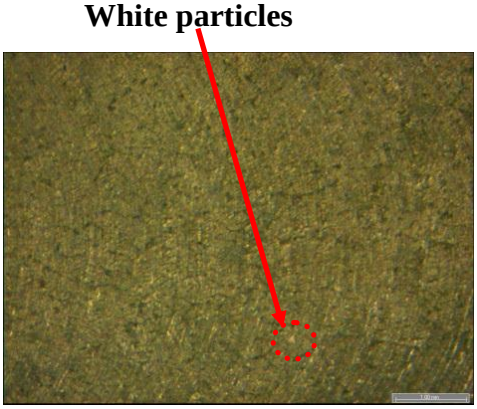
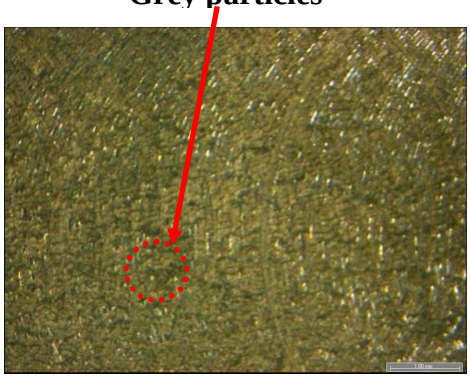
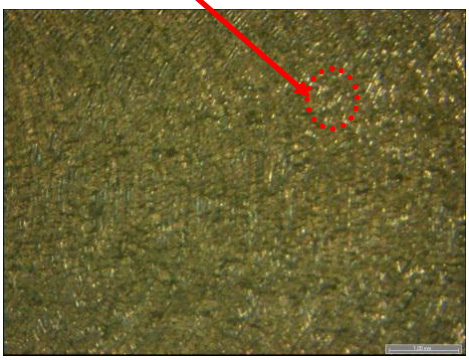
Table 4.12 depicts details on the machined surface quality between conventional machining and RUAEM (no Slurry) for all the runs. Generally, it can be observed that the machined work piece surface produced for all the runs consists a formation of cutter feed marks grooves which follows accordingly with the cutter teeth rotation direction. In addition, (referring to the experimental surface roughness value) the machined surface quality by using RUAEM produces more uniform and smooth cutter marks pattern as compared with conventional machining process for all the machining parameters condition. The best surface machined quality was observed at Run 26 with 0.19 μm for the combinations of 90 rpm (cutting speed), 5 mm/min (feed rate), 20 μm (depth of cut), 27 kHz (frequency vibration) and 3 μm (vibration amplitude).

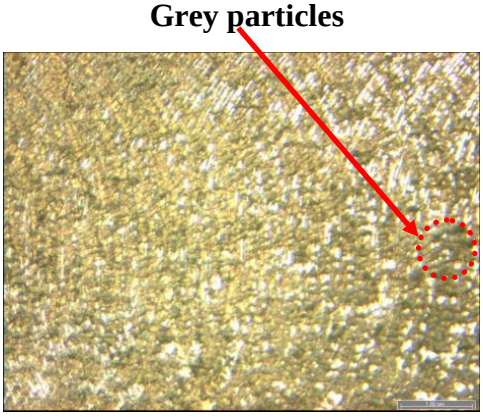
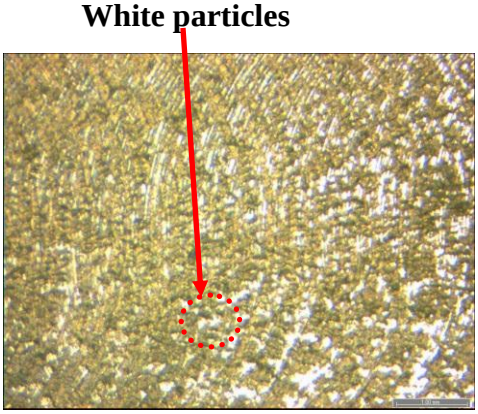
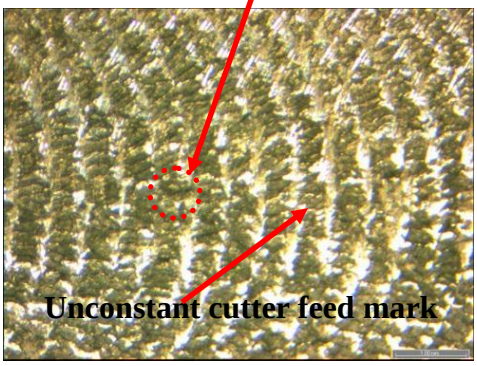
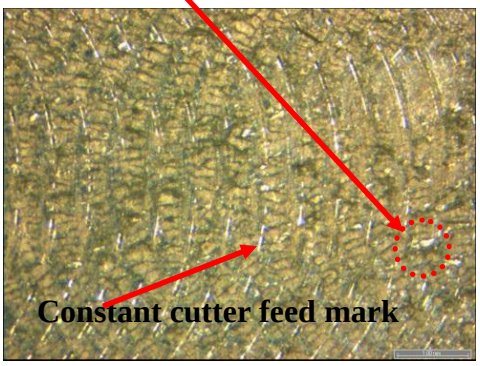
Table 4.12: Machined surface quality between conventional machining and RUAEM (no slurry)

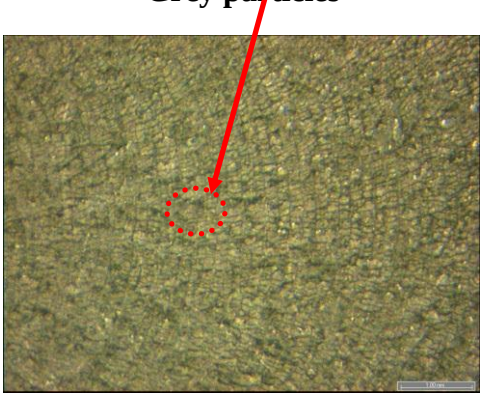
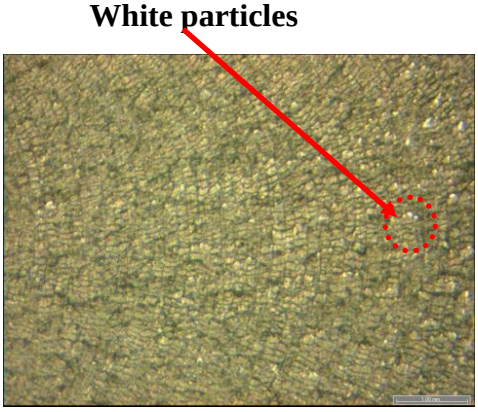
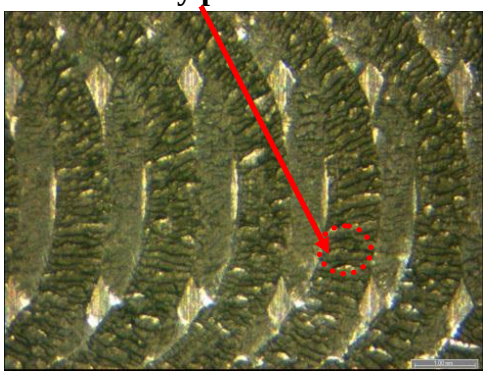
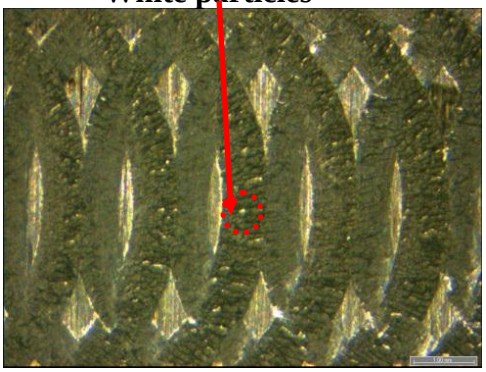
Runs No.	**Machining Parameters**	**Conventional Machining**	**Ultrasonic Machining with No Aluminum Oxide Slurry**
1	Vc = 90 rpm Feed = 45 mm/min Doc = 10µm	**Grey particles**  **Ra = 5.50 µm**	**White particles**  **Ra = 2.15 µm**
	Frequency	None	23 kHz
	Amplitude	None	2µm
2	Vc = 90 rpm Feed=25 mm/min Doc= 30µm	**Grey particles**  **Ra = 5.07 µm**	**White particles**  **Ra = 4.54 µm**
	Frequency	None	20 kHz
	Amplitude	None	1 µm

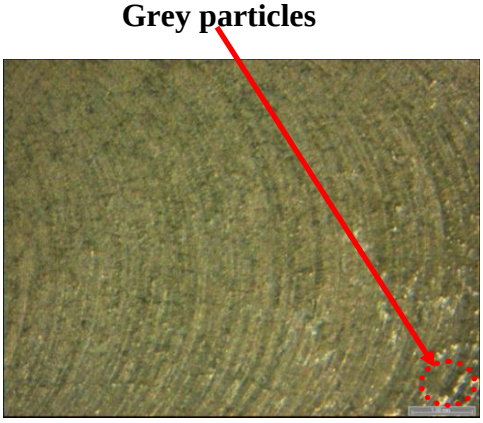
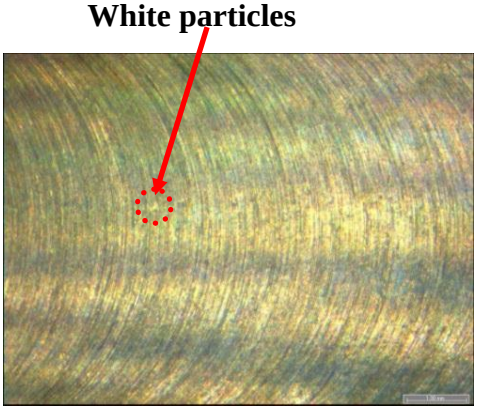
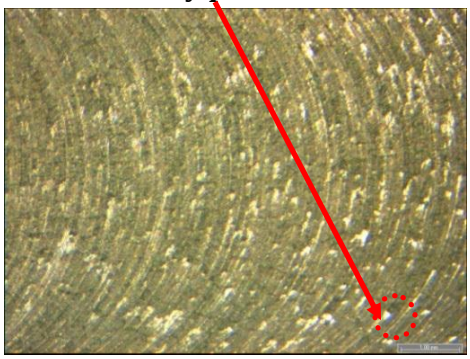
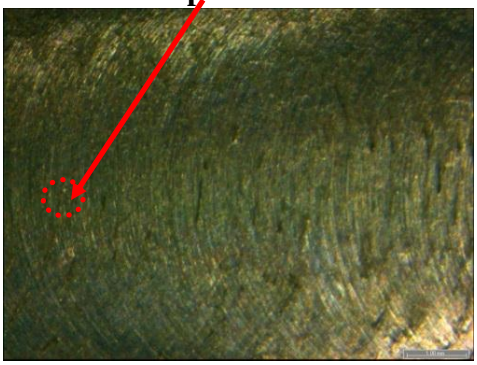
3	Vc = 90 rpm Feed=25 mm/min Doc=30µm	**Grey particles**  **Ra = 5.04 µm**	**White particles**  **Ra = 3.15 µm**
	Frequency	None	20 kHz
	Amplitude	None	2µm
4	Vc = 150 rpm Feed= 45 mm/min Doc= 20µm	**Grey particles**  **Ra = 5.14 µm**	**White particles**  **Ra = 4.59 µm**
	Frequency	None	20 kHz
	Amplitude	None	1 µm

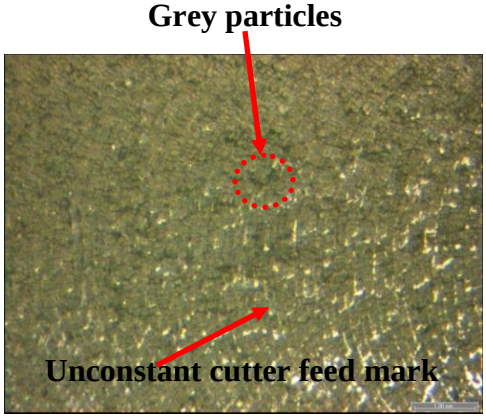
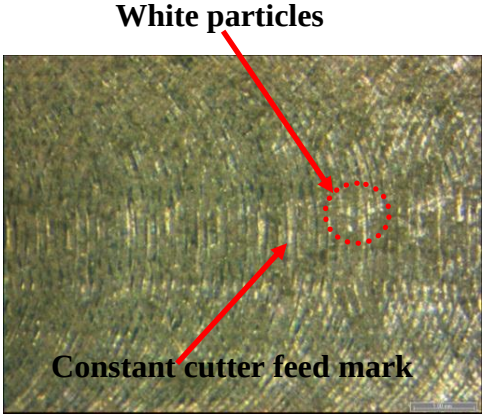
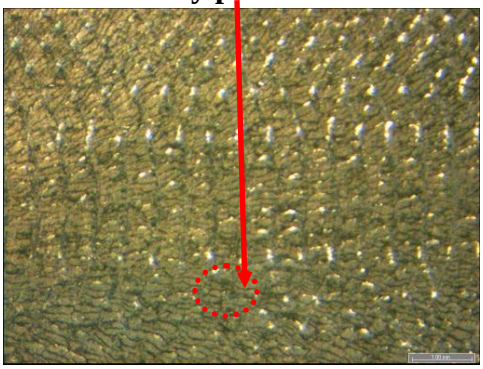
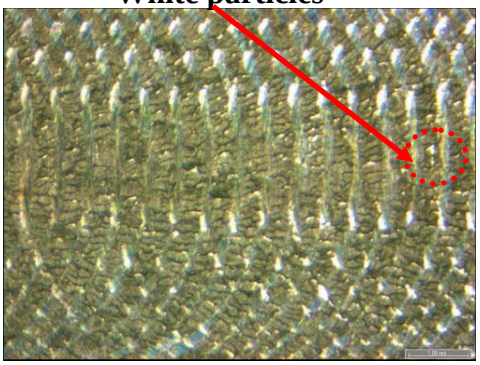
5	Vc = 150 rpm Feed= 45 mm/min Doc= 20µm	**Grey particles**  **Ra = 5.16 µm**	**White particles**  **Ra = 3.57 µm**
	Frequency	None	20 kHz
	Amplitude	None	2 µm
6	Vc = 90 rpm Feed= 5 mm/min Doc= 20 µm	**Grey particles**  **Ra = 1.87 µm**	**White particles**  **Ra = 1.60 µm**
	Frequency	None	27 kHz
	Amplitude	None	1 µm

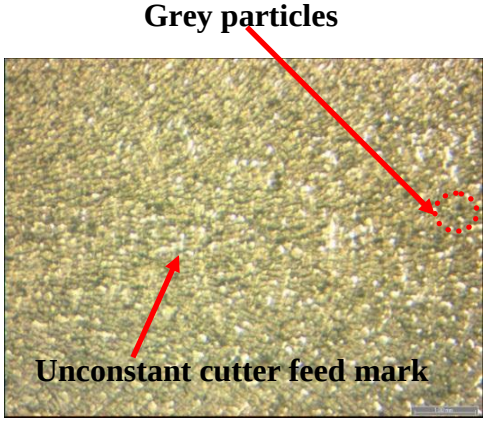
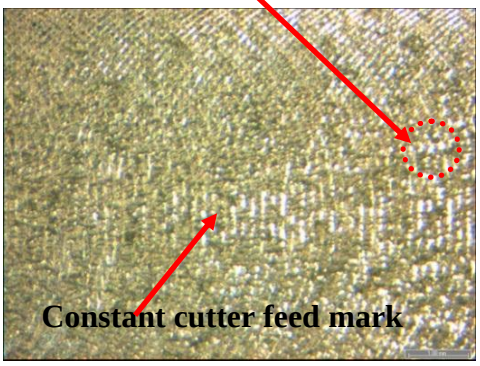
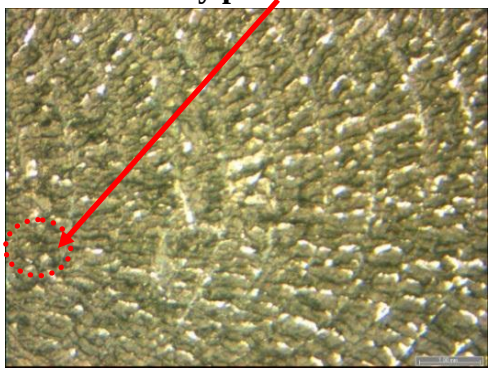
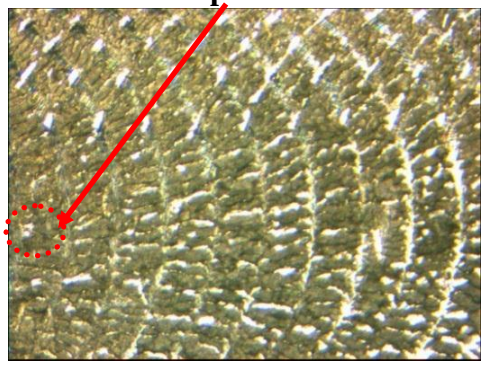
7	Vc = 90 rpm Feed= 5 mm/min Doc= 20 µm	**Grey particles**  **Ra = 1.89 µm**	**White particles**  **Ra = 1.84 µm**
	Frequency	None	27 kHz
	Amplitude	None	2 µm
8	Vc = 150 rpm Feed= 25 mm/min Doc= 10 µm	**Grey particles**  **Ra = 3.82 µm**	**White particles**  **Ra = 2.88 µm**
	Frequency	None	27 kHz
	Amplitude	None	3µm

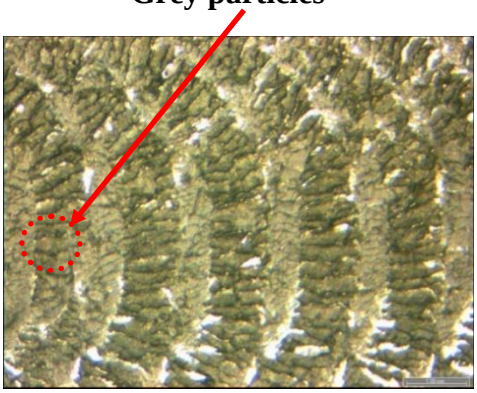
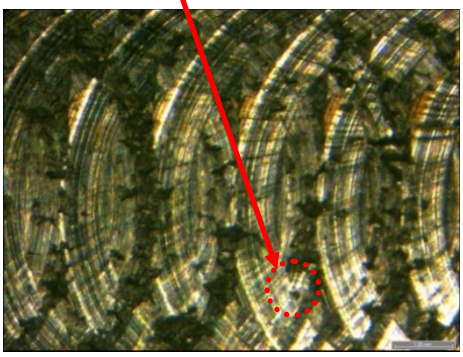
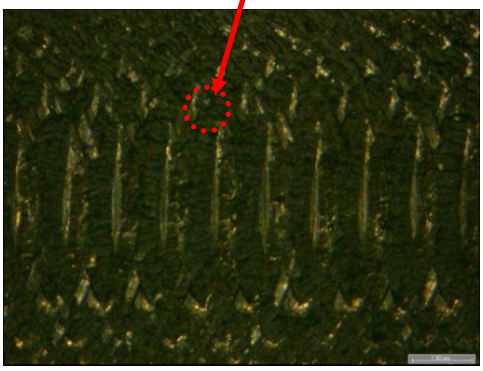
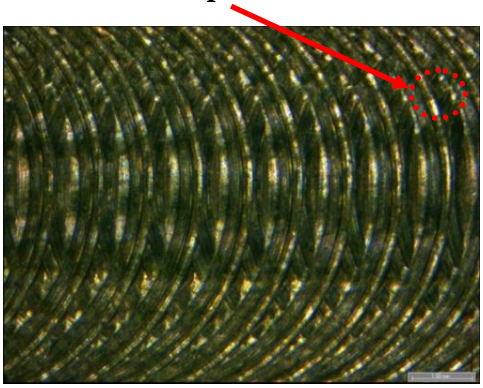
9	Vc = 150 rpm Feed= 25 mm/min Doc= 10µm	**Grey particles**  **Ra = 3.85 µm**	**White particles**  **Ra = 3.24 µm**
	Frequency	None	27 kHz
	Amplitude	None	2µm
10	Vc = 90 rpm Feed= 45 mm/min Doc= 10µm	**Grey particles**  **Unconstant cutter feed mark** **Ra = 5.55 µm**	**White particles**  **Constant cutter feed mark** **Ra = 2.86 µm**
	Frequency	None	23 kHz
	Amplitude	None	3µm

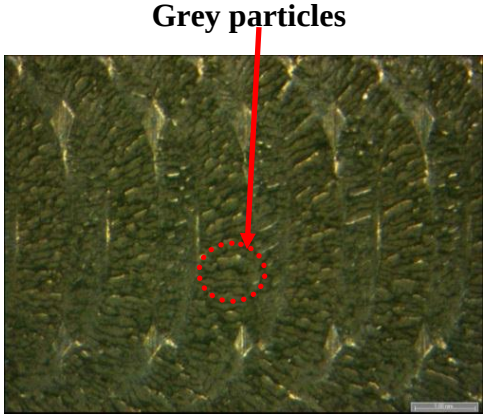
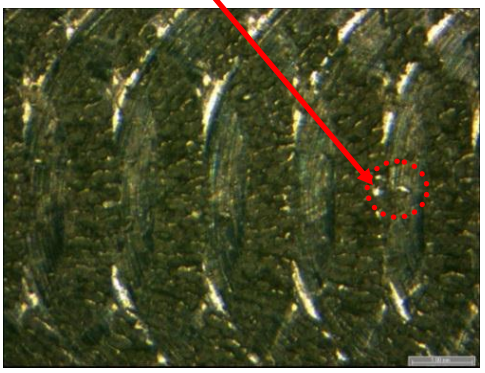
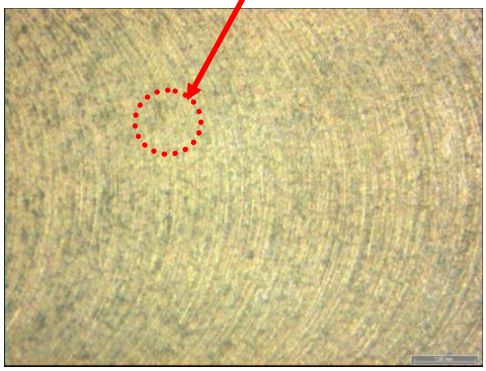
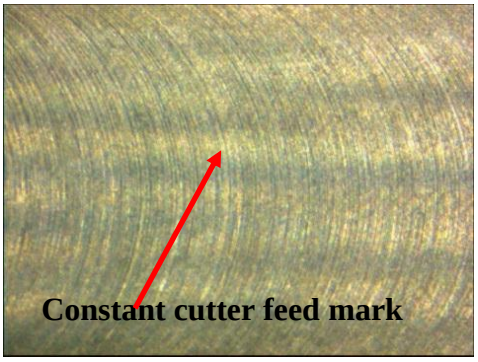
11	Vc = 30 rpm Feed= 5 mm/min Doc= 10 µm	**Grey particles**  **Ra = 4.02 µm**	**White particles**  **Ra = 3.62 µm**
	Frequency	None	20 kHz
	Amplitude	None	1 µm
12	Vc = 30 rpm Feed= 45 mm/min Doc= 30 µm	**Grey particles**  **Ra = 6.31 µm**	**White particles**  **Ra = 3.06 µm**
	Frequency	None	27 kHz
	Amplitude	None	1 µm

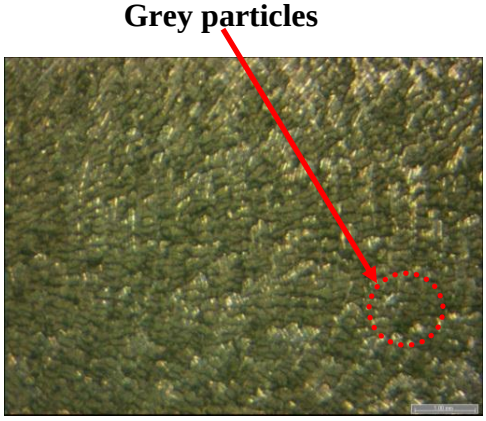
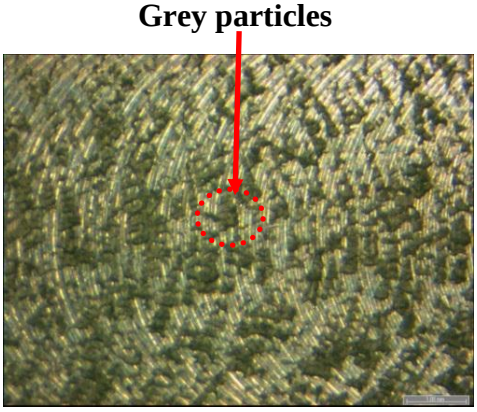
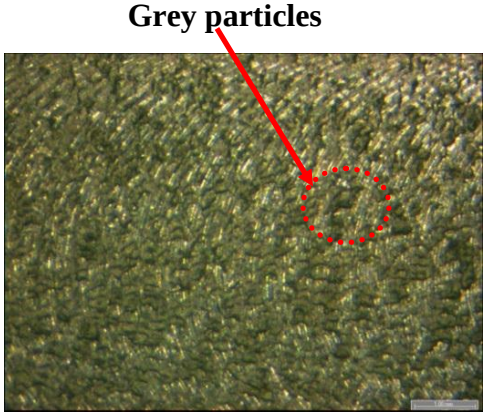
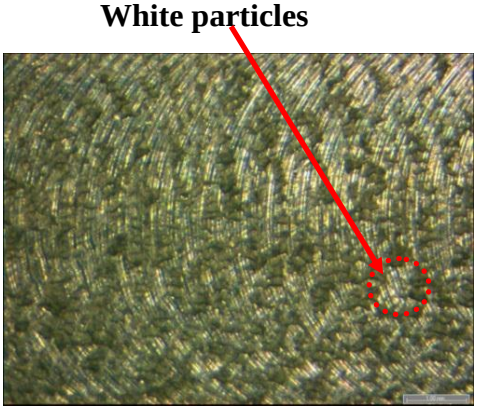
13	Vc = 150 rpm Feed= 5 mm/min Doc= 30 µm	**Grey particles**  **Ra = 1.93 µm**	**White particles**  **Ra = 0.91 µm**
	Frequency	None	23 kHz
	Amplitude	None	2 µm
14	Vc = 150 rpm Feed= 5 mm/min Doc= 30 µm	**Grey particles**  **Ra = 1.94 µm**	**White particles**  **Ra = 0.35 µm**
	Frequency	None	23 kHz
	Amplitude	None	1 µm

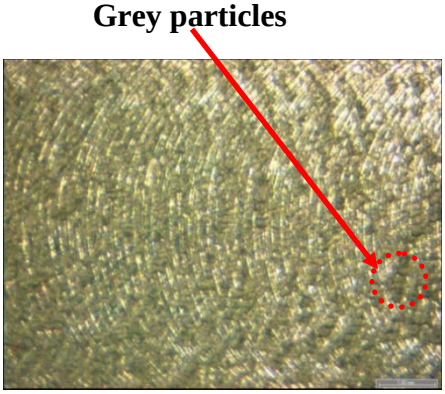
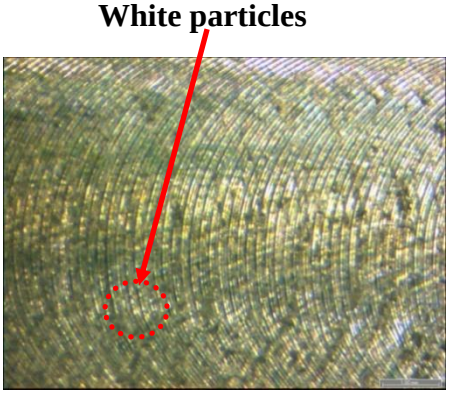
15	Vc = 30 rpm Feed= 5 mm/min Doc= 10μm	**Grey particles**  **Ra = 4.04 μm**	**White particles**  **Ra = 2.60 μm**
	Frequency	None	20 kHz
	Amplitude	None	3μm
16	Vc = 90 rpm Feed= 45 mm/min Doc= 10 μm	**Grey particles**  **Ra = 5.54 μm**	**White particles**  **Ra = 3.66 μm**
	Frequency	None	23 kHz
	Amplitude	None	1 μm

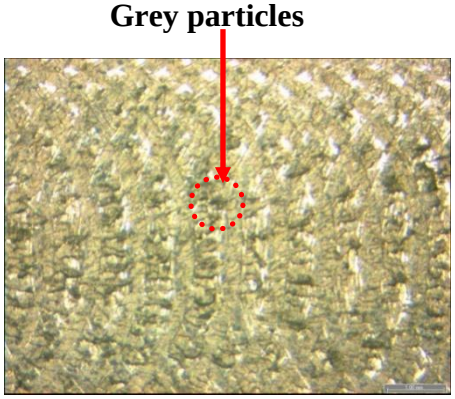
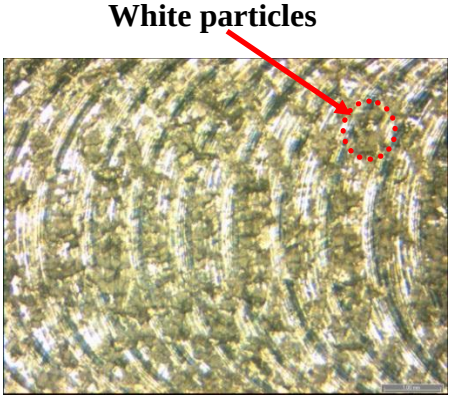
17	Vc = 30 rpm Feed= 5 mm/min Doc= 10µm	**Grey particles**  **Ra = 4.00 µm**	**White particles**  **Ra = 2.94 µm**
	Frequency	None	20 kHz
	Amplitude	None	2µm
18	Vc = 30 rpm Feed= 25 mm/min Doc= 20µm	**Grey particles**  **Ra = 6.37 µm**	**White particles**  **Ra = 5.50 µm**
	Frequency	None	23 kHz
	Amplitude	None	1µm

19	Vc = 30 rpm Feed = 45 mm/min Doc= 30 µm	**Grey particles**  **Ra = 6.65 µm**	**White particles**  **Ra = 3.25 µm**
	Frequency	None	27 kHz
	Amplitude	None	3µm
20	Vc = 30 rpm Feed = 25 mm/min Doc= 20 µm	**Grey particles**  **Ra = 6.49 µm**	**White particles**  **Ra = 5.28 µm**
	Frequency	None	23 kHz
	Amplitude	None	3 µm

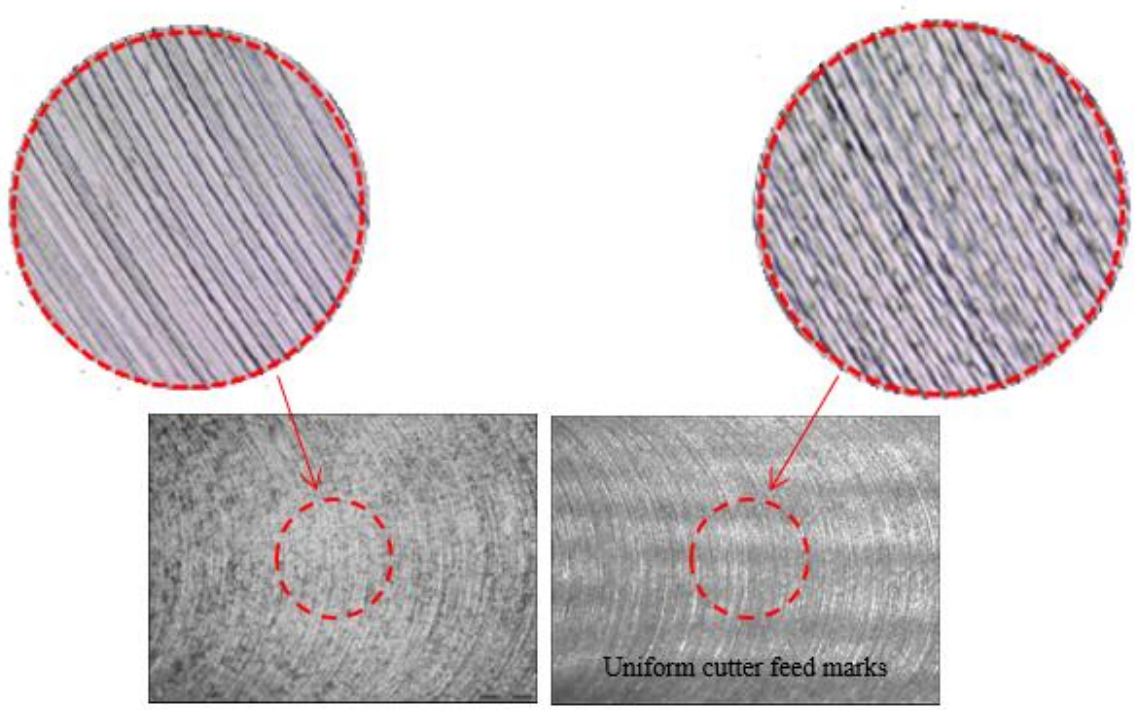
21	Vc = 30 rpm Feed= 45 mm/min Doc = 30 µm	**Grey particles**  **Ra = 6.10 µm**	**White particles**  **Ra = 4.86 µm**
	Frequency	None	27 kHz
	Amplitude	None	2 µm
22	Vc = 150 rpm Feed = 5 mm/min Doc = 30 µm	**Grey particles**  **Ra = 1.95 µm**	 **Constant cutter feed mark** **Ra = 0.70 µm**
	Frequency	None	23 kHz
	Amplitude	None	3 µm

23	Vc = 150 rpm Feed = 45 mm/min Doc = 20 µm	**Grey particles**  **Ra = 5.14 µm**	**Grey particles**  **Ra = 2.91 µm**
	Frequency	None	20 kHz
	Amplitude	None	3 µm
24	Vc = 90 rpm Feed= 25 mm/min Doc= 30 µm	**Grey particles**  **Ra = 5.03 µm**	**White particles**  **Ra = 2.72 µm**
	Frequency	None	20 kHz
	Amplitude	None	3 µm

25	Vc = 150 rpm Feed = 25 mm/min Doc = 10 µm	**Grey particles**  **Ra = 3.86 µm**	**White particles**  **Ra = 0.78 µm**
	Frequency	None	27 kHz
	Amplitude	None	1 µm
26	Vc = 90 rpm Feed = 5 mm/min Doc = 20 µm	**Grey particles**  **Ra = 1.81 µm**	 **Ra = 0.19 µm**
	Frequency	None	27 kHz
	Amplitude	None	3 µm

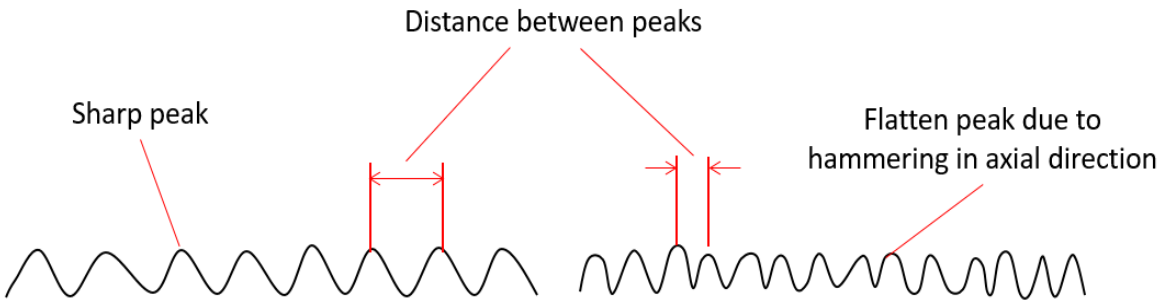
27	Vc = 30 rpm Feed= 25 mm/min Doc = 20 μm	**Grey particles**  **Ra = 6.22 μm**	**White particles**  **Ra = 5.15 μm**
	Frequency	None	23 kHz
	Amplitude	None	2 μm

Also, the machined surface produced by RUAEM are more smooth and has a shiny appearance which indicate a good quality surface as compared to conventional machining. Apart from that, it shows that the range of studied machining parameter have a significant effect on the produced surface quality. Figure 4.32, shows the macroscopic observation of machined surface generated from RUAEM (Run 26) with a uniform cutter feed mark with constant peak to peak value. Due to the presence of ultrasonic vibration in the vertical axis has created a hammering impact in cutting zone between the rotating cutter and work piece surfaces as well as minimize the distance between the two's peak that result in improved surface finish value as depicted in Figure 4.33.



Conventional machining RUAEM

Figure 4.32: Macroscopic observation for run 26 between conventional and RUAEM

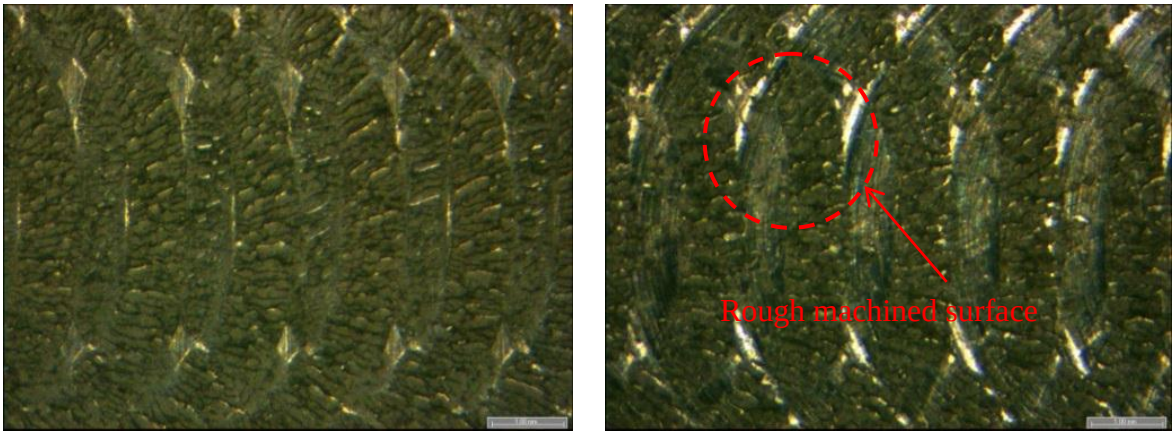


Conventional machining RUAEM

Figure 4.33: Machined surface topography between conventional and RUAEM

However, the hammering impact created from the vibration amplitude did not show any significant improvement on the machined surface quality if high cutting speed and high feed rate were employed. Hence, the interaction between parameters has a direct effect on the kinematic of the cutting process such chaotic chatter with random direction

movement which eliminate the axial direction movement. Figure 4.34 shows the insignificant hammering impact towards the machined surface in RUAEM cutting zone for Run 21.



Conventional machining RUAEM

Figure 4.34: Macroscopic observation of machined surface for run 21

4.6.1.1 Surface analysis

To further analyze the machined surface condition, a micrograph or surface topography were taken using scanning electron microscopy (SEM) machine. Figure 4.35 shows the microstructure of the machined surface generated by conventional machining (Run 22). The microstructure of machined surface has deformed due to the shearing of material by the cutter teeth. Furthermore, the SEM image showed that the high cutting speed and low feed rate resulted in small cutter feed marks with minor scratches and inconsistent marks appeared at the bottom surface. Other than that, when the high cutting speed was employed, the cutter feed marks produced are leveled off due to rapid occurrence on the machined surface (Chern and Chang, 2006). High cutting speed caused a high cutting force acting above the machined surface which affected the chips ejection process in the cutting zone and damaged the machined surface.

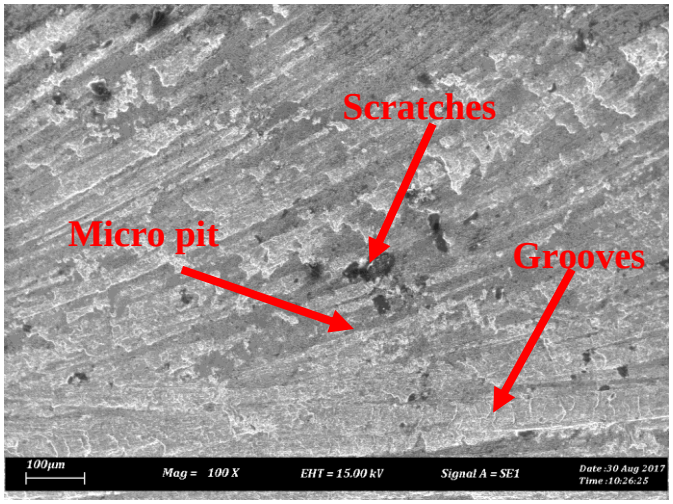


Figure 4.35: Microstructure of machined surface for run 22 (run 22C) by conventional machining at cutting speed of 150 rpm, feed rate of 5 mm/min, doc of 30 µm

As shown in Figure 4.36, the surface microstructure for conventional machining (Run 26) with low cutting speed and low feed rate indicated the consistency of cutter feed marks and the improvement of machined surface quality. Larger cutter feed marks with few scratches on the machined surface would appear when using a low cutting speed, low feed rate and low depth of cut. In addition, the feed marks produced on the machined surface work piece were leveled due to stable cutting condition such as low vibration occurred on the machined surface. In short, to machine hardened tool steel material using a lower cutting speed, lower feed rate and lower depth of cut is favorable for controlling the machined surface quality such as stable cutting condition, consistent cutter feed marks and minimum scratches.

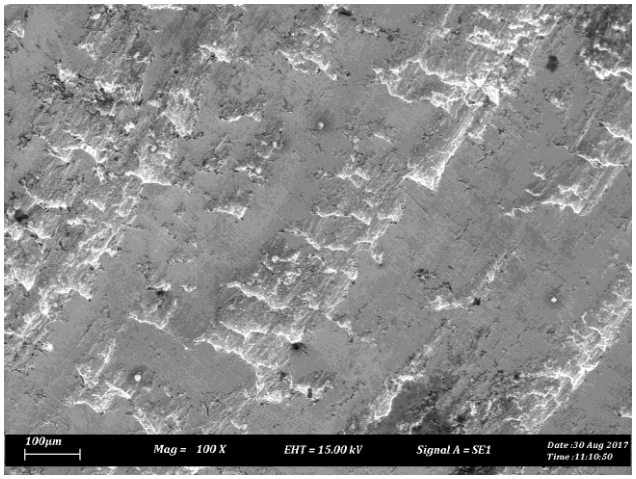


Figure 4.36: Microstructure of machined surface for run 26 by conventional machining (run 26 C) at cutting speed of 90 rpm, feed rate of 5 mm/min, doc of 20 µm

In RUAEM, the machined surface indicated the occurrence of plastic deformation as well as the formation of grooves and scratches along the cutting direction. The cracks initiation and scratches direction were found to be perpendicular to the cutting direction. In addition, the quantity of micro pit significantly increased when the cutting speed increased due to the occurrence of high compressive stress. As compared to conventional milling, the vibration force produced fine scratches and micro groove area as shown in Figure 4.37. In certain applications, this surface formation characteristic is important for the lubrication purpose.

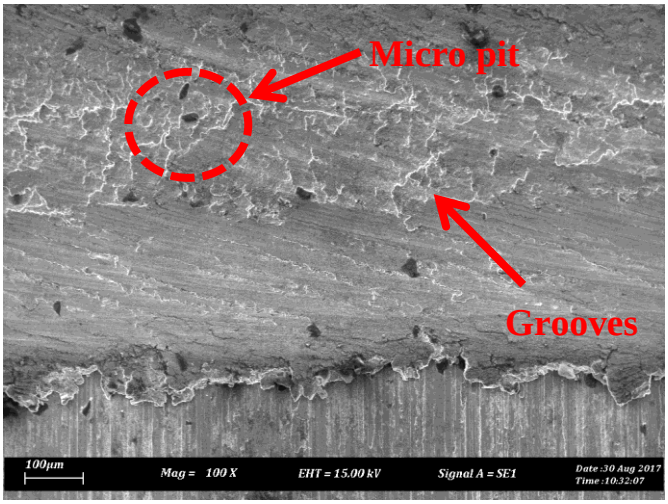


Figure 4.37: Microstructure of machined surface for run 22 (run 22 US) by RUAEM machining at cutting speed of 150 rpm, feed rate of 5 mm/min, doc of 30 µm, Frequency of 23 kHz and amplitude vibration of 3µm

However, employing low cutting speed and low feed with RUAEM process greatly improved the machined surface formation. Smooth machined surface and minimum micro-crack with micro size sub grains were observed on the machined surface as shown in Figure 4.38. Apart from the micro size sub grains that decrease the crack propagation rate, the improvement can be explained in terms of ways in which the machining process is slow (low speed and feed) so the axial direction vibration has sufficient time to impact on the instantaneous cutting surface as compared to fast process (high speed and feed) that flattened the cutter marks left by the cutter teeth, thus, reducing the peak height and improving the surface roughness value. Thus, in RUAEM, the selection of cutting parameters and vibrating parameters affects the topography of machined surface and has a direct impact on the surface roughness value.

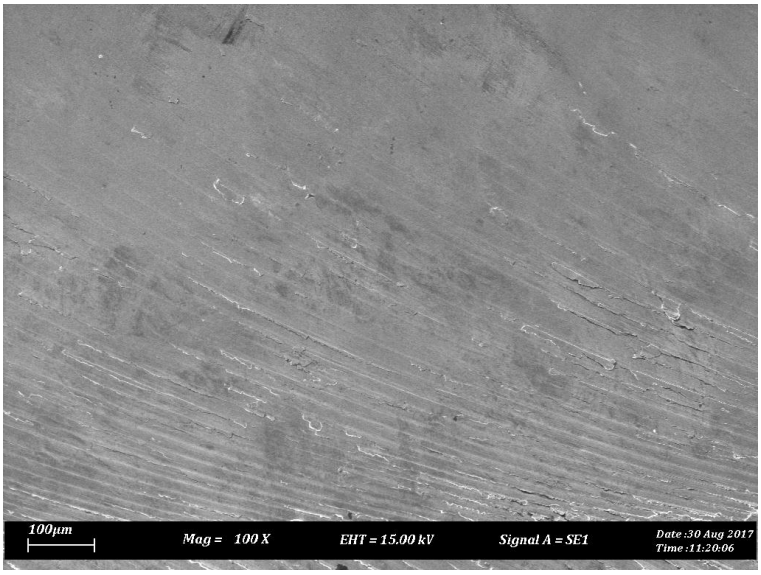


Figure 4.38: Microstructure of machined surface for run 26 (run 26 US) by RUAEM machining at cutting speed of 90 rpm, feed rate of 5 mm/min, doc of 20 µm, frequency of 27 kHz and amplitude vibration of 3 µm

4.6.1.2 Cross sectional analysis

Carl Zeiss scanning electron microscopy (SEM) machine was used to observe the cross-sectional images of machined surface. Cross sectional images provide an important information in determining the machined surface quality with respect to the machining parameter. Figure 4.39 shows the cross-sectional microstructure resulting from the conventional machining process. It can be observed that when high cutting speed was employed (Vc = 150 rpm), the microstructures tended to have a higher compressive stress zone, causing the atoms in the material changed to strain condition. The machined surface microstructure indicated that plastic deformation has taken place, leading to severe deformed layers of microstructure alteration at the subsurface level. In the strain condition, some of the atoms were separated from the original boundaries and moved to the new areas between planes, causing an elongation of grain boundaries. The figure showed that the

microstructure and grain boundaries tended to elongate to the bottom area due to the high cutting speed.

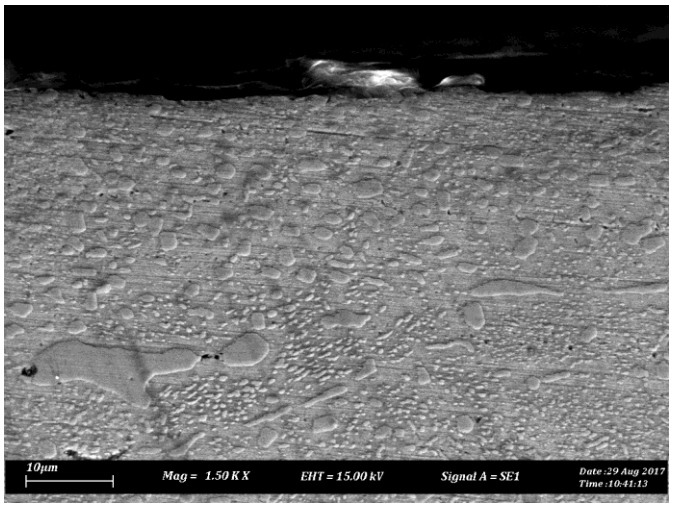


Figure 4.39: Microstructure of cross-sectional work piece machined surface for run 22 by conventional machining (run 22 C) at cutting speed of 150 rpm, feed rate of 5 mm/min, Doc of 30 µm with 1500 X magnification

Conversely, for lower cutting speed (Vc = 90 rpm), the grain boundaries were in a constant phase and produced less boundary elongation. One of the possible reasons is due to the occurrence of low compressive stress which minimized the atoms movement such as slight change to the strain condition as shown in Figure 4.40.

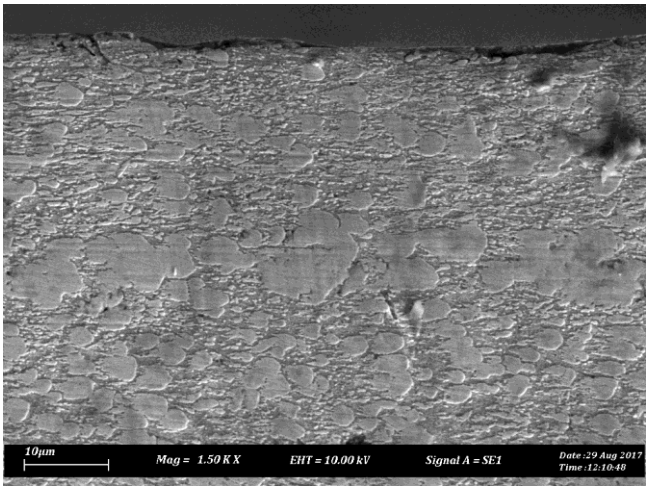


Figure 4.40: Microstructure of cross-sectional work piece machined surface for run 26 by conventional machining (RUN 26 C) at cutting speed of 90 rpm, feed rate of 5 mm/min, doc of 20 μm with 1500 X magnification

In RUAEM process, the cross-sectional observation indicated that the plastic deformation and grain distortion occurred on the top layer which was the closest to the work piece machined surface as compared to conventional milling. The presence of vibration frequency and amplitude minimizes the elongation of grain boundaries. However, the effects of cutting parameters on microstructure alteration based on cross sectional observation had little effects as compared to the machined surface as shown in Figure 4.41 (Run 22) and Figure 4.42 (Run 26).

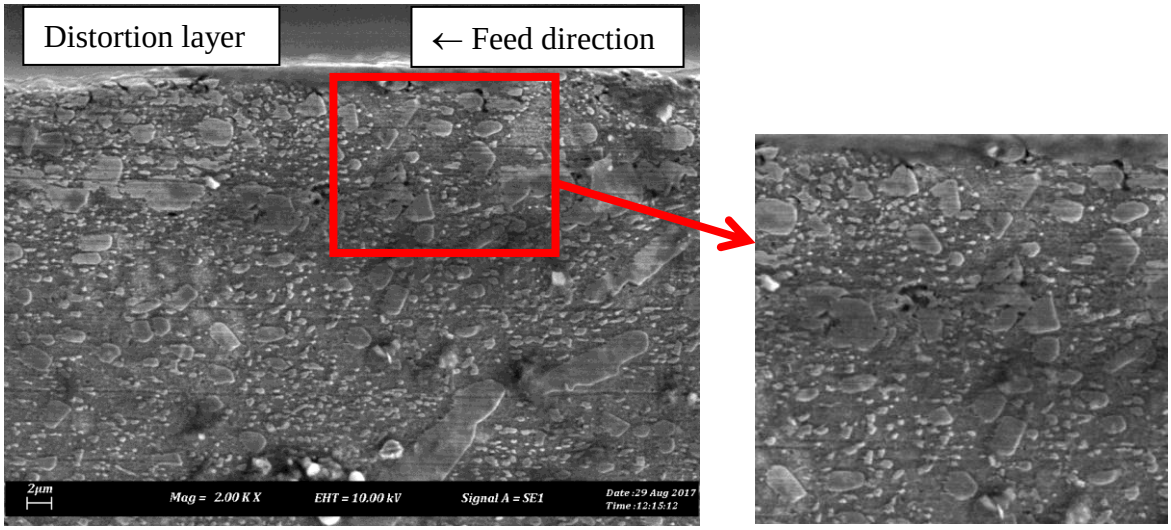


Figure 4.41: Microstructure of cross-sectional work piece machined surface for run 26 by RUAEM (run 26 US) at cutting speed of 90 rpm, feed rate of 5 mm/min, doc of 30 μm with 2000 X magnification

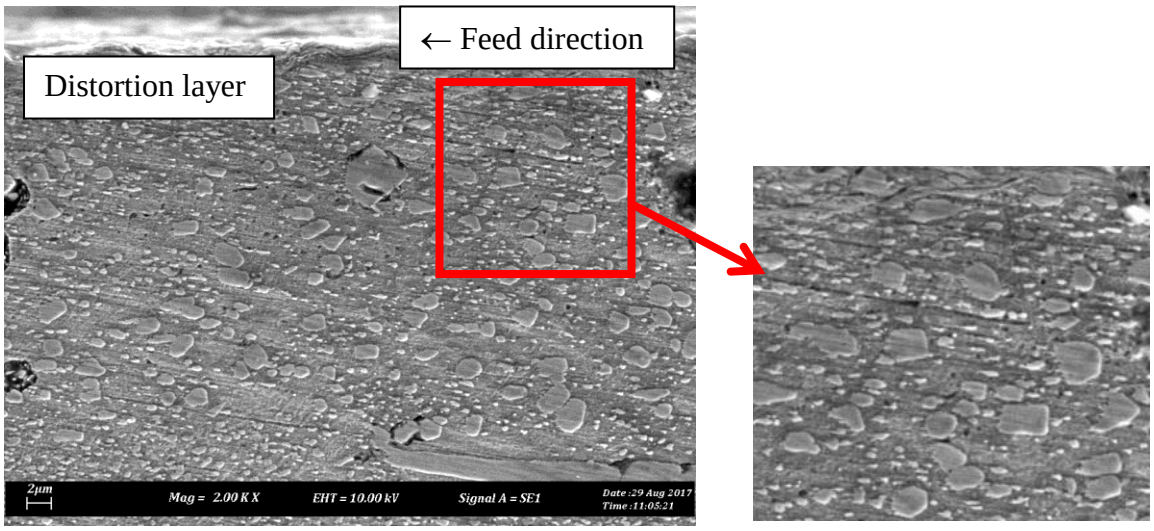


Figure 4.42: Microstructure of cross-sectional work piece machined surface for run 22 by RUAEM (run 22 US) at cutting speed of 150 rpm, feed rate of 5 mm/min, doc of 30 μm with 2000 X magnification

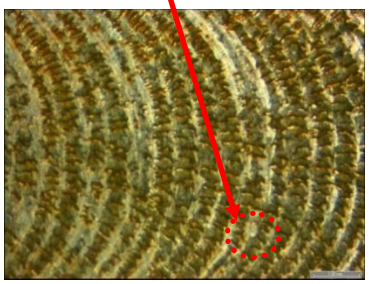
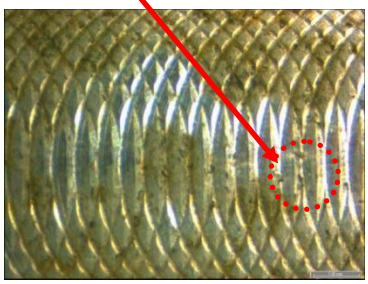
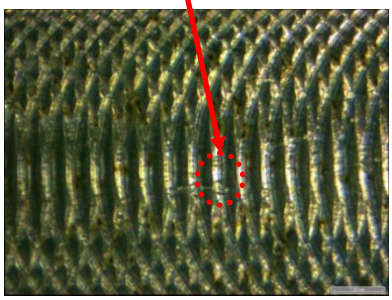
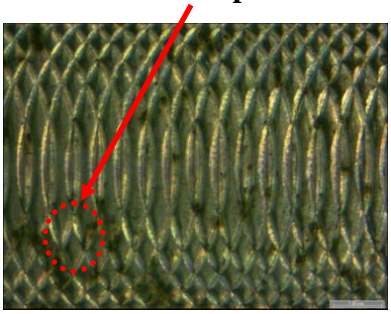
4.6.2 Machined surface quality for RUAEM with alumina oxide slurry

As for the second category, discussion is made based on the rotary ultrasonic assisted machining with different compositions of aluminum oxide slurry (5%, 10%, 15% and 20% concentration).

Table 4.13 depicts details on the RUAEM machined surface quality with different slurry concentrations and machining parameters. Generally, the machined work piece surface for all the runs consisted of a formation of cutter feed marks grooves which followed according to with the cutter teeth rotation direction. In addition, (referring to the experimental surface roughness value) the machined surface quality improved with the presence of alumina oxide slurry. Hence, at certain locations along the cutter feed marks, the peak surfaces were flattening due to the effect of vibration frequency on alumina oxide particles that created a hammering abrasion process on machined surface.

The best machined surface was obtained from Run 15 with 0.12 μm surface roughness using the combination of machining parameters (speed of 30 rpm, 5 mm/min feed rate, 10 μm depth of cut, frequency of 20 kHz, 3 μm amplitude and 15% concentration).

Table 4.13: RUAEM machined surface quality with different slurry concentrations and machining parameters

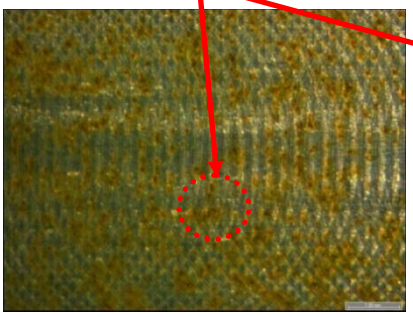
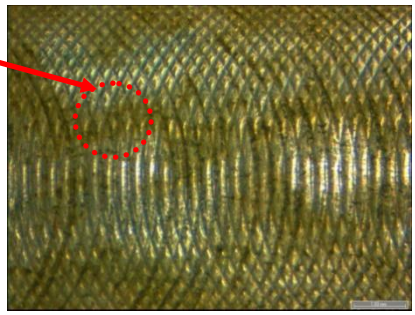
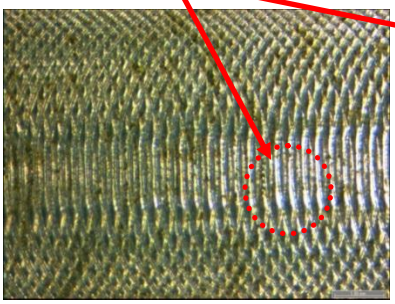
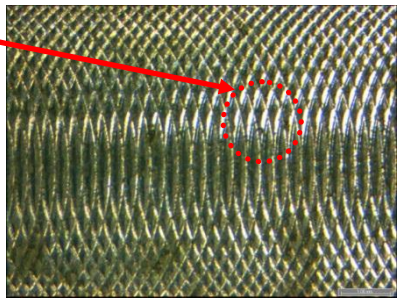
Runs No.	**Machining Parameters**	**Rotary Ultrasonic Assisted Machining with Slurry Concentration of Alumina Oxide**	
		5 %	10%
1	Vc = 90 rpm Feed = 45 mm/min Doc = 10µm Freq.=23 kHz Amp. = 2µm	**Alumina oxide particles**  **Ra = 2.62 µm**	**Alumina oxide particles**  **Ra = 1.85 µm**
		15 %	20 %
		Alumina oxide particles  **Ra = 2.52 µm**	**Alumina oxide particles**  **Ra = 2.28 µm**

<table>
<tr><td rowspan="4">2</td><td rowspan="4">Vc = 90 rpm

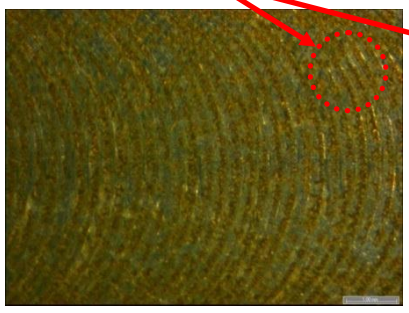
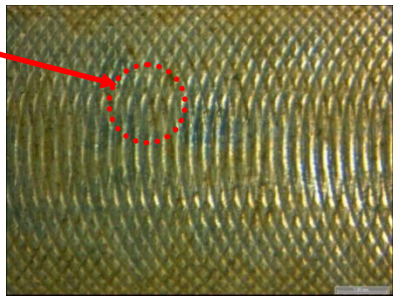
Feed = 25
mm/min

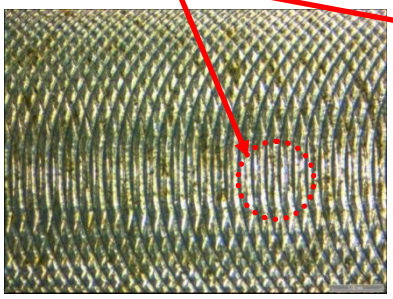
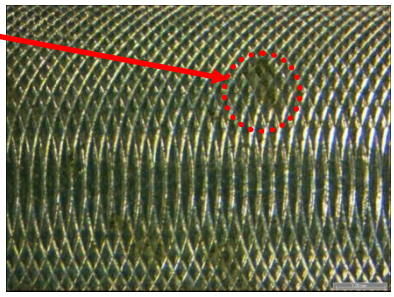
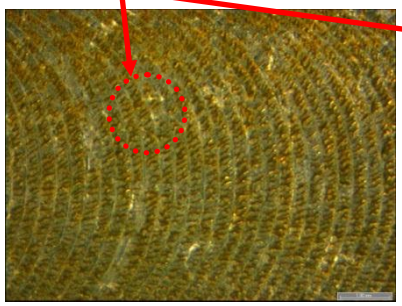
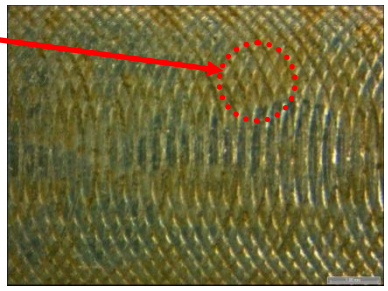
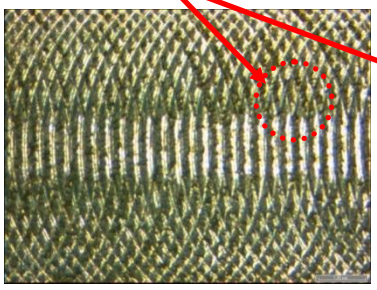
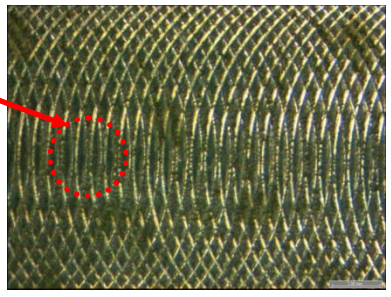
Doc = 30µm

Freq.=20
kHz

Amp. = 1 µm</td><td>5 %</td><td>10%</td></tr>
<tr><td>Alumina oxide particles

Ra = 0.83 µm</td><td>
Ra = 1.93 µm</td></tr>
<tr><td>15 %</td><td>20 %</td></tr>
<tr><td>Alumina oxide particles

Ra = 1.81 µm</td><td>
Ra = 2.00 µm</td></tr>
<tr><td rowspan="3">3</td><td rowspan="3">Vc = 90 rpm

Feed = 25
mm/min

Doc = 30µm</td><td>5 %</td><td>10%</td></tr>
<tr><td>Alumina oxide particles

Ra = 1.47 µm</td><td>
Ra = 1.70 µm</td></tr>
</table>

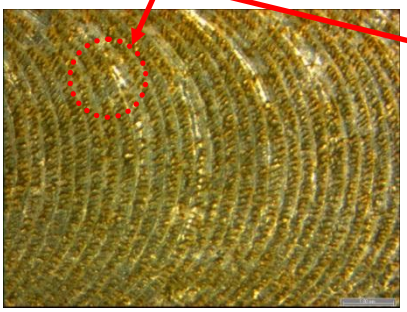
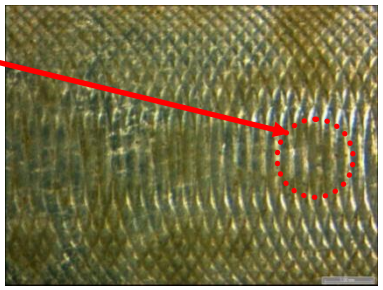
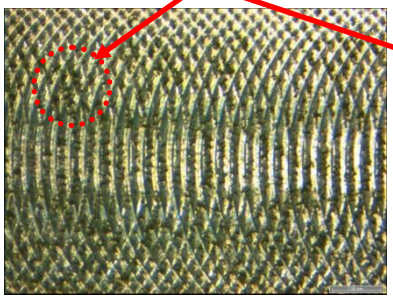
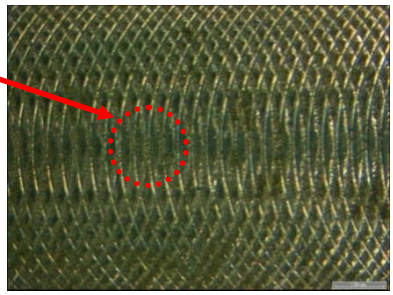
	Freq.=20 kHz Amp. = 2 µm	15 %	20 %
		Alumina oxide particles  **Ra = 1.86 µm**	 **Ra = 1.70 µm**
4	Vc = 150 rpm Feed = 45 mm/min Doc = 20µm Freq.=20 kHz Amp. = 1 µm	5 %	10%
		Alumina oxide particles  **Ra = 2.87 µm**	 **Ra = 1.29 µm**
		15 %	20%
		Alumina oxide particles  **Ra = 2.07 µm**	 **Ra = 1.91 µm**

<table>
<tr><td rowspan="4">5</td><td rowspan="4">Vc = 150 rpm

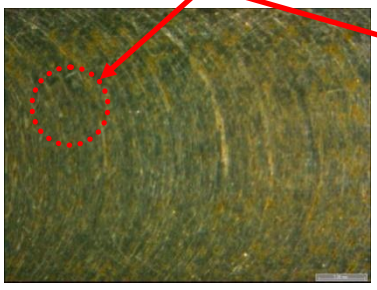
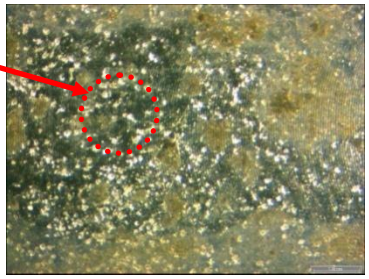
Feed = 45 mm/min

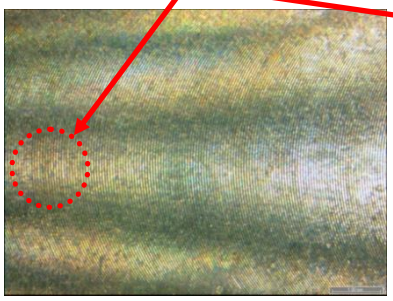
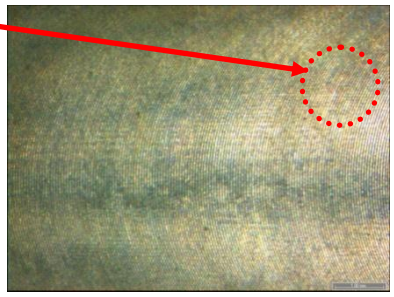
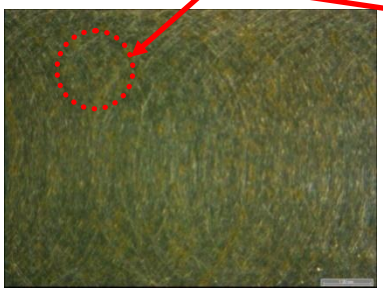
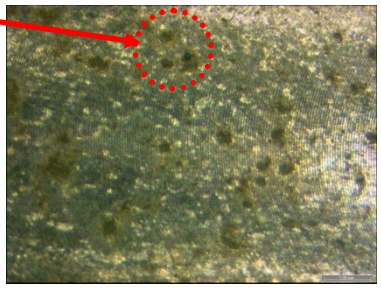
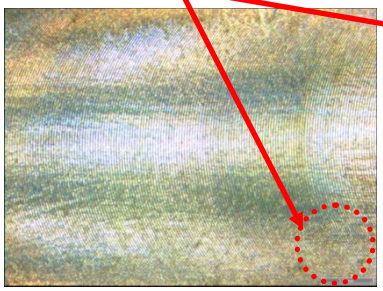
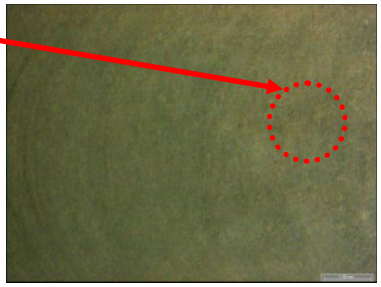
Doc = 20µm

Freq.=20 kHz

Amp. = 2 µm</td><td>5 %</td><td>10%</td></tr>
<tr><td>Alumina oxide particles

Ra = 2.87 µm</td><td>
Ra = 1.16 µm</td></tr>
<tr><td>15 %</td><td>20%</td></tr>
<tr><td>Alumina oxide particles

Ra = 2.20 µm</td><td>
Ra = 1.74 µm</td></tr>
<tr><td rowspan="3">6</td><td rowspan="3">Vc = 90 rpm

Feed = 5 mm/min

Doc = 20µm</td><td>5 %</td><td>10%</td></tr>
<tr><td>Alumina oxide particles

Ra = 0.30 µm</td><td>
Ra = 0.28 µm</td></tr>
</table>

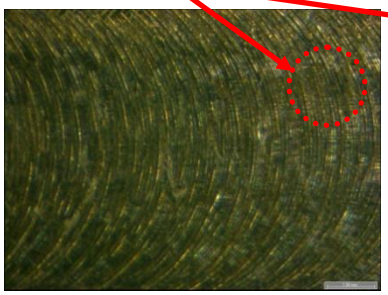
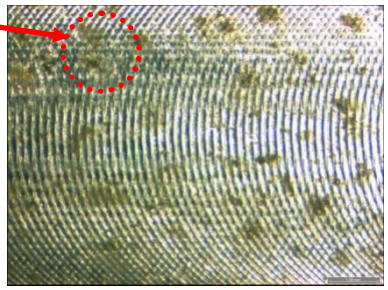
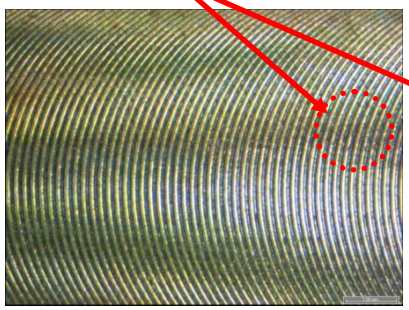
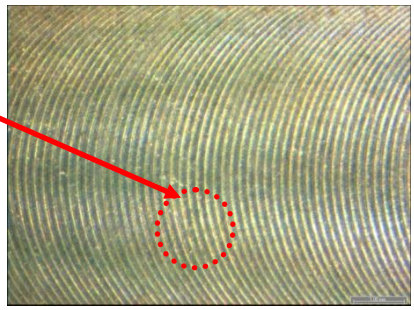
	Freq.=27 kHz Amp. = 1 µm	15 %	20%
		Alumina oxide particles  **Ra = 1.07 µm**	 **Ra = 0.88 µm**
7	Vc = 90 rpm Feed = 5 mm/min Doc = 20µm Freq.=27 kHz Amp. = 2µm	5 %	10%
		Alumina oxide particles  **Ra = 0.25 µm**	 **Ra = 0.39 µm**
		15 %	20%
		Alumina oxide particles  **Ra = 0.83 µm**	 **Ra = 0.36 µm**

<table>
<tr><td rowspan="4">8</td><td rowspan="4">Vc = 150 rpm

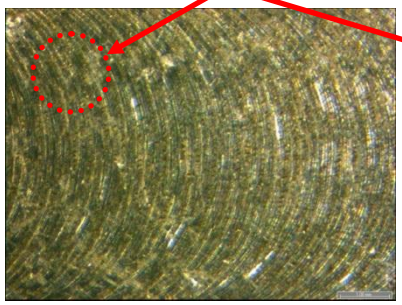
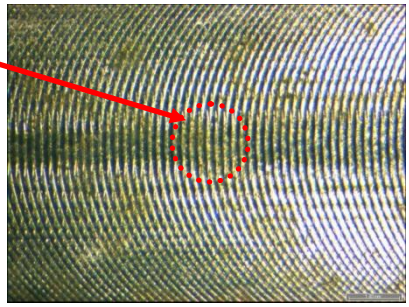
Feed = 25 mm/min

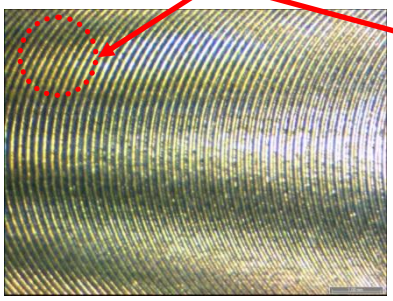
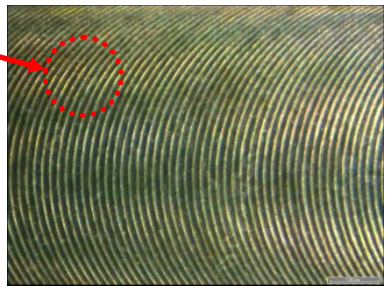
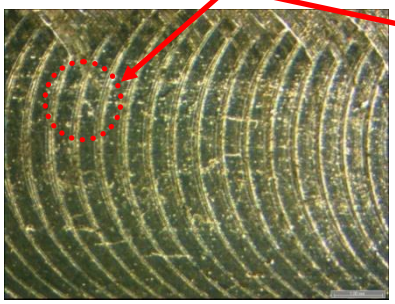
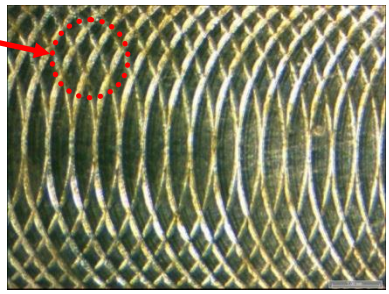
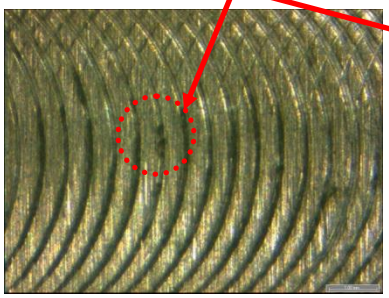
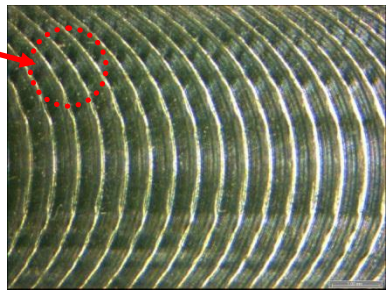
Doc = 10µm

Freq.=27 kHz

Amp. = 3µm</td><td>5 %</td><td>10%</td></tr>
<tr><td>Alumina oxide particles

Ra = 0.86 µm</td><td>
Ra = 1.23 µm</td></tr>
<tr><td>15 %</td><td>20%</td></tr>
<tr><td>Alumina oxide particles

Ra = 1.01 µm</td><td>
Ra = 0.70 µm</td></tr>
<tr><td rowspan="3">9</td><td rowspan="3">Vc = 150 rpm

Feed = 25 mm/min

Doc = 10µm</td><td>5 %</td><td>10%</td></tr>
<tr><td>Alumina oxide particles

Ra = 1.39 µm</td><td>
Ra = 1.48 µm</td></tr>
</table>

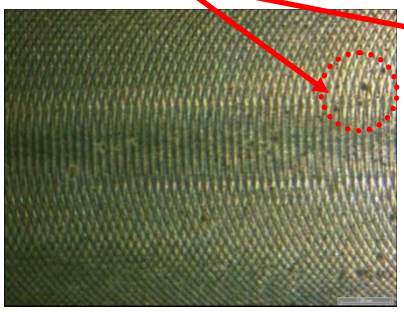
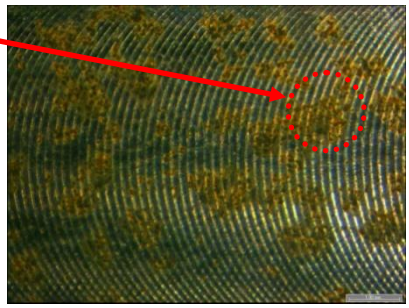
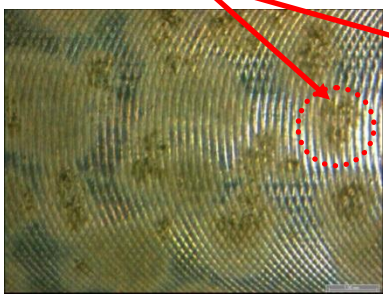
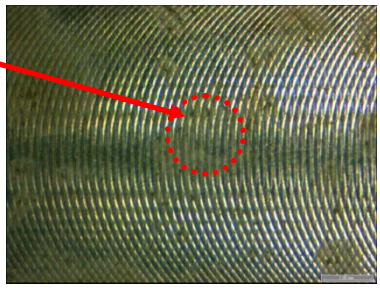
	Freq.=27 kHz Amp. = 2µm	15 %	20%
		Alumina oxide particles  **Ra = 1.09 µm**	 **Ra = 0.46 µm**
10	Vc = 90 rpm Feed = 45 mm/min Doc = 10µm	5 %	10%
		Alumina oxide particles  **Ra = 1.62 µm**	 **Ra = 1.65 µm**
	Freq.=23 kHz Amp. = 3µm	15 %	20%
		Alumina oxide particles  **Ra = 1.03 µm**	 **Ra = 1.94 µm**

<table>
<tr><td rowspan="4">11</td><td rowspan="4">Vc = 30 rpm

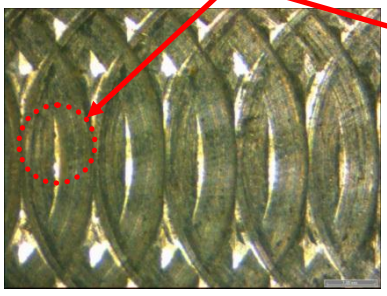
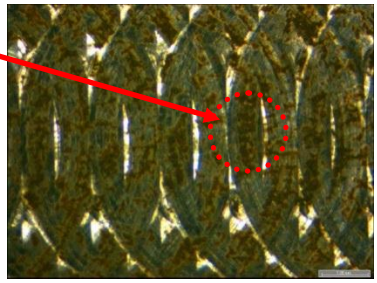
Feed = 5
mm/min

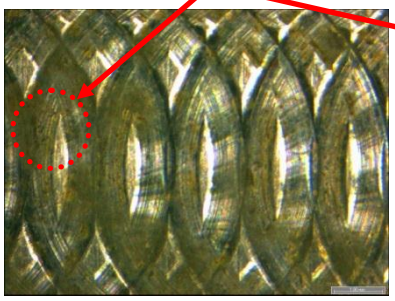
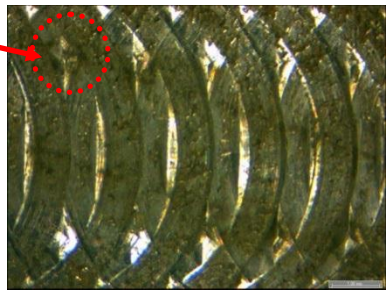
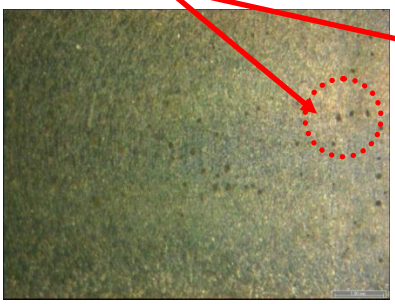
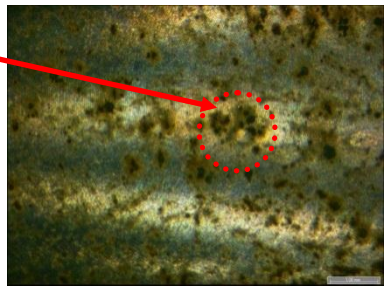
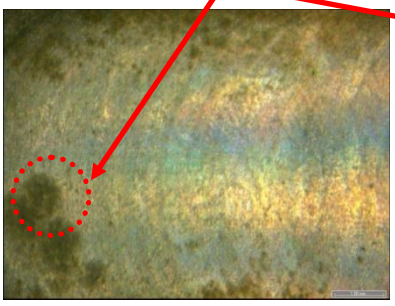
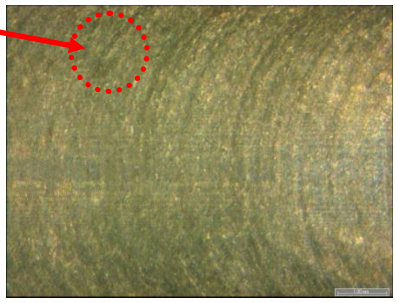
Doc = 10µm

Freq.=20
kHz

Amp. = 1µm</td><td>5 %</td><td>10%</td></tr>
<tr><td>Alumina oxide particles

Ra = 0.37 µm</td><td>
Ra = 0.79 µm</td></tr>
<tr><td>15 %</td><td>20%</td></tr>
<tr><td>Alumina oxide particles

Ra = 0.71 µm</td><td>
Ra = 0.69 µm</td></tr>
<tr><td rowspan="3">12</td><td rowspan="3">Vc = 30 rpm

Feed = 45
mm/min

Doc = 30µm</td><td>5 %</td><td>10%</td></tr>
<tr><td>Alumina oxide particles

Ra = 1.69 µm</td><td>
Ra = 2.59 µm</td></tr>
</table>

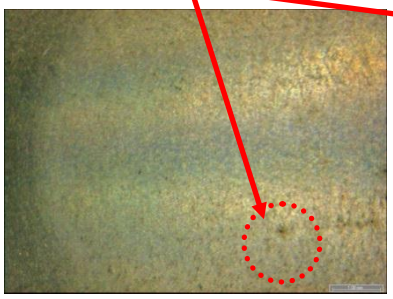
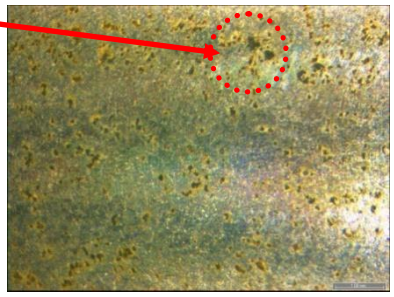
	Freq.=27 kHz Amp. = 1µm	15 %	20%
		Alumina oxide particles  **Ra = 1.50 µm**	 **Ra = 3.37 µm**
13	Vc = 150 rpm Feed = 5 mm/min Doc = 30µm	5 %	10%
		Alumina oxide particles  **Ra = 0.22 µm**	 **Ra = 0.54 µm**
		15 %	20%
	Freq.=23 kHz Amp. = 2µm	**Alumina oxide particles**  **Ra = 0.41 µm**	 **Ra = 0.52 µm**

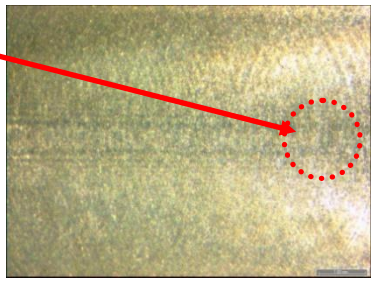
<table>
<tr><td rowspan="4">14</td><td rowspan="4">Vc = 150 rpm

Feed = 5 mm/min

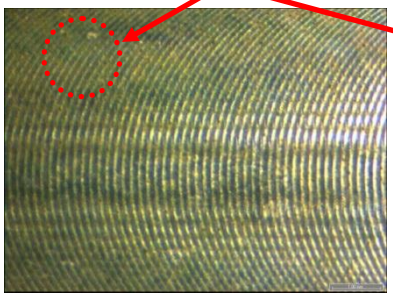
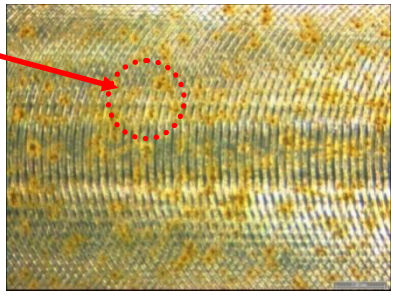
Doc = 30µm

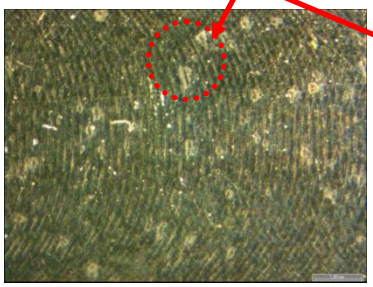
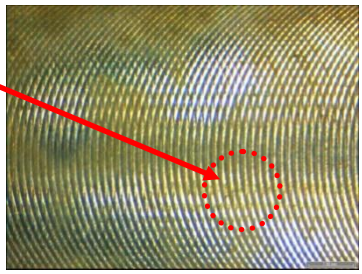
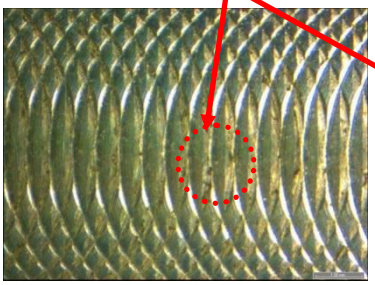
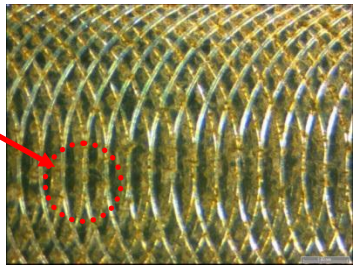
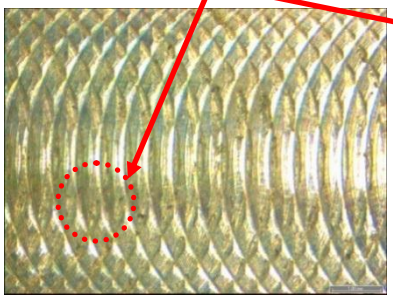
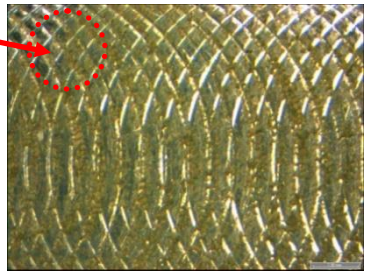
Freq.=23 kHz

Amp. = 1µm</td><td>5 %</td><td>10%</td></tr>
<tr><td>Alumina oxide particles

Ra = 0.29 µm</td><td>
Ra = 0.21 µm</td></tr>
<tr><td>15 %</td><td>20%</td></tr>
<tr><td>Alumina oxide particles

Ra = 0.25 µm</td><td>
Ra = 0.31 µm</td></tr>
<tr><td rowspan="2">15</td><td rowspan="2">Vc = 30 rpm

Feed = 5 mm/min

Doc = 10µm</td><td>5 %</td><td>10%</td></tr>
<tr><td>Alumina oxide particles

Ra = 0.90 µm</td><td>
Ra = 1.19 µm</td></tr>
</table>

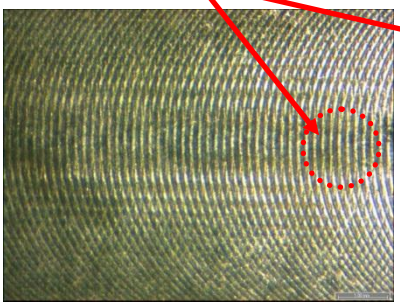
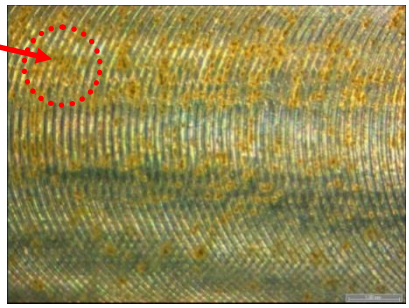
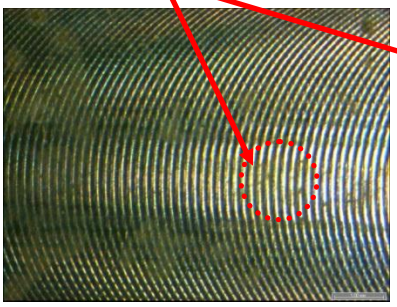
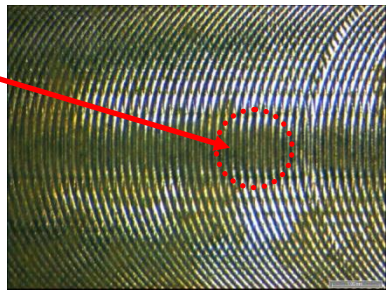
	Freq.=20 kHz Amp. = 3µm	15 %	20%
		Alumina oxide particles  **Ra = 0.12 µm**	 **Ra = 0.78 µm**
16	Vc = 90 rpm Feed = 45 mm/min Doc = 10µm Freq.=23 kHz Amp. = 1µm	5 %	10%
		Alumina oxide particles  **Ra = 1.59 µm**	 **Ra = 1.22 µm**
		15 %	20%
		Alumina oxide particles  **Ra = 1.87 µm**	 **Ra = 3.30 µm**

<table>
<tr><td rowspan="4">17</td><td rowspan="4">Vc = 30 rpm

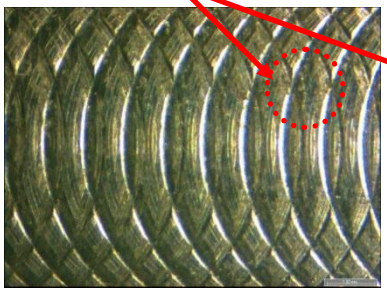
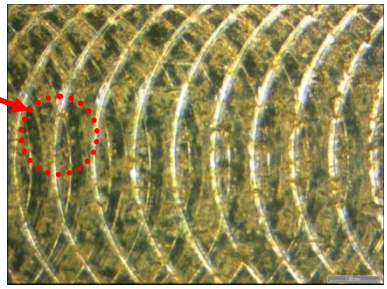
Feed = 5
mm/min

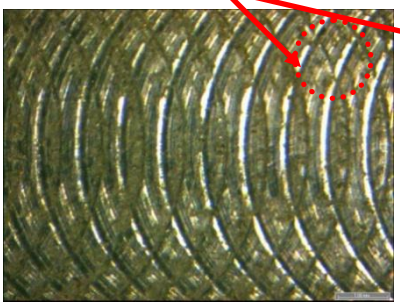
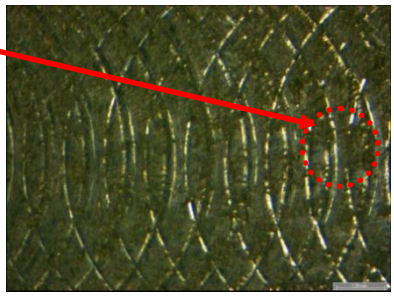
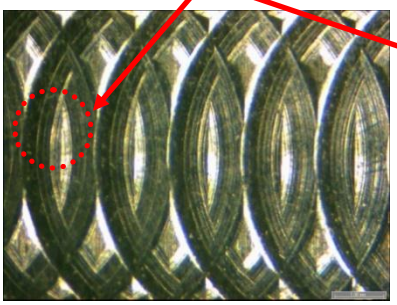
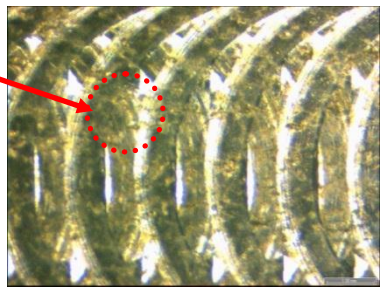
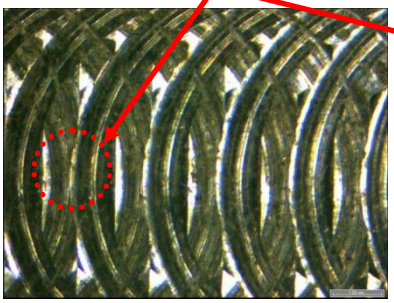
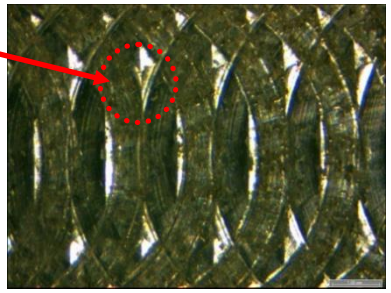
Doc = 10µm

Freq.=20
kHz

Amp. = 2µm</td><td>5 %</td><td>10%</td></tr>
<tr><td>Alumina oxide particles

Ra = 0.73 µm</td><td>
Ra = 0.86 µm</td></tr>
<tr><td>15 %</td><td>20%</td></tr>
<tr><td>Alumina oxide particles

Ra = 0.89 µm</td><td>
Ra = 0.94 µm</td></tr>
<tr><td rowspan="4">18</td><td rowspan="4">Vc = 30 rpm

Feed = 25
mm/min

Doc = 20µm</td><td>5 %</td><td>10%</td></tr>
<tr><td>Alumina oxide particles

Ra = 1.97 µm</td><td>
Ra = 1.41 µm</td></tr>
</table>

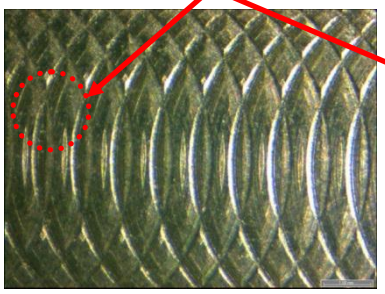
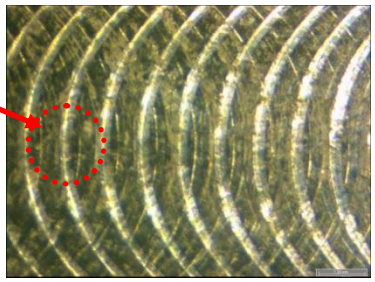
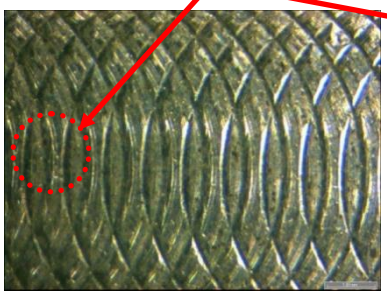
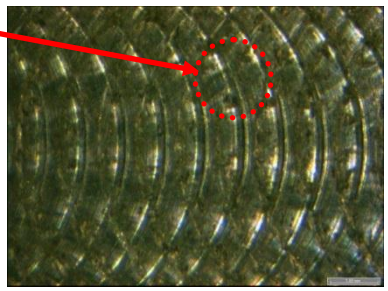
	Freq.=23 kHz Amp. = 1µm	15 %	20%
		Alumina oxide particles  **Ra = 1.82 µm**	 **Ra = 2.97 µm**
19	Vc = 30 rpm Feed = 45 mm/min Doc = 30µm Freq.=27 kHz Amp. = 3 µm	5 %	10%
		Alumina oxide particles  **Ra = 1.32 µm**	 **Ra = 1.83 µm**
		15 %	20%
		Alumina oxide particles  **Ra = 1.98 µm**	 **Ra = 2.03 µm**

<table>
<tr><td rowspan="4">20</td><td rowspan="4">Vc = 30 rpm

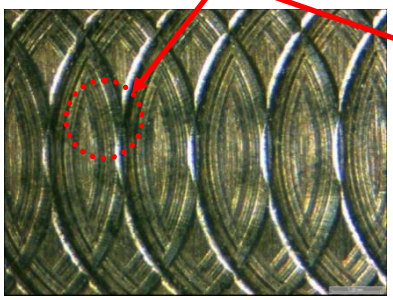
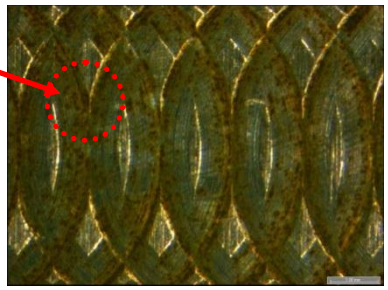
Feed = 25
mm/min

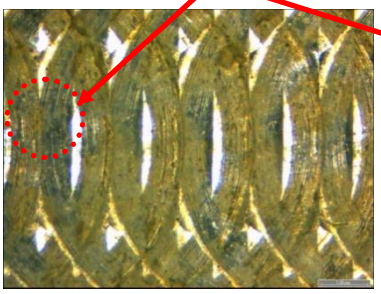
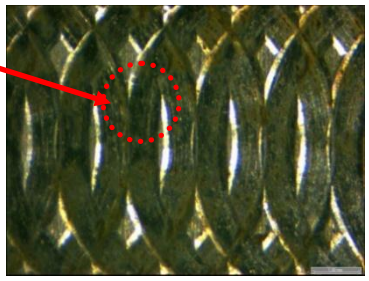
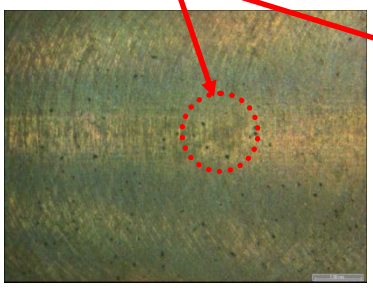
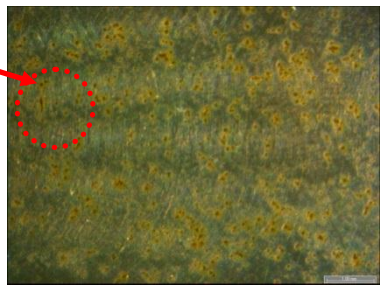
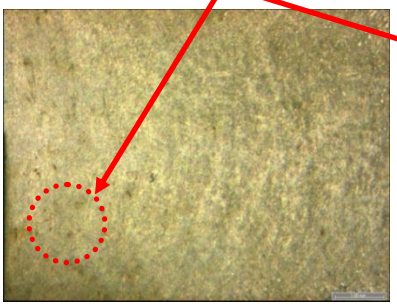
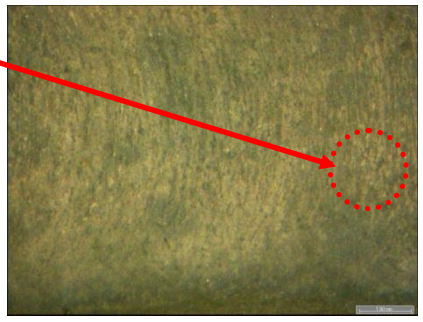
Doc = 20µm

Freq.=23
kHz

Amp. = 3 µm</td><td>5 %</td><td>10%</td></tr>
<tr><td>Alumina oxide particles

Ra = 1.73 µm</td><td>
Ra = 1.04 µm</td></tr>
<tr><td>15 %</td><td>20%</td></tr>
<tr><td>Alumina oxide particles

Ra = 1.52 µm</td><td>
Ra = 1.55 µm</td></tr>
<tr><td rowspan="3">21</td><td rowspan="3">Vc = 30 rpm

Feed = 45
mm/min

Doc = 30 µm</td><td>5 %</td><td>10%</td></tr>
<tr><td>Alumina oxide particles

Ra = 1.56 µm</td><td>
Ra = 1.17 µm</td></tr>
</table>

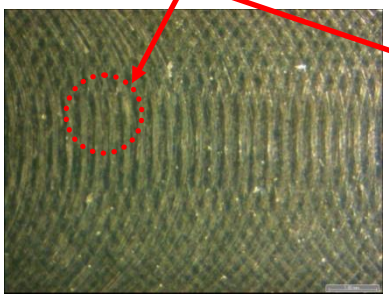
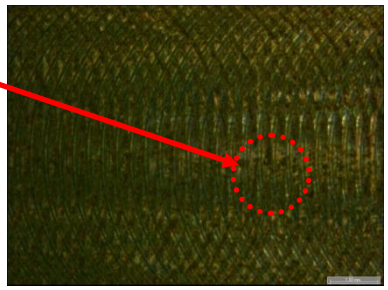
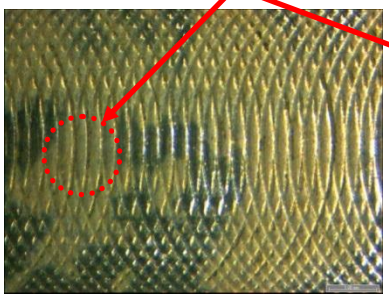
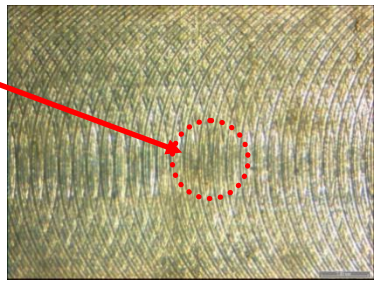
	Freq. = 27 kHz Amp. = 2 µm	15 %	20%
		Alumina oxide particles  **Ra = 1.96 µm**	 **Ra = 2.18 µm**
22	Vc = 150 rpm Feed = 5 mm/min Doc = 30 µm Freq. = 23 kHz Amp. = 3µm	5 %	10%
		Alumina oxide particles  **Ra = 0.20 µm**	 **Ra = 0.15 µm**
		15 %	20%
		Alumina oxide particles  **Ra = 0.19 µm**	 **Ra = 0.21 µm**

<table>
<tr><td rowspan="4">23</td><td rowspan="4">Vc = 150 rpm

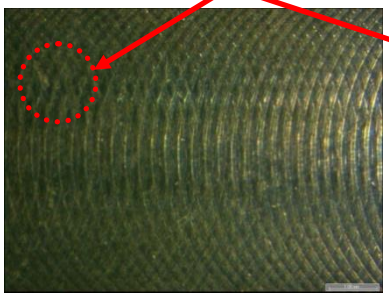
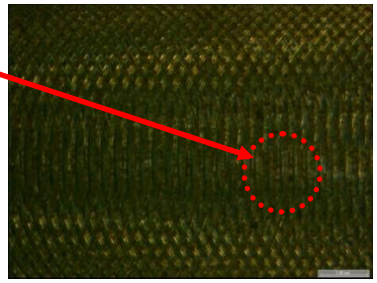
Feed = 45 mm/min

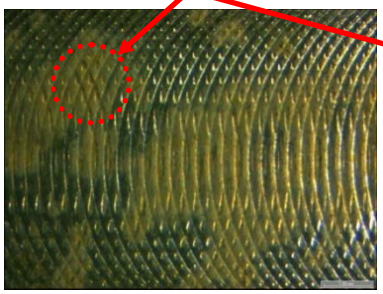
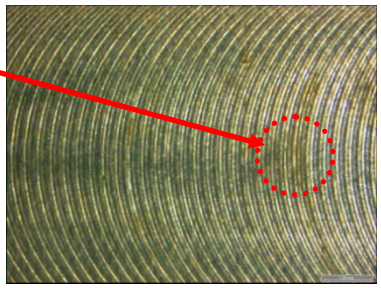
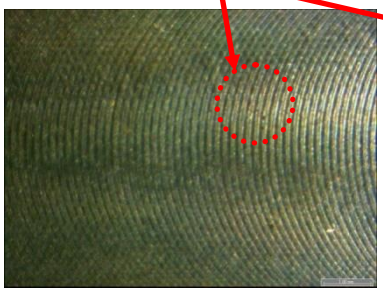
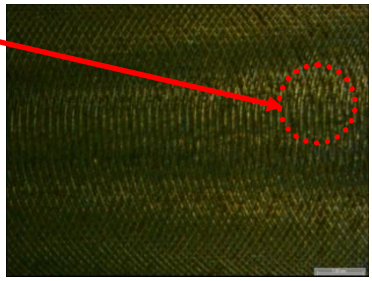
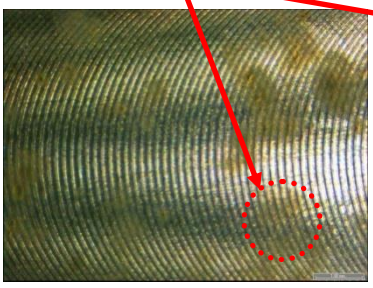
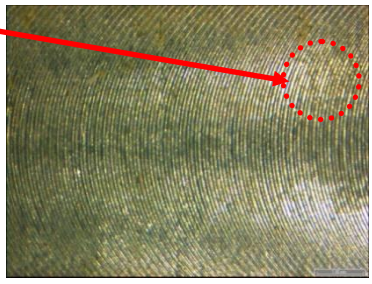
Doc = 20 µm

Freq. = 20 kHz

Amp. = 3µm</td><td>5 %</td><td>10%</td></tr>
<tr><td>Alumina oxide particles

Ra = 0.71 µm</td><td>
Ra = 0.63 µm</td></tr>
<tr><td>15 %</td><td>20%</td></tr>
<tr><td>Alumina oxide particles

Ra = 1.48 µm</td><td>
Ra = 0.81 µm</td></tr>
<tr><td rowspan="3">24</td><td rowspan="3">Vc = 90 rpm

Feed = 25 mm/min

Doc = 30 µm</td><td>5 %</td><td>10%</td></tr>
<tr><td>Alumina oxide particles

Ra = 0.78 µm</td><td>
Ra = 0.60 µm</td></tr>
</table>

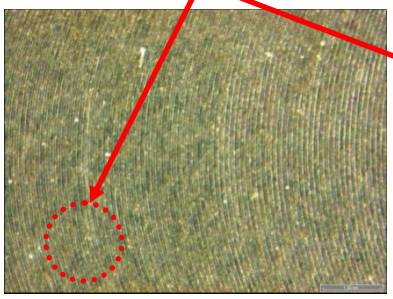
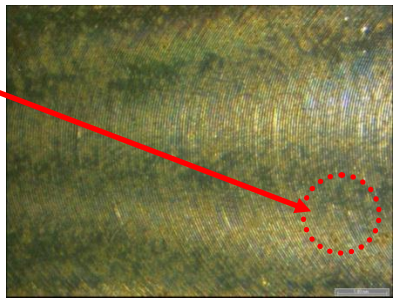
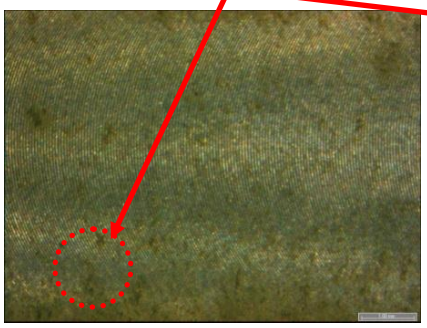
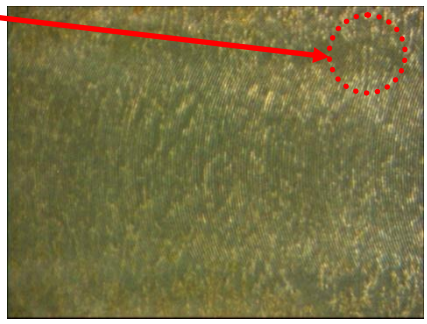
	Freq. = 20 kHz Amp. = 3µm	15 %	20%
		Alumina oxide particles  **Ra = 1.56 µm**	 **Ra = 0.85 µm**
25	Vc = 150 rpm Feed = 25 mm/min Doc = 10 µm Freq. = 27 kHz Amp. = 1µm	5 %	10%
		Alumina oxide particles  **Ra = 0.57 µm**	 **Ra = 0.32 µm**
		15 %	20%
		Alumina oxide particles  **Ra = 1.09 µm**	 **Ra = 0.71 µm**

<table>
<tr><td rowspan="4">26</td><td rowspan="4">Vc = 90 rpm

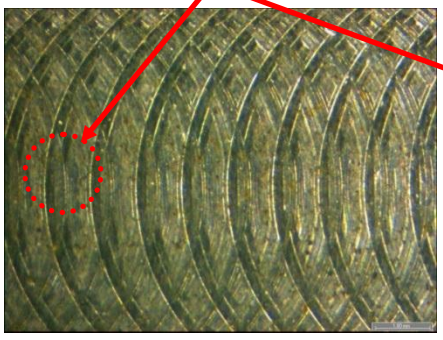
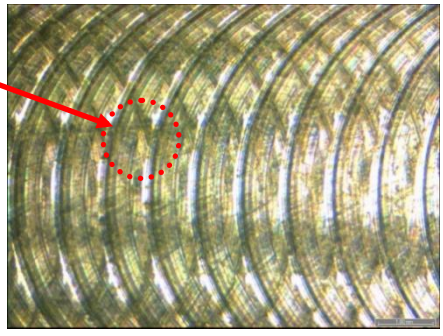
Feed = 5
mm/min

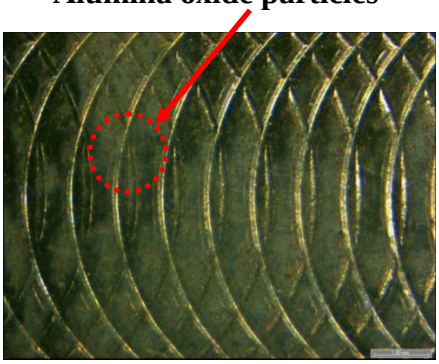
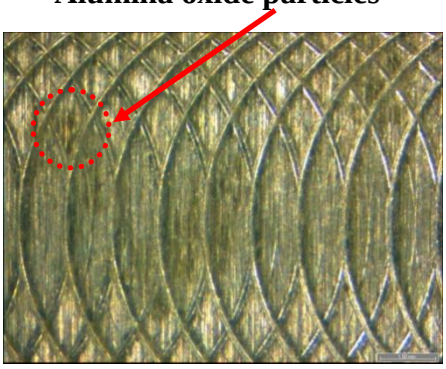
Doc = 20 µm

Freq. = 27
kHz

Amp. = 3µm</td><td>5 %</td><td>10%</td></tr>
<tr><td>Alumina oxide particles

Ra = 0.69 µm</td><td>
Ra = 0.19 µm</td></tr>
<tr><td>15 %</td><td>20%</td></tr>
<tr><td>Alumina oxide particles

Ra = 0.67 µm</td><td>
Ra = 0.28 µm</td></tr>
<tr><td rowspan="4">27</td><td rowspan="4">Vc = 30 rpm

Feed = 25
mm/min

Doc = 20 µm</td><td>5 %</td><td>10%</td></tr>
<tr><td>Alumina oxide particles

Ra = 0.87 µm</td><td>
Ra = 0.76 µm</td></tr>
</table>

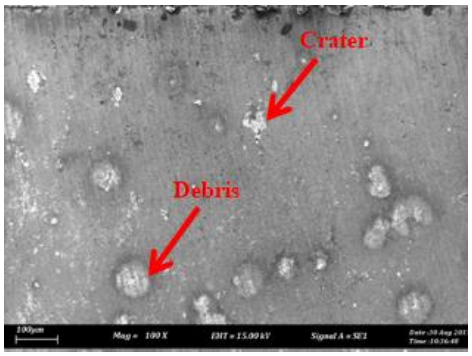
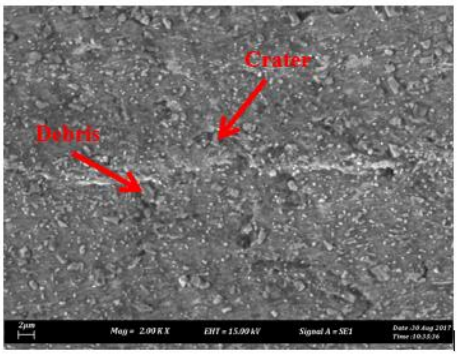
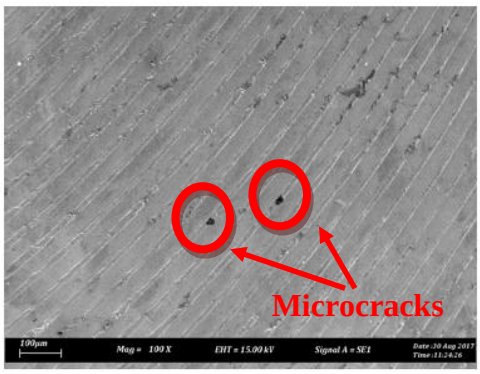
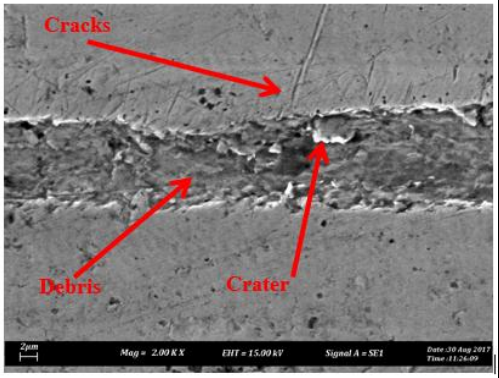
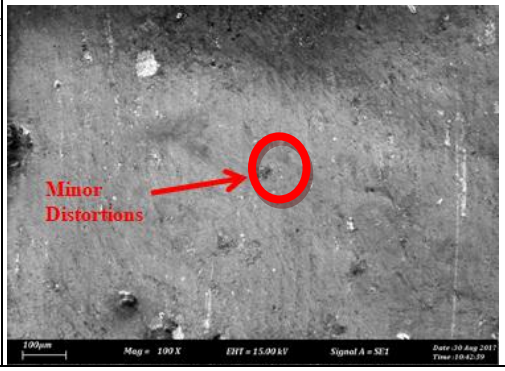
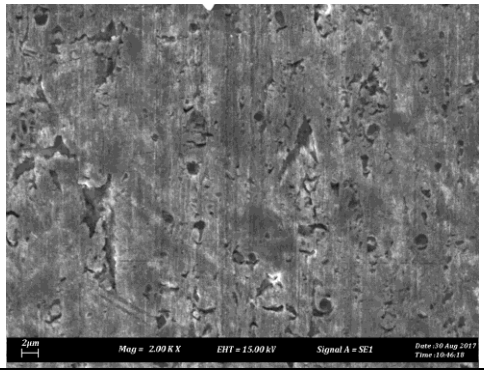
	Freq. = 23 kHz Amp. = 2μm	15 %	20%
		Alumina oxide particles  **Ra = 1.62 μm**	**Alumina oxide particles**  **Ra = 1.04 μm**

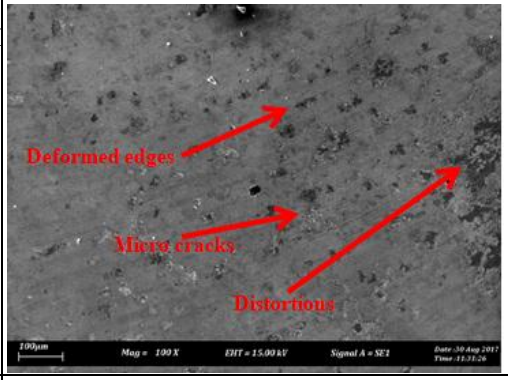
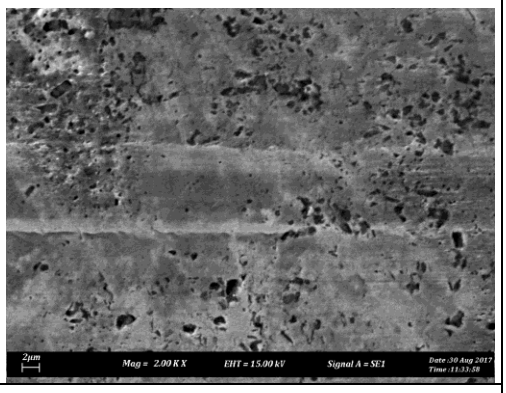
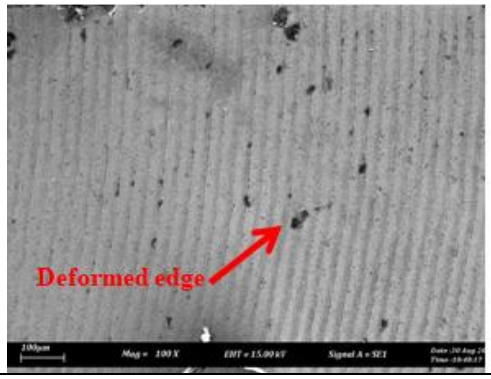
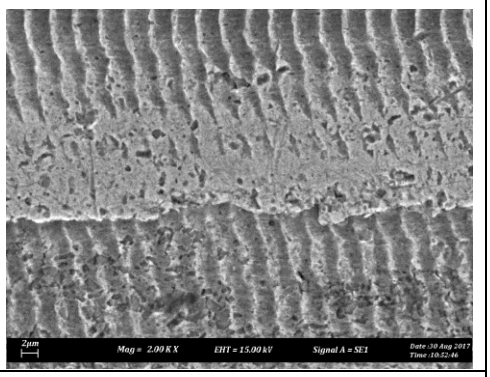
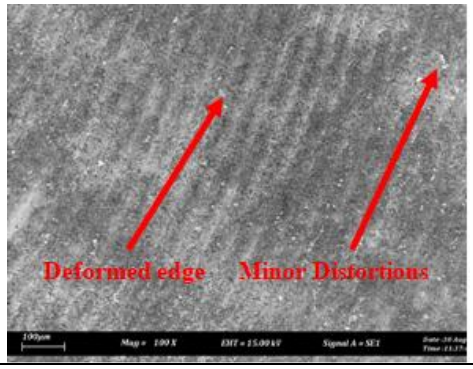
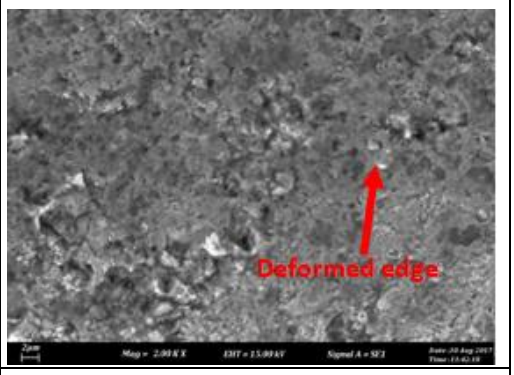
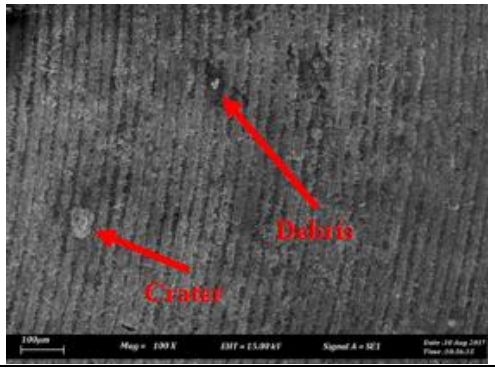
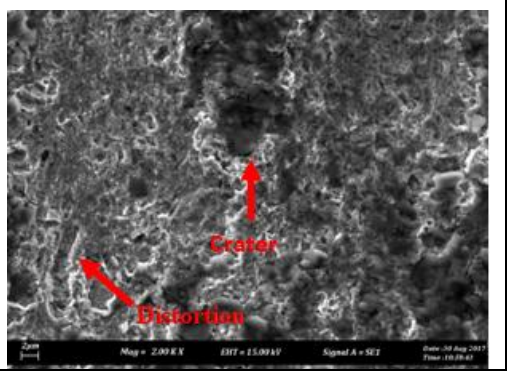
In addition, the optimum percentage of slurry concentrations and the combination of right cutting parameters produced a shiny like mirror surface, indicating a fine surface finish (<0.5μm). However, if the concentrations were too high, the slurry became too viscous that prevented it from effectively penetrated into the cutting zone, thus, increasing the roughness values. Another thing to be highlighted is because the slurry was mixed with distilled water, the formation of corrosion at the machined surface occurred rapidly as shown in Table 4.13.

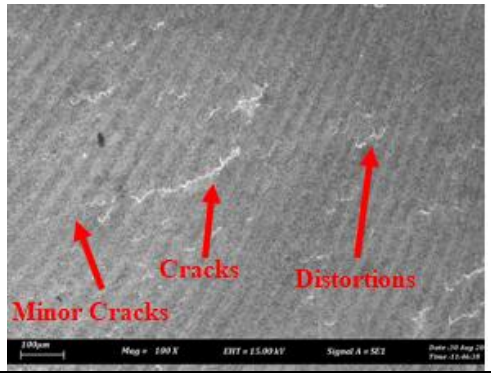
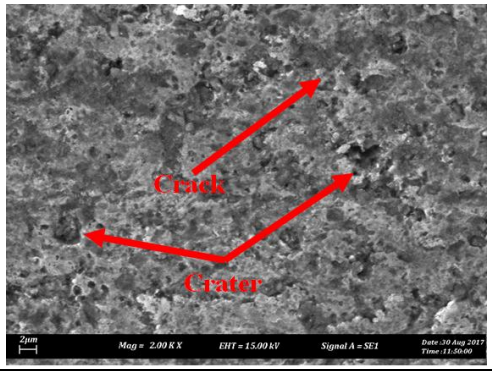
4.6.2.1 Surface analysis

To further analyze the machined surface condition, a micrograph or surface topography was taken using scanning electron microscopy (SEM) machine. Table 4.14 shows the microstructure of the machined surface generated by RUAEM with different alumina oxide slurry concentrations such 5, 10, 15 and 20% for Run 15 and 22. The microstructure surface analysis would only be taken by these two runs due to the lowest surface roughness produced.

Table 4.14: Microstructure of machined surface generated by RUAEM with different alumina oxide slurry concentration such 5, 10, 15 and 20% for run 15 and run 22

Alumina Oxide %	Run No.	100X	2000X
5%	15		
	22		
10%	15		

10%	22		
15%	15		
	22		
20%	15		

20%	22		

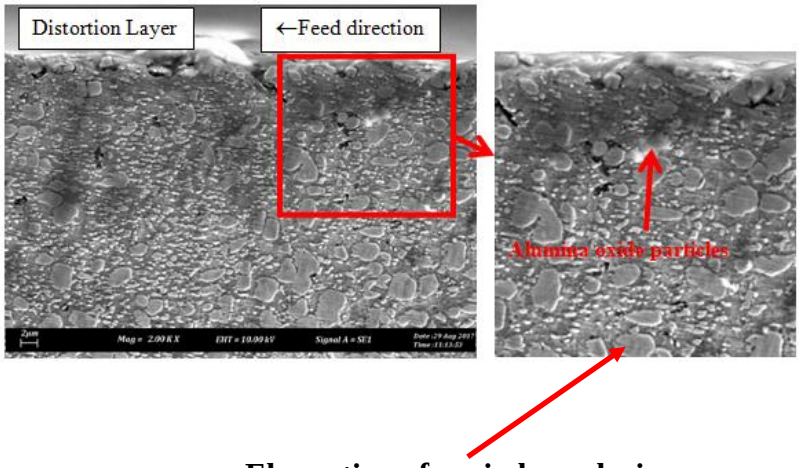
As with conventional milling, the microstructure of machined surface was deformed due to the shearing of material by the cutter teeth. Furthermore, the SEM image shows an additional mechanic of cutting mechanism namely direct hammering of abrasive grits and abrasion of abrasive grits parallel to the direction of the cutting due to the presence of alumina oxide slurry as evident by the occurrences of micro pits and surface scratch. In addition, the occurrences of debris such as alumina particle/grit on the surface were also observed.

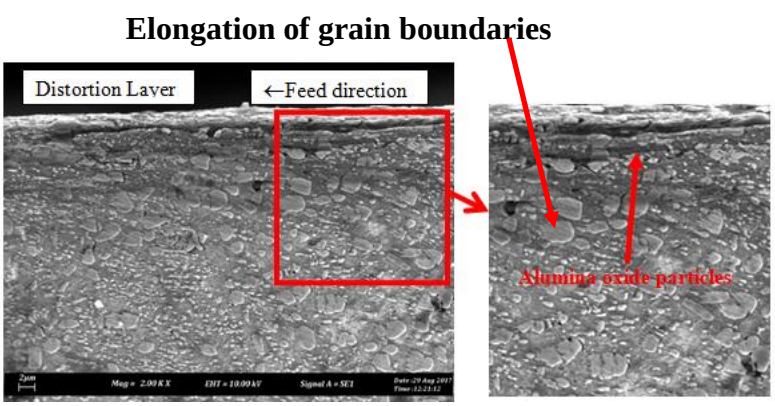
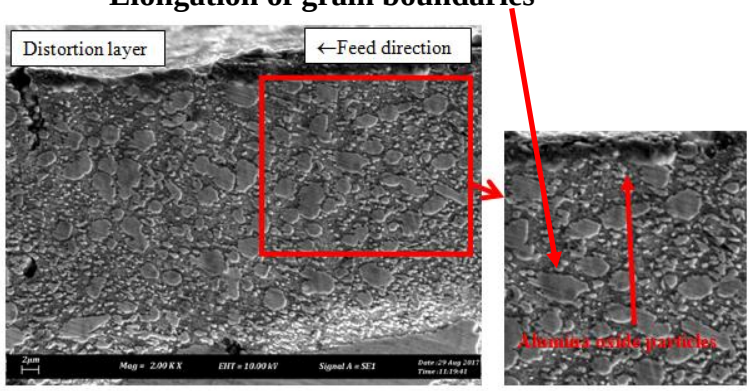
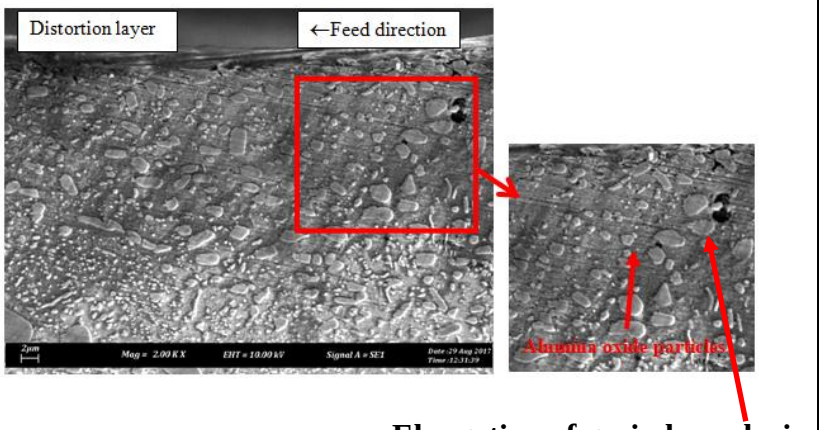
As the alumina oxide slurry concentration increased, the surface roughness value decreased up to certain concentration value, for this case 15% and started to increase beyond this limit. One of the possible reasons for this cause can be related with the slurry viscosity that prevents it from effectively penetrates into the cutting zone, thus, increasing the roughness values. Therefore, the optimal alumina oxide slurry concentration is the vital factor for the success of machining for RUAEM. Apart from that, alumina oxide slurry concentration has a direct effect on the MRR and cutting force values. As the concentration increases both factors will also increase which can be evident with the increasing numbers of micro pits and surface scratch.

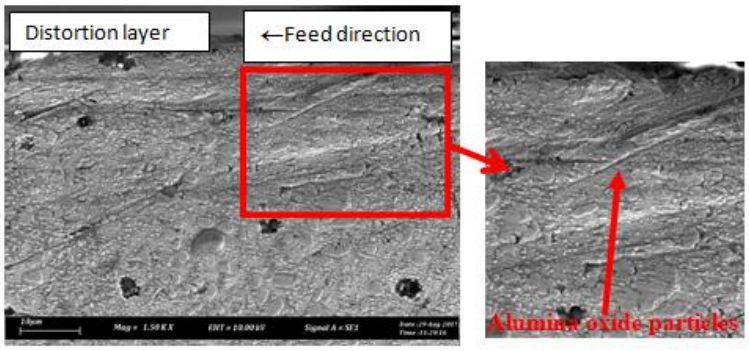
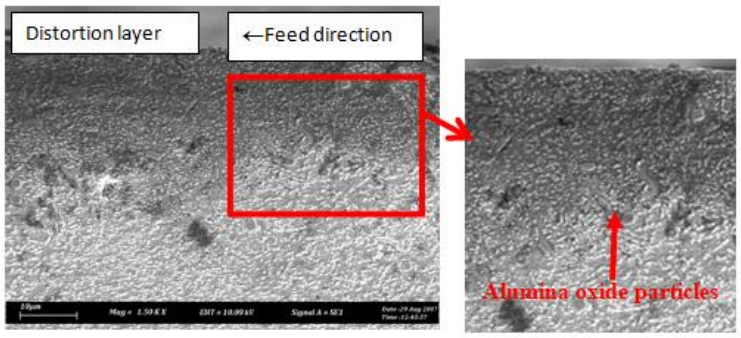
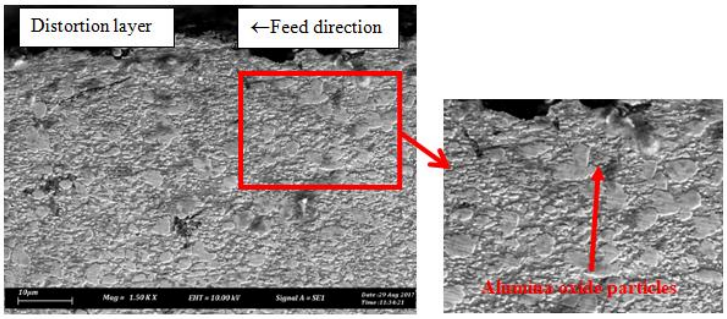
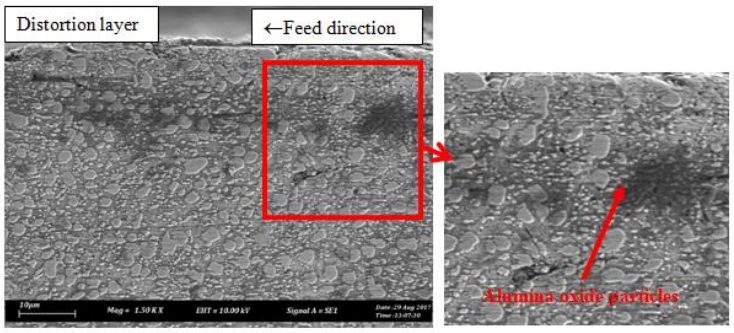
4.6.2.2 Cross sectional machined surface

Carl Zeiss scanning electron microscopy (SEM) machine was used to observe the cross-sectional images of machined surface with different alumina oxide slurry concentrations. Cross sectional images provide an important information in determining the machined surface quality with respect to the slurry concentration. Table 4.15 shows the cross-sectional microstructure of the machined surface generated by RUAEM with different alumina oxide slurry concentrations such 5, 10, 15 and 20% for Run 15 and Run 22. The cross-sectional microstructure surface analysis would only be taken by these two runs due to the lowest surface roughness produced.

Table 4.15: Cross sectional microstructure of machined surface generated by RUAEM with different alumina oxide slurry concentrations such 5, 10, 15 and 20% for run 15 and run 22

Alumina Oxide %	**Run No.**	**2000X Magnification**
5%	R15	

	R22	
10%	R15	
	R22	

15%	R15	
	R22	
20%	R15	
	R22	

It can be observed, as the alumina oxide slurry concentration increased, the microstructures tended to have a higher compressive stress zone, causing the atoms in the material changed to strain condition. In addition, for all the runs, the machined surface microstructure indicated that plastic deformation occurred, leading to severe deformed layers of microstructure alteration at the subsurface level. In the strain condition, some of the atoms were separated from the original boundaries and move to the new area between planes, causing an elongation of grain boundaries. Table 4.15 clearly shows that the microstructure and grain boundaries tend to elongate to the bottom area. A detail picture of microstructure and grain boundaries tend to elongate to the bottom area for run 15 with 10 % slurry concentration alumina oxide (2000 X magnification) is shown in Figure 4.43 below.

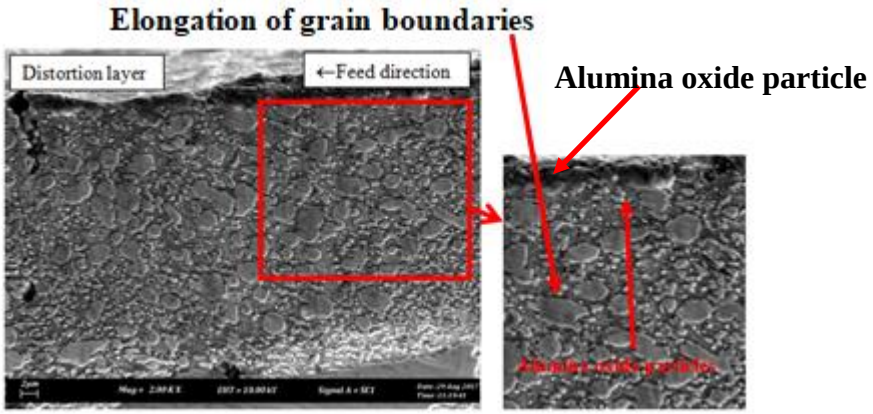


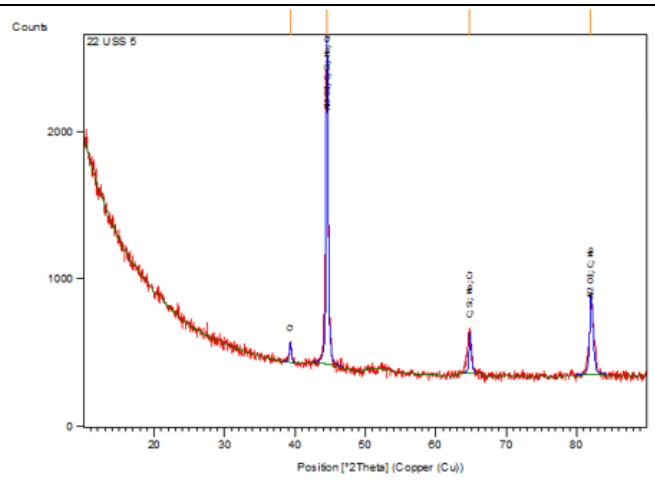
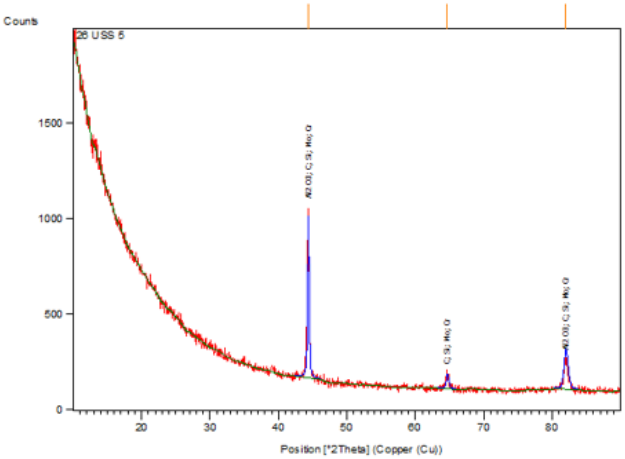
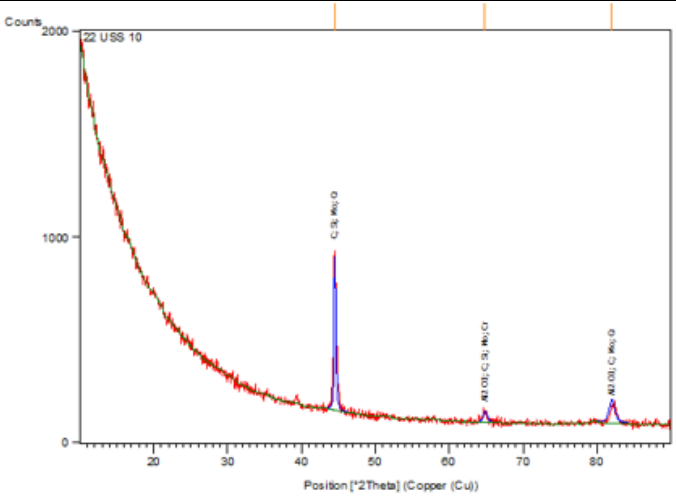
Figure 4.43: Microstructure of cross-sectional work piece machined surface and grain boundaries tend to elongate for run 15 with 10 % slurry concentration alumina oxide (2000 X magnification)

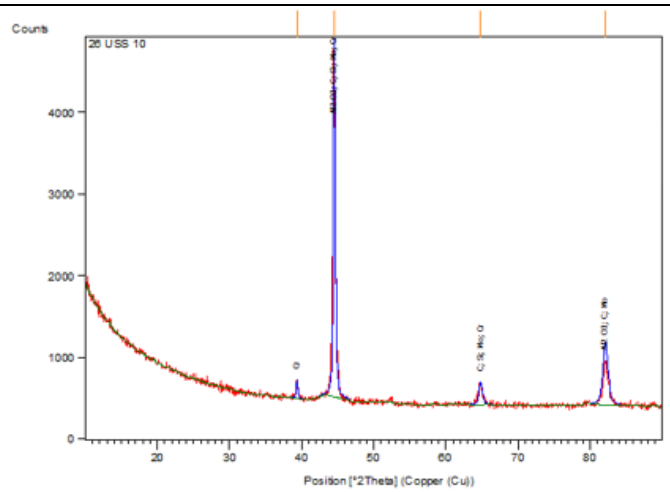
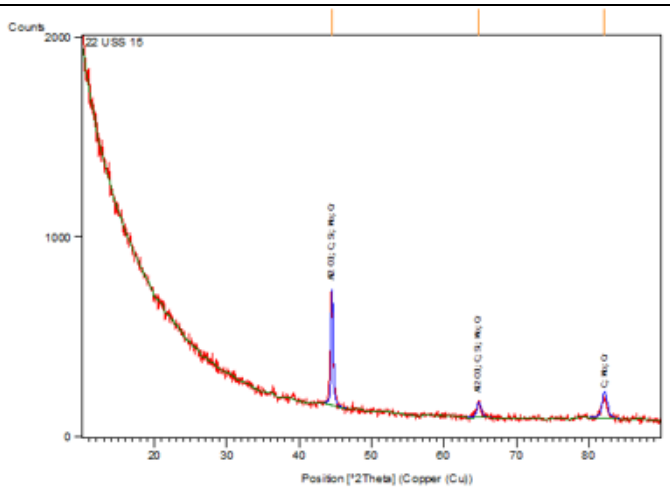
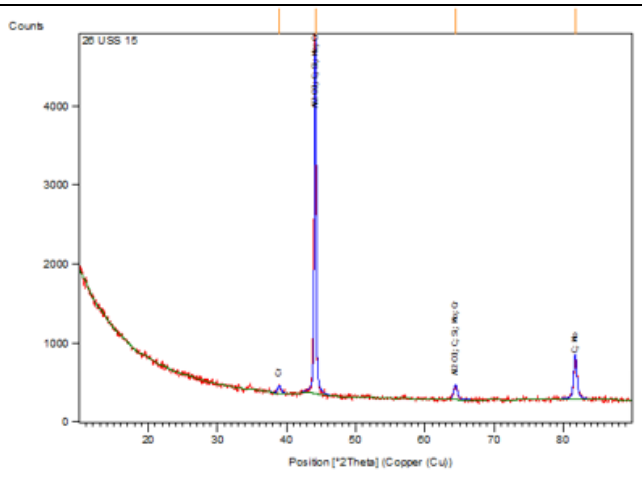
Furthermore, it shows that the formation of oxide layer (black layer) on the top surface indicates that the alumina oxide particles seep into the grain size that can alter the material properties.

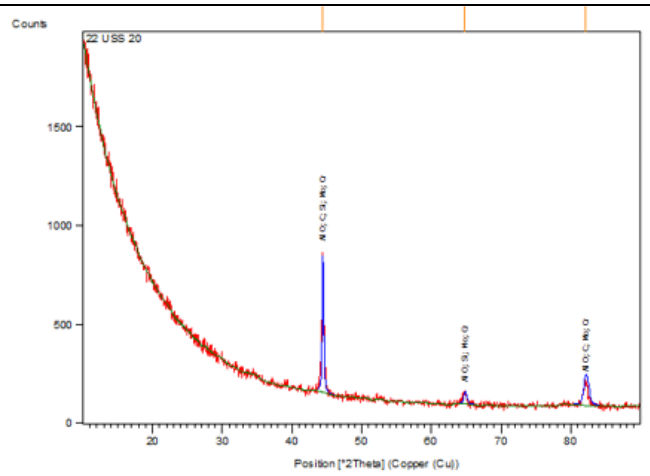
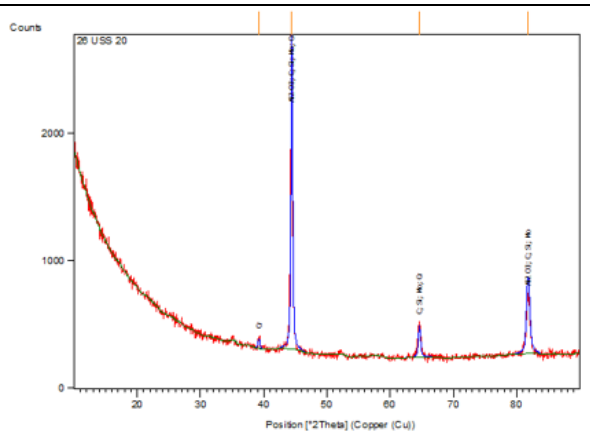
4.6.2.3 XRD measurement for analysis of alumina oxide particles affected surface roughness

The presence of alumina oxide particles as an abrasive slurry on top of machined surface was confirmed with a trace of alumina element on the machined surface area as shown in XRD measurement analysis in Table 4.16. The analysis showed that as the alumina oxide slurry concentrations increased, few peaks decreased in intensity which indicated the possibility of phase changes and the occurrence of residual stress that could alter the material properties. However, the quantities of alumina particle embedded into the material could not be quantified through this XRD measurement.

Table 4.16: The presence of alumina oxide particles on top of machined surface shown in XRD measurement analysis

Alumina Oxide %	**Run No.**	**EDX**
5%	Run 15	
	Run 22	
10%	Run 15	

	Run 22	
15%	Run 15	
	Run 22	

20%	Run 15	
	Run 22	

The analysis the presence of alumina oxide particles as an abrasive slurry on top of machined surface area has been proven by XRD measurement analysis and SEM analysis as shown in Figure 4.44. The presence of alumina oxide as abrasive slurry during RUAEM machining help to increase quality of machined surface finishing and improving the stability of cutting process which reducing machining force. Also, the use of appropriate alumina oxide as abrasive slurry is mostly affected the material removal rate of work piece and reducing machining temperature during machining (Singh, 2012).

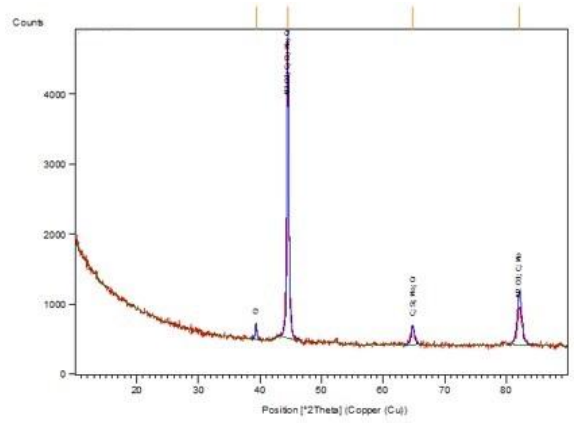
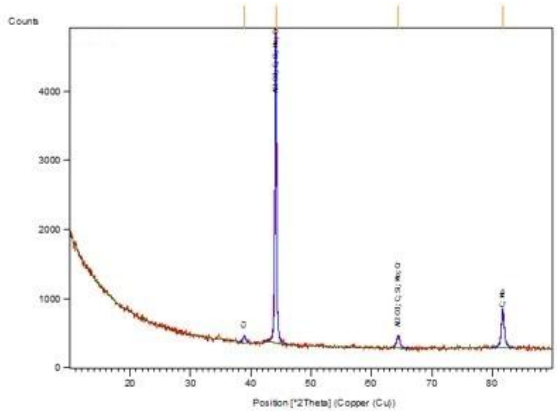
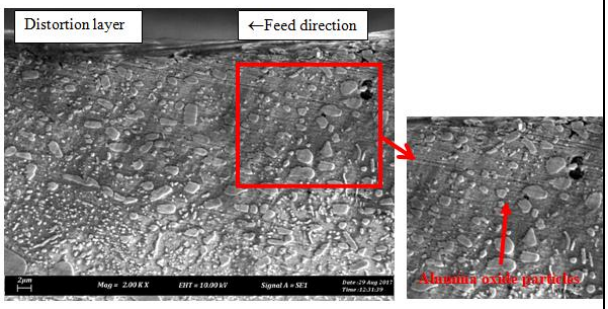
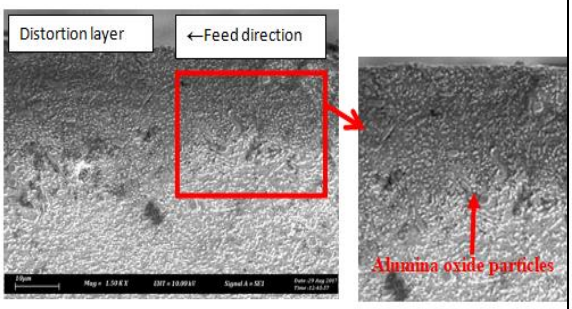
Run 22	
Alumina oxide slurry concentrations (10 %)	**Alumina oxide slurry concentrations (15 %)**
XRD measurement	**XRD measurement**
	
SEM analysis	**SEM analysis**
	

Figure 4.44: Analysis the presence of alumina oxide particles on top of machined surface area proven by XRD measurement analysis and SEM analysis

From the XRD measurement analysis and SEM analysis (Figure 4.44), it indicated that the highest presence abrasive slurry of alumina oxide with 15 % concentration improved on the top machined surface with alumina oxide particles seep into machined surface and the enough concentration quantity of alumina oxide has shear the top machined surface perfectly with spherical in shape of top machined surface. Alumina oxide slurry of 15 % concentration is continuously pumped through cutting zone, it keeps the machining

zone is cool, flush away the debris, reduce interaction force between machined surface and tools with causing a creating small grain particle size on top machined surface. Also, the enough concentration quantity of alumina oxide (15 % concentration) has shear the top machined surface perfectly with spherical in shape of top machined surface causing a reduction in surface roughness value because alumina oxide as abrasive slurry has shear the machined surface perfectly during milling machining process.

Otherwise, insufficient alumina oxide slurry concentration (10% concentration), caused the machining zone temperature to heat up and increased the pressure interaction between the cutting tool and the machined surface, which generate the coarse grains particle size in the top the machined surface. This is due to the difficulty of the alumina oxide slurry of 10 % concentration to lubricate the machined surface and cutting tool during milling machining due to insufficient alumina oxide concentration.

4.7 Heat and thermal effect in RUAEM machining

Heat and thermal affected during slot milling in RUAEM is influenced by the thermo chemical stability of the cutting tool material and increased speed generate more heat dissipated to the cutting tool and resulting high temperature leading to failure of the cutting tool (Soković et al., 2004). Abrasive slurry such as alumina oxide is pumped through the center core of the cutting tool and cutting zone to wash out the chips debris can prevent the cutting zone from overheating (Ning et al., 2016). The ultrasonic assisted milling removes heat effectively with reduce tool wear and extended tool life of cutting tool (Tsai et al., 2016). Gaitonde et al. 2009 reported that increasing depth of cut causing increases the thrust force and generating more heat during machining in cutting zone which resulting in higher surface roughness (Ra) value. The amplitude vibration applied in rotary ultrasonic assisted machining directly influenced the gap between the work piece and

cutting tool. The increased of the gap due to the increase in vibration amplitude allows more cutting fluids to carry away the heat generated in cutting zone area during ultrasonic milling machining (Chern and Chang, 2006). Figure 4.45 shows the heat and thermal flow during conventional machining processes between cutting tool and work pie machined surface. Conventional machining processes difficult to carry away the heat and thermal generated between cutting tool and work piece machined surface during slot milling machining. Next, Figure 4.46 shows the heat flow during RUAEM machining processes between cutting tool and work piece machined surface. It indicated that the RUAEM machining process easily to carry away the heat generated between cutting tool and work piece machined surface due to the amplitude vibration effect during slot milling machining.

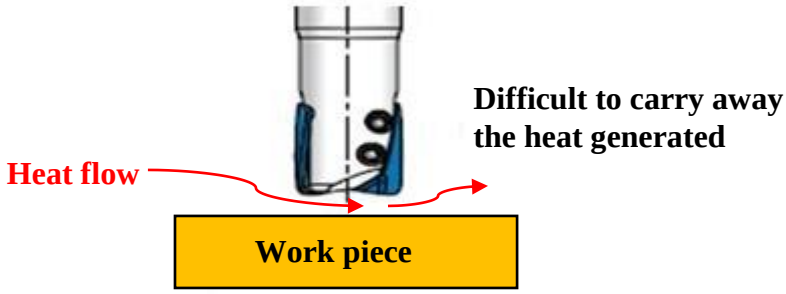


Figure 4.45: Conventional machining for carry away heat generated

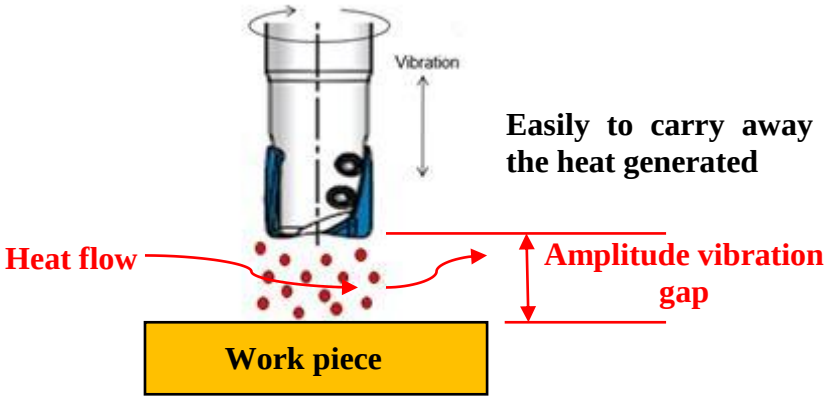


Figure 4.46: RUAEM machining for carry away heat generated

Figure 4.47 (a) and 4.47 (b) shows cutting temperature on slot milling for conventional machining and rotary ultrasonic assisted end milling (RUAEM) with alumina oxide slurry concentration, respectively. Temperature normally generated in the cutting zone due to the plastic deformation and high friction between the cutting tool and the work piece machined surface (Rehman and Maqsood, 2015).

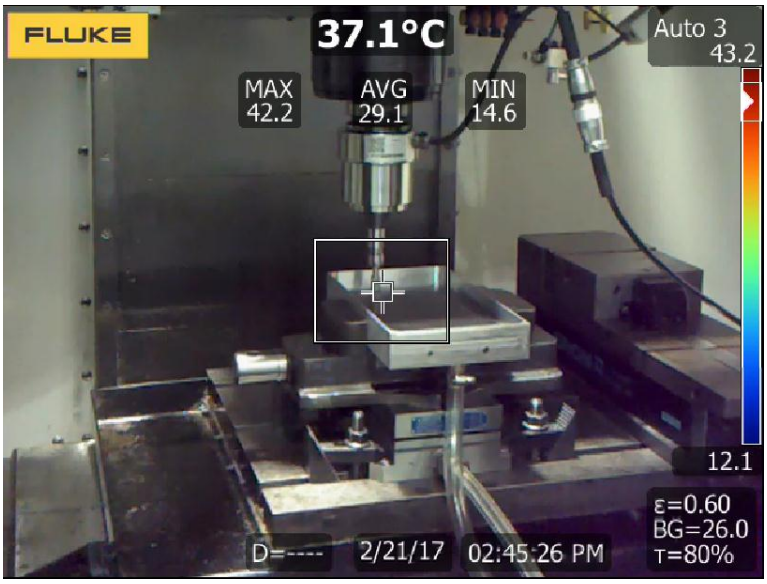


Figure 4.47 (a): Temperature reading on slot milling for conventional milling

As shown in Figure 4.47 (a), the temperature reading by thermal imager on slot milling for conventional milling is 37.1 °C. Heat and thermal generated for conventional machining very high compared RUAEM with 10 % slurry concentration of alumina oxide slurry because highest contact area and high friction between the cutting tool and work piece machined surface during conventional machining.

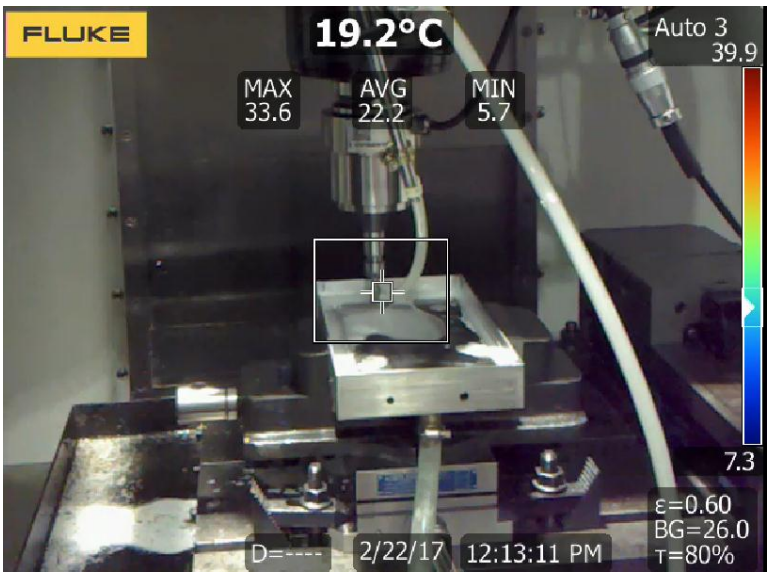


Figure 4.47 (b): Temperature reading on slot milling for RUAEM with 10 % slurry concentration of alumina oxide

While the temperature reading by thermal imager on slot milling for RUAEM with 10 % slurry concentration of alumina oxide is 19.2 °C. From this Figure 4.47 (b), it indicated that the temperature reading on slot milling for RUAEM with 10 % slurry concentration of alumina oxide is lower than conventional because of the effect alumina oxide slurry as coolant and lubricant which reduced the cutting temperature at cutting zone between cutting tool and work piece machined surface. These findings confirm that RUAEM machining with slurry concentration of alumina oxide easily carry away, move and fast movement out of heat and thermal generated from the cutting zone area between cutting tool and machined surface interface compared conventional machining with causes lowest cutting force generated during slot milling.

4.8 Summary

In summary, from the experimental work, a mathematical model of the performance correlated with the machining parameter is developed and used for the optimization model.

Based on the selected criteria and input limits, solution number 1 and 2 have the highest desirability index with 0.87. However, based on a compromised decision between responses and the constraints such as cost, efficiency and practicality, solution number 1 has been selected as the best solution for the optimization of machining parameters (combination of 111.45 rpm, 5.75 mm/min feed rate, 27.05 µm depth of cut, 20.91 kHz vibration frequency, 3 µm amplitude and 13.26 % abrasive concentration) based on the combination of targeted surface roughness value of 0.1 µm, minimum resultant force and maximum material removal rate value which are predicted to be 19.43 Newton and 9.78 mg/min respectively. The trade between solution 1 and 2 is made based on the highest predicted MRR value which affects the production time and can significantly reduce the machining cost. Although the resultant forces from solution 2 are slightly lower than solution 1 to ~4 Newton, the force increment value is not too severe and does not impair the cutting tool and work piece surface due to the presence of the abrasive slurry.

Based on the selected optimized cutting parameters, a triplicate experiment is set up to validate the effectiveness of the optimization model. Validation processes are done to assess the amount of relative errors between the predicted and experimental results. It is found that average relative error for each performance such as, surface roughness, resultant force and material removal rate are in the range of the accepted value which confirms the proposed optimization model validity.

Scanning electron microscope (SEM) is performed to evaluate the machined surface quality and support the findings for both techniques such as conventional machining and RUAEM with different alumina oxide slurry concentrations (5%, 10%, 15%, 20%).

CHAPTER 5

CONCLUSION AND RECOMMENDATION FOR FUTURE WORK

5.1 Conclusion

The experimental study has been successfully conducted which involves experimentation, analysis, modeling, optimization and validation on slot milling of AISI D2 hardened mould and die material using conventional rotary ultrasonic assisted end milling (RUAEM) with different % volumetric slurry concentration of alumina oxide-distilled water mixture. The RUAEM parameters involved in this study are cutting speed, feed rate, depth of cut, frequency vibration, amplitude vibration and % volumetric slurry concentration of alumina oxide-distilled water mixture. The machining performances analyzed in this study are surface roughness (Ra) value, resultant force (F_R) and material removal rate (MRR). Analysis of variances (ANOVA) test is used to determine the significant factors that influence responses such as surface roughness, cutting force and material removal rate during experiments on slot milling using the historical data analysis in the response surface methodology (RSM) tools which are often used for the optimization process. Historical data method used in the response surface methodology (RSM) is to analyze the interaction between independent variables and machining responses. Overall, the results were summarized and concluded as follows:

1. Firstly, the results of the analysis of variances (ANOVA) for conventional machining, conventional rotary ultrasonic assisted end milling (RUAEM) with 5%, 10%, 15%, 20% volumetric of alumina oxide slurry concentration-distilled water mixture indicate that the machining parameters (factors) like speed, feed rate, amplitude vibration and alumina oxide slurry concentration are significant and

strongly affected value of average surface roughness (Ra). However, the other two (2) parameters of depth of cut and frequency do not affect surface roughness value (Ra). Then, the ANOVA results indicate that the factors that are significant and strongly affect resultant cutting force (R_F) value are speed, feed rate, depth of cut, frequency and amplitude vibration. In addition, ANOVA results also yield that the main factors that are significant and strongly affect material removal rate (MRR) value for conventional and rotary ultrasonic assisted end milling (RUAEM) with 5%, 10%, 15%, 20% volumetric of alumina oxide slurry concentration-distilled water mixture on slot milling of hardened mould and die material are cutting speed, feed rate, depth of cut and amplitude vibration.

2. Secondly, the regression model is developed for conventional machining, conventional rotary ultrasonic assisted end milling (RUAEM) with 5%, 10%, 15%, 20% volumetric of alumina oxide slurry concentration-distilled water mixture on slot milling of hardened mould and die material to establish the relationships between RUAEM parameters and machining performances namely surface roughness, resultant cutting force and material removal rate. The final mathematical equation polynomial quadratic model is generated by analysis of variance (ANOVA) in terms of actual factors to characterize the relationships between the machining performance and all significant factors for rotary ultrasonic assisted end machining (RUAEM). The mathematical model for surface roughness (Ra), resultant force (F_R) and material removal rate (MRR) is developed and shown as Equation 4.1, 4.2 and 4.3 respectively. The optimization is achieved through response surface methodology (RSM) statistical technique. Multiple response routine with desirability function technique is employed for the level of multi

objective optimization process. The set of optimized RUAEM parameters associated with the machining performance outcome has been achieved.

3. Thirdly, the aim of the optimization process is to establish an optimum set of machining RUAEM parameter that can produce a combination of low surface roughness, low cutting force and high material removal rate. Multiple response is used for optimization solution processes. The main goal of this thesis is to eliminate the manual grinding polishing process with the targeted surface roughness values in the range between 0.1 to 0.2 μm and the weight is 5. A total of 17 solutions with their desirability levels are proposed and the proposed solutions have the desirability index in the range of 0.19 to 0.87. The proposed solution gives the high desirability index of 0.87. The high desirability index represents the closest the response towards the target or ideal value. In this optimization solution results for this experiment, the proposed solution number 1 is chosen as the best solution for the optimization of machining parameter (a combination of 111.45 rpm, 5.75 mm/min feed rate, 27.05 μm depth of cut, 20.91 kHz vibration frequency, 3 μm amplitude and 13.26 % abrasive concentration) based on a combination of targeted surface roughness value of 0.1 μm, minimum resultant force and maximum material removal rate value which are predicted to be 19.43 Newton and 9.78 mg/min respectively.

4. Fourthly, the experiment for this validation is done by comparing the results of surface roughness (Ra) value of machined surface, resulting force (F_R), material removal rate (MRR) between predicted values and actual experiments. The validation results for surface roughness (Ra) values show the correlation between experimental and selected solution which ranges between 76.0% to 92.0% with an average correlation of 89.7%. The low average relative errors of approximately

10% from the predicted values clearly indicate that the model fits the experimental data very well. The validation results for resultant force (F_R) values shows the correlation between experimental and selected solution which is in the range between 81.0% to 85.9% with an average correlation of 84.1%. Although the average relative errors of approximately 15.9% from the predicted values are high from a practical standpoint, the errors are still in the considerable accepted range due to the unstable and dynamic of the cutting force generated during slot machining. Besides, validation results for material removal rate (MRR) values show the correlation between experimental and selected solution which is in the range between 76.0% to 92.0% with an average correlation of 89.7%. The low average relative errors of approximately 10% from the predicted values clearly indicate that the model fits the experimental data very well. From all the validation results, the percentage of residual error is less than 10% for each machining response which validates the proposed optimized RUAEM parameters. The comparison between the predicted model and experimental results of surface roughness, resultant force and material removal rate on slot milling has proved that the model is deemed successful.

5. Fifthly, the surface roughness (Ra) value of machined surface of slot milling using RUAEM is 0.12 µm at runs no. 15-d with machining parameters with speed of 30 rpm, 5 mm/min feed rate, 10 µm depth of cut, frequency of 20 kHz, 3 µm amplitude, 48 volt (voltage) and 15% concentration of slurry concentration alumina oxide-water mixture. The results of the study indicate that an appropriate slurry concentration of 15% concentration conveyed to the cutting zone between the tool interface and the surface being machined during slot milling using rotary ultrasonic assisted end milling (RUAEM), produces a mirrored surface of the machined

surface about 0.12 μm. Then, the lowest of resultant force (F_R) obtained from RUAEM experiments is at combination of runs no. 6-c (Speed of 90 rpm, 5 mm/min feed rate, 20 μm depth of cut, frequency of 27 kHz, 1μm amplitude and 10% concentration volumetric of slurry concentration alumina oxide-water mixture with 4.98 N value. It can be observed that the use of appropriate slurry which is accurately conveyed to cutting zone between cutting tool and surface being machined during slot milling using rotary ultrasonic assisted machining causes repetitive impacts of the tool on the grains of the abrasive material grains slurry to fall onto the treated surface, causing the fracture of the work piece material with mirror machined surface. Then the highest of material removal rate (MRR) acquired from slot milling of hardened steel material using RUAEM machining is at combination of runs no. 12-e (Speed of 30 rpm, 45 mm/min feed rate, 30 μm depth of cut, frequency of 27 kHz, 1 μm amplitude and 20% of concentration volumetric of slurry concentration alumina oxide-water mixture with an average value of 161.58 mg/min.

5.2 Recommendations for future works

This thesis focuses on rotary ultrasonic assisted end milling (RUAEM) on slot milling of hardened mould and die material using a new cutting tool of straight shank type EPH Hybrid TAC mills with a code of EPH11R010M06.0-2. Through the completed experimental work, it is found that there are a number of issues that can be studied further. A few recommendations for future works are as follows:

1. This study can be conducted using rotary ultrasonic assisted end milling (RUAEM) machining with different shapes of horns and different materials such as steel or brass.

2. In this study, the experiments are conducted using RUAEM machining with a single type of abrasive slurry namely alumina oxide. For further experimental works, different abrasive slurry namely silicon carbide (SiC), boron carbide (B_4C) can be used using different grit sizes of abrasive slurry.
3. In this experiment, the slot milling using rotary ultrasonic assisted end milling (RUAEM) machining with different concentrations of volumetric alumina oxide-distilled water mixture. The future experiments might use different concentrations of volumetric silicon carbide, boron carbide with the highest different concentration of volumetric abrasive slurry (silicon carbide, boron carbide)-different types of water mixture.

REFERENCES

Abou-El-Hossein, K. A., Kadirgama, K., Hamdi, M., and Benyounis, K. Y., 2007. Prediction of cutting force in end-milling operation of modified AISI P20 tool steel. *Journal of Materials Processing Technology*, 182(1–3), pp. 241–247.

Abou-El-Hossein, K. A., and Yahya, Z., 2005. High-speed end-milling of AISI 304 stainless steels using new geometrically developed carbide inserts. *Journal of Materials Processing Technology*, pp. 596–602.

Abd Halim, M. A., Kasim, M. S., Sulaiman, M., Effendi, M., and Teruaki, I., 2014. Effect Cutting Parameters on Surface Roughness during End Milling of AISI D2 Tool. *Conference Design and System, Japan Society of Mechanical Engineers* 24(1), pp. 2308–2314.

Agarwal, S., 2015a. International Journal of Machine Tools and Manufacture On the mechanism and mechanics of material removal in ultrasonic machining. *International Journal of Machine Tools and Manufacture*, 96, pp. 1–14.

Agarwal, S., 2015b. On the mechanism and mechanics of material removal in ultrasonic machining. *International Journal of Machine Tools and Manufacture*, 96, pp. 1–14.

Agarwal, S., 2015c. On the mechanism and mechanics of material removal in ultrasonic machining. *International Journal of Machine Tools and Manufacture*, 96 pp. 1-14.

Alabdullah, M., Polishetty, A., and Littlefair, G., 2016. Microstructural and Surface Texture Analysis due to Machining in Super Austenitic Stainless Steel. *Journal of Metallurgy*, 2016(1), pp. 1-8.

Altan, T., Lilly, B., and Yen, Y. C., 2001. Manufacturing of dies and molds. *CIRP Annals - Manufacturing Technology*, 50(2), pp. 404–422.

Altan, T., Lilly, B., and Yen, Y. C., 2001. Manufacturing of Dies and Molds. *CIRP Annals - Manufacturing Technology*, 50(2), pp. 404–422.

Amin, K. M. N., Dolah, S. B., Mahmud, M. B., and Lajis, M. A., 2008. Effects of workpiece preheating on surface roughness, chatter and tool performance during end milling of hardened steel D2. *Journal of Materials Processing Technology*, 201(1–3), pp. 466–470.

Aremu, M. O., Oke, E. O., Arinkoola, A. O., and Salam, K. K., 2014. Development of Optimum Operating Parameters for Bioelectricity Generation from Sugar Wastewater Using Response surface methodology. *Journal of Scientific Research and Reports*, 3(15), pp. 2098–2109.

Arsecularatne, J. A., Zhang, L. C., Montross, C., and Mathew, P., 2006. *On machining of hardened AISI D2 steel with PCBN tools*. 171, pp. 244–252.

Astashev, V. K., Babitsky, V., 2014. *Ultrasonic Processes and Machines*. Retrieved from http://books.google.co.uk/books?id=saEqz_LKkdEC.

Axinte, D., and Dewes, R., 2002. Surface integrity of hot work tool steel after high speed milling-experimental data and empirical models. *Journal of Materials Processing Technology*, 127(3), pp. 325–335.

Azlan, R., Izamshah, R., Kasim, M. S., Akmal, M., and Nawi, M., 2017. Improvement of Machining Performance using Hybrid Rotary Ultrasonic Milling (HRUAM) for Hardened D2 Tool Steel Materials. *International Journal of Applied Engineering Research ISSN*, 12(23), pp. 13506–13513.

Baptista, R., and Antune Simões, J. F., 2000. Three and five axes milling of sculptured surfaces. *Journal of Materials Processing Technology*, 103(3), pp. 398–403.

Becze, C. E., Worswick, M. J., and Elbestawi, M., 2001. High Strain Rate Shear Evaluation And Characterization of AISI D2 Tool Steel In Its Hardened State. *Machining Sciences and Technology*, 5(1), pp. 131–149.

Begic-Hajdarevic, D., Cekic, A., and Kulenovic, M., 2014. Experimental Study on the High Speed Machining of Hardened Steel. *Procedia Engineering*, 69, pp. 291–295.

Bertsche, E., Ehmann, K., and Malukhin, K., 2013. Ultrasonic slot machining of a silicon carbide matrix composite. *International Journal of Advanced Manufacturing Technology*, 66(5–8), pp. 1119–1134.

Brehl, D. E., and Dow, T. A., 2008a. Review of vibration-assisted machining. *Precision Engineerin,* 32(3), pp. 153–172.

Brehl, D. E., and Dow, T. A., 2008b. Review of vibration-assisted machining. *Precision Engineering*, 32(3), 153–172.

Bourithis, L., Papadimitriou, G. D., and Sideris, J., 2006. Comparison of wear properties of tool steels AISI D2 and O1 with the same hardness. *Tribology International*, 39(6), pp. 479–489.

Budak, E., Lazoglu, I., and Guzel, B. U., 2004. Improving Cycle Time in Sculptured Surface Machining Through Force Modeling. *CIRP Annals - Manufacturing Technology*, 53(1), pp. 103–106.

Chen, J. S., Huang, Y. K., and Chen, M. S., 2005. Feedrate optimization and tool profile modification for the high-efficiency ball-end milling process. *International Journal of Machine Tools and Manufacture*, 45(9), pp. 1070–1076.

Cakir, M. C., Irfan, O., and Cavdar, K., 2005. An expert system approach for die and mold making operations. *Robotics and Computer-Integrated Manufacturing*, 21(2), pp. 175–183.

Campatelli, G., and Scippa, A., 2012. Prediction of milling cutting force coefficients for aluminum 6082-T4. *Procedia CIRP*, 1(1), pp. 563–568.

Camuşcu, N., and Aslan, E., 2005. A comparative study on cutting tool performance in end milling of AISI D3 tool steel. *Journal of Materials Processing Technology*, 170(1–2), pp. 121–126.

Cao, H., Zhou, K., and Chen, X., 2015. Stability-based selection of cutting parameters to increase material removal rate in high-speed machining process. *Journal of Engineering Manufacture*, 1, pp. 1–14.

Chavoshi, S. Z., and Luo, X., 2015. Hybrid micro-machining processes : A review. *Precision Engineering*, 41, pp. 1–23.

Chen, W., 2000. Cutting forces and surface finish when machining medium hardness steel using CBN tools. *International Journal of Machine Tools and Manufacture*, 40(3), pp. 455–466.

Chern, G. L., and Chang, Y. C., 2006. Using two-dimensional vibration cutting for micro-milling. *International Journal of Machine Tools and Manufacture*, 46(6), pp. 659–666.

Chinchanikar, S., and Choudhury, S. K., 2015. Machining of hardened steel—Experimental investigations, performance modeling and cooling techniques: A review. *International Journal of Machine Tools and Manufacture*, 89, pp. 95–109.

Churi, N., 2010. Rotary ultrasonic machining of hard-to-machine. *PhD Thesis, Kansas University, Manhattan, Kansas.*

Churi, N. J., Pei, Z. J., and Treadwell, C., 2007. Rotary ultrasonic machining of titanium alloy (Ti-6Al-4V): Effects of tool variables. *International Journal of Precision Technology*, 1(1), pp. 301-321.

Coldwell, H., Woods, R., Paul, M., Koshy, P., Dewes, R., and Aspinwall, D., 2003. Rapid machining of hardened AISI H13 and D2 moulds, dies and press tools. *Journal of Materials Processing Technology*, 135(2–3), pp. 301–311.

Cong, W. L., Pei, Z. J., Deines, T. W., and Treadwell, C., 2011. Rotary ultrasonic machining of CFRP using cold air as coolant: feasible regions. *Journal of Reinforced Plastics and Composites*, 30(10), pp. 899–906.

Cong, W. L., Pei, Z. J., Mohanty, N., Van Vleet, E., and Treadwell, C., 2011. Vibration Amplitude in Rotary Ultrasonic Machining: A Novel Measurement Method and Effects of Process Variables. *Journal of Manufacturing Science and Engineering*, 133(3), pp. 1-6.

Daud, R., Hasfa, N. K., Tomadi, S. H., Hassan, M. A., Kadirgama, K., Noor, M. M., and Rejab, M. R. M., 2009. Prediction of Chatter in CNC Machining based on Dynamic Cutting Force for Ball End Milling. *Proccedings of the International Multi Conference of Engineers and Computer Scientist*, pp. 1-6.

Dawes, R. C., and Aspinwall, D. K., 1997. A review of ultra high speed milling of hardened steels. *Journal of Materials Processing Technology* 69(1997), pp. 1-17.

Ding, H., Ibrahim, R., Cheng, K., and Chen, S. J., 2010. Experimental study on machinability improvement of hardened tool steel using two dimensional vibration-assisted micro-end-milling. *International Journal of Machine Tools and Manufacture*, 50(12), pp. 1115–1118.

Donghao, L. I. U., 2018. Die Manufacturing Process-The Best Flow From Idea To Delivery. *Thesis, Politecnic*.

Douglas C. Montgomery., 2009. *Design and Analysis of Experiments,* 7th ed., Arizona State University: John Wiley and Sons, Inc.

EI-Hofy, H., 2005. *Advanced machining processes*. https://doi.org/10.1036/0071466940

Elhadie, M., Karim, A. N. M., and Amin, A. K. M. N., 2011. Cost model for end-milling of AISI D2 tool steel. *2011 National Postgraduate Conference*, pp. 1–6.

Fallböhmer, P., Rodríguez, C. A., Özel, T., and Altan, T., 2000. High-speed machining of cast iron and alloy steels for die and mold manufacturing. *Journal of Materials Processing Technology*, 98(1), pp. 104–115.

Feucht, F., Ketelaer, J., Wolff, A., Mori, M., and Fujishima, M., 2014. Latest machining technologies of hard-to-cut materials by ultrasonic machine tool. *Procedia CIRP*, 14(1), pp. 148–152.

Gaitonde, V. N., Karnik, S. R., Figueira, L., and Paulo D. J., 2009. Machinability investigations in hard turning of AISI D2 cold work tool steel with conventional and wiper ceramic inserts. *International Journal of Refractory Metals and Hard Materials*, 27(4), pp. 754–763.

Gaitonde, S. R., Maciel, C. H. A., Rubio, J. C. C., and Abrao, A. M., 2016. Machinability Evaluation in Hard Milling of AISI D2 Steel. *Materials Research*, 19(2), pp. 360–369.

Ghani, J. A., Choudhury, I. A., and Hassan, H. H., 2004. Application of Taguchi method in the optimization of end milling parameters. *Journal of Materials Processing Technology*, 145, pp. 84–92.

Goswami, D., and Chakraborty, S., 2015. Parametric optimization of ultrasonic machining process using gravitational search and fireworks algorithms. *Ain Shams Engineering Journal*, 6(1), pp. 315–331.

Grandguillaume, L., Lavernhe, S., Quinsat, Y., and Tournier, C., 2015. Mold Manufacturing Optimization: A Global Approach of Milling and Polishing Processes. *Procedia CIRP*, 31, pp. 13–18.

Grzesik, W., 2008. *Influence of tool wear on surface roughness in hard turning using differently shaped ceramic tools*. 265, pp. 327–335.

Gundogar, E., and Findik, F., 1997. Developing A Knowledge Based Decision Making System To Select Of Dies For Sheet Metal Forming. *SAU Fen Bilimleri Enstitusi Dergisi*, 2(1), pp. 129–136.

Gupta, A., Mehta, J. S., and Madan, R., 2013. Micro Ultrasonic Machining: A Brief Outlook. *American Council for an Energy-Efficient Economy*, pp. 1–6.

Güvenç, L., and Srinivasan, K., 1997. An Overview of Robot-Assisted Die and Mold Polishing with Emphasis on Process Modeling. *Journal of Manufacturing Systems*, 16(1), pp. 48–58.

Heo, J. Y., Cho, S. H., Je, T. J., Kim, K. H., Lee, H. W., and Kang, M. C., 2011. Effects of Honing Treatment on AIP-TiN and TiAlN Coated End-Mill for High Speed Machining. *Transactions of Nonferrous Metals Society of China (English Edition)*, 21(1), pp. 83-87.

Horst, R. T., Tromp, N., Haan, M. D., Navarro, R., Venema, L., and Pragt, J., 2008. International Conference on Space Optics — ICSO 2008 Toulouse , France 14 – 17 October 2008 Menno de Haan Ramon Navarro. *International Conference on Space Optics*, 10566(October 2008), pp. 1–8.

Hosseini, A., Hussein, H. M., and Kishawy, H. A., 2016. On the machinability of die or mold D2 steel material. *International Journal Advanced Manufacturing Technology*, 1(85), pp. 735–736.

Ibrahim, R., Bateman, R., Cheng, K., Wang, C., and Au, J., 2011. Design and analysis of a Desktop Micro-Machine for Vibration-Assisted Micromachining. *Proceedings of the Institution of Mechanical Engineers, Part B: Journal of Engineering Manufacture*, 225(8), pp. 1377–1391.

Izamshah, R., Azam, M. A., Hadzley, M., Md Ali, M. A., Kasim, M. S., and Abdul Aziz, M. S., 2013. Study of Surface Roughness on Milling Unfilled-Polyetheretherketones Engineering Plastics. *Procedia Engineering*, 68, pp. 654–660.

Jain, V., Sharma, A. K., and Kumar, P., 2011. Recent Developments and Research Issues in Microultrasonic Machining. *ISRN Mechanical Engineering*, pp. 1–15.

Jasni, N. A. H., Lajis, M. A., and Kamdani, K., 2012. Tool Wear Performance of TiAlN / AlCrN Multilayer Coated Carbide Tool in Machining of AISI D2 Hardened Steel. *Advance Materials Research*, pp. 462–467.

Jawahir, I. S., Brinksmeier, E., M'Saoubi, R., Aspinwall, D. K., Outeiro, J. C., Meyer, D., and Jayal, A. D., 2011. Surface Integrity in Material Removal Processes: Recent Advances. *CIRP Annals - Manufacturing Technology*, 60(2), pp. 603–626.

Joshua, O. S., David, M. O., and Sikiru, I. O., 2015a. Experimental Investigation of Cutting Parameters on Surface Roughness Prediction during End Milling of Aluminium 6061 under Minimum Quantity Lubrication (MQL). 5(1), pp. 1–13.

Joshua, O. S., David, M. O., and Sikiru, I. O., 2015b. Experimental Investigation of Cutting Parameters on Surface Roughness Prediction during End Milling of Aluminium 6061 under MQL (Minimum Quantity Lubrication), 5(1), pp. 1–13.

Jung, H., Shamoto, E., Ueyama, T., and Hamada, S., 2012. Mirror Surface Finishing of Hardened Die Steel by High Power Ultrasonic Elliptical Vibration Cutting. *Journal of Machine Engineering*, 16(1), pp. 5–14.

Kalpakjian, S., and Schmid, S. R., 2014. Manufacturing Engineering and Technology. *United States: Pearson*, 7(1), pp. 1–16.

Kang, M. C., Kim, K. H., Shin, S. H., Jang, S. H., Park, J. H., and Kim, C., 2008. Effect of the minimum quantity lubrication in high-speed end-milling of AISI D2 cold-worked die steel (62 HRC) by coated carbide tools. *Surface and Coatings Technology*, 202(22–23), pp. 5621–5624.

Karaguzel, U., Bakkal, M., and Budak, E., 2016. Modeling and Measurement of Cutting Temperatures in Milling. *Procedia CIRP Conference on High Performance Cutting*, 46, pp. 173–176.

Kasim, M. S., Che Haron, C. H., Ghani, J. A., Sulaiman, M. A., and Yazid, M. Z. A., 2013. Wear mechanism and notch wear location prediction model in ball nose end milling of Inconel 718. *Wear*, 302(1–2), pp. 1171–1179.

Kasim, M. S., Haron, C. H. C., Ghani, J. A., Azam, M. A., Izamshah, R., Ali, M. A. M., and Aziz, M. S. A., 2014. The Influence Of Cutting Parameter on Heat Generation in High-Speed Milling Inconel 718 under MQL Condition. *Journal of Scientific and Industrial Research*, 73(1), pp. 62–65.

Kasim, M. S., Haron, C. H. C., Ghani, J. a, and Sulaiman, M. A., 2013. Prediction Surface Roughness in High-Speed Milling of Inconel 718 under Mql Using Rsm Method. *Middle-East Journal of Scientific Research*, 13(3), pp. 264–272.

Kei-lin, K. U. O., and Chung-chen, T., 2012. Rotary ultrasonic-assisted milling of brittle materials. *Transactions of Nonferrous Metals Society of China*, 22, pp. 793–800.

Khoo, C. Y., Hamzah, E., and Sudin, I., 2008. A Review on the Rotary Ultrasonic Machining of Advanced Ceramics. *Journal Mecanical*, (25), pp. 9–23.

Kiswanto, G., Zariatin, D. L., and Ko, T. J., 2015. The Effect Of Spindle Speed, Feed-Rate and Machining Time to the Surface Roughness and Burr Formation of Aluminum Alloy 1100 in Micro-Milling Operation. *Journal of Manufacturing Processes*, 16(4), pp. 435–450.

Kita, Y., Furuike, H., Kakino, Y., Nakagawa, H., and Hirogaki, T., 2001. Basic Study of Ball End Milling on Hardened steel. *Journal of Materials Processing Technology*, 111(1–3), pp. 240–243.

Komaraiah, M., Manan, M. a., Narasimha Reddy, P., and Victor, S., 1988. Investigation of Surface Roughness and Accuracy in Ultrasonic Machining. *Precision Engineering*, 10(2), pp. 59–65.

Koshy, P., Dewes, R. C., and Aspinwall, D. K., 2002. High Speed End Milling of Hardened AISI D2 Tool Steel (58 HRC). *Journal of Materials Processing Technology*, 127(2), pp. 266–273.

Kovac, P., Rodic, D., Pucovsky, V., Savkovic, B., and Gostimirovic, M., 2012. Application of Fuzzy Logic and Regression Analysis for Modeling Surface Roughness in Face Milling. *Journal of Intelligent Manufacturing*, 24(4), pp. 1–8.

Kumar, J., Khamba, J. S., and Mohapatra, S. K., 2008a. An investigation into the Machining Characteristics of Titanium Using Ultrasonic Machining. *International Journal of Machining and Machinability of Materials*, 3(1/2), pp. 143–161.

Kumar, J., Khamba, J. S., and Mohapatra, S. K., 2008b. An investigation into the Machining Characteristics of Titanium Using Ultrasonic Machining. *International Journal of Machining and Machinability of Materials*, 3(1/2), pp. 143–161.

Kumar, M. N., Subbu, S. K., Krishna, P. V., and Venugopal, A., 2014. Vibration Assisted Conventional and Advanced Machining: A Review. *Procedia Engineering*, 97, pp. 1577–1586.

Kumar, V., and Khamba, J. S., 2007. Statistical Analysis of Experimental Parameters in Ultrasonic Machining of Tungsten Carbide Using the Taguchi Approach. *Journal of the American Ceramic Society*, 91(1), pp. 92–96.

Kundor, N. F., Awang, N. W., and Berahim, N., 2016. Tool Wear and Surface Roughness in Machining AISI D2 Tool Steel. *Indian Journal of Science and Technology*, 9(18), pp. 1-7.

Kuo, K. L., and Tsao, C. C., 2012. Rotary Ultrasonic-Assisted Milling of Brittle Materials. *Transactions of Nonferrous Metals Society of China (English Edition)*, 22(3), pp. 793–800.

Kuruc, M., and Peterka, J., 2014. Rotary Ultrasonic Machining of Poly-Crystalline Cubic Boron Nitride. *Slovak University of Technology Journal*, 22(1), pp. 103–108.

Lamikiz, A., De Lacalle, L. N. L., Sánchez, J. A., and Salgado, M. A., 2004. Cutting force estimation in sculptured surface milling. *International Journal of Machine Tools and Manufacture*, 44(14), pp. 1511–1526.

Latif, A. A., Ibrahim, M. R., Amran, A., and Rahim, E., 2017. A study on the effect of feed rate and cutting speed on surface roughness and material removal rate of mild steel. *4th International Conference on Mechanical Engineering Research (ICMER2017)*, 1(1), pp. 1–8.

Lauwers, B., Bleicher, F., and Haaf, P. T. E. N., 2010. Investigation of the Process-Material Interaction in Ultrasonic Assisted Grinding of ZrO2 based Ceramic Materials. *Proceeding of CIRP International Conference on Hign Performance Cutting*, 1(4), pp. 1–6.

Lauwers, B., Plakhotnik, D., Vanparys, M., and Liu, W., 2008. Tool Path Generation Functionality and Ultrasonic Assisted Machining of Ceramic Components using Multi-axis Machine Tools. *Machine Tool Technologies Foundation*, 1(1), pp. 1–6.

Lee, M. H., 2008. *Parameters Optimization of Rotary Ultrasonic Machining of Glass Lens for Surface Roughness Using Statistical Taguchi's Experimental Design*. pp. 214–219.

Lee, T. C., and Chan, C. W., 1997. Mechanism of the Ultrasonic Machining of Ceramic Composites. *Journal of Materials Processing Technology*, 71(2), pp. 195–201.

Lian, H., Guo, Z., Huang, Z., Tang, Y., and Song, J., 2013. Experimental Research of Al6061 on Ultrasonic Vibration Assisted Micro-Milling. *Procedia CIRP International Conference on Hign Performance Cutting*, 6, pp. 561–564.

Liu, C. S., Zhao, B., Gao, G. F., and Jiao, F., 2002. Research on the Characteristics of the Cutting Force in the Vibration Cutting of a Particle-Reinforced Metal Matrix Composites SiCp/Al. *Journal of Materials Processing Technology*, 129(1–3), pp. 196–199.

Liu, J., Zhang, D., Qin, L., and Yan, L., 2012. Feasibility study of the rotary ultrasonic elliptical machining of carbon fiber reinforced plastics (CFRP). *International Journal of Machine Tools and Manufacture*, 53(1), pp. 141–150.

Ma, C., Shamoto, E., Moriwaki, T., and Wang, L., 2004. Study of machining accuracy in ultrasonic elliptical vibration cutting. *International Journal of Machine Tools and Manufacture*, 44(12–13), pp. 1305–1310.

Masmiati, S. A. A., 2015. Optimizing Cutting Parameters in Inclined End Milling for Minimum Surface Residual Stress – Taguchi Approach. *Measurement*, 60, pp. 267-275.

Marcel, K., Marek, Z., and Jozef, P., 2014. Investigation of Ultrasonic Assisted Milling of Aluminum Alloy AlMg4.5Mn. *Procedia Engineering*, 69, pp. 1048–1053.

Marcos, A., Erthal, R., Padua, E., Silveira, L., and Am, L., 2008. Talanta Response surface methodology (RSM) as a Tool for Optimization in Analytical Chemistry. 76, pp. 965–977.

MIDA, 2016. Malaysian Manufacturers to Enhance Operational Efficiency, Adopt Appropriate Technologies and Explore New Markets.

Mishra, V., Khan, G. S., Chattopadhyay, K. D., Nand, K., and Sarepaka, V., 2014. Effects of Tool Overhang on Selection of Machining Parameters and Surface Finish During Diamond Turning. *Measurement*, 55, pp. 353-361.

Mizayu. Stamping die [online] Available at: http://www.miyazu.com.my/v2/index.php?option=com_content&view=article&id=30&Itemid=169 [Accessed on 25 March 2017].

Moriwaki, T., Shamoto, E., Song, Y., and Kohda, S., 2004. Development of a Elliptical Vibration Milling Machine. *CIRP Annals - Manufacturing Technology*, 53(1), pp. 341–344.

Narasimha, P., 1993. A Study on The Influence of Workpiece Properties in Ultrasonic Machining. *International Journal Machining Tools Manufacturing*, 33(3), pp. 495–505.

Naresh, N., Rajasekhar, K., and Reddy, P. V., 2013. Parametric Analysis of GFRP Composites in CNC Milling Machine using Taguchi Method. *International Journal of Mechanical and Civil Engineering*, 6(1), pp. 102–111.

Nath, C., and Rahman, M., 2008. Effect of Machining Parameters in Ultrasonic Vibration Cutting. *International Journal of Machine Tools and Manufacture*, 48(9), pp. 965–974.

Neto, H. K., Diniz, A. E., and Pederiva, R., 2016. *Influence of tooth passing frequency , feed direction , and tool overhang on the surface roughness of curved surfaces of hardened steel*. pp. 753–764.

Nguyen, H., and Hsu, Q. C., 2016. Surface Roughness Analysis in the Hard Milling of JIS SKD61 Alloy Steel. *Applied Sciences*, 6(172), pp. 1–15.

Ning, F. D., Cong, W. L., Pei, Z. J., and Treadwell, C., 2016. Rotary ultrasonic machining of CFRP : A comparison with grinding. *Ultrasonics*, 66, pp. 125–132.

Noordin, M. Y., Venkatesh, V. C., Sharif, S., Elting, S., and Abdullah, A., 2004. Application of Response surface methodology in Describing the Performance of Coated Carbide Tools when Turning AISI 1045 Steel. 145, pp. 46-58.

Oh, S., Rheem, S., Sim, J., and Kim, S., 1995. Optimizing Conditions for the Growth of Lactobacillus Casei YIT 9018 in Tryptone-Yeast Extract-Glucose Medium by using Response surface methodology. 61(11), pp. 3809–3814.

Okada, M., Hosokawa, A., Tanaka, R., and Ueda, T., 2011. Cutting performance of PVD-coated carbide and CBN tools in hardmilling. *International Journal of Machine Tools and Manufacture*, 51(2), pp. 127–132.

Ozoegwu, C. G., Omenyi, S. N., Ofochebe, S. M., Obaseki, E., Uzoh, C. F., and Nwangwu, C. C., 2012. Comparison of up Milling and Down Milling Modes of End Milling Process. *Research Journal in Engineering and Applied Sciences*, 1(5), pp. 314–322.

Paulo, D. J., and Monteiro, B. A., 2000. Relationship between Cutting Force and PCD Cutting Tool Wear in Machining Silicon Carbide Reinforced Aluminum. *Journal of Materials Processing Technology*, 103(3), pp. 417–423.

Pei, W., Yu, Z., Li, J., Ma, C., Xu, W., Wang, X., and Natsu, W., 2013. Influence of Abrasive Particle Movement in Micro USM. *Procedia CIRP*, 6, pp. 551–555.

Pei, Z. J., and Ferreira, P. M., 1999. Experimental Investigation of Rotary Ultrasonic Face Milling. *International Journal of Machine Tools and Manufacture*, 39(8), pp. 1327–1344.

Pei, Z. J., Ferreira, P. M., Kapoor, S. G., and Haselkorn, M., 1995. Rotary Ultrasonic Machining for Face Milling of Ceramics. *International Journal of Machine Tools and Manufacture*, 35(7), pp. 1033–1046.

Pimenov, D. Y., 2014. Experimental Research of Face Mill Wear Effect to Flat Surface Roughness. *Journal of Friction and Wear*, 35(3), pp. 250–254.

Pu, Z., and Singh, A., 2013a. High Speed Ball Nose End Milling of Hardened AISI A2 Tool Steel with PCBN and Coated Carbide Tools. *Journal of Manufacturing Processes*, 15(4), pp. 467–473.

Pu, Z., and Singh, A., 2013b. High Speed Ball Nose End Milling of Hardened AISI A2 Tool Steel with PCBN and Coated Carbide Tools. *Journal of Manufacturing Processes*, 15(4), pp. 467–473.

Raja, I., Mo, J. P. T., Ding, S., Arfauz, M., and Azam, M. S. K., 2014. Effect of Parameter Condition on Surface Roughness for Machining AISI D2 Hardened Tool Steel. *Journal of Advanced Manufacturing Technology*, 8(1), pp. 47–56.

Ramli, A., Izamshah, R., Hadzley, M., and Kasim, M. S., 2016. Surface evaluation of rotary ultrasonic assisted machining technique. *Advanced Processes and Systems in Manufacturing An International Conference 2016*, 1, pp. 11–12.

Rasidi, I. I., Rafai, N. H., Rahim, E. A., Ding, S. A. K. H., and Cheng, K., 2015. An Investigation of Cutting Mechanics in 2 Dimensional Ultrasonic Vibration Assisted Milling Toward Chip Thickness and Chip Formation. *MATEC Web of Conferences*, pp. 1-4.

Rasidi, I., Rahim, E. A., Ibrahim, A. A., Maskam, N. A., and Ghani, S. C., 2014. The Effect on the Application of Coolant and Ultrasonic Vibration Assisted Micro Milling on Machining Performance. *Applied Mechanics and Materials*, 660(1), pp. 65–69.

Rawangwong, S., Chatthong, J., Boonchouytan, W., and Burapa, R., 2014. Influence of Cutting Parameters in Face Milling Semi-solid AA 7075 Using Carbide Tool Affected the Surface Roughness and Tool Wear. *Energy Procedia*, 56, pp. 448–457.

Rehman, A., and Maqsood, S., 2015. *Finite Element Analysis of Tool Wear in Ultrasonically Assisted Turning*. pp. 64–68.

Routara, B. C., Sahoo, A. K., Rout, A. K., and Thatoi, D. N., 2011. Optimization of Multiple Performance Characterstic in Ultrasonic Machining Process using Grey Relational Analysis. *International Conference on Mechanical Engineering*, 4, pp. 18–20.

Saedon, J. B., Soo, S. L., Aspinwall, D. K., and Barnacle, A. (2012). Micro-Milling of Hardened AISI D2 Tool Steel. *Advanced Materials Research*, 445(1), 62–67.

Said, M. S., Ghani, J. A., Kassim, M. S., Tomadi, S. H., Hassan, C., Haron, C., and Kedah, K., 2013. Comparison between Taguchi Method and Response surface methodology (RSM) In Optimizing Machining Condition Department of Mechanical and Materials Engineering. *International Conference on Robust Quality Engineering*, pp. 60–64.

Seifert, E., Abramo, L., and Thelin, B., 1998. Experimental Design and Optimization. *Chemometrics and Laboratory Systems*, 42, pp. 3–40.

Sekulic, M., Jurkovic, Z., Hadzistevic, M., and Gostimirovic, M., 2010. The Influence of Mechanical Properties of Workpiece Material. *Metalurgija*, 49(4), pp. 339–342.

Senthil Kumar, K., Senthilkumaar, J. S., and Srinivasan, A., 2013. Reducing Surface Roughness by Optimising the Turning Parameters. *South African Journal of Industrial Engineering August*, 24(2), pp. 78–87.

Shahrom, M. S., Yahya, N. M., and Yusoff, A. R., 2013. Taguchi Method Approach on Effect of Lubrication Condition on Surface Roughness in Milling Operation. *Procedia Engineering*, 53, pp. 594–599.

Shajari, S., Sadeghi, M. H., and Hassanpour, H., 2014. The influence of tool Path Strategies on Cutting Force and Surface Texture During Ball End Milling of Low Curvature Convex Surfaces. *The Scientific World Journal*, pp. 1-14.

Shamoto, E., Suzuki, N., Tsuchiya, E., Hori, Y., Inagaki, H., and Yoshino, K., 2005. Development of 3 DOF Ultrasonic Vibration Tool for Elliptical Vibration Cutting of Sculptured Surfaces. *CIRP Annals - Manufacturing Technology*, 54(1), pp. 321–324.

Shen, X. H., and Xu, G. F., 2017. Study of Milling Force Variation in Ultrasonic Vibration-Assisted End Milling. *Materials and Manufacturing Processes*, 33(9), pp. 1–7.

Shiou, F. J., and Ciou, H. S., 2008. Ultra-Precision Surface Finish of the Hardened Stainless Mold Steel using Vibration-Assisted Ball Polishing Process. *International Journal of Machine Tools and Manufacture*, 48(7–8), pp. 721–732.

Singh, N., and Gianender, K., 2012. USM for Hard or Brittle Material and Effect of Process Parameters on MRR or Surface Roughness: A Review. *International Journal of Applied Engineering Research*, 7(11), pp. 1–6.

Singh, G., Kumar, D., Sharma, N., and Kumar, B., 2014. Investigation into Machining Characteristics Of Tri - Alumane Zirconium Particle Reinforcement In Metal Matrix Composite Using Ultrasonic Machining Process. *International Journal of Research in Engineering and Technology*, 1(1), pp. 649–656.

Singh, K. J., 2014. Ultrasonic Machining Processes-Review Paper. *International Journal for Multi Disciplinary Engineering and Business Management*, 2(3), pp. 57–66.

Singh, R., and Khamba, J. S., 2008. Comparison of Slurry Effect on Machining Characteristics of Titanium in Ultrasonic Drilling. *Journal of Materials Processing Technology*, 197(1–3), pp. 200–205.

Singh, R., and Khamba, J. S., 2007. Taguchi Technique for Modeling Material Removal Rate in Ultrasonic Machining of Titanium. *Materials Science and Engineering*, pp. 365–369.

Singh, R., and Khamba, J. S., 2006. Ultrasonic machining of Titanium and its Alloys: A review. *Journal of Materials Processing Technology*, 173(2), pp. 125–135.

Singh, R. P., and Singhal, S., 2015. Rotary Ultrasonic Machining of Advanced Materials: A Review. *International Journal For Technological Research In Engineering*, 2(7), pp. 777–785.

Soković, M., Kopać, J., Dobrzański, L. A., and Adamiak, M., 2004. Wear of PVD-Coated Solid Carbide End Mills in Dry High-Speed Cutting. *Journal of Materials Processing Technology*, pp. 422–426.

Srinivasa, Y. V., and Shunmugam, M. S., 2013. Mechanistic Model for Prediction of Cutting Forces in Micro End-Milling and Experimental Comparison. *International Journal of Machine Tools and Manufacture*, 67, pp. 18–27.

Sun, S., Brandt, M., and Dargusch, M. S., 2010. Thermally enhanced machining of hard-to-machine materialsA review. *International Journal of Machine Tools and Manufacture*, 50(8), pp. 663–680.

Suzuki, N., Nakamura, A., Shamoto, E., and Harada, K., 2012. Ultraprecision sculpturing of Hardened Steel by Applying Elliptical Vibration Cutting. *International Symposium on Micromechatronics and Human Science*, 1(1), pp. 1–6.

Suzuki, N., 2012. Ultraprecision sculpturing of hardened steel by applying elliptical vibration cutting. *Proceedings of ISUPEN2011*, 1(1), pp. 1–6.

Tawakoli, T., and Azarhoushang, B., 2008. Influence of Ultrasonic Vibrations on Dry Grinding of Soft Steel. *International Journal of Machine Tools and Manufacture*, 48(14), pp. 1585–1591.

Taylor, P., and Kishawy, H. A., 2002. Experimental Evaluation Of Cutting Temperatures During High Speed Machining of Hardened D2 Tool Steel. *Machining Science and Technology*. pp. 37–41.

Thepsonthi, T., Hamdi, M., and Mitsui, K., 2009. Investigation into Minimal-Cutting-Fluid Application in High-Speed Milling of Hardened Steel Using Carbide Mills. *International Journal of Machine Tools and Manufacture*, 49, pp. 156–162.

Thoe, T. B., Aspinwall, D. K., and Wise, M. L. H., 1998. Review on Ultrasonic Machining. *Int. J. Mach. Tools Manufact*, 38(4), pp. 239–255.

Thomas, S., Ramesh, S., Jeykrishnan, J., 2016. Parametric Optimization of Powder Mixed Electro-Discharge Machining using Taguchi Technique. *International Journal of Latest Trends in Engineering and Technology*, 7(3), pp. 61–66.

Toh, C. K., 2006. Cutter path strategies in high speed rough milling of hardened steel. *Materials and Design*, 27(2), pp. 107–114.

Tomas, V., Jozef, P., Mario, K., and Ivan, B., 2014. The wear measurement process of ball nose end mill in the copy milling operations. *Procedia Engineering*, 69, pp. 1038–1047.

Tsai, C., Tong, L., and Wang, C., 2010. Optimization of Multiple Responses Using Data Envelopment Analysis and Response surface methodology. *Journal of Science and Engineering*, 13(2), pp. 197–203.

Tsai, M., Chang, C., and Ho, J., 2016. The Machining of Hard Mold Steel by Ultrasonic Assisted End Milling. *Applied Sciences*, 6(11), pp. 373.

Ucun, İ., Aslantas, K., and Bedir, F., 2013. An experimental investigation of the effect of coating material on tool wear in micro milling of Inconel 718 super alloy. *Wear*, 300(1–2), pp. 8–19.

Viswanath, A., Li, T., and Gianchandani, Y. B., 2014. High resolution micro ultrasonic machining (HR-μUSM) for post-fabrication trimming of fused silica 3-D microstructures. *Proceedings of the IEEE International Conference on Micro Electro Mechanical Systems (MEMS)*, *065017*, pp. 494–497.

Wang, C., Xie, Y., Zheng, L., Qin, Z., Tang, D., and Song, Y., 2014. Research on the Chip Formation Mechanism during the High-Speed Milling of Hardened Steel. *International Journal of Machine Tools and Manufacture*, 79, pp. 31–48.

Wojciechowski, S., and Konrad, K., 2012. Tool Life and Process Dynamics in High Speed Ball End Milling of Hardened Steel. *5th Conference on High Performance Cuting*, 1, pp. 289–294.

Wojciechowski, S., and Twardowski, P., 2012. Tool Life and Process Dynamics in High Speed Ball End Milling of Hardened Steel. *Procedia CIRP*, 1, pp. 289–294.

Wu, B., Yan, X., Luo, M., and Gao, G., 2013. Cutting Force Prediction for Circular End Milling Process. *Chinese Journal of Aeronautics*, 26(4), pp. 1057–1063.

Wu, J., Cong, W., Williams, R. E., and Pei, Z. J., 2011. Dynamic Process Modeling for Rotary Ultrasonic Machining of Alumina. *Journal of Manufacturing Science and Engineering*, 133(4), pp. 1-5.

Xing, D., Zhang, J., Shen, X., Zhao, Y., and Wang, T., 2013. Tribological Properties of Ultrasonic Vibration Assisted Milling Aluminium Alloy Surfaces. *Procedia CIRP*, 6, pp. 539–544.

Xuhuimold. Metal auto parts stamping die. [online]. Available at: http://www.xuhuimould.com/m/metal-auto-parts-stamping-die/stamping-dies-for-ChangAn -parts/metal-stamping-tool-dies-maker-manufacturers.html [Accessed on 24 December 2018].

Ya, G., Qin, H. W., Yang, S. C., and Xu, Y. W., 2002. Analysis of the Rotary Ultrasonic Machining Mechanism. *Journal of Materials Processing Technology*, 129(1–3), pp. 182–185.

Yan, L., Yang, W., Jin, H., and Wang, Z., 2011. Microstructure Changes of Machined Surfaces on Austenitic 304 Stainless Steel. *World Academy of Science, Engineering and Technology*, 81(9), pp. 1883-1887.

Yang, X., and Liu, C. R., 2002. A New Stress-Based Model of Friction Behavior in Machining and its Significant Impact on Residual Stresses Computed by Finite Element Method. *International Journal of Mechanical Sciences*, 44(1), pp. 703-723.

Yang, Y. K., Chuang, M. T., and Lin, S. S., 2009. Optimization of Dry Machining Parameters for High-Purity Graphite in End Milling Process via Design of Experiments Methods. *Journal of Materials Processing Technology*, 209, pp. 4395-4400.

Zeng, W. M., Li, Z. C., Pei, Z. J., and Treadwell, C., 2005. Experimental Observation of Tool Wear In Rotary Ultrasonic Machining Of Advanced Ceramics. *International Journal of Machine Tools and Manufacture*, 45(12–13), pp. 1468-1473.

Zhang., J., Cui, T., Ge, C., Sui, Y., and Yang, H., 2016. Review of Micro/Nano Machining by Utilizing Elliptical Vibration Cutting. *International Journal of Machine Tools and Manufacture*, 106, pp. 109–126.

Zhang, C., Zhang, J., and Feng, P., 2013. Mathematical model for cutting force in rotary ultrasonic face milling of brittle materials. *International Journal of Advanced Manufacturing Technology*, 69(1–4), pp. 161–170.

Zhang, J., Suzuki, N., and Shamoto, E., 2013. Investigation on Machining Performance of Amplitude Control Sculpturing Method in Elliptical Vibration Cutting. *Procedia CIRP*, 8(1), pp. 328–333.

Zhang, J. Z., Chen, J. C., and Kirby, E. D., 2007. Surface Roughness Optimization in an End-Milling Operation using the Taguchi Design Method. *Journal of Materials Processing Technology*, 184, pp. 233–239.

Zhang, X., Senthil K. A., Rahman, M., Nath, C., and Liu, K., 2011. Experimental Study on Ultrasonic Elliptical Vibration Cutting of Hardened Steel using PCD Tools. *Journal of Materials Processing Technology*, 211(11), pp. 1701–1709.

Zhixin, J., Jianhua, Z., and Xing, A., 1997. Study on a New Kind of Combined Machining Technology of Ultrasonic Machining and Electrical Discharge Machining. *International Journal of Machine Tools and Manufacture*, 37(2), pp. 193-199.

Zhou, M., Eow, Y. T., Ngoi, B. K. A., and Lim, E. N., 2003. Vibration-Assisted Precision Machining of Steel with PCD Tools. *Materials and Manufacturing Processes*, 18(5), pp. 825–834.

Zhou, M., Ngoi, B. K. A., Yusoff, M. N., and Wang, X. J., 2006. Tool wear and surface finish in diamond cutting of optical glass. *Journal of Materials Processing Technology*, 174(1–3), pp. 29–33.

Zou, P., Xu, Y., He, Y., Chen, M., and Wu, H., 2015. Experimental Investigation of Ultrasonic-Vibration Assisted Turning of 304 Austenitic Stainless Steel. *Shock and Vibration*, 2015(1), pp. 1–19.

APPENDIX A

Preliminary test

The preliminary test an experiment involves on slot milling of hardened steel materials by using rotary ultrasonic assisted end milling (RUAEM) machining.

1.1 Rotary ultrasonic assisted machining (RUAEM)

Rotary ultrasonic assisted end milling (RUAEM) machining is composed of machining method and a combination of ultrasonic vibrations with normal machining and it used in machining of difficult to cut materials (Zou et al., 2015; Thoe at al., 1998; Ya et al., 2002). RUAEM involves the use of ultrasonic vibration frequency, ranging between 20-40 kHz that is transmitted to the rotating cutting tool. According to Azlan et al. (2016), ultrasonic assisted machining is used for machining hardened steel to get a mirror machined surface and to eliminate the manual polishing process. By incorporating the ultrasonic frequency to the rotating cutting tool, the vibration oscillation amplitude of the tool is altered that had imposed a static pressure on the work piece surface grains, in which the work piece surface is hammered into, and finally a peening surface is produced that improved the surface finish by reducing the peak height produced from the milling cutter. In addition, the transmitted oscillating vibration also reduced the contact pressure between the cutting tool and the work piece, thus reducing the machining force and temperature that consequently prolongs the cutting tool life. It has been reported that the surface roughness of machined surface was improved from 0.60 μm to 0.26 μm (up to 57% reduction) when applying the ultrasonic assisted milling of hardened steel material and using solid carbide ball nose as tool materials. In machining of hardened steel material, surface roughness is

the most important factor to obtain a high quality of machined surface, dimensional accuracy of machined work piece and good of surface integrity (Izamshah et al. 2010).

1.2 Experimental design of preliminary test

A preliminary was conducted to identify the most influential factors that affected by machining performance, which has been studied, namely surface roughness, cutting force (Fx, Fy, Fz) during slot milling cutting using conventional and rotary ultrasonic assisted machining. This experiment was carried out with different cutting speed, feed rate, depth of cut and auto scanning of vibration frequency and amplitude vibration when machining of hardened steel materials. The full factorial design is a suitable method that has been used to carry out this preliminary study with two levels of each factor. The experimental matrix run was generated by Design-Expert 7.0. The 2 level of full factorial design showed all possible combinations of experiments run of minimum and maximum level for each cutting parameter which has the greatest effect on machining performance. The Table 1.1 and Table 1.2 shows the detail of cutting parameters and design an experimental matrix run was generated by Design-Expert 7.0.

Table 1.1: Two level of cutting parameters

Parameter	**Unit**	**Low (-1)**	**High (1)**
Cutting speed	m/min	0.6	3
Feed rate	mm/min	5	100
Depth od cut	µm	0.010	0.012

Table 1.2: Experiment run matrix design

Level	Cutting Speed, *Vc* (m/min)	Feed Rate, *f* (mm/min)	Depth of Cut, *Ap* (μm)
1	0.6	100	10
2	0.6	100	12
3	3	5	12
4	3	100	10
5	3	100	12
6	0.6	5	10
7	3	5	10
8	0.6	5	12

All experiment runs were conducted using 3 axis CNC (Computer numerical control) milling machine, type HAAS VF-1 and BT-40 ultrasonic tool holder as assisted machining tools with constant controlled of 23.83 kHz of vibration frequency and 2 μm of amplitude vibration. Figure 1.1 and Figure 1.2 shows the ultrasonic tool holder assisted machining and cutting tools that was used in the experiment, respectively.

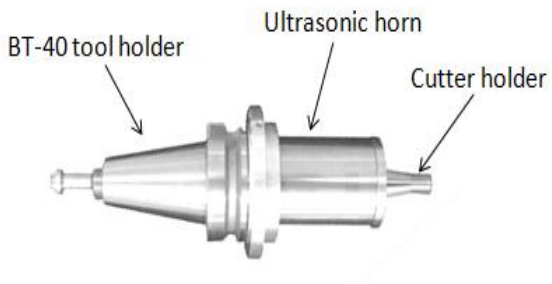


Figure 1.1: Ultrasonic Tool Holder Type BT40

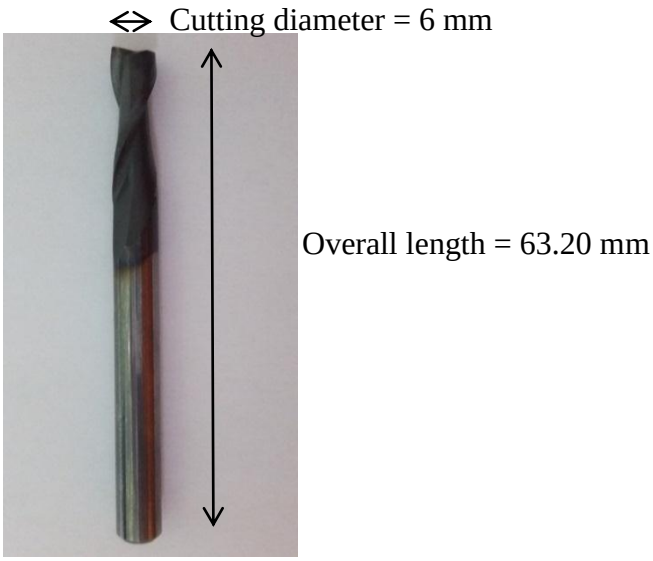


Figure 1.2: Cutting Tool Used In Preliminary Test

1.3 The result of preliminary test

Statistical analysis of preliminary test using 2 level factorial design with 3 factors with aims for screening many factors to find the significant few and contain the low and high range value of factors to allow the analysis process. The minimum for 'low' level machining parameters generated was 0.6 m/min (cutting speed), 5 mm/min (feed rate) and 10 μm (depth of cut). While, the maximum for 'high' level machining parameters generated was 3 m/min (cutting speed), 100 mm/min (feed rate) and 12 μm (depth of cut). The total of independent factors involved in preliminary test is 3 factors, namely cutting speed, feed rate and depth of cut. The 8 experimental run was generated by 2 level factorial design for measurement of machining performance (surface roughness, cutting force).

The machining parameter effects for surface roughness result of machined surface by rotary ultrasonic assisted machining of hardened steel is shown in Table 1.3 and illustrated in Figure 1.3. It can be seen from the data in Table 1.3, that the surface roughness value of machined surface of the hybrid rotary ultrasonic assisted machining process is lower and better compared to conventional machining with same parameters

cutting conditions. These results indicate that the range of the surface roughness value for hybrid rotary ultrasonic assisted machining between 0.27 μm to 1.11 μm. While, the range of the surface roughness value of conventional machining between 0.32 μm to 3.48 μm. The best and the lowest of the surface roughness value of machined surface achieved by hybrid rotary ultrasonic assisted end milling machining with 0.27 μm (Run 3) at 0.6 m/min (cutting speed), 5 mm/min (feed rate) and 12 μm (depth of cut).

Table 1.3: The preliminary result of the surface roughness of conventional machining and rotary ultrasonic assisted machining of hardened steel

Run	**Vc (m/min)**	***f* (mm/min)**	**Ap (μm)**	**Surface roughness Value, Ra (μm)**		
				Conventional	**Rotary Ultrasonic**	**% Ra Reduction**
1	0.6	100	10	0.87	0.69	20.69
2	0.6	100	12	0.83	0.77	7.23
3	3	5	12	0.32	0.27	15.63
4	3	100	10	3.47	2.59	25.36
5	3	100	12	3.48	0.52	85.06
6	0.6	5	10	3.33	0.87	73.87
7	3	5	10	2.36	0.48	79.66
8	0.6	5	12	2.84	1.11	60.92

While, for conventional machining, the lowest of the surface roughness of machined surface achieved was 0.32 μm at Run 3 with 0.6 m/min (cutting speed), 5 mm/min (feed rate) and 12 μm (depth of cut). A comparison of the two results reveals that the cutting speed of 0.6 m/min and feed rate of 5 mm/min is the best and an excellent machining parameter in the machining of hardened steel materials.

From the graph in Figure 1.3, it can be seen that the improvement of surface roughness value from Run 1 to Run 8 when applying of rotary ultrasonic assisted end milling (RUEAM) machining. The results obtained show an improvement on the quality of the machined surface by using RUAEM with a reduction of 85.05 % surface roughness values compared to conventional machining at machining Run 5 as shown in Table 1.3.

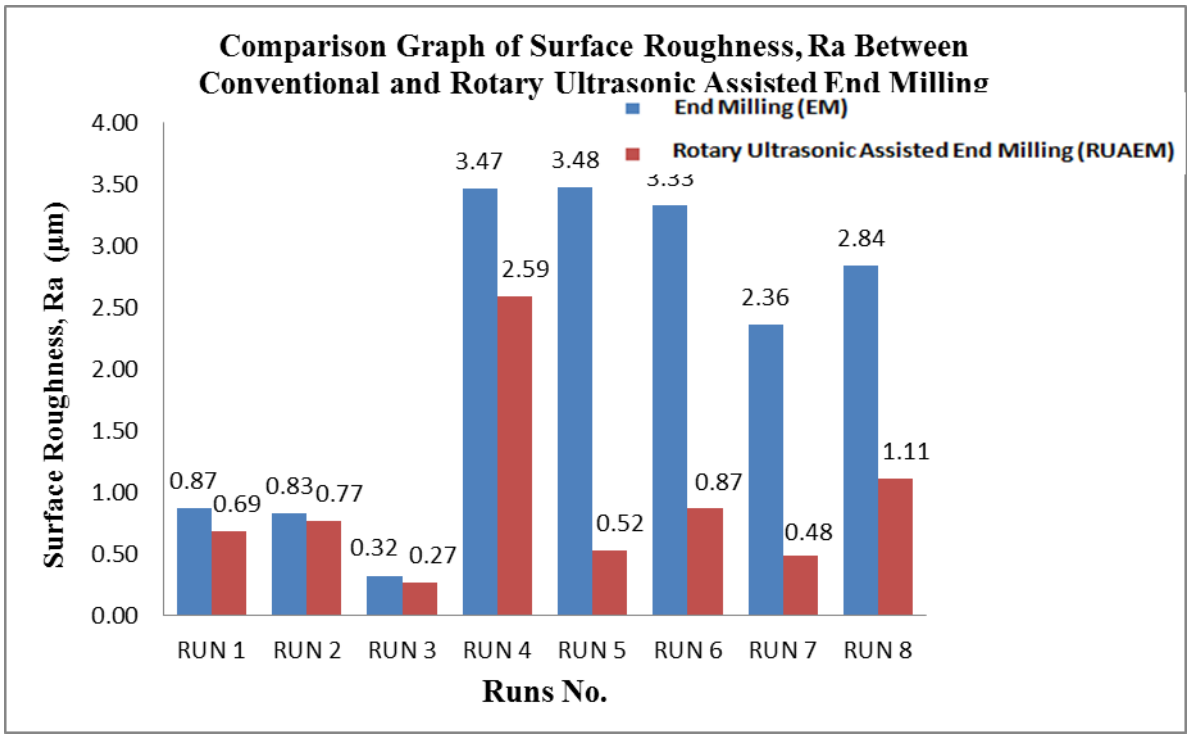


Figure 1.3: The comparison result of surface roughness value for conventional machining and rotary ultrasonic assisted end milling machining

1.4 Statistical analysis of preliminary test

Analysis of variances (ANOVA) was generated by Design Expert 7.0 software and was used to analyze a data obtained from the experiment. Analysis of variances (ANOVA) was used to determine the most significant factors that affected the machining performance namely surface roughness and cutting force. The analysis of variances (ANOVA) is the

statistical analysis was applied to the results of experiments in identifying the percent contribution of each factors at a significant level of confidence (Kumar and Khamba, 2008). The analysis of variances (ANOVA) with significant level of 5%, p-value of less than 0.050 was used to indicate the model is siginificant and identify which factors that affected to machining performance such as surface roughness and cutting force. From the ANOVA analysis, the main effects and interaction effects between factor and response can be plotted. The ratio of maximum response to a minimum response was 12.8889 when the range of value surface roughness response was from 0.27 μm to 3.48 μm. The model F-value of 3.95 implied that the model was significant. The Table 1.4 shows the ANOVA table for result of surface roughness when using hybrid rotary ultrasonic assisted machining. Analysis of variance (ANOVA) for response surface roughness in slot milling machining using square root transformation with full factorial analysis. The F value was derived from the mean square and converted into its corresponding p-value.

Table 1.4: The ANOVA table for result of surface roughness using hybrid rotary ultrasonic assisted end milling machining

Source	**Sum of Square**	**DF**	**Mean Square**	**F-Value**	**Prob>F**	
Model	2.94	8	0.37	3.95	0.04343	*significant*
A	0.328	1	0.328	0.071	0.7978	
B	0.040	1	0.040	0.43	0.5331	
C	0.26	1	0.26	2.75	0.1413	
D	0.97	1	0.97	10.46	0.0144	
AB	1.37	1	1.37	14.76	0.0064	
AC	0.26	1	0.26	2.78	0.1392	
AD	0.025	1	0.025	0.26	0.6227	
BC	0.284	1	0.284	0.061	0.8116	

Residual	0.65	7	0.093
Cor Total	3.59	15	

The analysis of variances (ANOVA) revealed that the value of probability was small, with the Prob>F, near 4.343 % ($p = 0.0062$). When the value of $p < 0.05$, it proves that the existence of the relationship between surface roughness with cutting speed, feed rate and depth of cut was statistically significant. Besides that, when the factors possessing the values less than 0.0500 of "Prob> F", it indicates that the model terms are significant (Izamshah et al., 2013). In this ANOVA analysis, it shows that cutting speed (A), feed rate (B) and ultrasonic assisted machining (D) were the main effects and strongly significant effect on the surface roughness value. Analysis of variance (ANOVA) found that the depth of cut (C) was not affected and did not have a significant effect on the surface roughness value when machining of hardened steel materials using hybrid rotary ultrasonic assisted machining. Also, the ANOVA result shows that the value of "Prob>F" was 0.0434 and less than 0.0500 where it proves that model terms were statistically significant.

Equations 1.1 show the statistical equation model of relationship for correlating the surface roughness considering output responses of machining parameters, i.e. spindle speed, feed rate and depth of cut. The statistical equation model was generated by ANOVA in terms of actual factors and is presented as follows in the form as equation:

$$\text{Surface roughness } (\mu m) \text{ ultrasonic} = 0.88472 + 0.88057A - 0.012574B + 0.043542C + 0.25596AB - 0.10602AC + 0.07280\,BC \quad (1.1)$$

This statistical equation model in terms of the actual factors depended on cutting speed, feed rate and depth of cut. The factor of determination of R-Squared and adjusted R-

Squared was 81.86 % and 61.12 % respectively. While, it can be proved that the average error between the predicted value and an experiment was less than 10 %.

This statistical equation model represented graphically by 3D response surface plots. The Figure 1.4 (a) to 1.4 (c) illustrates the graph of the 3D response surface graphical interactions between factors and machining performance namely surface roughness in the design space. It can be observed that the surface roughness value changed by the cutting speed and feed rate, while the depth of cut was constant. From the Figure 1.8 (a), it shows that a higher cutting speed with lower feed rate can reduce the value of surface roughness.

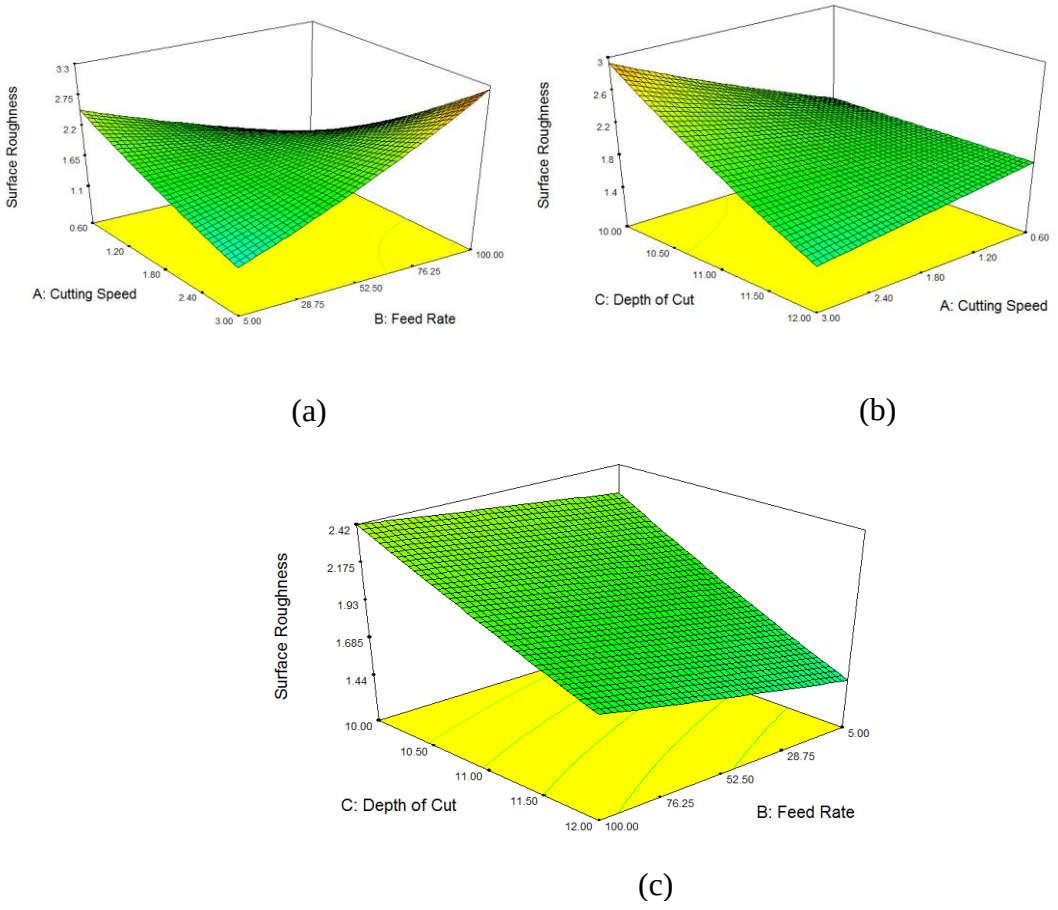


Figure 1.4: 3D response surface graph shows three (3) machining parameters (cutting speed, feed rate, depth of cut) which affect to surface roughness

From the Figure 1.4 (b), it can be observed that the lowest value of surface roughness could be achieved by increasing the depth of cut with lower cutting speed. Figure 1.4 (c) shows the 3D response surface for surface roughness in relation to the machining parameters of feed rate and depth of cut with surface roughness. From the graph in Figure 1.4 (c), it can be seen that the value of surface roughness decreased with the decreasing of a feed rate and increasing of depth of cut. From this Figure 1.4 (a) to (c), it is apparent that the minimum value of surface roughness was obtained at low feed rate (5 mm/min) and high depth of cut (12 μm). This is happening is due to the chip formed during machining process with low feed was continuous and it cause the tool-chips and workpiece-tool had less interaction between workpiece-tool which can reduce a friction between workpiece-tool interface (Joshua et al., 2015b). Overall, these results indicate that the low feed rate can decrease the value of surface roughness and concur with the results obtained by (Izamshah et al. 2010).

The normal plot of the residual graph for surface roughness was generated is as shown in the Figure 1.5. The normal probability plots of the residual graph present the data of the surface roughness value with followed a normal distribution in a straight line. The normal distribution data in straight line are good because all the points line up nicely. While, the Figure 1.10 shows the predicted versus actual plots of response, namely surface roughness and it is useful to detect outlier values that are predicted by the model.

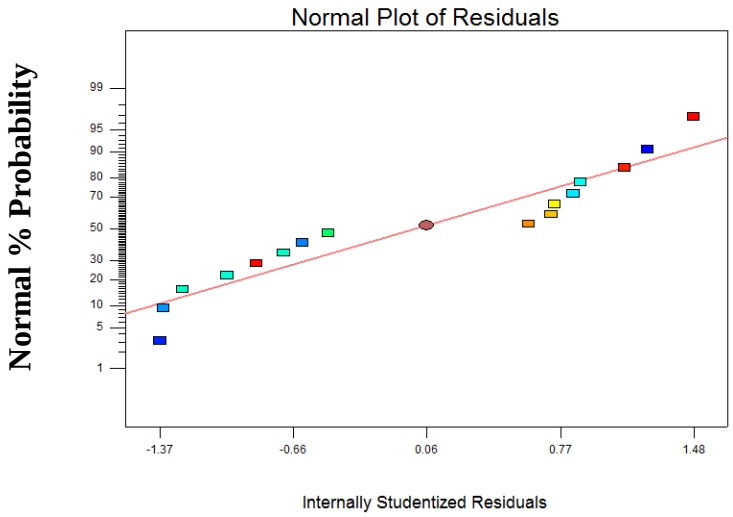


Figure 1.5: The normal plot of the residual graph for surface roughness

As can be seen from the Figure 1.6, it shows that the model generated was fitted very well with the observed values. In addition, there is an existing a good relationship between the predicted values of surface roughness acquired from the model and actual experimental data.

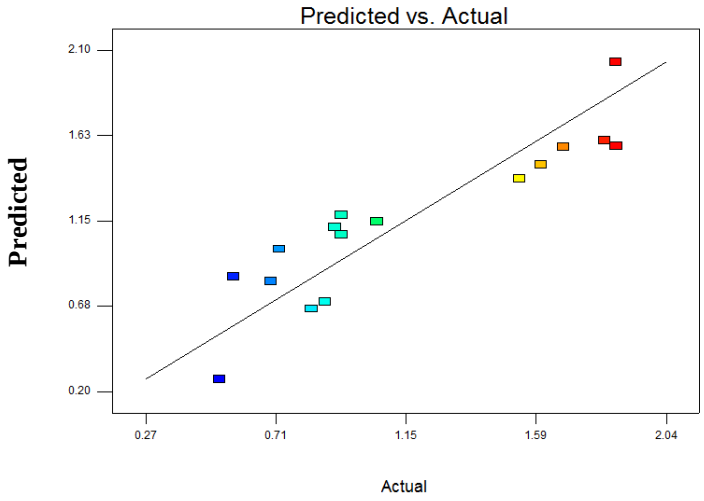
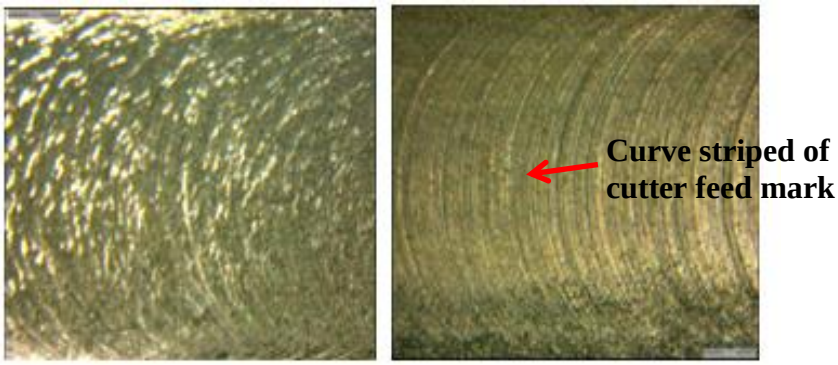


Figure 1.6: The predicted Vs. actual graph for surface roughness

1.5 Macroscopic observation for preliminary test

The another important analysis was performed through the macroscopic analysis with aims to evaluate the surface roughness of machined surface when machining of hardened steel materials using conventional and rotary ultrasonic assisted end milling (RUAEM) machining. The Figure 1.7 (a) and Figure 1.7 (b) presents the differences of macroscopic observation or macro surface profile in the conventional machining and the ultrasonic assisted machining of the hardened steel material using laboratory stereo microscope. From this Figure 1.7 (a) and Figure 1.7 (b), the macroscopic observation of machined surface produced from the ultrasonic assisted machining was uniform with consistent peak to peak value which improved the surface finish compare to conventional machining with bad of machined surface.



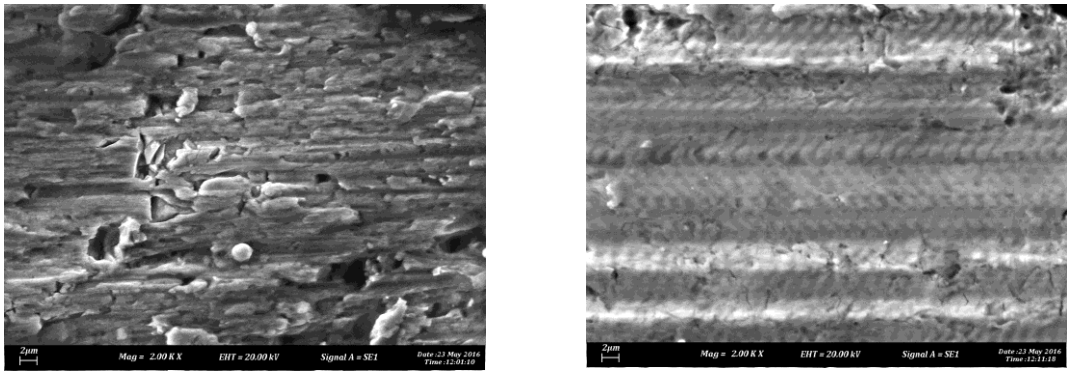
a) Conventional machining b) Ultrasonic assisted end milling machining

Figure 1.7: Macroscopic observation of machined surface of hardened steel material

When finished the milling process, existed a curve striped of cutter feed marks for conventional machining and ultrasonic assisted machining respectively. The macroscopic observation shows the curve striped of cutter feed marks generated by ultrasonic assisted

machining was consistent and had a low vibration with the smaller transverse marks compared to the conventional machining. The quality of machined surfaces produced by the rotary ultrasonic assisted machining were more shiny and luminous compare to the conventional machining. This outcome is equivalent to that of (Gao et al., 2002) who found that ultrasonic cutting generated by the smaller tranverse feed marks was caused by the low tool vibration compared to the common cutting.

Scanning Electron Microscopy (SEM) used for measuring micro surface topography for the surface finish of machined surface with comparison of conventional machining and ultrasonic assisted machining. Figure 1.8 (a) and Figure 1.8 (b) shows the micro surface topographies of machined surface by using SEM photos between conventional machining and rotary ultrasonic assisted end milling machining.



(c) Conventional machining (d) Rotary ultrasonic assisted end milling

Figure 1.8: The micro surface topographies by SEM with cutting speed, vc = 3 m/min, feed, f = 100 mm/min, depth of cut, a_p = 12 μm

As shown in Figure 1.8, there are many shallow surface depressions (pits) existed on the machined surface by conventional machining compared to rotary ultrasonic assisted end milling machining. In rotary ultrasonic assisted end milling machining process, the

quality of machined surface was very smooth with the consistency of feed mark. While, in conventional machining process, emerged a scratch on the machined surface by successively. From this Figure 1.8 (a) and Figure 1.8 (b), it proves that the surface quality of the machined surface by rotary ultrasonic assisted end milling machining is an excellent compared to conventional machining with the same cutting condition and machining accuracy improve greatly by ultrasonic assisted machining.

1.6 Summary of preliminary test result

Overall, the preliminary study result of statistical analysis and macroscopic observation indicates that the most significant factor that affected and strongly significant effect on the surface roughness value of machined surface was cutting speed (A), feed rate (B) and rotary ultrasonic assisted end milling machining (D). By analysis of variance (ANOVA), it found that the depth of cut (C) was not affected and did not have a significant effect on the surface roughness value when machining of hardened steel materials using rotary ultrasonic assisted machining. Macroscopic observation results indicate that machined surface produced from the ultrasonic assisted machining was uniform with consistent peak to peak value which improved the surface finish compare to conventional machining. The cutter feed marks of slot milling by rotary ultrasonic assisted end milling machining was consistent and had a low vibration with the smaller transverse marks compared to the conventional machining. By using the rotary ultrasonic assisted end milling machining, the machined surface generated was shiny, luminous, smooth and excellence compared to conventional machining.

Furthermore, this preliminary study result is similar to the study carried out by (Shamoto et al., 2005) that showing rotational ultrasonic machining is the best method to improved surface roughness of machined surface with mirror surface by machining

parameter with cutting speed of 0.2 m/min to 1.34 m/min (32 rpm to 213 rpm). Rotary ultrasonic assisted end milling machining using the average feed rate of 6 mm/min for milling process and the result show that improving a surface roughness of machined surface (Kuo and Tsao, 2012). From the result of an experimental study, the cutting speed, feed rate and hybrid rotary ultrasonic assisted end milling machining is a main factor which will be used for future research.

This experimental result proves that rotary ultrasonic assisted end milling machining was successfully improving of the machined surface and machining accuracy with the reduction of Ra values and consistency of cutting feed mark with the low tool vibration. The best and the lowest of the surface roughness value of machined surface achieved by rotary ultrasonic assisted end milling machining is 0.27 μm (Run 3) at 0.6 m/min (cutting speed), 5 mm/min (feed rate), 12 μm (depth of cut)with constant controlled of 23.83 kHz of vibration frequency and 2 μm of amplitude vibration.

According to these data, it can infer that the machining parameters was affecting the machining performance of surface roughness is cutting speed, feed rate and rotary ultrasonic assisted machining. From the graph of surface roughness (Ra) between conventional and rotary ultrasonic assisted end milling machining, it indicates that a higher cutting speed of 3 m/min with lower feed rate of 5 mm/min was affected the surface roughness, Ra value. Also, the vibration frequency of 23.83 kHz and amplitude vibration of 2 μm is the main effect and strongly significant effect of surface roughness value.

However, further experimental work need to be perform to obtain a lower surface roughness value, Ra with below 0.27 μm and aim to obtain mirror surface by applying rotary ultrasonic assisted end milling (RUAEM) machining.

APPENDIX B

Cutting process and surface facing a work piece



Figure 2.1: Cutting process of raw material using vertical milling machine



Figure 2.2: Surface facing process by using surface grinding machines

APPENDIX C

Procedure of EPH insert mounting

a. Firstly, the clamping screw must be loose and placing EPH insert in the pocket of the body.

b. The clamping screws lightly fasten in order of position A then B as shown in the Figure 1 below.

c. Then, tighten the clamping screw securely in order of position A then B.

d. Lastly, the condition of insert setting clearance the insert and insert pocket, the tool diameter and the peripheral edge run out must be checked before the machining process done.

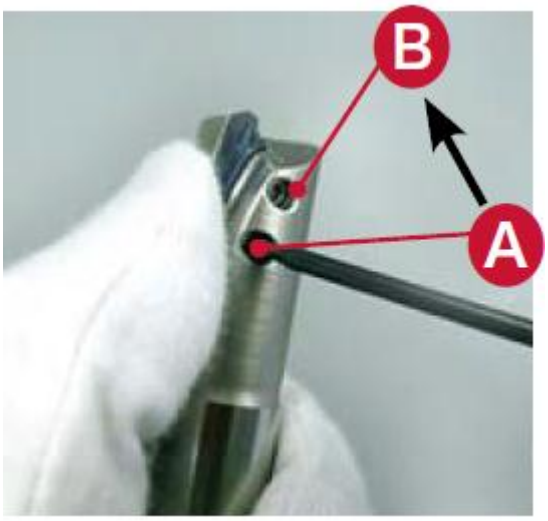


Figure 3.1: Procedure of EPH Insert Mounting

APPENDIX D

HAAS CNC milling machine VF-1 with 3 axis specification

TRAVELS	S.A.E	METRIC
X Axis	20 "	508 mm
Y Axis	16 "	406 mm
Z Axis	20 "	508 mm
Spindle Nose to Table (~ max)	24 "	610 mm
Spindle Nose to Table (~ min)	4 "	102 mm
TABLE	**S.A.E**	**METRIC**
Length	26 "	660 mm
Width	14 "	356 mm
T-Slot Width	5/8 "	16 mm
T-Slot Center Distance	4.92 "	125.0 mm
Number of Std T-Slots	3	3
Max Weight on Table (evenly distributed)	3000 lb	1361 kg
SPINDLE	**S.A.E.**	**METRIC**
Max Rating	30 hp	22.4 kW
Max Speed	8100 rpm	8100 rpm
Max Torque	90 ft-lb @ 2000 rpm	122 Nm @ 2000 rpm
Drive System	Inline Direct-Drive	Inline Direct-Drive
Max Torque w/opt Gearbox	250 ft-lb @450 rpm	339 Nm @ 450 rpm
Taper	CT or BT 40	CT or BT 40
Bearing Lubrication	Air/Oil Injection	Air/Oil Injection
Cooling	Liquid Cooled	Liquid Cooled
FEEDRATES	**S.A.E.**	**METRIC**
Rapids on X	1000 in/min	25.4 m/min
Rapids on Y	1000 in/min	25.4 m/min
Rapids on Z	1000 in/min	25.4 m/min
Max Cutting	650 in/min	16.5 m/min
AXIS MOTORS	**S.A.E.**	**METRIC**
Max Thrust X	2550 lb	11343 N
Max Thrust Y	2550 lb	11343 N
Max Thrust Z	4200 lb	18683 N
TOOL CHANGER	**S.A.E.**	**METRIC**
Type	Carousel (SMTC Optional)	Carousel (SMTC Optional)
Capacity	20	20
Max Tool Diameter (full)	3.5 "	89 mm
Max Tool Weight	12 lb	5.4 kg

Tool-to-Tool (avg)	4.2 sec	4.2 sec
Chip-to-Chip (avg)	4.5 sec	4.5 sec
GENERAL	**S.A.E.**	**METRIC**
Air Required	4 scfm, 100 psi	113 L/min, 6.9 bar
Coolant Capacity	55 gal	208 L

Source: http://www.haascnc.com

APPENDIX E

EDM (electro discharge machining) wire cut

Electro Discharge Machining (EDM) is a non-traditional machining with electro thermal process, where an electrical energy is used to generate an electrical spark and material removal caused by the thermal energy of the spark. An electric spark is generated between a work piece and an electrode. Electro discharge machining is often used for machining of difficult to cut materials and high strength temperature of resistant alloys. Machining processes for work piece materials using EDM wire cut must be electrically conductive. When the electrical current flows, the electric spark is generated. The electric spark is carefully controlled and localized to avoid any damage to the work piece surface because this electric spark will generate temperature up to 8000 to 12000 degrees of Celsius. The spark of EDM wire takes place in the dielectric of deionized water. Figure 3.18 shows a basic EDM process.

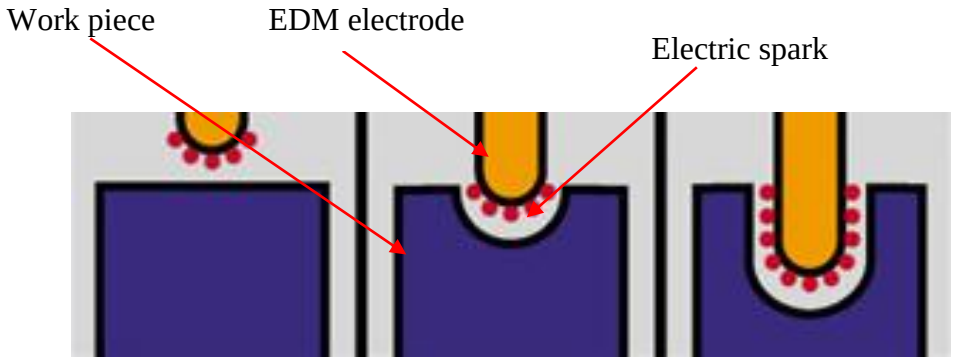


Figure 4.1: The basic EDM process

The electro discharge machine was used for cutting the finished slot machined work piece material into the sizes of 10 mm X 10 mm X 10 mm before investigating the

microstructure of materials using scanning electron microscopy (SEM). Table 3.6 shows the photo of EDM machine and cutting techniques of finished slot machined work piece using EDM machine into smaller sizes (10 mm X 10 mm X 10 mm) for ease of insertion into SEM (scanning electron microscopy) machine.

Ultrasonic cleaner

Ultrasonic cleaner is a process using ultrasonic in the cleaning process with the range of frequency between 20-400 kHz and using water as a cleaning solvent. Ultrasonic cleaning utilizes cavitation bubbles prompted by a high frequency pressure wave through a sound to shake water (cleaning solvent). The shaking delivers high force on contaminants sticking to substrates like metals, plastics, glass, rubber, and ceramics. This action additionally penetrates blind holes, cracks and recesses. The function is to completely evacuate all traces of contamination tightly adhering or embedded onto strong surfaces. Table 3.6 shows the ultrasonic cleaner used in experiments for cleaning the specimen before investigating the microstructure of material using scanning electron microscopy (SEM). The specimens are overlaid with oil to prevent corrosion process. Before the microstructure investigation process is done using machines of SEM (scanning electron microscopy), the specimen must be cleaned from the effects of oil. The specimen is soaked in a beaker filled with ethanol solution and shaken using an ultrasonic cleaner.

During the cleaning process of the specimen from the oil layer, specimen temperature for cleaning process is set to 0°C (zero degree Celsius) to avoid any effects to the specimens whereas the time set for the cleaning of specimens from oil layer is about 60 minutes. When the cleaning process of specimen from the oil layer finished, the specimen is removed from the beaker using a spatula and put in the airtight container to prevent any occurrence of chemical reaction. After the specimen is put in the airtight container, the

specimen is ready to be run for the microstructure investigation of machined surface (conventional and ultrasonic) using SEM (scanning electron microscopy) machine.

APPENDIX F

The setting of CNC machine datum

The setting of CNC machine datum is very important before machining experiment to ensure the position of a work piece is in flat position. The flat position of the work piece could be achieved using the milling vise (work holding device). The work holding device used for the position of a work piece in the flat position is a milling vise as shown in Figure 3.23. After the work piece was placed on the milling machine vise, the work piece alignment process was carried out as shown in Figure 3.24.



Figure 5.1: Milling vise use for holding the work piece in flat position



Figure 5.2: The alignment process for holding the work piece in flat position